

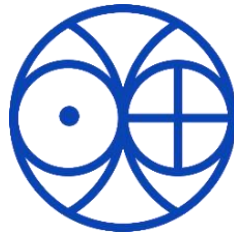


ICPEH 2024

**International Conference on
Planets, Exoplanets and Habitability**

5-9 February 2024

Physical Research Laboratory, Ahmedabad



Volume of Abstracts

Table of Contents

<i>SNo.</i>	<i>Title</i>	<i>page</i>
1.	"Other worlds in the cosmos? The search for planets similar to our Earth and... perhaps harbouring life !"	8
2.	HIGHLIGHTS FROM ILEWG LUNEX EUROMOONMARS & EUROSPACEHUB	9
3.	IS LUNAR WATER A RENEWABLE RESOURCE?.....	11
4.	DO GIANT IMPACTS KICKSTART ROCKY PLANET HABITABILITY?.....	12
5.	The Legacy of Extreme Precision Radial Velocity (EPRV) at PRL	13
6.	Ionosphere - thermosphere investigations of Planet Earth	14
7.	EXPOSED ROCK FRAGMENTS ENCOUNTERED BY PRAGYAN ROVER AT THE LANDING SITE OF CHANDRAYAAN-3 MISSION.	15
8.	SOME NEW INSIGHTS ON THE CHARACTERISTIC FEATURES OF THE LUNAR IONOSPHERE USING DFRS AND TWO-WAY OLR MEASUREMENTS FROM CHANDRAYAAN-2.....	16
9.	Evolution of magma sources revealed by the surface composition of the Mare on Moon	17
10.	All you need are spectra – with SIR-2 from Earth to the Moon and back.....	18
11.	Revolutionizing Our Understanding: Scientific Milestones from Sample Return Missions	19
12.	Solar X-ray Monitor (XSM) onboard Chandrayaan-2.....	20
13.	In-flight performance and initial results from Plasma Analyser Package for Aditya (PAPA) payload onboard Aditya-L1 mission.....	21
14.	FLUXGATE MAGNETOMETER ONBOARD ADITYA-L1 SPACECRAFT: THE JOURNEY SO FAR	22
15.	MINIATURE HIGH SENSITIVITY ACCELEROMETERS FOR PLANETARY SEISMIC ACTIVITY STUDIES	24
16.	LUNAR SWIRLS: FRESH INSIGHTS REVEALED BY GEOLOGICAL CONTEXT	25
17.	A LUNAR SAMPLE RETURN MISSION	26
18.	INSIGHTS INTO HIGHLY SIDEROPHILE ELEMENT ABUNDANCE IN LUNAR CRUST AND MANTLE FROM METEORITES A-881757, Y 981031, Y 983885 and Y-86032: CONSTRAINTS ON REGIONS BEYOND THE PROCELLARUM KREEP TERRANE (PKT) ..	28
19.	Magmatism Along the Eastern Limb of the Moon.....	30
20.	Integrated comparative study between lunar regional pyroclastic deposits	31
21.	EXPLORING FAN DEPOSITS ON MARS AND EARTH	32
22.	Evolution of Martian Volcanism and Lithosphere: Geochemical Insights from Noachian to Amazonian Volcanic Terrains	32
23.	Subsurface study of the Tharsis graben system using SHARAD data	35
22.	Characterizing Arsia Mons Clouds using OMEGA and CRISM.....	36
23.	AEOLIAN ACTIVITY AND DUNE MIGRATION OVER A GLOBAL DUST-STORM YEAR AROUND THE MARTIAN GALE CRATER	38
24.	DEVELOPMENT OF A COAXIAL ROTOR SYSTEM FOR MARS EXPLORATION	39
25.	EXOBASE AND HOMOPAUSE ALTITUDES IN THE MARTIAN UPPER ATMOSPHERE:	

VARIABILITIES AND SOURCES	41
26. RESULTS FROM THE MARS EXOSPHERIC COMPOSITION ANALYSER (MENCA) ONBOARD MARS ORBITER MISSION	42
27. THE IMPACT OF THE VENUSIAN PLASMA ENVIRONMENT DURING THE PASSAGE OF INTERPLANETARY CORONAL MASS EJECTIONS	43
28. CHARACTERISTIC FEATURES OF THE VENUS IONOSPHERE USING PHYSICS BASED IONOSPHERIC MODELS AND OBSERVATIONS.....	44
29. Whistler mode wave in Jovian magnetosphere	45
30. RESULTS FROM CHACE-2 ONBOARD CHANDRAYAAN-2 ORBITER	46
31. Effect of spacecraft orbital parameters on the spatiotemporal distribution of Solar Occultation measurements in the Venusian Atmosphere.....	47
32. Exploring rocky worlds with the HARPS-N, ESPRESSO and NIRPS spectrographs ...	49
33. Avoiding False Positive Exoplanet Detections in Centimeters-Per-Second Radial Velocity Data	50
34. CHEOPS observations of KELT-20 b/MASCARA-2 b: An aligned orbit and signs of variability from a reflective day side.....	51
35. Comprehensive homogeneous investigation of orbital ephemeris and atmospheric characterization of an Ultra-hot Jupiter: WASP-19 b.....	52
36. DESIGN AND DEVELOPMENT OF PRECISE TEMPERATURE CONTROLLER FOR PARAS-2	54
37. Double Scrambler Design and Implementation in PARAS-2 to achieve sub-m/s RV Precision.....	55
38. Precise Wavelength Calibration of PARAS-1 and PARAS-2 using Uranium lines for 1 m s ⁻¹ to sub-m s ⁻¹ RV measurements.....	56
39. Elevating precision: High-resolution spectroscopy with the Fabry-Perot wavelength calibration.....	57
40. Pushing the limits of precision RVs in the near-infrared and optical with HPF and NEID	58
41. The PLATO mission and the full characterisation of planetary systems	59
42. Curious case of two Extreme Density Close-in Giant Planets TOI-1789b and TOI-4603b around Evolved Stars	60
43. PUSHING THE BOUNDARIES OF PLANET DETECTION IN THE RADIAL VELOCITY METHOD USING ARTIFICIAL INTELLIGENCE.....	60
44. The Large Fiber Array Spectroscopic Telescope: A scalable ELT targeting Earth-like exoplanet atmospheres	62
45. Precise inference of limb-darkening using a regularization technique: application for a sample of Kepler and TESS exoplanet transit light curves.....	63
46. A search for auroral radio emission from β Pictoris b.	64
47. A NUMERICAL TRANSIT SIMULATOR FOR GENERATING LIGHTCURVES OF TRANSITING OBJECTS WITH WEIRD GEOMETRIES	65
48. UNVEILING AND EXPLORING THE ATMOSPHERIC COMPOSITION OF SUPER-EARTH EXOPLANETS IN THE JWST ERA.....	66
49. Exocomets, 35 years of discoveries	67
50. Exoplanet Demographics: Insights into Planet Formation Mechanisms and History ..	68
51. Age Distribution of Exoplanet Host Stars: Chemical and Kinematic Age Proxies from	

GAIA DR3.....	69
52. Investigating the influence of clouds on the reflectance spectra of exo-Earths using the HWO mission concept.....	70
53. First measurement of seasonal variations of surface pressure over Hellas and Argyre basins from EMIRS on board EMM: Comparison with MCD model.....	71
54. SUPRATHERMAL ELECTRON DEPLETIONS IN THE MARTIAN NIGHTSIDE UPPER ATMOSPHERE: ROLE OF MAGNETIC FIELD TOPOLOGY AND INDUCED MAGNETIC FIELDS.....	72
55. Electromagnetic Ion Cyclotron wave with magnetic model in Jovian Magnetosphere.	73
56. INTERPLANETARY DUST FLUX AT DIFFERENT PLANETS IN INNER SOLAR SYSTEM	74
57. ELECTROSTATIC CHARGING NEAR THE LUNAR POLAR REGION.	75
58. DEVELOPMENT OF PROCESSING PACKAGES FOR AKATSUKI RADIO SCIENCE EXPERIMENT OF VENUS ATMOSPHERE.....	77
59. DEVELOPMENT OF A COAXIAL ROTOR SYSTEM FOR MARS EXPLORATION	79
60. THE SEARCH FOR LIFE ON EXOPLANETS: THE RELIABILITY OF O2 AS A BIOSIGNATURE AND THE KEY ROLE OF UV SPACE TELESCOPES LIKE ASTROSAT AND INSIST	80
61. INSIGHTS INTO THE GEOLOGICAL IMPORTANCE OF IMPACT CRATERING EVENTS	81
62. Asteroid impact craters on terrestrial planets and opportunity for planetary habitability.....	83
63. End Member Models in Planet Formation: Constraints from different Achondrites	84
64. Search for the habitable worlds by their atmosphere characterization	85
65. The Curious Case of Argon.....	86
66. FROM PRESTELLAR CORE TO PLANETARY BODIES -ASTROCHEMICAL ORIGIN AND HABITABILITY	87
67. Exploring the scaling relations of exoplanets and characterization of a potential habitable exoplanet system.	88
68. ESTABLISHMENT OF LUNAR HABITAT: CONSIDERATIONS, REQUIREMENTS AND ESSENTIAL TECHNOLOGIES	89
69. NEXT GENERATION LUNAR SCIENCE THROUGH GEOPHYSICAL NETWORK ON THE MOON	90
70. Development of Spectro-polarimeter for HABITABLE Planet Earth (SHAPE) onboard Chandrayaan-3.....	91
71. PROCESS VIABILITY STUDY IN THE LUNAR ISRU – PRODUCTION OF OXYGEN FROM LUNAR REGOLITH.....	92
72. SIMULATION OF BRIGHTNESS TEMPERATURE FROM LUNAR SUBSURFACE FOR RADIOMETRIC MODE OBSERVATIONS OF DFSAR/CHANDRAYAAN-2.....	94
73. Surface and Subsurface Regolith Characterization of Lunar South Pole using Chandrayaan-2 Dual-frequency Synthetic Aperture Radar (DFSAR)	95
74. TERRESTRIAL IMPACT CRATERS AS AN IMPORTANT GEOMORPHIC FEATURE FOR THE FORMATION, PRESERVATION, AND IDENTIFICATION OF ENERGY RESOURCES ..	97
75. Role of ice in the Martian erosional valley formation: A study from Thaumasia	

highland and adjacent region, Mars	99
76. Morphological Scene Representations to Explore Small Solar System Bodies.....	100
77. Estimation of lunar soil parameters near southern polar regions of the moon from Chandrayaan-3 mission observations.....	101
78. Noble gas isotope study in Chondrules of Ordinary Chondrule.....	102
79. EXPLORING NUV M-DWARF FLARES AND THEIR IMPACT ON HABITABILITY.....	103
80. UNDERSTANDING HABITABILITY AND LIMITS OF LIFE: OPPORTUNITIES THROUGH INDIAN SPACE PROGRAMME	105
81. Using mid-IR spectroscopy to study interstellar ice analogues.....	107
82. Sustainable Lunar Habitat Design: Utilizing PEMFCs in Lava Tube for Creating an Artificial Atmosphere.....	108
83. DYNAMIC GEOPHYSICAL CONDITIONS AND PROBABILITY OF ADVANCED LIFE IN POTENTIALLY HABITABLE ROCKY EXOPLANETS.	109
84. LONGEVITY OF HYDROLOGICAL REGIME AND WATER ACTIVITY AS IMPORTANT PARAMETERS IN SEARCH FOR ASTROBIOLOGICAL TARGET SITES	111
85. Automatic Crater Detection on Lunar Surface.....	112
86. Lunar Launchpad to Cosmic Frontiers: Navigating Interplanetary Exploration from the Moon.....	113
87. Surface and Subsurface Regolith Characterization of Lunar South Pole using Chandrayaan-2 Dual-frequency Synthetic Aperture Radar (DFSAR)	115
88. Morphological, Mineralogical, and Chronological Mapping of Nernst Crater Using Lunar Remote Sensing Datasets	117
89. COMPOSITIONAL DIVERSITY OF MANILIUS CRATER AND SURROUNDING REGION USING CHANDRAYAN HYPERSPECTRAL DATASETS.	119
90. IMBRIAN TO ERATOSTHENIAN VOLCANISM AND THE COMPOSITIONAL DELINEATION OF MARE UNITS OF MARE INGENII USING M3 , IIRS, TMC-2, AND KAGUYA DATA.	121
91. AUTOMATIC CRATER DETECTION AND CLASSIFICATION ON LUNAR SURFACE USING NEURAL NETWORKS	123
92. DUST DETACHMENT FROM THE LUNAR SURFACE.....	124
93. Advance Lunar Surface Exploration: A Comparative Analysis of Deep Learning Models for Crater Detection Using Chandrayaan-2 OHRC Data.....	125
94. Mapping the Moon: A Deep Learning Strategy for Lunar Crater Detection from Chandrayaan-2 Satellite Captures	127
95. Towards Understanding Role of Transient Lunar Volcanism in Enriching Lunar Polar Volatile Deposits	128
96. ELECTROSTATIC CHARACTERISTICS OF ROCK-ICE MIXTURES AND DETECTION OF ICE ON LUNAR SURFACE.	130
97. VOLATILE MIGRATION ON THE LUNAR SURFACE.	132
98. Evaluating Latitudinal Dependency in Depth-to-Diameter Ratios of Lunar Polar Craters: Do They Truly Indicate the Presence of Water Ice?	134
99. EXPLORING THE POTENTIAL OF USING CHANDRAYAAN-2 IMAGING INFRA RED SPECTROMETER (IIRS) AND LRO-DIVINER DATA TO ESTIMATE SURFACE TEMPERATURES OVER PARTS OF THE ARISTARCHUS PLATEAU PYROCLASTIC DEPOSITS ON THE MOON	136

100. Differentiating wrinkle ridges for the analysis of displacement-length ratios in Mare Tranquillitatis.	138
101. INVESTIGATION OF TEMPERATURE DEPENDENT THERMAL CONDUCTIVITY OF LUNAR ANALOGUES UNDER SIMULATED LUNAR ENVIRONMENT.	139
102. MOON AS A GATEWAY FOR FUTURE SOLAR SYSTEM EXPLORATION	139
103. LABORATORY REFLECTANCE SPECTROSCOPY OF SITTAMPUNDI ANORTHOSITE, A LUNAR ANALOGUE	140
104. REFLECTANCE SPECTROSCOPY OF CLAY MINERALS FROM THE MATANUMADH LOCALITY, A MARTIAN ANALOGUE.	141
105. Transition of a pristine crater to sepulchered: A tale of Morella crater, Mars	142
106. Designing a toolkit to delineate the ejecta rays of fresh craters on lunar surface ...	144
107. STUDY OF TRACES OF BIO-SIGNATURES ON MARS AND INDIAN ANALOG SITES	144
108. Unraveling Martian Mysteries: Nakhrites as Key Proxies for Water Activity in the Younger Amazonian Epoch.....	146
109. COMPARATIVE STUDY OF LADAKH PERIGLACIAL FEATURES FROM MARTIAN ANALOGUE PERSPECTIVE.....	147
110. INSIGHTS ON MARTIAN ALTERATION PROCESS FROM TERRESTRIAL ANALOG STUDY ON OLIVINE-TO-CLAY REPLACEMENT.....	149
111. On the Relationship of Dichotomy of Mars and Occurrence of Dust Devils	150
112. MAGNETIC TOPOLOGY DEPENDENCE OF ELECTRON IMPACT IONIZATION FREQUENCY IN THE MARTIAN NIGHTSIDE IONOSPHERE	151
113. Characteristics of Gravity Waves in Lighter and Heavier Species	152
114. in the Martian Thermosphere	152
115. CHASING MARTIAN GLACIAL LANDFORMS: ANALYSIS OF ACHERON FOSSAE GLACIAL FORMATION USING HIGH RESOLUTION SATELLITE IMAGERY.....	153
116. GEOLOGICAL EVOLUTION OF A COMPLEX TOPOGRAPHIC DEPRESSION WITHIN TERRA SIRENUM, MARS.....	154
117. Archean stromatolites: a possible terrestrial analog to Mars.....	155
118. UNVEILING MARTIAN MAGMATIC PROCESSES: GEOCHEMICAL PERSPECTIVES ON POIKILITIC SHERGOTTITES	156
119. Volcano-tectonic and fluvial interplay on Mars: insights from geomorphic landforms in Syria Planum.....	158
120. Modeling of Schumann Resonance of Mars by using FDTD Method	159
121. Geological evaluation of the Martian analogue site in Kachchh basin of western India and its Geoheritage value.....	160
122. MORPHOLOGICAL CHARACTERIZATION OF LIU HSIN CRATER, MARS.....	162
123. Electromagnetic Ion Cyclotron wave with magnetic model in Jovian Magnetosphere	162
124. Understanding the effect of Fe in the interstellar nanosilicates : A first principles study	163
125. Unraveling Phaethon's Comet-Like Activity: Expected Spectral Variations in the December 2024 Encounter	164
126. Future Mining Candidate Among the Quili-hilda Group of Asteroid & Comet	165

127. Understanding the Mode of Occurrence of Granite and Other Felsic Rocks in Mars and Moon and their Role in Planetary Crustal Evolution: An Earth Analogous Study	166
128. Effect of Different Forces on IDP in Inner and Outer Solar System.....	167
129. HIGH-PRESSURE PHASES AND IMPACT-INDUCED TEXTURES IN SHOCKED INDIAN METEORITES.....	167
130. Insights on the Ion Composition of Comet 67P/C-G during the Rosetta Mission: A Multi-instrument Analysis	169
131. Venus Exploration Challenges and Future Research Opportunities.....	170
132. Observations of V0 layer from Venera 15 and 16.....	171
133. Ejection age and Noble Gas Study of Rantila Meteorite.....	172
134. Active radio sounding of Solar Corona - Results From MOM and Akatsuki Missions.	173
135. ELECTROSTATIC SOLITARY WAVES IN THE VENUSIAN PLASMA ENVIRONMENT	174
136. UTILIZING PSINSAR FOR MONITORING SUBSIDENCE IN RAMGARH CRATER, INDIA: AN INNOVATIVE APPROACH.....	175
137. Magnetosphere Formation of a Tidally Locked Planet or Satellite.	176
138. Autonomous Systems for Data Analysis on Space Probes	177
139. SPACE SURVEILLANCE NETWORK AS A MEANS OF MAXIMIZING SCIENTIFIC OUTPUT FROM SPACE MISSIONS	178
140. Advancements in volatiles and In-Situ Resource Utilization: Efficient Extraction Methods for Sustainable Space Exploration.....	180
141. Design and development of Neutral and Ion Mass Spectrometer (NIMS) for future planetary space missions.....	181
142. Characterization of Silicon Photomultipliers and Scintillators based detector modules for hard X-ray measurements.....	182
143. Development and Characterization of a Multi-Detector Large Area X-Ray Spectrometer using Silicon Drift Detectors with ASIC Based Readout	183
144. In-Situ Measurement of Water-ice on Moon for Future Missions: Challenges, Techniques and Current Understanding	184
145. Digital Pulse Processing based readout electronics for Alpha Particle Spectrometer (APS).....	185
146. Development of Cadmium Telluride (CdTe) based high-energy X-ray spectrometer for Venus Solar Soft X-ray Spectrometer (VS3) on-board Venus Orbiter	186
147. Developmental aspects of Impact Ionization Dust Detector	187
148. NEW WAY OF OPTIMIZING SURFACE MISSIONS TO INCREASE SCIENTIFIC OUTPUT	187
149. BUOYANT ASCENSION: AN INGENIOUS PROBE DESIGN USING CONTROLLED VOLUME EXPANSION.....	188
150. Optical Observation of Midnight Temperature Maximum using a Doppler Fabry-Perot Interferometer: First results from an equatorial Indian station.....	189
151. Design and development of speckle imager for PRL 2.5m telescope	191
152. DEVELOPMENT OF STABLE PRESSURE ENVIRONMENT FOR PARAS-2.....	191
153. Searching for Organic beyond the Visible: Unveiling Biosignature Potential in Super-Earths through Combined Near-Infrared Spectroscopy and Polarimetry	192

154. Further Probing the Plausible Causes of TTV in the TrES-2 system with TESS data	194
155. Pushing Efficiency of Planet Formation: Detection and Characterization of a Saturn around an M dwarf star	195
156. Comparative analysis of atmospheric characteristics of M-Dwarf Systems	196
157. SEARCHING FOR VARIABLE STARS AND MICROLENSING EVENTS IN THE GLOBULAR CLUSTERS PALOMAR 1 AND PALOMAR 2	197
158. Photometric and Spectroscopic observations of the transiting exoplanets from Devasthal Observatory	197
159. Estimating the fundamental limit to RV precision taking into account the stellar activity	198
160. Probing the Biosignatures on Rocky Exoplanets: Methods, Current hurdles and Future Horizons	198
161. EXOPLANET DETECTION USING NEURAL NETWORK FOR TIME SERIES DATA ...	199
162. Do low metallicity stars contain giant planets? Large exoplanet relation with stellar Metallicity around G class star	200
163. A Quench Level Approximation Approach for Rapid Retrieval of Chemical Abundances in Spectral Observations	201
164. EXOPLANET TRANSMISSION SPECTROSCOPY WITH 2m HIMALAYAN CHANDRA TELESCOPE	202
165. Unraveling the atmospheres of faraway worlds with adaptable planetary atmosphere model	202

1. "Other worlds in the cosmos? The search for planets similar to our Earth and... perhaps harbouring life !"

Mayor Michel, University of Geneva, Switzerland

Are there other worlds in the universe? Does life exist elsewhere in the cosmos? Today's technology has made it possible to transform this ancient dream into a fascinating field of astrophysics. Twenty-eight years after the discovery of the first planet orbiting a star like our Sun, several thousand planetary systems have been discovered. These initial discoveries have revealed the astonishing diversity of these systems, which are very different from our own solar system.

After the euphoria of these initial discoveries, the era of studying the atmospheres of exoplanets has now begun. Despite the enormous contrast between the luminosity of the star and the very low luminosity reflected by the planet, atmospheric analysis is beginning and will benefit from space and ground-based telescopes. The instrumentation developed by the Physical Research Laboratory, based at the Mont Abu Observatory, will contribute to this fascinating research.

Does life exist in other parts of the cosmos? - A dizzying question - Analysis of planetary atmospheres could reveal biosignatures, the spectral characteristics induced by the development of life. Advances in spectroscopic studies of exoplanets lead us to believe that the search for extraterrestrial life is possible.

2. HIGHLIGHTS FROM ILEWG LUNEX EUROMOONMARS & EUROSPACEHUB

B. Foing¹⁻¹⁰, H. Rogers², J. Pascual⁴, V. Purién⁴, F. Fazel^{3,4,5}, A. Roperó^{3,4}, K. Claeys^{2,3,4}, T. Ducai^{3,4,10}, S. Crotti^{3,4}, D. Tagne^{3,4}, S. Vleugels^{5,10}, O. Swida^{5,10}, R. Hoogenboom^{5,10}, D. Abbink^{5,10}, EuroSpaceHub Team⁴, A. Kolodziejczyk^{3,7}, I.R.Perrier^{3,7,9}, S. Baatout¹¹, S. Pavanello¹⁴, C. Stoker¹, P. Ehrenfreund^{1,19}, TaiSik Lee², M.Musilova², M. Heemskerck^{2,3}, C. Pouwels^{2,3,12}, A. Tavernier¹³, K. McGrath^{3,7,12,15}, C.Robertson^{3,10,15}, I. Horvatt^{3,10,15}, M.Balfe^{3,10,15}, J.Laffey^{3,10,15}, C.Tyndall^{3,10,15}, M.Harvey^{3,10,15}, A. Ehreiser¹⁶, L.Schlarmann^{3,4}, B. Reymens^{3,4}, P.Sol^{3,9,10}, K. Gautam^{3,4}, A. Wedler¹⁶, A. Autino¹⁷, S. Heinz¹⁷, J. Pelton¹⁷, J. Crisafulli¹⁷, V. Beldavs¹⁷, D.Tacchini¹⁰, A. Hutchinson^{3,4}, C.Dubouille^{10,21}, M. Gil Navidad^{19,10}, V. Foing¹⁰, B. Demir¹⁰, G. Reibaldi²⁰, J. Mankins²⁰, S.Molony^{3,10,15}, D.Osioanu^{3,10,15}, S. Ip-Jewell¹⁷, EuroMoonMars campaigns teams³, ¹ILEWG MDRS campaign teams (ESA ESTEC, NASA Ames, VU Amsterdam, GWU), ²EuroMoonMars-Intl MoonBase Alliance & HISEAs, ³ILEWG LUNEX EuroMoonMars, ⁴EuroSpaceHub, ⁵Leiden Observatory, ⁶ESA ESTEC, ⁷EMMPOL/AATC, ⁸Moon Gallery Foundation, ⁹IPSA, ¹⁰EuroSpaceHub Academy, ¹¹Politecnico Torino, ¹²EMM CHILL-ICE Iceland team, ¹³U of Atacama, Chile, ¹⁴U Padova, ¹⁵TU Dublin, ¹⁶DLR Institute of Mechatronics & ROBEX/ARCHES telerobotics Etna campaigns, ¹⁷Space Renaissance International, ¹⁸Fotonika U Latvia, ¹⁹ISU International Space University, ²⁰MVA Moon Village Association, ²¹ENS Ecole Normale Sup Paris-Saclay and HEC Hautes Etudes Commerciales (foing at strw.leidenuniv.nl)

Summary: We describe highlights from initiatives from ILEWG LUNEX EuroMoonMars, EuroSpaceHub Academy and partners contributing to Space and Planetary Research , Innovation , Astronautics and Entrepreneurship.

EuroMoonMars programme: EuroMoonMars is an ILEWG programme [1-229] in collaboration with space agencies, academia, universities and research institutions and industries. The programme includes research activities for data analysis, instruments tests and development, field tests in MoonMars analogue, pilot projects, training and hands-on workshops, technical visits and outreach activities (Fig.1). Extreme environments on Earth often provide similar terrain conditions to sites on the Moon and Mars. EuroMoonMars field campaigns have then been organised in specific locations of technical, scientific and exploration interest. Lunex EuroMoonMars, has been organizing in collaboration with ESA, NASA, European and US universities a programme of missions for students and researchers in different locations worldwide since 2009, including Hawaii HI-SEAs, Utah MDRS, Iceland, Etna/ Vulcano Italy, Atacama, AATC Poland, ESTEC Netherlands, Eifel Germany, etc... Over the course of these missions, students have access to special Space instrumentation, laboratories, Facilities, Science Operations, Human Robotic partnerships. In 2023 , EuroMoonMars and EuroSpaceHub Academy co-sponsored a series of EMMIHS missions at HI-SEAS Hawaii and EMMPOL Moonbase isolation simulation campaigns in Poland .

EuroSpaceHub programme for Space Innovation and Workforce Development: The EuroSpaceHub project to facilitate accessibility to the Aerospace sector. EuroSpaceHub is a European-led project with collaborators worldwide, funded by the EIT HEI initiative, led by EIT Manufacturing and EIT Raw Materials. The EIT HEI initiative - Innovation Capacity Building for Higher Education - is a key objective of the European Institute of Innovation and Technology as part of its Strategic Innovation Agenda 2021-2027. **ExoSpaceHab Xpress** (ESH-X) is an innovative portable lunar base simulator designed for education, analog missions and public outreach. This habitat has been funded by European consortium EuroSpaceHub and its partner LUNEX EuroMoonMars. After being exhibited at a conference and Padova Botanical Garden in Italy, ExoSpaceHab-X was invited in Sept-Oct at ENS Paris Saclay, and then installed from mid October at ESTEC SBIC and Leiden for further research and simulations.

Fig. 1 (left): Lectures and ESTEC visit for geology students of planetary science course organised by VUA/ EuroMoonMars. Fig.2 (right): ExoSpaceHab-Xpress Lunar Module developed by LUNEX EuroMoonMars for research training, astronautics simulations, business innovation & outreach

References:

[1-229]:

<https://ui.adsabs.harvard.edu/search/q=euromoonmars%20or%20eurogeomars%20or%20ilewg>

3. IS LUNAR WATER A RENEWABLE RESOURCE?

C. M. Pieters¹, ¹Brown University, Providence, RI, USA (carle_pieters@brown.edu)

Introduction: Based on a notably higher abundance of H observed at both poles of the Moon as early as 1998 [1], the lunar and planetary science community suspected that water exists in some form sequestered in cold, deeply shadowed areas at the lunar poles. A decade later in 2009, the surprising discovery was made by three independent spacecraft [2, 3, 4] that the lunar surface did indeed exhibit small amounts of hydration across its sunlit surface, with higher abundance found in the cooler regions at high latitudes.

Observations: Since then, the global data acquired by the Moon Mineralogy Mapper (M3) on Chandrayaan-1 over several lunations was shown to demonstrate that the degree of hydration varies with different time-of-day [5]. For any lunar surface area, local noon (with a relative higher surface temperature) exhibits the lowest hydration, but hydration returns as evening approaches and is not lost during the lunar night.

This cycle appears to repeat each lunar day. Lunar surficial hydration decreases from morning to noon but then is restored as cooler evening approaches. It is expected that solar wind H combines with oxygen of lunar surface materials to become the key source of lunar hydration, cycling on a diurnal basis. Surface hydration is temporarily lost as the surface becomes warmer but is also regained each lunar day.

Implications: In the future, it is worth contemplating how this lunar water might be ‘harvested’ during the lunar night and be replenished naturally during the lunar day.

[1] W. C. Feldman, S. Maurice, A. B. Binder, B. L. Barraclough, R. C. Elphic, D. J. Lawrence (1998) Fluxes of Fast and Epithermal Neutrons from Lunar Prospector: Evidence for Water Ice at the Lunar Poles, *Science* Vol 281, 1496-1500.

[2] C. M. Pieters, J. N. Goswami, R. N. Clark, M. Annadurai, J. Boardman, et al. (2009) Character and Spatial Distribution of OH/H₂O on the Surface of the Moon Seen by M3 on Chandrayaan-1, *Science* 326, 568-572.

[3] J. M. Sunshine, T. L. Farnham, L. M. Feaga, Olivier Groussin, Frédéric Merlin, et al. (2009) Temporal and Spatial Variability of Lunar Hydration as Observed by the Deep Impact Spacecraft, *Science* 326, 565-568.

[4] R. N. Clark (2009) Detection of Adsorbed Water and Hydroxyl on the Moon (2009) *Science* 326, 562-564.

[5] C. Wöhler, A. Grumpe, A. A. Berezhnoy, V. V. Shevchenko (2017) Time-of-day-dependent global distribution of lunar surficial water/hydroxyl, *Science Advances* 2017;3: e1701286 1-10.

4. DO GIANT IMPACTS KICKSTART ROCKY PLANET HABITABILITY?

R. Brasser¹

¹Konkoly Observatory; Budapest, Hungary (rbrasser@konkoly.hu)

Introduction: Earth is the only inhabited planet that we know of. Modern life has adapted to an oxygen-rich and therefore oxidising atmosphere, which is produced by photosynthesis that produces oxygen and sugars from carbon dioxide and water. Yet terrestrial-type life may have begun in an RNA-first world that would have benefitted from a strongly reducing environment¹. The gases emitted from Earth's volcanoes are predominantly oxidised, which presents us with a paradox as to how ancient life may have started under the current atmospheric conditions. On Earth life may have begun about 4.36 billion years ago¹ in the aftermath of a colossal impact with a lunar-sized object some 4.48 billion years ago² that produced a temporary hydrogen atmosphere due to the reaction of the impactor's metal core with terrestrial surface water³. This atmosphere provided the strongly reducing environment that created the pre-biotic molecules that may have been suitable to begin life. Since a rocky planet's mantle oxidation state is somewhat dependent on its mass, the question arises whether colossal impacts facilitate the kickstarting of origins of life on planets whose masses are in excess of 0.5 Earth mass, on what timescale and with what frequency these impacts take place.

Methods: We ran numerical N-body simulations of exoplanet formation around low-mass stars (M8 to K5) to establish the frequency and timing of large impacts in such systems. All simulations were run with the N-body integrator GENGA on A100 graphics cards⁴.

Results: We find that the frequency of planet-planet collisions decreases monotonically until about 15 Myr of simulation time, after which most systems have settled into a quasi-stable state. This is much earlier than in the terrestrial planet region of the solar system. Since crust formation on Mars did not start until about 20 Myr in the history of the solar system⁵, it is plausible that most large collisions in systems of close-in rocky exoplanets in the habitable zone of low-mass stars are over before they have begun to form a crust. In that case rocky planets in the habitable zone of more massive stars could be preferred to kickstart origins of life.

References:

- [1] Benner, S. A. et al. (2020). *ChemSystemsChem* 2, e1900035. [2] Brasser, R. et al. (2016). *Earth & Planetary Science Letters* 455, 85-93. [3] Genda, H. et al. (2017). *Earth & Planetary Science Letters* 480, 25-32. [4] Grimm, S. & Stadel, J. (2014). *The Astrophysical Journal* 796, A23. [5] Bouvier, L. C. et al. (2018). *Nature* 558, 586–589.

5. The Legacy of Extreme Precision Radial Velocity (EPRV) at PRL

Abhijit Chakraborty¹, Kapil Kumar Bhardwaj¹, Neelam Prasad¹, Kevi Kumar Lad¹, Rishikesh Sharma¹, Ashirbad Nayak¹ and Nikita Jitendran¹

¹Physical Research Laboratory Navarangpura, Ahmedabad 380009, email: abhijit@prl.res.in,
achak966@gmail.com

At PRL we initiated in the study of exoplanets detections and characterizations using EPRV about a decade ago. This was a pioneering research work for the first time in the country (India). At PRL we designed and developed the high-resolution optical fiber-fed stabilized spectrograph called **PRL Advanced Radial-velocity Abu-sky Search (PARAS-1)**^{1,2} and is coupled to the PRL 1.2m telescope. PARAS-1 works at a resolution of ~ 65000 under temperature stability of $\pm 0.005^\circ\text{C}$ at 25°C and under vacuum. It became operational for science observations in 2013 and demonstrated 3 to 5m/s RV precision and discovered three exoplanets namely: K2-236b³, TOI1789b⁴ and TOI4603b⁵ and as well as did other sciences. Subsequently, at PRL we began developing PARAS-2⁶ with a resolution of $\sim 110,000$ and a precision of sub-1m/s for the PRL 2.5m telescope. PARAS-2 being the highest resolution optical astronomical stabilized spectrograph in India will enable detections of super-Earths (4 to 10 earth mass planets). PARAS-2 began observations from January 2023 and has already demonstrated sub-1m/s (20cm/s to 50cm/s) radial velocity precision in terms instrument precision. PARAS-2 basic optics design, instrument performance, and on-sky performance will be presented. Also a few new interesting science results on TESS candidates will be discussed.

References:

- [1] Chakraborty, Abhijit; Mahadevan, Suvrath; Roy, Arpita*; Dixit, Vaibhav*; Richardson, Eric Harvey; Dongre, Varun*; Pathan, F. M.*; Chaturvedi, Priyanka*; Shah, Vishal; Ubale, Girish P.; Anandarao, B. G, 2014, "The PRL Stabilized High- Resolution Echelle Fiber-fed Spectrograph: Instrument Description and First Radial Velocity Results", *PASP*, 126, 133-147
- [2] Fischer, Debra A.; Anglada-Escude, Guillem; Arriagada, Pamela; Baluev, Roman V.; Bean, Jacob L.; Bouchy, Francois; Buchhave, Lars A.; Carroll, Thorsten; Chakraborty, Abhijit; Crepp, Justin R.; and 46 coauthors, 2016, "State of the Field: Extreme Precision Radial Velocities", *PASP*, 128, 066001
- [3] Chakraborty, Abhijit; Roy, Arpita*; Sharma, Rishikesh*; Mahadevan, Suvrath; Chaturvedi, Priyanka*; Prasad, Neelam J. S. S. V.*; Anandarao, B. G. 2018AJ....156,3C; Evidence of a Sub-Saturn around EPIC 211945201
- [4] Khandelwal, Akanksha*; Chaturvedi, Priyanka*; Chakraborty, Abhijit; Sharma, Rishikesh*; Guenther, Eike W. ; Persson, Carina M. ; Fridlund, Malcolm; Hatzes, Artie P.; Prasad, Neelam J. S. S. V.*; Esposito, Massimiliano; Chamarthi, Sireesha; Nayak, Ashirbad*; Dishendra*; Howell, Steve B., Discovery of an inflated hot Jupiter around a slightly evolved star TOI-1789; 2022 MNRAS. 509. 3339K
- [5] Khandelwal, Akanksha*; Sharma, Rishikesh*; Chakraborty, Abhijit; Chaturvedi, Priyanka*; Ulmer-Moll, Solène; Ciardi, David R.; Boyle, Andrew W.; Baliwal, Sanjay*; Bieryla, Allyson; Latham, David W.; Prasad, Neelam J. S. S. V.*; Nayak, Ashirbad*; Lendl, Monika; Mordasini, Christoph, 2023, Discovery of a massive giant planet with extreme density around the sub-giant star TOI-4603, 2023, *Astron. & Astrophys.*, 672, L7
- [6] Chakraborty, Abhijit; Thapa, Nitesh; Kumar, Kapil; Neelam, Prasad J. S. S. V.; Sharma, Rishikesh; Roy, Arpita; PARAS-2 precision radial velocimeter: optical and mechanical design of a fiber-fed high resolution spectrograph under vacuum and temperature control; 2018SPIE10702E..6GC [SEP]

6. Ionosphere - thermosphere investigations of Planet Earth

D. Pallamraju¹, D. Chakrabarty¹, R. P. Singh¹, M. Shanmugam¹, T. K. Pant², S. Thampi², C. Vineeth², S. Sarkhel³, S. Narendranath⁴ and DISHA team

¹Physical Research Laboratory, Navrangpura, Ahmedabad (raju@prl.res.in); ²Space Physics Laboratory, VSSC, Trivandrum; ³Indian Institute of Technology, Roorkee; ⁴UR Rao Satellite Centre, Bangalore

The sun emits radiation, magnetic fields, and particles. This radiation interacts with the planetary atmospheres to produce ionosphere. The solar magnetic field embedded in the particles of solar origin interacts with the geomagnetic field of the planetary body to cause space weather effects on the planetary atmosphere. Earth is a planet with active geo-dynamo and thus its interaction with the interplanetary magnetic field of solar wind origin gives rise to geomagnetic disturbances wherein currents are generated in the ionosphere and neutral waves and winds are generated in the thermosphere. The ionosphere and thermosphere of the Earth acts as a system, as they share the same volume, i.e., the dynamics of neutrals species are communicated to the plasma and vice-versa. The existence of geomagnetic field lines in the earth's upper atmosphere makes the ionosphere a birefringent medium and so the motion of ionospheric plasma along and across the magnetic fields are different in different directions. Therefore, under the influence of differential heating of the neutrals in the thermosphere, which is both location and time dependent, several processes are engendered. The ionosphere-thermosphere region of the earth extends from about 60 – 1000 km and gets influenced directly by the forcing of solar origin. This is the region which is adversely affected due to the incidence of solar flares, coronal mass ejections, interplanetary electric and magnetic fields, etc. Incidentally, this is also the region where most of the Low Earth Orbiting (LEO) satellites that cater to the societal applications are present. As a consequence, these space weather effects not only do various plasma-neutral phenomenon are engendered, but also several of the societal applications do get adversely affected. The Earth's ionosphere-thermosphere regions do get affected not only due to the forcing from above, but also to the lower atmospheric forcing of planetary waves and gravity waves from below. In order to investigate the nature, properties, behavior of the solar-terrestrial interactions during both geomagnetic storm, sub-storm and quiet times, a space mission has been conceived by the Indian Space Research Organization. The proposed mission is called, the Disturbed and quiet time Ionosphere-thermosphere System at High Altitudes (DISHA), will address fundamental science questions to understand the upper atmospheric processes that are present at different latitudes/longitudes as a function of time, season and solar flux conditions. DISHA mission is proposed to be a dual satellite mission with both high and low inclination angles orbiting for a common duration. DISHA mission will yield critical information on the space weather effects. In addition to addressing fundamental science questions of upper atmospheric interest, the DISHA mission will help in a better description of the influence of varying conditions of space weather on space based technological systems and sub-systems. With a continued increase in space missions and a growing requirement of placing satellites in LEO, which is within the ionosphere thermosphere region, it is right time that systematic satellite borne studies are carried out to characterize this region on a global scale. The proposed measurements of DISHA mission are electron densities, plasma waves of different scale sizes, major ion densities, ion drifts, ion temperatures, electron temperatures, neutral densities, and airglow emissions in X-ray and visible wavelength regions. The DISHA mission will not only address the understanding of the ionosphere-thermosphere regions of the planet Earth, but will also help in the scientific understanding of processes of other planets.

7. EXPOSED ROCK FRAGMENTS ENCOUNTERED BY PRAGYAN ROVER AT THE LANDING SITE OF CHANDRAYAAN-3 MISSION.

R. K. Sinha^{1*}, S. Vijayan¹, J. Laha², A. Maji², A. K. Prashar³, K. V. Iyer³, Amitabh³, N. P. S. Mithun¹, A. Patel¹, S. Vadawale¹, M. Shanmugam¹, N. Srivastava¹, A. D. Shukla¹, A. Basu Sarbadhikari¹, K. Suresh³, A. Suhail³, A. Medha³, S. Verma³, Anil Bhardwaj¹

(¹Physical Research Laboratory, Ahmedabad, India rishitosh@prl.res.in, ²Laboratory For Electro Optics Systems, Indian Space Research Organisation, Bengaluru, India, ³Space Applications Centre, Indian Space Research Organisation, Ahmedabad, India)

On 23 August 2023, India became the first nation to successfully land a mission in the southern high-latitude region of the Moon. The Vikram lander of the Chandrayaan-3 mission landed at 69.37° S, 32.32° E (within the

~3.9 Ga old Nectarian plains region), which is located between the Manzinus and Boguslawsky craters. The Pragyan rover of the Chandrayaan-3 mission, deployed and commanded by Vikram lander, moved about 103 meters on the lunar surface within a single lunar day. During the traverse, the Pragyan rover encountered small rock fragments (~1–11.5 cm) distributed around the rim, wall slopes, and floor of small craters (diameter ≤ 2 m) at the southern high-latitude landing site. The number and size of rock fragments increased when the Pragyan rover navigated ~39 m toward the west of the landing site. A plausible source for the encountered rock fragments could be a ~10 m diameter crater (western crater). We propose that this crater excavated and redistributed the rock fragments around the west of the landing site, which was buried several times by the lunar regolith overturning mechanism, and eventually exposed by the small craters encountered by the Pragyan rover. Two of the rock fragments indicated evidence of degradation, implying that they have been subjected to space weathering. These results support the previous studies that suggested gradual coarsening of rock fragments in the interior of lunar regolith.

8. SOME NEW INSIGHTS ON THE CHARACTERISTIC FEATURES OF THE LUNAR IONOSPHERE USING DFRS AND TWO-WAY OLR MEASUREMENTS FROM CHANDRAYAAN-2.

R. K. Choudhary¹, Keshav R. Tripathi, and K. M. Ambili¹, ¹ Space Physics Laboratory, VSSC, ISRO, Trivandrum – 695022, India; e-mail : rajkumar.choudhary@gmail.com

Introduction: Previous lunar missions, such as Luna-19, 20, SELENE, and Chandrayaan-1, have shown the presence of a plasma population in the lunar exosphere of the order varying from a few tens to hundreds per cc [1, 2, 3]. These observations highlight that electron density peaks at the lunar surface and decreases with altitude, up to 50 km above the lunar surface. However, the electron density profiles in the lunar ionosphere have been sporadically measured, providing insufficient data to unveil the temporal and spatial evolution of the lunar ionosphere. In this study, we have used measurements from the Dual Frequency Radio Science (DFRS) payload on board the Chandrayaan-2 orbiter to study temporal and spatial variations in the Lunar ionosphere. Regular radio occultation measurements are being conducted using two coherent radio signals of DFRS. These signals are generated by a highly stable crystal oscillator, the Evacuated Miniaturized Crystal Oscillator (EMXO), having a stability of 10-12 Hz/Hz over a 0.1-second integration time [4]. In addition, experiments are being conducted in two-way mode too in which X-band radio signals (~ 8.4 GHz), duly stabilized by ground-based MASER, are used in occultation mode to study the Lunar ionosphere.

Results : DFRS measurements have shown that the ionosphere in the lunar wake region could be much higher compared to the dayside [5]. Notably, the results demonstrated a substantial electron density near the lunar polar regions during the solar transition period. These observations are distinctive as they indicate post-sunset enhancements in the integrated electron density, contrary to findings from earlier missions. Furthermore, these results validate recent predictions from a theoretical model for the lunar ionosphere [6], providing novel insights into the lunar plasma environment. Further investigations using two-way Open Loop Receiver (OLR) data, conducted when the Moon was located within Earth's geotail, reveal an exceptionally active nature of plasma density in the lunar ionosphere. The temporal and spatial variations in lunar plasma, spanning from the equator to the pole, as observed by Chandrayaan-2 under varying solar conditions, will be discussed in detail .

References: [1] Vyshlov, A. S. (1976), Preliminary results of circumlunar plasma research by the Luna 22 spacecraft, *Space Res.*, 16, 945 – 949. [2] Imamura, T., et al. (2012), Radio occultation measurement of the electron density near the lunar surface using a subsatellite on the SELENE mission, *Journal of Geophysical Research: Space Physics*, 117(A6). [3] Choudhary, R. K., K. M. Ambili, S. Choudhury, M. B. Dhanya, and A. Bhardwaj (2016), On the origin of the ionosphere at the Moon using results from Chandrayaan-1 S band radio occultation experiment and a photochemical model, *Geophysical Research Letters*, 43(19), 10 – 025. [4] Choudhary, R.K., Bindu, K.R., Harshit, K., Karkara, R., Ambili, K.M., Pant, T.K., Shenoy, D., Kumar, C., Reddy, N., Rajendran, T.K. and Nazer, M., 2020. Dual Frequency Radio Science experiment onboard Chandrayaan-2: a radio occultation technique to study temporal and spatial variations in the surface-bound ionosphere of the Moon. *Current Science* (00113891), 118(2). [5] Tripathi,

K.R., Choudhary, R.K., Ambili, K.M., Bindu, K.R., Manikantan, R. and Parikh, U., 2022. A study on the characteristic features of the lunar ionosphere using Dual Frequency Radio Science (DFRS) experiment onboard Chandrayaan-2 orbiter. *Monthly Notices of the Royal Astronomical Society: Letters*. [6] Ambili, K.M. and Choudhary, R.K., 2022. Three-dimensional distribution of ions and electrons in the lunar ionosphere originated from the photochemical reactions. *Monthly Notices of the Royal Astronomical Society*, 510(3), pp.3291-330

9. Evolution of magma sources revealed by the surface composition of the Mare on Moon

Shyama Narendranath K.C.¹, Netra S Pillai^{1,2} and Ramananda Chakrabarti², ¹U.R. Rao Satellite Centre, Indian Space Research Organisation, Bengaluru (netra@urisc.gov.in), ²Centre for Earth Sciences, Indian Institute of Science, Bengaluru.

Introduction: Moon has a long history of volcanism from ~4 Ga to as young as 1.2 Ga [1] which led to the formation of the mare regions. Thermal evolution of the magma sources affects the composition of the erupted material thereby resulting in wide ranges in observed elemental abundances of the surface regolith. Samples collected by Chang'e 5 from Oceanus Procellarum have confirmed the occurrence of young volcanism [2]. Being one of the largest mare basins on Moon, Oceanus Procellarum is suspected to have a history of possible multiple episodes of eruption and therefore is a good location to study the evolution of the source. Gravity anomalies over this region also indicate the complexity of the sub-surface structures underlying this region, having major implications in understanding the impact and volcanic history of Moon [3].

Methods: Chandrayaan-2 Large Area Soft X-ray Spectrometer (CLASS) measures the elemental abundances of major elements present in the lunar regolith at the largest coverage and best possible spatial resolution till date [4]. We use the global maps prepared by CLASS [5] to study the heterogeneity in composition over Oceanus Procellarum. Magnesium number ($Mg/(Mg+Fe)$) provides clues to the temperature conditions at which the magma was extracted and hence we study its relationship to the age determined from crater counting chronology.

Results: We observe a large range in Mg number (20-50) over Oceanus Procellarum with typically higher values in the Western part compared to the Eastern part. Correlating to the age estimates reveal the systematic trend where older portions have higher Mg number due to its extraction at higher temperatures. The wider range in the Mg number values for eruptions with similar ages indicate heterogeneity in the same source or the possibility of multiple sources.

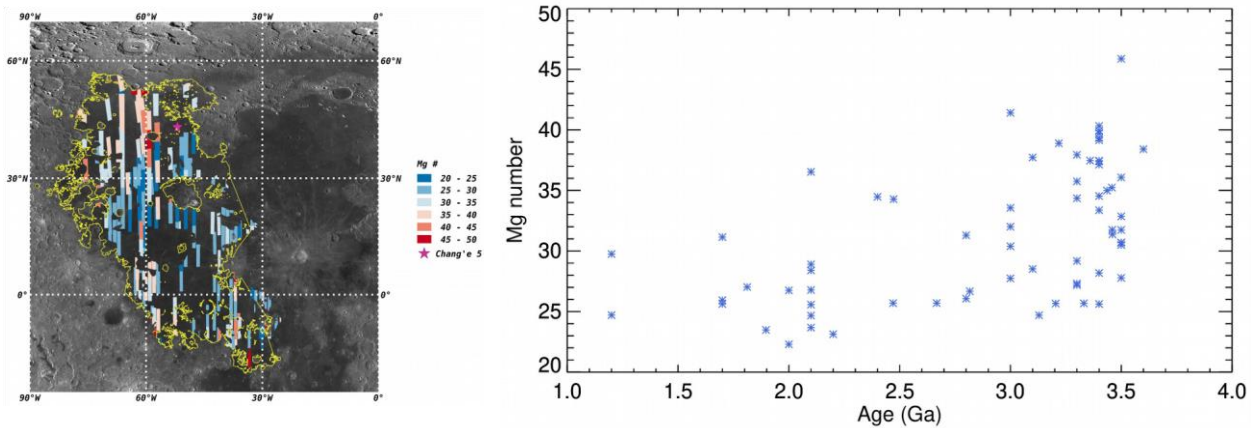


Figure: (Left) Mg number measured by CLASS. (Right) Relationship between age and Mg number showing the increasing value for older regions

References: [1] Hiesinger H. et al. (2011) Recent advances and current research issues in lunar stratigraphy, 477, 1-51. [2] Che X. et al. (2021) Science, 374, 887-890. [3] Deutsch A.N. et al (2019) Icarus, 331, 192-208. [4] Vatedka R. et al. (2020) Current Science, 118, 219. [5] Narendranath S. et al. (2024) Icarus, 410

10. All you need are spectra – with SIR-2 from Earth to the Moon and back

Urs Mall

Max-Planck Institute for Solar System research

The surfaces of planetary bodies reflect their evolution through primary surface shaping via their continuous evolution over time. Surface formation and degradation processes need to be understood in detail to infer the timescales over which these processes operate.

The Moon, with its lack of atmosphere, low seismicity and simpler mineralogical composition is a unique laboratory to investigate some of the processes which shape the surface of rocky planets over time.

Fifteen years after Chandrayaan-1, we look back on how VIS-NIR data from India's first mission to the Moon has opened a new window into planetary science. We show with an example of how Chandrayaan-1's data is currently used in concert with data provided by ongoing missions to shed light on open questions in planetary science by looking at large clasts, referred to usually as boulders, which have been recognized as a major surface feature on solid planets and small bodies, including asteroids and comets. Interest in these clasts range from practical applications relevant for landing site selection to characterization of geomechanical parameters of the soil on which they rest, to an understanding of their size frequency distributions relevant for an understanding of the processes leading to their formation and their erosion, and the mass wasting processes involved.

11. Revolutionizing Our Understanding: Scientific Milestones from Sample Return Missions

K. K. Marhas

Physical Research Laboratory, Ahmedabad.

Space missions have brought about surprising and new understanding of the cosmos. The planetary missions since 1960's have set in stones of evidences on origin and evolution, hitherto unimagined. Various sample return missions have brought extra-terrestrial materials from various chosen 'Type' celestial bodies within our Solar system that often gave not only novel but contrarian evidences of then prevalent understanding and knowledge. Starting from 1970s, various attempts of sample returns of lunar rock and soil samples (382 kilograms, Apollo mission 11th to 17th) led to explanation of the complex history of impacts, volcanism, and surface processes on Moon. The major result from Apollo mission, which vouched for "giant impact hypothesis" were based on results that the isotopic compositions of certain major elements were remarkably similar to those of Earth (suggesting a common origin). Apart from this, age differences obtained from samples from Lunar Mare and highlands and low amounts of water (~20 ppm) & volatile elements (potassium, rubidium, and phosphorus) in the basalts suggested that they originated from a mantle source, consistent with the aftermath of a giant impact. In fact, analysis of these Apollo samples indicated giant impact was followed by extensive volcanic activity. Whereas, Luna mission (~1969-76, sample retrieval 326 gms) revealed that the Moon's surface was extremely dry, with only trace amounts of water and volatile elements challenging theories of lunar pole ice, labelling moon as 'bone dry'. After ~45 years, lunar soil was again brought back by Change 5 (2020, amount 1.731kg), though from different region. One of the interesting results from Change 5 has been the abundance of water of ~170 ppm which is consistent with that result reported by the Moon Mineralogy Mapper (remote observation), Chandrayan-1.

After 1970s, 'Genesis' mission in 2004 brought back extra-terrestrial samples and provided the first 'direct' measurements of the elemental and isotopic composition of the solar wind, which consists of charged particles (ions) emitted by the Sun. The isotopic ratios of elements such as Oxygen, Nitrogen, and noble gases in the solar wind samples and by inference of the Sun, gave important insights into the composition of the early solar nebula from which the solar system formed.

A series of sample return projects were and are lined up since then. First one, being 'Stardust' mission, that returned ~4.8 gms of cometary dust in 2006 (Comet Wild 2). The study identified various organic compounds, including amino acids, which are the building blocks of proteins. In addition, stardust analyses heavily favoured 'X-wind model' with finding of CAI type material mixed with low temperature matrix minerals suggesting an amalgamation of inner and outer solar system material.

Sample return mission from Moon to Comet had a long time gap, but a jump to asteroid sample returns were quick. Starting with Hayabusa returning in 2010 from stony asteroid 25143 Itokawa (<1 mg) followed by Carbonaceous asteroid sample returns from 162173 Ryugu asteroid (5.4 gms, Hayabusa-2 in year 2020) and 101955 Bennu asteroid (250 gms, OSIRIS-REx in year 2023). Hayabusa-2 supported 'migration theory' of planets, based on oxygen isotopic compositions, which indicate they differ slightly from those found in meteorites from the inner solar system. While subtle, this discrepancy could be interpreted as evidence for formation in a distinct region. In addition, organic inventories (0.1 wt %) found on this stony asteroid also challenges the long-held assumption that organic molecules could only have formed under specific conditions. The latest sample returns from carbonaceous asteroids (Ryugu) indicates large abundance of organic molecules (~22 wt. %). Ryugu fragments contained more Carbon, Hydrogen and Nitrogen than any other known carbonaceous chondrite asteroids. Crystals found in the samples contain a lot of water indicating its parent asteroid formation beyond the CO₂ and H₂O snowlines. In nutshell, a few grains of materials returned to Earth have churned ocean worth of knowledge, understanding, and set new 'Rosetta stone' paradigms.

12. Solar X-ray Monitor (XSM) onboard Chandrayaan-2

S. V. Vadawale¹, N. P. S. Mithun¹, M. Shanmugam¹, A. R. Patel¹, H. L. Adalja¹, T. Ladiya¹, S. K. Goyal¹, C. S. Vaishnav¹, B. Saiguhan¹, A. Sarkar¹, A. Bhardwaj¹,

¹Physical Research Laboratory, Navarangpura, Ahmedabad – 380058, Gujarat, India.

The Solar X-ray Monitor (XSM) payload onboard the Chandrayaan-2 orbiter, along with the companion payload CLASS, forms the remote X-ray Fluorescence X-ray spectroscopy experiment with the main scientific objective of generating global maps of the abundance of major elements on the lunar surface. The XSM provides simultaneous measurement of the incident solar X-ray spectrum, which is essential to quantitatively interpret the X-ray spectra of the lunar surface measured by CLASS. For this purpose, XSM employs a state-of-the-art Silicon Drift Detector (SDD) along with an innovative instrument design, which provides consistent X-ray spectral measurements covering the extremely large range of solar X-ray intensity with an unprecedented cadence of one second. Such measurements are also highly useful to understand a variety of solar phenomena. The XSM has been operational in the lunar orbit for the past four and half years and has been providing excellent quality X-ray spectroscopic observations of the Sun. This presentation will highlight the unique features of the XSM, provide an overview of the solar X-ray observations, and discuss some of the significant scientific results obtained using XSM observations so far.

13. In-flight performance and initial results from Plasma Analyser Package for Aditya (PAPA) payload onboard Aditya-L1 mission

R. Satheesh Thampi¹, M B Dhanya¹, Mathin Chemukula Yadav¹, Aneesh A.N¹, Ankush Bhaskar¹, Govind G Nampoothiri¹, Pritesh Meshram¹, A K Abdul Samad², G Subha Varier², G Sajitha², Sundar B³, Sheeja Mathews², Pradeep Kumar P², Amarnath Nandi⁴, Ullekh Pandey³, Neha Naik², Sabooj Ray², Vijay Kumar Sen⁴, Shishir Kumar S Chandra², Ganesh Varma², R Manoj³, Akash J. B⁴, Dersana Sasidharan², Rosmy John², Tincy M Wilson² and Naresh S².

1. *Space Physics Laboratory, Vikram Sarabhai Space Centre (VSSC), Thiruvananthapuram ,Kerala, India, satheesh_thampi@vssc.gov.in*, 2. *Avionics entity, Vikram Sarabhai Space Centre (VSSC), Thiruvananthapuram, Kerala, India*, 3. *Aeronautics entity, Vikram Sarabhai Space Centre (VSSC), Thiruvananthapuram, Kerala, India*, 4. *Electronics systems and actuators entity, Vikram Sarabhai Space Centre (VSSC), Thiruvananthapuram, Kerala, India*

Aditya-L1 mission is the first space based observatory from ISRO for exploring the Sun, which will make the comprehensive measurement of radiation, particles and magnetic field using seven state-of the art scientific payloads [1] onboard. Plasma Analyser Package for Aditya (PAPA) payload is one among the seven payloads onboard Aditya-L1 spacecraft aims at studying the composition of solar wind and its energy distribution (in the range from 0.01 - 3 keV for electrons and 0.01 to 25 keV for ions) continuously throughout the mission's lifetime. PAPA contains two sensors; Solar Wind Electron Energy Probe (SWEEP) to measure the solar wind electron flux and Solar Wind Ion Composition AnalyseR (SWICAR) to measure the ion flux and composition as a function of direction and energy. SWEEP will measure only electron parameters whereas SWICAR has two modes of operation – ion mode where ion parameters are measured and electron mode where electron parameters are measured and is synchronized with SWEEP electron observations. These two modes in SWICAR are mutually exclusive. All the three modes of PAPA payload were exercised in the commissioning phase of payload operation that collected the electron/ion data continuously during the cruise phase from 11th December 2023 onwards as well as after the halo orbit insertion around L1 point which occurred on 06th January 2024. Here we present the in-flight performance of both sensors of PAPA payload and the and the initial results showing the response to the transient event/s as well as its comparison with the observations made by similar instruments onboard the already existing spacecrafts which are at or near L1 point.

References:

[1] P. Janardhan, Santosh Vadawale , Bhas Bapat , K. P. Subramanian , D. Chakrabarty , Prashant Kumar , Aveek Sarkar, Nandita Srivastava, R. Satheesh Thampi , Vipin K. Yadav , M. B. Dhanya , Govind G. Nampoothiri , J. K. Abhishek, Anil Bhardwaj and K. Subhalakshmi (2017), *Current Science*, 113, 620– 624, doi: 10.18520/cs/v113/i04/620-624

14. FLUXGATE MAGNETOMETER ONBOARD ADITYA-L1 SPACECRAFT: THE JOURNEY SO FAR

Vipin K. Yadav¹, Y. Vijaya², B. Krishnam Prasad², Srikar P.T.³, Monika Mahajan², K.V.L.N. Mallikarjun², Syeeda N. Zamani², M.M. Kandpal², S. Narendra³, Abhijit A. Adoni³, Vijay S. Rai³, Veerasha D.R.³, Nandita Srivastava⁴, Geeta Vichare⁵

¹ Space Physics Laboratory (SPL), Vikram Sarabhai Space Centre, Thiruvananthapuram 695022, India
Email: vipin_ky@vssc.gov.in ² Laboratory Electro-Optical Systems (LEOS), 1st Cross, 1st Phase, Peenya, Bengaluru 560058, India ³ U R Rao Satellite Centre (URSC), Old Airport Road, Vimanpura, Bengaluru 560017, India ⁴ Udaipur Solar Observatory, Physical Research Laboratory (USO-PRL), Badi Road, Dewali, Udaipur 313001, India ⁵ Indian Institute of Geomagnetism (IIGm), Near Kalamboli Highway, New Panvel, Navi Mumbai 410218, India

Abstract

Magnetic field measurements are routinely done in space onboard spacecraft in space or around a planetary body to understand the local magnetic environment with fluxgate magnetometers (FGMs) due to their high sensitivity in observing the interplanetary magnetic field (IMF) coming from the Sun towards the Earth. The first Lagrangian or Liberation (L1) point is an ideal location for this away from the Earth's magnetic environment.

The MAG payload onboard Aditya-L1 spacecraft is a dual set of tri-axial magnetic sensors mounted at the centre and at the extreme edge of a 6 m boom away from the spacecraft so as to eliminate the effect of spacecraft magnetic contamination when operating in the differential mode. The MAG payload is designed to measure 8 vectors per second during the operations and the MAG sensors are capable of observing ≈ 1 nT variation in the magnetic field variation above the noise in the range ± 256 nT, default operating range at the L1 point. The main science objectives of this MAG payload is to observe the Earth-directed coronal mass ejection (CME) as and when it passes through the L1 point; to study the effect of CMEs and co-rotating interaction regions (CIRs) and to observe the signatures of solar plasma waves at L1 point [1]. This will also enable us to record the passage of interplanetary shock, sheaths and magnetic clouds associated with CMEs.

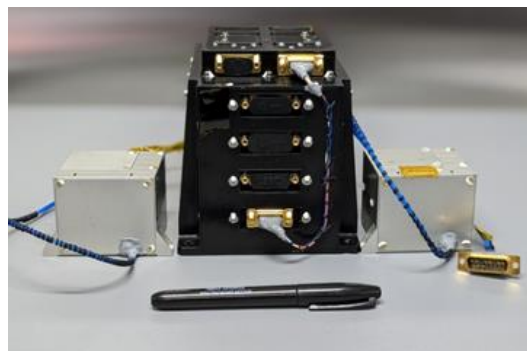


Figure: The Flight Model of MAG Payload

The Aditya-L1 mission was launched on September 02, 2023 and is now approaching the L1 point where it is going to be placed in a halo orbit to continuously monitor and study the Sun from there with seven instruments onboard. The MAG payload is switched ON, in the stowed condition, on October 16, 2023 and since then the payload performance is observed to be normal. The magnetic field data acquired so far is being analyzed to observe the signature of extreme solar events taken place so far.

References:

[1] Vipin K. Yadav, Nandita Srivastava, et al., (2018) *Advances in Space Research*, 61 (2):749–758

15. MINIATURE HIGH SENSITIVITY ACCELEROMETERS FOR PLANETARY SEISMIC ACTIVITY STUDIES

J John*, V Thamarai, Teena Choudhary, Ashwini Jambhalikar, M M Mehra, Mayank Garg, D Praveena, Gaurav Saxena, M N Srinivas, Shila K V, Krishna Kummari, Gogulapati Supriya, M S Giridhar, Kalpana Arvind, K V Sriram

Laboratory for Electro-Optics Systems (LEOS), ISRO, Peenya 1st Stage, 1st Cross, Bangalore 560058, India

*jjohn@leos.gov.in

Chandrayaan 3 is the first ever mission to land at the south polar region of the Moon. The Lander payload, Instrument for Lunar Seismic Activity studies (ILSA) had the objective of studying the seismicity at the landing site. After the seismic experiments carried out around fifty years ago at the lunar equatorial region by the Apollo missions, it is ILSA that has recorded seismic activities at Moon. The uniqueness of the instrument lies in the fact that it is for the first time an instrument based on relatively new silicon micro machining technology, also called Micro Electro Mechanical Systems (MEMS) technology is used in a lunar science experiment.

ILSA has been designed for recording ground accelerations and was deployed on the lunar surface. It had three orthogonally arranged high sensitivity accelerometers in it. ILSA was operated during the lunar day spanning over 24 August 2023 to 02 September 2023. The instrument has recorded several distinct events that caused ground vibrations of which the cause is known for many of them including the navigation of the rover and operation of science instruments involving mechanical activities. Some of the events are not correlated to any known activity. ILSA experiment proves that properly designed miniature high sensitivity accelerometers can function as very effective short period seismometers. This paper presents the approach in developing such instruments for seismic studies in planetary environment and ideas to further miniaturize them with enhanced performance parameters and lesser power consumption thereby laying a foundation for maximizing the possible scientific output.

16. LUNAR SWIRLS: FRESH INSIGHTS REVEALED BY GEOLOGICAL CONTEXT

Deepak Dhingra, Department of Earth Sciences, Indian Institute of Technology Kanpur, Kanpur, UP
208016, India.

(Email: deepdpes@gmail.com, ddhingra@iitk.ac.in)

Introduction: Lunar swirls remain one of the most enigmatic features which have been extensively studied and yet a thorough understanding of their origin and time of formation remains incomplete [1-6]. The key properties of swirls include their high albedo, curvilinear geometry, association with strong magnetic field and very surficial character. The latter indicates that they do not extend to any significant depth and appear to drape over the existing landscape. In addition, they have been shown to have weak hydration signatures (especially associated with the bright regions) due to shielding from the solar wind by the ambient magnetic field [7]. Recent work has also suggested some topographic association with swirls [8].

We are characterizing the geologic context of selected swirl occurrences utilizing imaging, spectral and topography data from multiple missions. The detailed evaluation of the swirls involves variability across the interface of the swirls and the surroundings, including any association with geological feature. We are also characterizing the variability within the swirl region in various parameters.

Early Results: Our work is revealing new insights about the association of swirls with their surrounding terrain. We have identified selected regions where swirl material seems to have been disturbed. This observation has important implications as swirls are nominally regarded as one of the youngest geomorphological features in the region of their occurrence which have not been subsequently modified. We are carrying out a detailed characterization of these regions and will present the obtained results.

References:

[1] Blewett, D. T. et al. 2011, *J. Geophys. Res. (Planets)*, 116, E02002. [2] Denevi, B. W. et al. 2016, *Icarus*, 273, 53. [3] Garrick-Bethell, I., Head, J. W., & Pieters, C. M. 2011, *Icarus*, 212, 480 [4] Glotch, T. D., Bandfield, J. L., Lucey, P. G., et al. 2015, *Nat. Commun.*, 6, 6189 [5] Bruck Syal, M., & Schultz, P. H. 2015, *Icarus*, 257, 194 [6] Bhatt et al. 2023 *A&A* 674, A82, <https://doi.org/10.1051/0004-6361/202245356> [7] Kramer G Y et al. 2011 *J. Geophys. Res.*, 116 E00G18. [8] John R. Weirich et al, 2023 *The Planetary Science Journal*. DOI: 10.3847/PSJ/ace2b8

17. A LUNAR SAMPLE RETURN MISSION

D. Banerjee, Physical Research Laboratory, Ahmedabad.

Introduction: Our views regarding the formation and evolution of the Moon were fundamentally changed after the Apollo and Luna sample return missions. Before Apollo landed on Moon, several theories were proposed for the origin of the moon: fission from earth, co-accretion with earth and capture by earth. We know now that the moon formed at around 4.5 billion years ago (Ga), as a result of a grazing collision of an impactor of the size of Mars with the early earth, and ejected material from the earth and impactor which accreted to form the Moon. Further the discovery of anorthosite, an igneous rock, in returned samples suggested that a large part of the Moon was likely to be molten, with the anorthositic crust being formed by flotation above the crystallizing magma. This is the widely accepted “magma ocean” model for early lunar differentiation. Here we discuss some science questions to be addressed in future sample return missions.

Late Heavy Bombardment: The lunar surface also provides a record of bombardment; indeed, radiometric ages of lunar samples suggest a spike in impact activity and that a “late heavy bombardment(LHB)” phase occurred around 3.9 Ga. It is also presumed that several large lunar basins on the nearside formed at this time due to a considerable increase in the influx rate of bombarding planetesimals. However, additional ages of lunar samples from new missions are necessary to determine whether the record of older impacts is reset by younger impacts, and whether Late Heavy Bombardment may signify the end of a diminishing rate of impact activity on Moon. The ~2 billion-year age reported for lunar basalts returned by Change-5 implies that the impact flux rate may have been lower than previous estimates based on youngest Apollo and Luna basalts, but requires confirmation from future studies.

KREEP-poor vs KREEP-rich origin of basalts: Radioisotope dating of basaltic samples returned by Apollo and Luna missions have revealed that basaltic magmatism occurred on the Moon between 4.4 Ga and 2.9 Ga. Pb-Pb ages of 2 Ga have been reported for basalt fragments returned by the Change-5 mission providing confirmation that lunar volcanism continued at least until 2 Ga. Additional radiometric ages are necessary from future missions to confirm this finding and to provide calibration points for ages determined using crater counting. Further, the source of the melt which formed the basalt was suggested to be a KREEP-poor source. Determination of new uranium, thorium and potassium in young KREEP-rich basalts from lander or rover platforms are necessary to determine whether these heat-producing elements are significantly higher in such samples in order to explain how a KREEP-poor source could result in extended volcanic activity on Moon. Models for thermal evolution of the Moon may need revision, and inclusion of a non-KREEP origin for the youngest basalts of the Procellarum KREEP Terrane.

Dating and Compositional Analyses: Radiometric dating of samples (impact melt, breccia) is necessary from a large lunar impact basin (e.g. South Pole Aitken, i.e., SPA) for an improved understanding of lunar stratigraphy. Age determination of samples from the lunar farside is important to understand compare the nature of volcanism on the nearside and the farside of the Moon. Further, the South Pole Aitken Basin is presumed to have excavated the lower crust and perhaps the upper mantle. Mafic compositions with higher Th, Fe values characterize the SPA floor, perhaps representing melt rocks from SPA event containing mixtures of pre-existing crust and mantle rocks. The possibility of KREEP in SPA, with implications regarding magma ocean hypothesis, cannot be ruled out until Th, K and REEs measurements are performed in-situ or on returned samples. Finally, the timing of the SPA events is not precisely known and is only constrained by the Imbrium impact event at 3.9 Ga. A sample return mission from the South Pole Aitken basin would significantly add to our present knowledge of the lunar interior and its early evolution history.

18. INSIGHTS INTO HIGHLY SIDEROPHILE ELEMENT ABUNDANCE IN LUNAR CRUST AND MANTLE FROM METEORITES A-881757, Y 981031, Y 983885 and Y-86032: CONSTRAINTS ON REGIONS BEYOND THE PROCELLARUM KREEP TERRANE (PKT)

Y. Srivastava¹, A. Basu Sarbadhikari¹, J. M. D. Day², E. V. S. S. K. Babu³, T. Vijaya Kumar³ and A. Yamaguchi⁴ ¹Physical Research Laboratory, Ahmedabad 380009, India; ²Scripps Institution of Oceanography, University of California San Diego, CA 92093-0244, USA; ³National Geophysical Research Institute, Hyderabad, 500007 India, ⁴National Institute of Polar Research (NIPR), Tokyo 190-8518, Japan.

Introduction: Highly siderophile elements (HSE: Re, Os, Ir, Ru, Rh, Pt, Pd, and Au) are important tracers for the understanding of the formation and accretion history of the Moon (e.g., [1, 2]). Most of our present understanding of the lunar highly siderophile elements is biased by the samples from the PKT (Apollo 12, 14, 15, Chang'E 5) and its adjacent (Apollo 11, 16, 17, Luna 16, 20 and 24) regions, having a relatively high abundance of incompatible trace elements. It is therefore important to better constrain the abundance of highly siderophile elements of the lunar mantle and crust using the samples from the non-PKT regions. In this study, the abundance of the HSE in the lunar mantle and crust is targeted using lunar meteorites A-881757, Y 981031, Y 983885 and Y-86032.

Methods: Back-scattered electron imaging, X-ray mapping and mineral chemical analysis were carried out using an electron probe microanalyzer. In-situ trace element composition of mineral clasts was measured using LAICPMS. The bulk major and trace element analyses were performed on the powdered bulk rock using an ICPMS. Highly siderophile elements and Os isotopes were measured by digesting the remaining sample powder with appropriate amounts of reagent and isotopically enriched spikes in Carius tubes. Osmium isotope dilution (ID) concentration and isotopic composition was analyzed by N-TIMS while the remaining HSE were analyzed for ID concentrations by ICP-MS (e.g., [3]).

Results and Discussion: Composition of metal grains. Nickel/cobalt of metal grains can record the effect of impact contamination as most plausible impactors (chondrites and iron meteorites) have relatively high Ni/Co [4]. The average measured Ni/Co of metals in A-881757 is 3.6 for Type-I and 0.3 for Type-II. The average Ni/Co of metals in MET 01210 is ~23.6, indicative of exogenous input of chondritic materials [4]. The measured Ni/Co for A-881757 metal grains indicate that they are pristine, free from impactor contamination and, therefore, can be used to estimate BSM HSE contents in non-PKT regions. Metal grains in regolith breccias Y 981031 and Y 983885 show 10.40 ± 1.53 (n=6) and 11.70 ± 2.84 (n=20) Ni/Co, respectively. This value is similar to Ni/Co of metal grains present in Apollo 16 impact melt breccias (~ 11.6) but lower than value observed in lunar breccia meteorite MET 01210 and PCA 02007 (~27) [4]. The intermediate Ni/Co of Apollo 16 impact melt breccias has been interpreted as signature of mixing between low Ni/Co endogenous component and high Ni/Co exogenous components [4].

HSE abundance and Re-Os isotopes. The HSE plot of A-881757 shows a fractionated pattern as seen in case of low-Mg mare basalt meteorites. The absolute and relative abundance of the HSE in A-881757 lies within the range of values observed for Apollo mare basalts [5]. The isotopic ratio $^{187}\text{Os}/^{188}\text{Os}$ of A-881757 (0.1247 ± 0.0003) is slightly sub-chondritic but within the error range of its paired counterpart MIL 05035 (0.1244 ± 0.0002). The studied regolith breccia meteorites have the HSE concentrations that range from approximately 0.01 to 0.1 times CI chondrite values and most data fall within the range of impact melt breccias, feldspathic granulites and fragmental matrix breccias [3 and references therein]. Among all the three studied samples, Y-86032 exhibit relatively flat HSE pattern while Y 981031 and Y 983885 display HSE fractionation pattern. Sample Y 981031 is enriched in Pt and Pd, while the sample Y 983885 is enriched in only Pd. Conclusively, the Re-Os isotope systematics and HSE abundance in A-881757 yield valuable insights into the abundance of these elements in the KREEP-free lunar mantle,

while the brecciated lunar meteorites offer constraints on the HSE abundance at the lunar crust. The inter-elemental HSE ratio of lunar regolith breccia Y-86032 implies late accretion of an ordinary chondrite-type impactor, while Y 981031 and Y 983885 show fractional crystallization and metal segregation within impact melt sheets, resembling the HSE enrichment observed in the terrestrial impact settings.

References: [1] Walker R. J. (2009) *Chemie der Erde* 69, 101–125. [2] Day J. M. D., et al., (2016). *Reviews in Mineralogy and Geochemistry* 81, 161–238. [3] McIntosh E. C., et al., (2020) *Geochimica et Cosmochimica Acta* 274, 192–210. [4] Day, J. M. D. (2020). *Meteoritics and Planetary Science*, 55(8), 1793-1807. [5] Day J. M. D., et al., (2007) *Science* 315, 217–219.

19. Magmatism Along the Eastern Limb of the Moon

Neha Panwar^{1,2}(neha@prl.res.in), Neeraj Srivastava¹, Megha Bhatt¹, Anil Bhardwaj¹

¹Planetary Remote Sensing Section, Planetary Sciences Division, Physical Research Laboratory, Ahmedabad 380009, India; ²Discipline of Earth Sciences, Indian Institute of Technology, Gandhinagar, India

The volcanism on the Moon is mainly confined to large-scale impact structures either occurring in the central portion of multi-ring basins as basin-filling volcanic deposits or in troughs concentric to the basin [1,2]. The eastern nearside farside boundary provides a unique window to study this relationship between the impact processes and magmatism on the Moon. The boundary acts as a zone of transition between the thinner nearside crust and the thicker farside crust hosting a unique style of volcanism. The basalts in this region are emplaced within Mare Australe (47.77°S, 91.99°E), Mare Marginis (13.3°N, 86.1°E) and pre-Nectarian Smythii Basin (1.3°N, 87.5°E). Results from the GRAIL data suggested the presence of an ~880 km impact basin in the northern part of the Mare Australe, identifying it as Australe North Basin (35.5°S, 96°E) [3] that displays visibly no topographic signatures. A large part of the Mare Australe basalts lies outside the proposed basin, i.e. Australe North. Late-stage volcanism at ~1.7 Ga has also been reported for the first time inside the Bowditch Crater within the Australe North Basin suggesting that even the ancient basins on the Moon can be hosts to recent volcanism [4]. Similarly, Mare Marginis hosts extensive volcanism within topographic low situated outside the partially infilled Smythii Basin. The results from Clementine mission showed that the basalts of Mare Smythii and Mare Marginis are compositionally similar in terms of their FeO weight percentage (wt.%) (15–17 wt.%) and TiO₂ wt.% (2.6–3.6 wt.%) suggesting a common source for these basalts [5]. However, our study showed that the basalts within Mare Marginis show a range of compositions [6]. It also highlights the role of the ancient structural discontinuities in causing volcanism in the region.

The presence of partially infilled basins and widespread volcanism outside the pre-Nectarian basins in the region provides an opportunity to look at the complex volcanic processes and the controls multi-ring basins exert on magmatism on the Moon. In the studies discussed above, we have carried out a detailed topographical, morphological, and mineralogical investigation of the North-eastern part of the proposed Australe North Basin and the basalts of Mare Marginis and Mare Smythii lying at the eastern nearside farside boundary of the Moon using remote sensing datasets to understand the processes responsible for lunar volcanism away from the KREEP.

References: [1] Head J. W. (1976) *Rev. Geophys.*, 14(2), 265–300. [2] Head J. W. and Wilson L. (1992) *Geochim. Cosmochim. Acta.*, 56(6), 2155–2175. [3] Neumann G. A. et al. (2015) *SciAdv.* 1(9), e1500852. [4] Panwar N. and Srivastava N. (2024) *Icarus*, 408, 115841. [5] Gillis J. J. and Spudis, P. D. (2000) *JGR Planets*, 105(E2), 4217–4233. [6] Panwar N. et al. (2023). *Icarus*, 395, 115496.

20. Integrated comparative study between lunar regional pyroclastic deposits

D. Misra^{1,2}, C. Wöhler³, N. Rai^{4,5}, and M. Bhatt¹.

¹Physical Research Laboratory, Ahmedabad-380009, India (dibyendu@prl.res.in) ² Indian Institute of Technology Gandhinagar, Gandhinagar-382055, India, ³ Image Analysis Group, TU Dortmund University, Otto-Hahn-Str. 4, 44227 Dortmund, Germany, ⁴Department of Earth Sciences, Indian Institute of Technology Roorkee, Roorkee-247667, India, ⁵Centre for Space Science and Technology, Indian Institute of Technology Roorkee, Roorkee-247667, India.

Lunar pyroclastic deposits (LPDs) are a distinctive lithological unit associated with volcanic features (e.g., rilles, vents, fractures, wrinkle ridges, etc.) and the dark mantle deposits (DMDs) within and around major mare-filled basins [1,2]. Pyroclasts in the form of partially crystallized Fe-Ti-bearing volcanic glass droplets [3] are a key to understanding the early lunar mantle composition [4]. These glasses have overlapping spectral characteristics with common major lunar minerals in the visible to near-infrared (VIS-NIR) wavelength range. Separation by remote sensing becomes feasible only when the mafic mixture contains over 70 wt.% of volcanic glass [5]. Based on the areal distribution, LPDs are broadly classified into regional (>1000 km²) and local deposits [6]. In order to systematically detect and study LPDs, a methodology is developed using the Moon Mineralogy Mapper (M³) global Moon coverage [7]. We will present a case study focusing on two extensively documented regional pyroclastic deposits located around the Aristarchus crater (23.7° N, 47.5° W) and the Sinus Aestuum region (12.1° N, 8.3° W). The detailed scientific analysis of LPDs at Aristarchus and Sinus Aestuum includes the integration of morphology, mineralogy, composition, and grain size variations within these deposits. Despite both DMDs being products of explosive volcanic eruptions during a similar period (~3.2-3.8 Ga) [8], we find differences in mineralogy and regolith grain sizes indicating different source regions at different depths. Our multidimensional approach of studying LPDs will further be applied on a global scale, with the goal of a better understanding of the links between explosive and effusive volcanism on the Moon.

References: [1] Head, J. W. (1974), LPSC, 5, 207-222. [2] Hawke et al. (1989), LPSC, 19, 255-268. [3] Delano, J. W. (1986), JGR: Solid Earth, 91 (B4), 201-213. [4] Gaddis et al. (1985), Icarus, 61 (3), 461-489. [5] Horgan et al. (2014), Icarus, 234, 132-154. [6] Gaddis et al. (2003), Icarus, 161(2), 262-280. [7] Green et al. (2011), JGR: Planets, 116 (E10). [8] Head III, J., and Wilson, L. (1979), LPSC, 10, 2861-2897.

21. EXPLORING FAN DEPOSITS ON MARS AND EARTH

S. Vijayan, Anil Chavan, Kimi KB

Planetary Sciences Division, Physical Research Laboratory, Ahmedabad, India, vijayan@prl.res.in

Fan deposits on Mars retain the record of ancient environments and prevailing climatic conditions, whereas Mid-latitude fans of the Hesperian-Amazonian period are of great interest as they may represent fluvial activity occurred in those regions. Fans on Mars generally found within the basins or craters which are linked with incised channels and alcove on the crater rim, and extensive fan deposits are reported. Whereas on Earth such large number of fan deposits are associated to mountain valleys. One such region on Earth, where large fan deposits associated is the Himalayan region. The Himalaya region is known for its vast high rise mountains with snow covers, and the seasonal changes over this region lead to significant snow melts, which feeds the valley and also a major source for sedimentary deposits all along the foothills. Alluvial fan deposits are a common stochastic depositional process that may account for the significant contribution of sediments produced in Himalaya mountain foothills. Determining how sedimentary deposit processes contribute to the evolution of the fan is complicated because some depositional or erosional are continuous, while others are stochastic. The alluvial fan and the deposition on Mars and Earth gather more recognition that they represent a continuum of depositional processes from small debris cones to characteristics of past environments. Several analogue locations are emerging recently for the Mars alluvial fan and sedimentary deposits, however, the nature of climatic condition prevailed, source and nature of deposits all need to be comparable to establish the most suitable analogue locations. In this regard, the Himalaya region which is semi-arid, snow deposits and seasonal melt, dearth of current precipitation, multiple mountain ranges providing sediment supply will be an apt location to explore and bring out more realizable analogue to Mars. This work explores the environmental conditions that prevailed in the mid-latitude of Mars near Eridania Basin, part of Terra Sirenum. This region is chosen because of their past large scale fluvial activities, followed by glacial activities. For the analogue location, a similar environment prevailed in the Ladakh region over the Himalayas. The analogue site provides an unprecedented focus on the cold period and their associated environments. Both the regions on Mars and Earth is known for its fluvial activities and cold, arid conditions. The current cold and arid conditions on Ladakh is similar to the past Martian environment. We examined several craters over the Terra Sirenum region and found their fan deposits associated to alcoves, degradation and mantling of ice deposits over the fan deposits, graben/fracture associated knobs with possible linkage to fluvial activity, mineralogical assemblage of these locations with CRISM. Interestingly, these mid-latitude landforms are glacial covered and draped by many recent glacial features. This work discusses the analogue deposits from Himalayan region to the Mars.

22. Evolution of Martian Volcanism and Lithosphere: Geochemical Insights from Noachian to Amazonian Volcanic Terrains

Alka Rani^{1,2*}, Amit Basu Sarbadhikari², Yash Srivastava², Lujendra Ojha³, Heidi Fuqua Haviland⁴ and Suniti Karunatillake⁵

¹NASA Post-doctoral Program Fellow, Marshall Space Flight Center, Huntsville, AL, USA (alka.rani@nasa.gov); ²Physical Research Laboratory, Navrangpura, Ahmedabad, India; ³Department of

Earth and Planetary Sciences, Rutgers University, Piscataway, NJ, USA; ⁴NASA Marshall Space Flight Center, Huntsville, AL, USA; and ⁵Department of Geology and Geophysics, Louisiana State University, Baton Rouge, LA, USA

Introduction: The lithosphere of Mars has played a crucial role in shaping its geological features, influencing volcanic activity, climate shifts, and the planet's early habitability. Understanding the evolution of Mars' lithosphere through different geological eons has been challenging due to weathering and resurfacing affecting the study of early Noachian volcanic chemistry. Therefore, in our study we have focused on recently discovered Noachian volcanic terranes [1-2], along with Hesperian and Amazonian volcanic terranes [3], to trace the evolution of the Martian lithosphere and thermal flux. The composition of igneous rock formed from the eruption of magma tends to preserve the record of thermal properties viz. pressure, temperature, or degree of partial melting at which it forms. Therefore, Martian volcanic provinces are of great geologic interest; they have been active throughout its history, from Noachian (>3.7 Ga) to the Late Amazonian (<500 Ma) [4]. Earlier studies focused on the evolved magmatism from Hesperian to Amazonian [4], but the type and style of Noachian-aged volcanism remain to be understood. We have investigated the geochemical compositions of Noachian volcanic provinces and compared them with relatively younger volcanic provinces on Mars using remote sensing (Mars Odyssey Gamma Ray and Neutron Spectrometer suite-GRS) and in-situ observations. Furthermore, petrologic modeling is performed to understand magmatic processes and thermal evolution.

Our findings reveal distinct Pressure-Temperature (P - T) conditions across different Martian geological eras. In the Noachian terranes, we model P - T conditions ranging from 1.3-1.6 GPa and temperatures between 1340-1360°C. Conversely, the Hesperian volcanic terrane exhibits variations between 1.6-1.7 GPa and temperatures spanning 1360-1365°C. For the Amazonian volcanic terrane, P - T conditions ranged notably higher, from 1.9-2.8 GPa with temperatures between 1415-1425°C. Based on our modeling, we estimated the corresponding lithospheric thicknesses and depths of melting for each eon. In the Noachian, the lithospheric thickness ranged from 125-145 km. Meanwhile, for the Hesperian terranes, it varied between 145-150 km, and for the Amazonian, it extended from 195-260 km. We also calculated partial melting percentages (F), observing a range of 8-12% for the Noachian, 10-11% for the Hesperian, and 10-12% for the Amazonian. Mantle potential temperatures (T_p) were calculated to illustrate variations across these geological eons. Our estimates of heat flux depicted temporal changes, showing ranges from 51-68 mW/m² for the Noachian, 43-45 mW/m² for the Hesperian, and 27-41 mW/m² for the Amazonian.

Our study implies that the lithosphere remained consistently uniform until the Hesperian eon, indicating sustained weaker volcanic systems from mid-Noachian to Hesperian. This contrasts with fewer deep-seated plumes observed in the Amazonian era. These variations suggest potential implications for Martian climatic conditions which show a milder climate prevailed until the Hesperian, differing from Mars' current cold, arid conditions.

References:

[1] Michalski J.R. and Bleacher J. E. (2013). Nature, 502, 47–52. [2] Rani A. et al., (2021). Journal of Geophysical Research: Planets. 126, e2020JE006748. [3] Tanaka et al., (2014). U.S. Geological Survey Geologic Investigations. [4] Baratoux D. et al., (2011). Nature, 472, 338–341.

23. Subsurface study of the Tharsis graben system using SHARAD data

Rajiv R. Bharti^{1,4}, Isaac B. Smith^{2,3}, Shital H Shukla⁴

1 . Physical Research Laboratory, Navrangpura, Ahmedabad, India 380009

2 . York University, Toronto, Ontario, Canada, M3J 1P3

3 . Planetary Science Institute, Lakewood, CO, USA 80401

4 . Gujarat University, Ahmedabad, India 380009

Mars' crust has an extensive graben system that covers a region more than 8,000 km in diameter and nearly one-third of the planet's circumference. Many of them trend radially outward from the Tharsis Montes. They are long-lived crucial features to determining the evolution of the tectonic and volcanic history of Mars. These thousands of grabens were discovered in the early 1970s and have been studied extensively with different hypotheses about their formation throughout the literature. These hypotheses include the formation process being either tectonic or a combination of tectonic and magmatic processes, but no consensus has been reached so far. For the first time, we explore the subsurface of narrow graben systems using SHARAD data to understand and support the formation hypothesis of the martian graben system. We found multiple subsurface reflections in a narrow range of time delay at the rim of Mangala Fossa and at the floor of Labeatis Fossa. The loss tangent of the subsurface unit is in the range of 0.009 to 0.03, consistent with low to moderate-density basalt. The presence of a basaltic subsurface unit at these locations confirms that magmatism is involved during the formation process of these two graben systems (<https://doi.org/10.1016/j.icarus.2023.115681>).

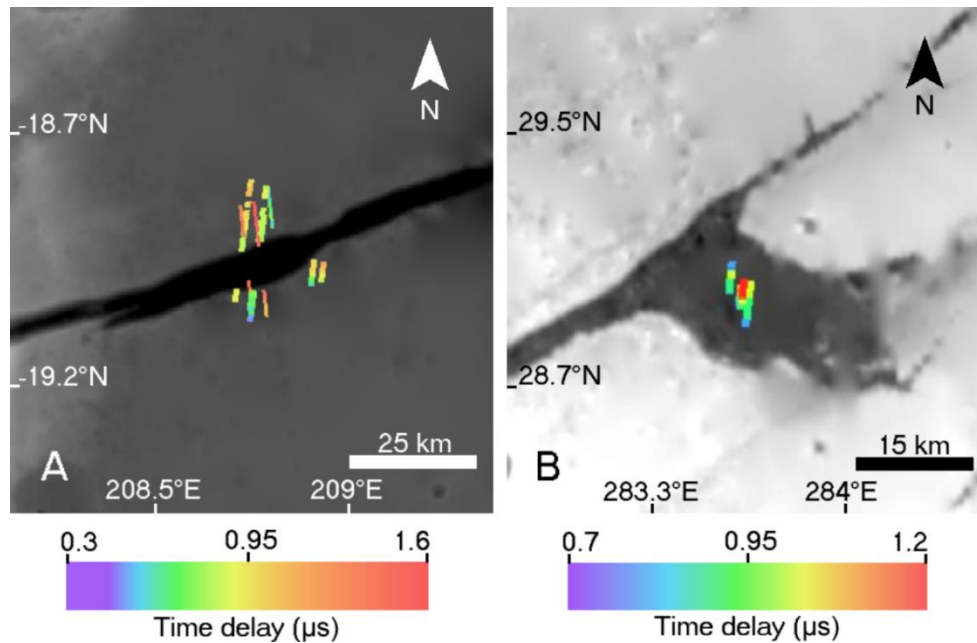


Fig. A: Mangala Fossa and **Fig B:** Labeatis Fossa. SHARAD ground track colors illustrate the two-way time delay of the subsurface reflections over the region.

References:

[1] Banerdt, W.B., et al. (1992). Stress and tectonics on Mars. In: Kieffer, H.H., et al. (Eds.), Mars, Univ. Arizona Press, pp. 249–297.

- [2] Carter, L. M., Campbell, B. A., Holt, J. W., Phillips, R. J., Putzig, N. E., Mattei, S., Seu, R., Okubo, C. H., and Egan, A. F. (2009). Dielectric properties of lava flows west of Ascraeus Mons, Mars. *Geophys. Res. Lett.*, 36, L23204. [10.1029/2009GL041234](https://doi.org/10.1029/2009GL041234).
- [3] Choudhary, P., Holt, J.W., Kempf, S.D., 2016. Surface Clutter and Echo Location Analysis for the Interpretation of SHARAD Data From Mars. *IEEE Geoscience and Remote Sensing Letters* PP, 1–5. [10.1109/LGRS.2016.2581799](https://doi.org/10.1109/LGRS.2016.2581799)
- [4] Seu, R., Phillips, R. J., Biccari, D., Orosei, R., Masdea, A., Picardi, G., Safaeinili, A., Campbell, B. A., Plaut, J. J., Marinangeli, L., Smrekar, S. E., & Nunes, D. C. (2007a). SHARAD sounding radar on the Mars Reconnaissance Orbiter. *J. Geophys. Res.* 112, E05S05. [10.1029/2006JE002745](https://doi.org/10.1029/2006JE002745)

22. Characterizing Arsia Mons Clouds using OMEGA and CRISM

Ashwathy Nair¹, Frank van Ruitenbeek² and Wim Bakker³ ¹University of Twente (nairashwathy99@gmail.com), ²University of Twente (f.j.a.vanruitenbeek@utwente.nl), ³University of Twente (w.h.bakker@utwente.nl)

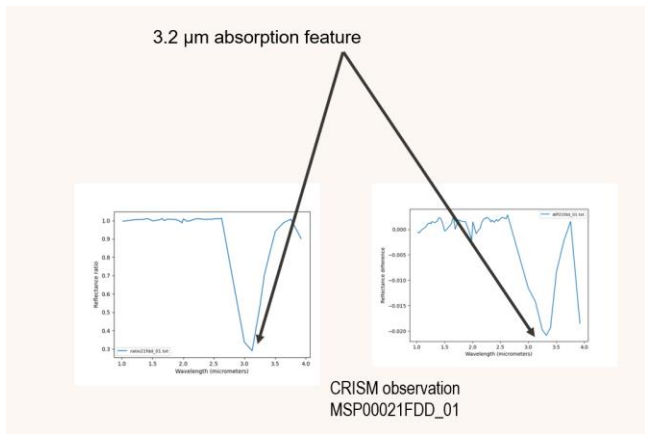
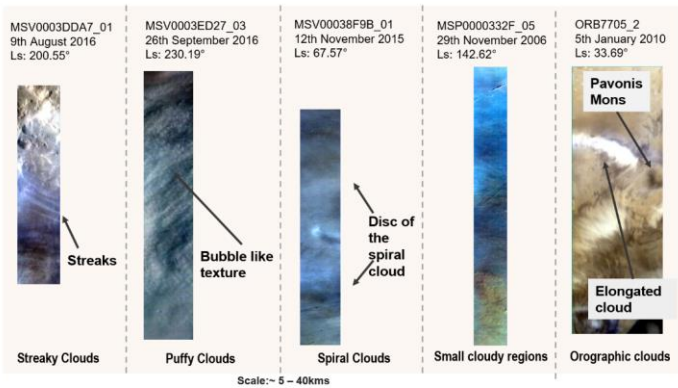
Abstract

Characterizing clouds over Arsia Mons using OMEGA and CRISM

Mars, our neighboring planet, has been a source of fascination for scientists and planetary enthusiasts for its unique atmospheric phenomena. Clouds are an intriguing feature observed on Mars, which play a crucial role in influencing the planet's weather patterns and climate system. Arsia Mons is a Martian volcanic mountain that experiences distinct types of cloud occurrences, including the recently discovered mysterious elongated cloud called the AMEC (Arsia Mons Elongated Cloud). This research focuses on investigating the clouds observed over the Martian volcanic mountain, Arsia Mons using spectral datasets to gain insights into the cloud occurrences in this area with respect to its morphology and composition. Data obtained over a period of 18 years from OMEGA and CRISM spectrometers was utilized to search for new cloud images, characterize clouds based on their morphologies and investigate cloud constituents using spectral analysis techniques. The study compiled a total of 102 cloud images from both OMEGA and CRISM. A novel observation of an elongated cloud was discovered at the volcanic mountain Pavonis Mons, situated adjacent to the Arsia Mons volcano. Additionally, a distinct cloud morphology was identified in the Pavonis Mons region, referred to as the 'puffy' cloud in this research. The study also adds an observation of a rarely observed spiral cloud in the Arsia Mons region along with other cloud morphologies such as streaky clouds, orographic clouds and small cloud regions. Spectral analysis of the clouds to investigate cloud constituents and confirm the presence of dust, H₂O ice, and CO₂ ice showed no contribution of dust and CO₂ ice in the clouds. H₂O ice was detected in the examined clouds characterized by the 3.2 μm absorption feature. New cloud observations, their observed morphologies and inferred cloud constituents in this study will be useful to add to our current knowledge and understanding of clouds in the Arsia Mons region.

Introduction: Mars, our neighboring planet, has been a source of fascination for scientists and planetary enthusiasts for its unique atmospheric phenomena. Clouds are an intriguing feature observed on Mars, which play a crucial role in influencing the planet's weather patterns and climate system. Arsia Mons is a Martian volcanic mountain that experiences distinct types of cloud

occurrences, including the recently discovered mysterious elongated cloud called the AMEC (Arsia Mons Elongated Cloud) [1]. This research focuses on investigating the clouds observed over the Martian volcanic mountain, Arsia Mons using spectral datasets to gain insights into the cloud occurrences in this area with respect to its morphology and composition. Data obtained over a period of 18 years from OMEGA and CRISM spectrometers was utilized to search for new cloud images, characterize clouds based on their morphologies and investigate cloud constituents using spectral analysis techniques. The study compiled a total of 102 cloud images from both OMEGA and CRISM. A novel observation of an elongated cloud was discovered at the volcanic mountain Pavonis Mons, situated adjacent to the Arsia Mons volcano. Additionally, a distinct cloud morphology was identified in the Pavonis Mons region, referred to as the ‘puffy’ cloud in this research. The study also adds an observation of a rarely observed spiral cloud in the Arsia Mons region along with other cloud morphologies such as streaky clouds, orographic clouds and small cloud regions. Spectral analysis of the clouds to investigate cloud constituents and confirm the presence of dust, H₂O ice, and CO₂ ice showed no contribution of dust and CO₂ ice in the clouds. H₂O ice was detected in the examined clouds characterized by the 3.2 μm absorption feature. New cloud observations, their observed morphologies and inferred cloud constituents in this study will be useful to add to our current knowledge and understanding of clouds in the Arsia Mons region.



References

[1] J. Hernández-Bernal, A. Sánchez-Lavega, T. del Río-Gaztelurrutia, E. Ravanis, A. CardesínMoineiro, K. Connour, D. Tirsch, I. Ordóñez-Etxeberria, B. Gondet, S. Wood and D. Titov, "An Extremely Elongated Cloud over Arsia Mons Volcano on Mars: I Life Cycle," *Journal of Geophysical Research: Planets*, 2021.

23. AEOLIAN ACTIVITY AND DUNE MIGRATION OVER A GLOBAL DUST-STORM YEAR AROUND THE MARTIAN GALE CRATER

Nayama Valsa Scariah^{1*}, Mili Ghosh Nee Lala^{1**}, A.P. Krishna^{1***}

Department of Remote Sensing, Birla Institute of Technology, Mesra, Ranchi¹

*e-mail:phdrs10003.17@bitmesra.ac.in,**e-mail:mili@bitmesra.ac.in,***e-mail:
apkrisha@bitmesra.ac.in

Abstract: Dune dynamics analysis is crucial for assessing the influence of circulation pattern and climatic parameters on Martian morphology. Climate, topography and dune morphometry measure the dune dynamics. In this study, MRO CTX image was used for the estimation of the dune migration from non-dust storm season to dust storm season over MY34, a reported global dust storm year. Climatic parameters were acquired from MCD and curiosity rover. Climate, topography and dune morphometry measure the dune dynamics in terms of distance and direction. Climatic parameters such as surface temperature, pressure, wind speed, wind direction and atmospheric optical depth were analyzed as indicators of the dune dynamics. The dune morphometric parameters such as area, perimeter and height of the dune as well as the topographic parameters such as slope, aspect and elevation were also analyzed.

It was observed that the southern region of Gale crater had high dune migration rate of about 1.91m/Martian month whereas, western region of Gale crater had the lowest migration rate of about 0.22m/Martian month. Seasonal dune dynamics in Gale crater region have direct correlation with all the morphometric parameters which is unlike dune migration trends on Earth [1]. Drift potential is the most prime indicator that measures the ability of a surface to carry the sediment. It varies with varying surface properties of the area. In this study, southern region of the Gale crater has the highest seasonal dune migration rate and highest drift potential whereas, western region has the lowest dune migration as well as lowest drift potential. Largest dune migration was observed where the AOD and atmospheric pressure were low with high temperature. Dynamic seasonal movement of particles in the southern region and north-eastern region of Gale crater have been significantly influenced by the topography of the location.

Global dust storms have prodigious effect on the surface temperature, which affect the climatic parameters as well. THEMIS data was chosen corresponding to Martian global dust storm for MY34 to match the available CTX data and used to analyze the seasonal surface temperature and dune dynamics respectively. The difference in temperature between a normal Martian year (MY30) and MY34 was observed to be almost 10°K derived from Curiosity Rover data. Thus, such excessive dust loading also could hinder the effect of climatic parameters on dune migration which was evident in temperature observations over these two different reference years.

References :[1] Yang Z., Qian G., Dong Z., Tian M. and Lu J., (2021), *Geomorphology*, 378 , 107615, [2] Almeida M.P., Parteli E.J.R., Andrade J.S. and Herrmann H.J., (2008), *Proceedings of the National Academy of Sciences*, [3] Xu P. and Greeley R., (1992), *Workshop on the Martian Surface and Atmosphere Through Time*

24. DEVELOPMENT OF A COAXIAL ROTOR SYSTEM FOR MARS EXPLORATION

Ajo Joseph Anto¹, Vellingiri Ramanujam R², Abraham George M³, Ranjith Mohan⁴ and Shamrao⁵

¹M.S Scholar, Dept. of Aerospace Engineering, IIT Madras, ²Research Associate, Dept. of Aerospace Engineering, IIT Madras, ³Project Associate, Dept. of Aerospace Engineering, IIT Madras, ⁴Associate Professor, Dept. of Aerospace Engineering, IIT Madras, ⁵Scientist/Engineer-‘SG’, Space Mechanics Group, URSC - Bangalore

Introduction: The research focusses on the development of a helicopter rotor system for operation in the Martian atmosphere which is approximately 100 times less dense than Earth’s atmosphere. On Mars, 98% of the atmosphere is composed of CO₂ and has an average surface temperature of 210K. In order for the helicopter to generate the necessary thrust at low density, a higher rotating speed of rotor is necessary which combined with low temperatures leads to a high Mach number flow. A coaxial helicopter rotor system is designed with aerodynamic profiles of the rotor blades being optimized for operation on Mars.

Experimental studies and Prototype development: A 2.4m vacuum chamber is set-up for simulating the atmospheric density on Mars. Experimental rotor is mounted on a test stand installed inside the chamber with an electric motor drive mechanism. Multi-axis loadcells are employed to measure the thrust and power. The test setup includes all essential components for the helicopter, although not optimized for weight. The experimental data consisting of thrust and power coefficients are compared with numerical results obtained from blade element momentum theory and RotCFD (a commercial tool that is specific for rotor applications and based on momentum source approach). Test data that brings out the effect of Reynolds number on propellers are also presented.

Keywords: Mars, Helicopter, Reynolds number, Mach number, BEMT, RotCFD

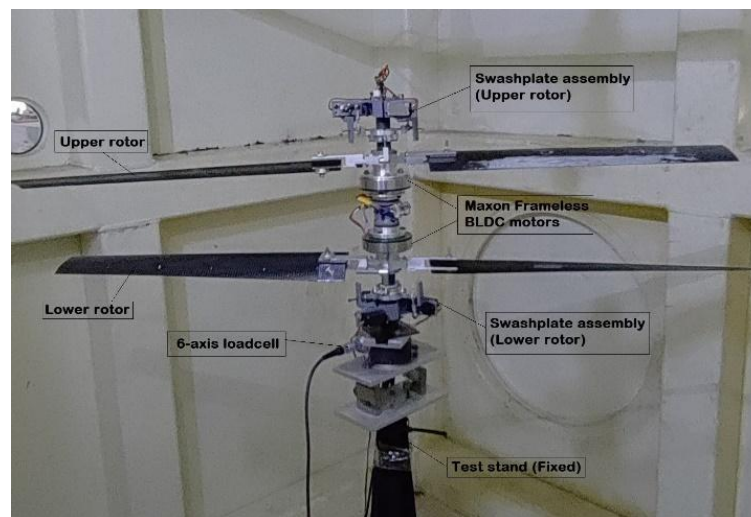


Figure 1: Coaxial rotor system prototype being tested inside a vacuum chamber

References:

[1] Young, L.A., et al. “Rotorcraft as mars scouts.” Proceedings, IEEE Aerospace Conference. Vol. 1. IEEE, 2002.

[2] J. Balaram, et. Al. "Mars Helicopter Technology Demonstrator", 2018 AIAA Atmospheric Flight Mechanics Conference, AIAA 2018-0023.

[3] Leishman, J. G., and Ananthan, S. "Aerodynamic Optimization of a Coaxial Proprotor," Proceedings of the 62nd Annual Forum of American Helicopter Society, Phoenix, AZ, May 2006.

25. EXOBASE AND HOMOPAUSE ALTITUDES IN THE MARTIAN UPPER ATMOSPHERE: VARIABILITIES AND SOURCES

N. V. Rao¹, V. Leelavathi¹, and Neha Gupta²

¹*National Atmospheric Research Laboratory, Gadanki, India (nvrao@narl.gov.in)*

²*NSSTC, UAE University, P.O. Box 15551, Al Ain, United Arab Emirates*

Understanding the composition of volatile gases in the Martian exosphere and the mechanisms governing their escape into outer space is crucial for unravelling the mysteries of planetary evolution. Two significant neutral atmospheric boundaries, namely the exobase and the homopause, hold particular importance in this context. Exobase marks the altitude at which transition occurs from a collisional region on the lower side to a collisionless region on the higher side. Planetary volatiles reaching this region with sufficient energy are more likely to escape into outer space, and it is widely believed that most of the gaseous escape from Mars occurs above the exobase. Homopause lies at altitudes below which atmospheric gases are effectively mixed due to large-scale mixing and above which the vertical distribution of gases is governed by molecular diffusion. Thus, homopause acts as a determining factor for the altitude at which gases establish their own scale-height, thereby playing a vital role in dictating the abundance of lighter species, such as H and He, that reach the exobase region. In this study, we conducted a detailed analysis of the exobase and homopause altitudes derived from measurements by the Neutral Gas and Ion Mass Spectrometer (NGIMS) aboard the Mars Atmosphere and Volatile Evolution (MAVEN) spacecraft. Exobase altitudes typically range from 140 to 200 km, with 165 km being the most probable altitude and homopause altitudes are predominantly found between 90 km and 135 km, 111 km being the most probable altitude. Exobase altitudes are typically 41-68 km higher than homopause altitudes. Both exobase and homopause altitudes display sinusoidal variations, primarily attributed to diurnal changes. While the exobase altitudes show a clear local time, seasonal and latitudinal variations that are in-phase with local solar insolation, the homopause altitudes display complex variability. The phase relation between the exobase and homopause altitudes, and their relation to the thermospheric background temperatures provide clues on the sources of their variability. We found that the phase relation between the homopause and homopause altitudes is not constant and varies with solar forcing from top and dust forcing bottom.

26. RESULTS FROM THE MARS EXOSPHERIC COMPOSITION ANALYSER (MENCA) ONBOARD MARS ORBITER MISSION

Smitha V. Thampi¹, M. B. Dhanya¹, Vipin K. Yadav¹, R. Satheesh Thampi¹, Tirtha Pratim Das², and Anil Bhardwaj³

1. *Space Physics Laboratory, VSSC, Trivandrum, India, smitha_vt@vssc.gov.in*

2. *ISRO HQ, Bengaluru, India*

3. *Physical Research Laboratory, Ahmedabad, India*

Mars, being an unmagnetised planet with low gravity compared to Earth, atmospheric escape has been very important, that determined the present day conditions on the planet. Study of the composition and the variability of the Martian exosphere may help in understanding the escape processes of the Martian atmosphere, which is responsible for making it a cold, dry planet as we see it today. This is the region being explored *in-situ* by MENCA (Mars Exospheric Neutral Composition Analyser) experiment aboard the Mars Orbiter Mission (MOM). During its initial phase of operations in December 2014, MENCA measured the abundances of the major gases viz. atomic Oxygen (O with mass 16 amu), Carbon Monoxide (CO) and Nitrogen molecule (N₂) (both have mass 28 amu) and Carbon Dioxide (CO₂ with mass 44 amu) during Martian evening hours from 265 km to 400 km altitude. These measurements were conducted when Mars was closer to the Sun in its elliptical orbit, known as the perihelion period. The observations also showed that the abundance of O exceeds that of CO₂ at an altitude of ~260 km during Martian evening hours [1]. During this period, MENCA instrument could also measure the neutral Argon-40 (Ar) concentrations in the Martian exosphere. The altitude profiles revealed that on certain orbits, the scale height over the 250-300 km region is found to be higher compared to 'normal' values. The corresponding increase in temperature is found to be about 100 K compared to the 'normal' exospheric temperature. The increase in temperature indicates the significant presence of suprathermal heavy neutral atoms in Martian exosphere [2]. The discovery has important implications in the context of understanding the energy deposition in the Martian upper atmosphere, and this will help scientists understand why the Martian atmospheric escape rates are higher than what was believed previously. These results will be discussed in detail.

References:

[1] Anil Bhardwaj, Smitha V. Thampi, Tirtha Pratim Das, M. B. Dhanya et al. (2016), *Geophysical Research Letters*, 43, 1862– 1867, doi:10.1002/2016GL067707

[2] Anil Bhardwaj, Smitha V. Thampi, Tirtha Pratim Das, M. B. Dhanya et al (2017), *Geophysical Research Letters*, vol. 44, doi:10.1002/2016GL072001

27. THE IMPACT OF THE VENUSIAN PLASMA ENVIRONMENT DURING THE PASSAGE OF INTERPLANETARY CORONAL MASS EJECTIONS

Diptiranjana Rout¹, S. V. Thampi², Y. Miyoshi³, T. Pant², A. Bhardwaj⁴

¹National Atmospheric Research Laboratory, Gadanki, India

²Space Physics Laboratory, Vikram Sarabhai Space Center, Kerala, India

³Institute for Space-Earth Environmental Research, Nagoya University, Nagoya, Japan

⁴Physical Research Laboratory, Ahmedabad, India

Email: diptipr189@gmail.com

Abstract: The present investigation explores the dynamic interaction between interplanetary coronal mass ejections (ICMEs) and the induced magnetosphere of Venus. Utilizing data from the Venus Express (VEX) mission, we studied four ICME events. The peak magnetic field of the magnetic barrier is found to be more than 100 nT during all these events. The altitude of the inbound bow shock and ionopause at Venus are comprehensively studied during the passage of these ICMEs. The ionopause altitude is observed to be around 800 km during the quiet days. However, during the passage of ICMEs, the ionopause altitude experienced significant compression due to the high solar wind dynamic pressure within the induced magnetosphere, and the ionosphere was also found to be highly magnetized. Interestingly, the position of the bow shock did not show any significant changes as compared to the previous quiet days. It shows that the location of ionopause is more sensitive toward the solar wind pressure change during ICME than the bow shock location. Further, the increase in heavy-ion density is found to be 4-10 times higher than the previous days during the passage of these ICMEs. This study shows that ICMEs can lead to an increase in the atmospheric loss of Venus and can also cause a significant reduction in the ionopause location.

28. CHARACTERISTIC FEATURES OF THE VENUS IONOSPHERE USING PHYSICS BASED IONOSPHERIC MODELS AND OBSERVATIONS

K M Ambili, R K Choudhary and Keshav R Tripathi

Space Physics Laboratory, VSSC, ISRO, Trivandrum, 695022

Venus, being the closest planet to Earth, has been a subject of numerous planetary missions aimed at studying its atmospheric and ionospheric composition and density. The Venus ionosphere is formed by the photoionization of the neutral atmosphere by solar EUV and X-ray radiations and, as a secondary effect, by photo-electron impact ionization at lower altitudes. In addition to the V2 layer, Venus is known to have the presence of a secondary layer of enhanced ionization at the lower height (~125 km) as well [1,2]. Though Venus has been thoroughly explored in the past various missions, there are still outstanding questions even related to the formation of the different layers. In the present study some of these outstanding scientific issues are addressed using both Radio occultation measurements and physics based ionospheric model.

One of such outstanding issue is the formation of the V1 layer. Measurements from earlier missions like Mariner 5/10, Venera 9/10, and PVO, had shown pieces of evidence, albeit limited, for the existence of a layer of enhanced ionization at about 125 km. A more detailed study addressing the characteristic features of V1 layer such as peak altitude, peak density, and morphological changes with respect to SZA and solar activity better were done by Venus Express radio occultation (VeRa) observations [2]. Though, VeRa reported different types of V1 layer, no theoretical understanding has been developed so far which could explain the occurrence of different types. Another interesting feature is the enhanced ionization below 120 km. This is known as V0 layer. Though there are different mechanisms possible for the formation of an ionization at the lower altitude, the exact reason is not yet sort out. The study of the formation and characteristics of different layers enable us to understand the physics of that region and its variability. Though there are observations reporting an additional layer above 160 km (V3 layer), its origin is still not understood. In addition to these, the variabilities observed in the ionosphere such as day and night, ionopause and the upper atmosphere etc are not understood completely.

References:

- [1] Cravens, T., Kliore, A., Kozyra, J., Nagy, A., 1981. The ionospheric peak on the venus dayside. *J. Geophys. Res.* 86, 11323–11329. [2] Girazian, Z., Withers, P., Häusler, B., Pätzold, M., Tellmann, S. and Peter, K., 2015. Characterization of the lower layer in the dayside Venus ionosphere and comparisons with Mars. *Planetary and Space Science*, 117, pp.146-158. [3] Imamura, T., Ando, H., Tellmann, S., Pätzold, M., Häusler, B., Yamazaki, A., Sato, T.M., Noguchi, K., Futaana, Y., Oschlisniok, J. and Limaye, S., 2017. Initial performance of the radio occultation experiment in the Venus orbiter mission Akatsuki. *Earth, Planets and Space*, 69(1), pp.1-11. [4] Ambili, K.M., Babu, S.S. and Choudhary, R.K., 2019. On the relative roles of the neutral density and photo chemistry on the solar zenith angle variations in the V2 layer characteristics of the Venus ionosphere under different solar activity conditions. *Icarus*, 321, pp.661-670.

29. Whistler mode wave in Jovian magnetosphere

R.S. Pandey¹ and Ankita²

^{1,2}Department of Physics, Amity Institute of Applied Sciences, Amity University, Sector –125
Noida, Uttar Pradesh, India rspandey@amity.edu¹ ankitachauhan625@gmail.com²

ABSTRACT

The whistler waves observed by Ulysses in Jovian magnetosphere have been investigated in this paper. Various types of large frequency radio emissions by mechanism of resonant interaction have been observed in Jovian magnetosphere. In the present study, the phenomenon of wave particle interaction between electromagnetic waves along with magnetic field lines and fully ionized magnetospheric plasma particles has been considered with Oblique and parallel propagation of wave to evaluate the detailed dispersion relation with generalized distribution in collision-less Jovian magnetosphere at 17 R_J by using the method of characteristics solution and kinetic approach, the expression for growth rate has been derived. The growth rate has been calculated for oblique and parallel propagation using suitable data in magnetosphere of Jupiter.

30. RESULTS FROM CHACE-2 ONBOARD CHANDRAYAAN-2 ORBITER

M. B. Dhanya¹, Smitha V. Thampi¹, R. Satheesh Thampi¹, Tirtha Pratim Das², and Anil Bhardwaj³

1. Space Physics Laboratory, VSSC, Trivandrum, India, mb_dhanya@vssc.gov.in

2. ISRO HQ, Bengaluru, India

3. Physical Research Laboratory, Ahmedabad, India

Composition of the lunar exosphere, especially beyond the equatorial regions of the Moon are poorly explored. CHandra's Atmospheric Composition Explorer-2 (CHACE-2) experiment, which is a neutral gas mass spectrometer, aboard the Chandrayaan-2 orbiter samples the lunar exosphere at ~100 km altitude [1]. CHACE-2 has unambiguously detected Argon-40, which is an important noble gas in the lunar exosphere, upto the mid-latitude regions of the Moon. Though the presence of Ar-40 in the lunar exosphere has been confirmed by previous missions like Apollo-17 [2] and LADEE [3] in the near equatorial regions, CHACE-2 has provided for the first time, the global distribution (within $\pm 60^\circ$ latitude). The diurnal variation in the number density (with respect to the solar longitude) showed pre-sunrise, sunrise and sunset peaks, as well as nightside minima. These features are typical of a condensable gas and are in agreement with the earlier low latitude observations. CHACE-2 observations shows that these features extend up to the mid-latitude regions as well. Apart from this, the observations revealed significant spatial heterogeneity in the number density of Ar-40 as well as enhancements over certain longitude sectors. Comparison with the map of potassium-40 (K-40) from the Lunar Prospector indicated the Ar-40 enhancements in some of the southern hemisphere regions coincide with the K-40 rich KREEP terrain and the South Pole Aitken (SPA) terrain. In addition, there are a few more regions of Ar-40 enhancements observed in the northern hemisphere. These observations are indicative of unknown or additional loss processes, role of Moon quakes or regions with lower activation energies, which need further investigation and call for a better understanding of the surface-exosphere interactions and source distributions. These results along with the detection of other gases like CO₂ in the lunar exosphere will be presented.

References:

- [1] Das, T. P., Thampi, S. V., Dhanya, M. B., Naik, N., Sreelatha, P., Pradeepkumar, P., et al. (2020). *Current Science*, 118, 202–209
- [2] Hodges, R. R., Jr, & Hoffman, J. H. (1974). In *Lunar and planetary science conference proceedings*. (Vol. 3, pp. 2955–2961).
- [3] Benna, M., Mahaffy, P. R., Halekas, J. S., Elphic, R. C., & Delory, G. T. (2015). *Geophysical Research Letters*, 42, 3723–3729. <https://doi.org/10.1002/2015GL064120>.

31. Effect of spacecraft orbital parameters on the spatiotemporal distribution of Solar Occultation measurements in the Venusian Atmosphere

Jayadev Pradeep^{1,*} and S. V. Sunilkumar¹

¹Space Physics Laboratory, Vikram Sarabhai Space Centre, ISRO, Thiruvananthapuram-695022, Kerala

*E-mail: jayadevpradeep07@gmail.com

Solar occultation is a versatile and well-proven technique for high-resolution vertical profiling of planetary atmospheres from satellite-based platforms [1]. Due to the distinctive observational geometry involved, the deduction of the spatiotemporal coverage of solar occultation measurements as a function of the spacecraft (S/C) orbit is non-trivial. In light of this, we have implemented PYTHON-based 3D orbital simulations of the occultation-viewing geometry for hypothetical Solar Occultation Experiments (SOE) to explore the atmosphere of Venus [2]. The simulations incorporate planetary motions and orbital propagation using the ASTROPY and POLIASTRO packages, computing the instantaneous line-of-sight (LoS) tangent point using 3D vector algebra. SPICAV/SOIR solar occultation data from the Venus Express mission [3] was used to validate the simulations, confirming excellent agreement. Using the simulations, a first-of-its-kind theoretical study was carried out on the effect of different spacecraft orbital elements on the spatiotemporal distribution of solar occultation measurements in the Venusian atmosphere, revealing a highly sensitive dependence. The semimajor axis (a) and inclination (i) of the spacecraft orbit are found to influence the latitudinal extent of observations and the nature/duration of occultation seasons, while the eccentricity (e) and argument of periapsis (ω) determine the distinct regions of sparse observations (RSOs). The spatiotemporal spread of individual solar occultation profiles is found to depend on the orbital parameters as well as the solar beta angle. Our results show that spacecraft orbits can be designed with appropriate parameters to optimize the coverage of SOE measurements in view of achieving specific science goals, thereby providing valuable inputs for upcoming missions to Venus that aim to implement the solar occultation technique. The 3D orbital simulations developed in this work are further adaptable to different planetary environments, enabling the simulation and optimization of a range of space-borne observational geometries for various future interplanetary missions.

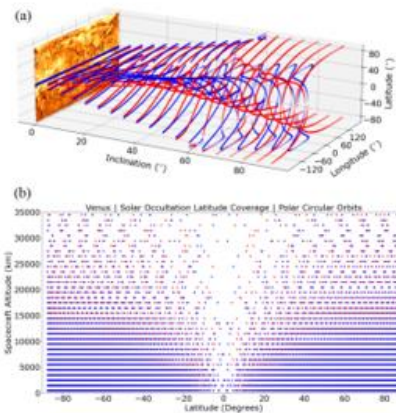
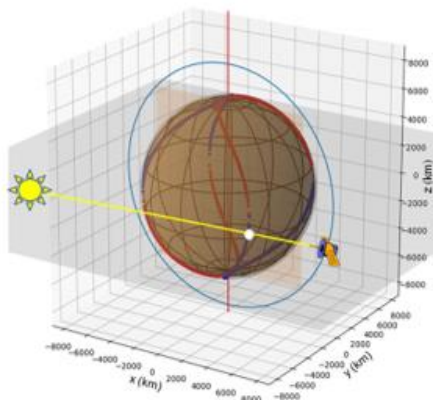


Figure 1: 3D visualization of a 2500 km circular polar orbit (blue curve) simulated around Venus, with the yellow line depicting instantaneous solar occultation LoS between spacecraft and the sun. The red dots correspond to sunrise (egress) events and blue dots correspond to sunset (ingress) events. **Figure 2:** Results from 3D orbital simulation studies for Venus: (a) Effect of S/C orbit inclination (i) on the spatial distribution of SOE measurements for 1000 km circular orbits. (b) Effect of S/C orbit semimajor axis (a) on latitude distribution of SOE measurements for polar circular orbits.

References: [1] Vandaele, A. C., et al. (2008), *Journal of Geophysical Research: Planets*, 113, E00B23. [2] Pradeep, J. and Sunilkumar, S. V. (2023), *RAS Techniques and Instruments*, 2(1), 324-344. [3] Wilquet, V., et al. (2014). *EGU General Assembly Conference Abstracts* (p. 11491).

32. Exploring rocky worlds with the HARPS-N, ESPRESSO and NIRPS spectrographs

F. Pepe¹, X. Dumusque, and F. Bouchy¹, ¹Departement of Astronomy of the University of Geneva, Chemin de Pegasi 51, 1290 Versoix, Switzerland, Francesco.pepe@unige.ch

Abstract : High-spectral fidelity measurements are essential to explore the diversity of small-mass planets to put further constraints on the formation and evolution of exoplanets. Recent developments in understanding better stellar systematics and instrumental signals allow us now to start exploring the population of rocky worlds.

In this field, the HARPS-N and ESPRESSO spectrographs have made tremendous contributions these last years, mainly thanks to 10 years of HARPS-N Guaranteed Time of Observations (GTO) and 4 years of ESPRESSO GTO. The consortia of those instruments focused their efforts on three main projects: 1) the precise measurement of bulk density for the small transiting planets found by Kepler, TESS and CHEOPS, 2) a blind search for rocky worlds orbiting around the closest stars to the solar system and 3) the characterization of planetary atmospheres by transmission spectroscopy. I will highlight during this talk the main results obtained from those instruments.

Looking at the future, significant contribution will come from the NIRPS spectrograph, with its 725 nights of GTO over the next 5 years. Thanks to its wavelength range centered on the NIR and an exquisite precision below the m/s, NIRPS will be sensitive to rocky worlds in the habitable zone of their host M dwarf. Such planets will represent key targets for future atmospheric characterization and direct imaging using future facilities like the ELT and HabEx. In addition to this science case, NIRPS is also focusing on measuring the bulk-density of transiting planet, to further constrain the formation and evolution of exoplanets orbiting cool dwarfs.

The Legacy of Extreme Precision Radial Velocity (EPRV) at PRL

33. Avoiding False Positive Exoplanet Detections in Centimeters-Per-Second Radial Velocity Data

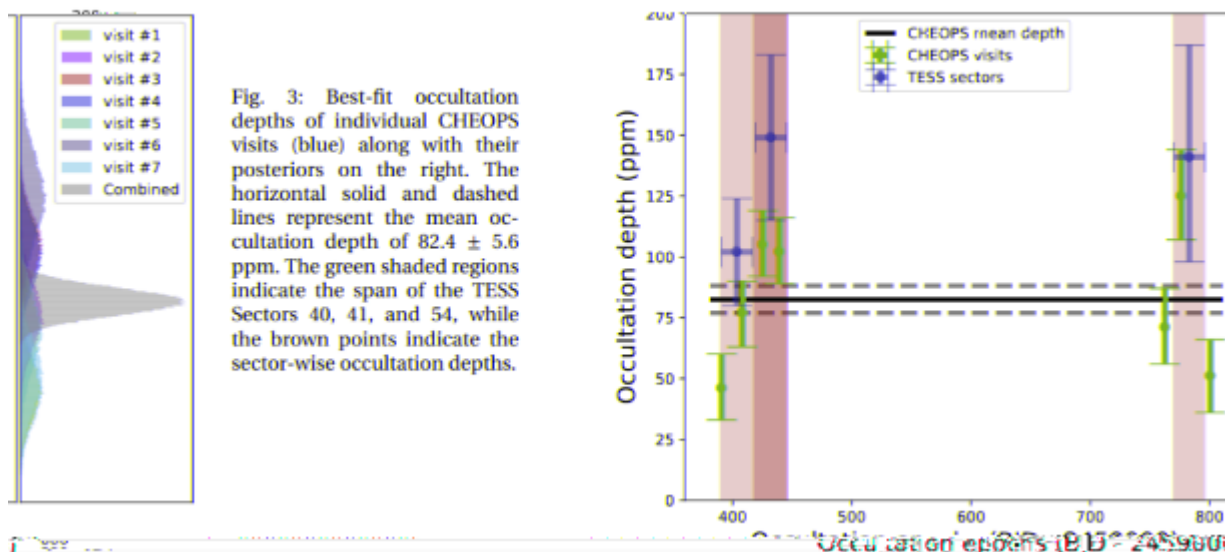
P. Robertson¹, ¹Department of Physics & Astronomy, University of California Irvine, 4129 Frederick Reines Hall, Irvine, CA 92697, USA, paul.robertson@uci.edu

Ultra-precise Radial Velocity (RV) time series are subject to various sources of noise originating from the instrument, Earth's atmosphere, and the surface of the target star. Some of these noise sources simply obscure true Doppler variability, but others—particularly those associated with stellar rotation—create quasiperiodic signals which may be incorrectly interpreted as Doppler motion from exoplanets. As new RV spectrometers with measurement stability below the 1 m/s threshold begin to dominate the field, we will see RV signals from stellar rotation for all targets. I will review the process by which false positive exoplanet signals appear, and highlight some examples showing how temporal sampling and starspot lifetimes can make false positives extremely difficult to avoid. I will also discuss novel ways in which data products from new ultra-precise RV spectrometers may be used to identify and mitigate stellar activity signals which might otherwise create false positive exoplanet detections.

34. CHEOPS observations of KELT-20 b/MASCARA-2 b: An aligned orbit and signs of variability from a reflective day side

V. Singh¹ and The CHEOPS science team, ¹Affiliation (INAF – Osservatorio Astrofisico di Catania, via santa sofia 78, Catania, Italy. E-mail: vikash.singh@inaf.it)

Introduction: Occultations are windows of opportunity to indirectly peek into the dayside atmosphere of exoplanets. We aim to precisely measure the planetary radius and geometric albedo of the ultra-hot Jupiter KELT-20b as well as the system's spin-orbit alignment. We obtained optical high-precision transits and occultations of KELT-20b with CHEOPS in conjunction with simultaneous TESS observations. We further used the host star's gravity-darkened nature to measure the system's obliquity. We present time-averaged precise occultation depth of $82(6)$ ppm measured with seven CHEOPS visits, and $131(+8/-7)$ ppm from four sectors of TESS photometry. We interpret the occultation measurements together with archival infrared observations to measure the planet's geometric albedo and dayside temperatures. The comparably high geometric albedo of KELT-20 b corroborates a recent known trend of strongly irradiated planets being more reflective. Finally, we tentatively detect signs of temporal variability in the occultation depths, which might indicate variable cloud cover advecting onto the planetary day side.



Article accepted to be published in A&A. The preprint can be found on astro-ph: <https://arxiv.org/abs/2311.03264>

35. Comprehensive homogeneous investigation of orbital ephemeris and atmospheric characterization of an Ultra-hot Jupiter: WASP-19 b

A. R. Rajkumar¹ and J. Tregloan-Reed¹, ¹Affiliation (Instituto de Investigación en Astronomía y Ciencias Planetarias, Universidad de Atacama, Chile; anitha.raj.21@alumnos.uda.cl).

Exoplanets with ultra-short periods ($P < 1$ day) might experience orbital decay due to the tidal dissipation effect with the host star. As these orbital decay occurs on a human time scale, with consistent observation it is possible to verify these orbital decay which occur in a system [1]. This work allows verification of the orbital ephemeris of the WASP-19 b with the availability of long-term high-precision photometric and spectroscopic data including 28 unpublished transits from the Danish telescope (Refer Figure 1). The transit timings were fitted with linear, quadratic and cubic ephemeris. This place limits on the modified tidal quality factor Q^* and set the lower limit on orbital decay was determined.

The same data allows for a detailed study of the atmospheric properties of WASP-19 b, via transmission photometry and spectroscopy. WASP-19 A is an active host star with a surface strewn with starspots [2], which if not correctly modeled, systematics are introduced into the transit timing measurements and transit depth, which latter affects the exoplanetary transmission spectrum [3]. Additionally the signal from stellar inhomogeneities can outweigh the signal from planetary spectral characteristics [4]. As a result, modeling the starspots using PRISM [5][6] we perform the most complete, detailed, homogeneous analysis of all available data to estimate Q^* and study the atmospheric properties of WASP-19 b with the help of ground-based and space-based archival data.

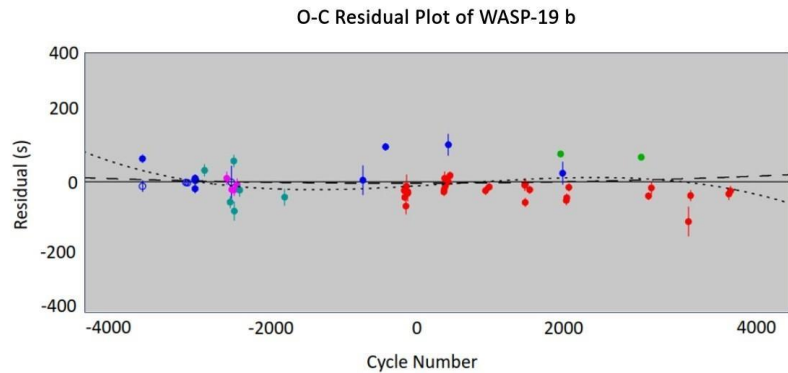


Figure 1: The O-C residuals of WASP-19 b using 28 unpublished transits from the Danish telescope (red datapoints) and the remaining data are from the literature. The plot shows the best fitting linear ephemeris (black line), the best-fitting quadratic ephemeris model (black dashed line) and the best-fitting cubic ephemeris model (black dotted line).

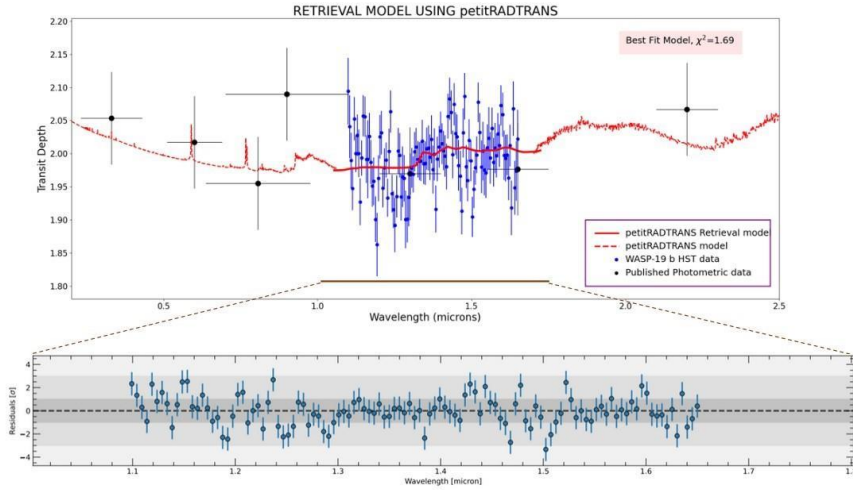


Figure 2: The figure illustrates the petitRADTRANS model fitting of WASP-19 b spectroscopic (blue points) and photometric data (black points). The spectroscopic data [9] is obtained from the HST archive and is fitted using the petitRADTRANS retrieval model and its residual shown below. The photometric data are the result of multiple transits obtained in the same filter are combined via their weighted mean to provide a single data point for that particular passband. The vertical bars represent errors in the measurements and horizontal bars show the FWHM transmission of the passbands used.

References:

- [1] Southworth. J., et al. 2022, MNRAS, 515, 3212-3223.
- [2] Rackham. B V., et al. 2023, arXiv:2303.15418.
- [3] Mancini. L., et al. 2013a, A & A, 551, A11.
- [4] TregloanReed, J., et al. 2013, MNRAS, 428, 3671.
- [5] TregloanReed, J., et al. 2015, MNRAS, 450, 1760.

36. DESIGN AND DEVELOPMENT OF PRECISE TEMPERATURE CONTROLLER FOR PARAS-2

Neelam J S S V Prasad*¹, Kapil Bharadwaj¹, Kevi Kumar¹, Rishikesh Sharma¹, Ashirbad Nayak¹, Nafees Ahmed¹ and Abhijit Chakraborty¹

¹*Physical Research Laboratory, Ahmedabad, Gujarat, India-380009*

**prasadgn@prl.res.in*

PARAS-2 is a High Resolution Spectrograph, which uses radial velocity technique for detection of exoplanets. For achieving sub-meter per second radial velocity measurements, demanding an instrument devoid of drift. Even minute alterations in temperature can induce drift in radial velocity measurements, a one-degree Celsius temperature shift fluctuation results in a substantial 100 m/sec [1] drift. To surmount this challenge, we devised a sophisticated temperature control mechanism to ensure precision control of temperature throughout observations. The temperature control system was meticulously crafted based on theoretical calculations. The spectrograph is housed within two concentric insulated chambers made up of thick layers of insulation. The temperature of the outer chamber is regulated using a commercially available PID controller, maintaining it within the range of $18 \pm 0.5^\circ\text{C}$. Spectrograph temperature is controlled by indigenously developed controller. It incorporates Pt100 sensors, a Micro K temperature reader for accurate measurements, and a controller utilizing a 12-bit DAC and ultra-precise, low-drift amplifiers. This intricate setup sends precise voltages to heaters through a programmable power supply, adjusting based on the disparity between the measured and set-point temperatures. Through this system, we achieved the targeted precision in temperature control. Across a typical observing night, we observed peak-to-valley variations of 0.0024 degrees Celsius at 24C and root mean square deviations of 0.0005 degrees Celsius.

I will present the intricate design parameters, the challenges we encountered during the development of this system, and the consequential results. It highlights our commitment to addressing and overcoming the intricacies associated with achieving sub-meter per second radial velocity measurements.

[1] Pepe, F., Mayor, M., et al. 2002. The Messenger , 110:9–14.

37. Double Scrambler Design and Implementation in PARAS-2 to achieve sub-m/s RV Precision

Kapil Kumar, KV, Neelam Prasad, Abhijit Chakraborty

Achieving the precision necessary for detecting super Earth-sized planets through Radial Velocity (RV) measurements demands an accuracy range of approximately 30 cm/s to 70cm/s or sub-1m/s velocity precision. To achieve such RV precision using high-resolution Doppler spectroscopy, an unparalleled level of long-term instrument stability is required. Among the key technical challenges in enhancing instrument stability lies the need to stabilize instrument illumination uniformly. Here we present the optical, opto-mechanical design and implementation of a double scrambler for the PARAS-2 high-resolution spectrograph (R~110,000). Coupled with octagonal fibers, this scrambler is anticipated to provide significant scrambling gains (SGs) in terms of the long term uniform illumination of the slit position of the spectrograph. Its use will effectively minimize the impact of input illumination variations on the fiber output, thereby enhancing the stability of the spectrograph's instrument profile and thus improving the Doppler measurement precision. Additionally, the output becomes remarkably insensitive to the variations in input pupil, effectively isolating the spectrograph from fluctuations in telescope illumination and changes in atmospheric seeing conditions up to an extent.

38. Precise Wavelength Calibration of PARAS-1 and PARAS-2 using Uranium lines for 1 m s⁻¹ to sub-m s⁻¹ RV measurements

Rishikesh Sharma*¹, Sanjay Baliwal¹, Nikitha Jithendran¹, Abhijit Chakraborty¹

¹ Physical Research Laboratory, Ahmedabad, Gujarat, India-380009*rishikesh@prl.res.in

Astronomical spectrographs with high resolution ($R > 50,000$) and exceptional thermal stability possess unique scientific capability of detecting subtle Doppler shifts that signify the presence of small exoplanets. Generally, for exoplanet detection, the precision of radial velocity (RV) measurements of stars is more influenced by the accuracy of the calibration source than by intrinsic photon noise. Traditionally, thorium-argon (Th-Ar) lamps have been the first choice for wavelength calibration in the visible spectrum. Unfortunately, these lamps with high-purity thorium cathodes (up to 99%) are no longer available. The commercially available replacements have cathodes made of thorium oxide (ThO), which, as confirmed by studies, contaminate the spectra with unwanted molecular oxide bands and obscure faint thorium atomic lines. This makes them unsuitable for wavelength calibration, hindering precise tracking and characterization of thorium lines, eventually degrading the RV precision.

Consequently, we proposed an alternative approach by utilising Uranium, which shares similarities with Thorium at the sub-atomic level. Approximately 1500 well-resolved Uranium lines (with a separation of $\geq 2 \cdot \text{FWHM}$) were identified and characterized using the PARAS-1 spectrograph. These lines were incorporated into the PARAS data analysis framework for both wavelength calibration and instrumental drift calculations. The study revealed that Uranium lines effectively measured instrumental drifts and stellar RVs comparable to Thorium lines. Subsequently, during the initial testing phase of the PARAS-2 spectrograph commissioned in 2021, operating at a resolution of 107,000, the same Uranium linelist was employed for wavelength calibration. The line identification and characterization efforts were extended with PARAS-2, identifying approximately 3000 well-resolved Uranium lines. This new linelist replaced the existing PARAS-1 linelist. The use of these newly identified Uranium lines allowed us to measure the dispersion of instrumental differential drift at a level of 30–50 cm s⁻¹, consistently.

In this presentation, I will delve into the process of identifying Uranium lines from UAr spectra, the selection criteria for the final linelist, and various results obtained with both PARAS-1 and PARAS-2 utilizing the Uranium lines.

39. Elevating precision: High-resolution spectroscopy with the Fabry-Perot wavelength calibration

Shubhendra Nath Das¹, Kapil Kumar¹, Abhijit Chakraborty¹, Rishikesh Sharma¹, Prasad Neelam¹ 1A&A Division, Physical Research Laboratory, Ahmedabad
E-mail: shubhendra@prl.res.in

The radial velocity (RV) technique stands out as the leading tool for discovering extra-solar planets, achieving precision below or equal to the sub-meter per second. This advancement has expanded detection capabilities to super-Earths, yet realising the identification of Earth-like planets necessitates reaching a precision of approximately 10 cm/s or below. Overcoming instrumental limitations, particularly in wavelength calibration, becomes crucial. Emission lamps, with uneven line distributions and limited coverage, pose challenges, exacerbated by the scarcity of pure uranium or thorium hollow cathode lamps. Seeking alternatives, molecular absorption cells, Fabry-Perot etalon (FP), and laser frequency combs (LFC) are popular calibration methods. While LFCs are infrequently used due to their high cost and complexity, FP etalon, demonstrated to achieve 10 cm/s stability in a controlled environment during one night[1][2], emerges as a promising alternative.

Here at PRL, with our state-of-the-art spectrograph, PARAS-2[3], we intend to employ FP etalon as the method for wavelength calibration. This approach aims to enhance RV precision and potentially enables the exploration of low-mass planets orbiting F, G, and K-type stars. We are currently in the design phase of this instrument. In this oral presentation, we will present the calculations and considerations involved in selecting the FWHM and free spectral range parameter of the FP etalon. Additionally, we will address aspects such as pressure and temperature stability, along with mechanical stability and operating pressure as well[4].

Furthermore, we have conducted simulations to assess the radial velocity (RV) precision limited by the fundamental photon noise, when using this FP etalon with PARAS-2. We have achieved an RV precision of the order of 1 cm/s, with this we aspire to achieve RV precision less than or equal to 20 cm/s on brighter targets.

References:

- [1]Wildi, F., Pepe, F., Chazelas, B., Lo Curto, G., & Lovis, Ch. (2010). "A Fabry-Perot calibrator of the HARPS radial velocity spectrograph: performance report." In *Ground-based and Airborne Instrumentation for Astronomy III*, Proceedings of SPIE, Vol. 7735, Article ID 77354X. Doi: 10.1117/12.857951.
- [2]Wildi, F., Chazelas, B., & Pepe, F. (2012). "A passive cost-effective solution for the high accuracy wavelength calibration of radial velocity spectrographs." In *Ground-based and Airborne Instrumentation for Astronomy IV*, Proceedings of SPIE, Vol. 8446, Article ID 84468E. doi: 10.1117/12.926841
- [3]Chakraborty, A., Thapa, N., Kumar, K., Neelam, P. J. S. S. V., Sharma, R., & Roy, A. (2018). "PARAS-2 precision radial velocimeter: optical and mechanical design of a fiber-fed high resolution spectrograph under vacuum and temperature control." In C. J. Evans, L. Simard, & H. Takami (Eds.), *Ground-based and Airborne Instrumentation for Astronomy VII* (Vol. 10702, p. 107026G). Society of Photo-Optical Instrumentation Engineers (SPIE) Conference Series. doi:10.1117/12.2313055

[4]Cersullo, F., Wildi, F., Chazelas, B., & Pepe, F. (2017). "A new infrared Fabry-Pérot-based radial-velocity-reference module for the SPIRou radial-velocity spectrograph." *Astronomy & Astrophysics*, 601, A102. doi:10.1051/0004-6361/201629972.

40. Pushing the limits of precision RVs in the near-infrared and optical with HPF and NEID

S. Mahadevan¹, ¹Department of Astronomy and Astrophysics, The Pennsylvania State University, 525 Davey Lab, University Park, PA-16802, USA. Email: suvrath@astro.psu.edu

In this talk I will outline the path that led to the design choices of the Habitable Zone Planet Finder and NEID precision RV spectrometers, including lessons learnt from the PARAS instrument that impacted some of these choices. I will then discuss both the intrinsic stability of these instruments, the capability to precisely and accurately calibrate these drifts with laser frequency combs that both instruments are equipped with and discuss new calibration challenges (eg. chromatic etalon drifts) that these ultra-precise measurements are revealing. I will also discuss some recent discoveries with HPF, that challenge our understanding of planet formation theories around the lowest mass stars and discuss also efforts with HPF and NEID to understand and tackle stellar activity noise – including observations with the dedicated NEID Solar Telescope. Finally, I will discuss how discoveries emerging from HPF and NEID have led to large follow-up programs with JWST, highlighting the synergy of ground and space in addressing compelling questions of planet formation and planetary atmospheres.

41. The PLATO mission and the full characterisation of planetary systems

Stephane Udry Geneva Observatory, Switzerland

PLATO (PLAnetary Transits and Oscillations of stars) is an ESA space-based photometric mission whose primary focus is the detection and characterisation of transiting Earth-like planets out to the habitable zone of Sun-like stars. The payload of PLATO will carry 24 normal and 2 fast cameras, where the former will operate in white light and take images of the sky every 25 seconds while the latter will include colour information and operate at a sampling of 2.5 sec.

PLATO will be launched towards the end of 2026 and will deliver observations of hundreds of thousands stars in two long pointing fields (nominal mission) of 2232 squared degrees for a total duration of minimally two years each. The required photometric precision of the PLATO instrument is 50 ppm in 1 hour for stars brighter than $m_V = 11$. These performances completed with a dedicated ground-based follow-up will provide planetary and stellar masses, radii, and ages of asteroseismically active hosts with a precision better than 15%, 2%, and 10%, respectively (for a $m_v = 10$ G0V reference star). These values will allow for the characterisation of the internal composition of individual planets, studies of statistical properties of planet population, as well as the full characterisation of planetary systems taking advantage of complementary detection methods and a deep understanding of planetary dynamics. In addition to the core science, the PLATO mission will also have a rich complementary science program open to the worldwide community via Guest Observer calls, with the ultimate goal to maximise the scientific return of the mission.

42. Curious case of two Extreme Density Close-in Giant Planets TOI-1789b and TOI-4603b around Evolved Stars

Authors: Akanksha Khandelwal¹, Rishikesh Sharma¹, Abhijit Chakraborty¹, Priyanka Chaturvedi², Sanjay Baliwall¹ et al.

¹ Physical Research Laboratory, Ahmedabad

² Thüringer Landessternwarte Tautenburg, Sternwarte 5, 07778 Tautenburg, Germany

Hot Jupiters (with $MP > 0.25MJ$) were the first kind of exoplanets discovered around the stars and surprised us with their presence in close-in orbits ($P < 10$ days). They are a perfect example of how exoplanets have challenged planetary system formation and evolution theories. Despite more than twenty-eight years since the first hot Jupiter discovery, these intriguing giants remain poorly understood. Of particular interest are hot Jupiters around evolved stars, a subset more captivating due to the potential engulfment of planets by their host stars. Currently, the count of such hot Jupiters is limited to 90, comprising a mere 2% of the total known exoplanets. These planets exhibit a wide range of diversity in density, and many of these (including main-sequence counterparts) have inflated radii, presenting challenges to existing theoretical models.

At PRL, we initiated an exoplanet search program around evolved stars utilizing the PRL's high-resolution spectrograph PARAS-1 and PRL 1.2m telescope, which led to the discovery of two such planets, TOI-1789b and TOI-4603b. These planets possess masses of 0.70MJ and 12.89MJ and sizes of 1.44RJ and 1.004RJ, respectively, standing TOI-1789b an inflated (ρ of 0.28 cgs) hot Jupiter and TOI-4603b one of the most dense (ρ of 14.1 cgs) exoplanets. These diverse properties make them particularly interesting for further exploration. We will discuss the detailed results related to the discovery and characterization of these systems and will show how much more needs to be understood about these systems. The imperative to deepen our understanding of such planetary systems and their evolution in the later stages of stellar evolution motivates the detection of hot Jupiters around evolved stars. The program will be continued with PARAS-2 on the PRL 2.5m telescope as well.

43. PUSHING THE BOUNDARIES OF PLANET DETECTION IN THE RADIAL VELOCITY METHOD USING ARTIFICIAL INTELLIGENCE

Anoop Gavankar¹, Tanish Mittal², Joe Philip Ninan¹, Shravan Hanasoge¹

1. Department of Astronomy and Astrophysics, Tata Institute of Fundamental Research, Mumbai, Maharashtra, India-400005
2. Tanish Mittal, Birla Institute of Science and Technology, Pilani, Rajasthan, India-333031

Instruments for measuring radial velocity are now fast approaching the precision required for detecting earth-like exoplanets. However, at this precision, another source of noise becomes relevant: the parent star itself. Disentangling the signatures of spurious radial velocity changes because of fluid

flows in the photosphere is a complicated, multidimensional problem. Traditional methods, while successful to some extent, have not been able to make use of all the hidden information in the spectrum. Identifying hidden patterns and exploiting higher-order correlations is where machine learning algorithms shine. We used the NEID solar data observations spanning the period 2020 to 2022 for training the network and for the injection recovery tests. During this period, the stellar jitter had an rms value of 1.77 m/s. We show our machine learning-based algorithm can recover planetary signal periods and semi-amplitudes down to 95 cm/s in semi-amplitude, with high accuracy(>76%). They perform well for very low amplitude signals(up to 65 cm/s), even with irregularly spaced observations containing real stellar noise from the Sun, showcasing the potential of AI in EPRV studies.

[1] Lily L. Zhao, Debra A. Fischer, Eric B. Ford et al., The EXPRES Stellar Signals Project II. State of the Field in Disentangling Photospheric Velocities, *The Astronomical Journal* 163:171, (2022 April)

[2] Zoe L. de Beurs, Andrew Vandenburg et al., Identifying Exoplanets with Deep Learning. IV. Removing Stellar Activity Signals from Radial Velocity Measurements Using Neural Networks, *The Astronomical Journal* 164:49, (2022)

[3] Andrea S. J. Lin et al., Observing the Sun as a Star: Design and Early Results from the NEID Solar Feed, *The Astronomical Journal* 163:184, (2022)

44. The Large Fiber Array Spectroscopic Telescope: A scalable ELT targeting Earth-like exoplanet atmospheres

C. F. Bender¹ and the LFAST Team, ¹Steward Observatory, University of Arizona, 933 N Cherry Ave, Tucson, AZ, 85721, USA, cbender@arizona.edu

The Large Fiber Array Spectroscopic Telescope (LFAST) is currently being designed and prototyped at the University of Arizona's Steward Observatory in Tucson, Arizona. LFAST's primary objective is to provide large and scalable collecting area, equivalent to or greater than other Extremely Large Telescopes (ELTs) currently under construction, but at a dramatically reduced cost per square-meter of aperture. LFAST will be dedicated to scientific investigations that require spectroscopy at very large signal-to-noise or of very faint targets. In particular, LFAST will be well suited to characterizing the atmospheric chemistry of transiting exoplanets, including searching for bio-signatures in Earth-like planets with the goal of assessing habitability. The telescope will also be well suited to a variety of other exoplanet and non-exoplanet science cases across astronomy.

LFAST is an array telescope, and will combine the light from hundreds or thousands of individual "unit telescopes" into a single spectrograph. Each unit consists of a prime focus telescope with a 0.76-m diameter spherical primary mirror and a refractive prime focus corrector. One element of the corrector can move to compensate for both atmospheric dispersion and high-frequency jitter from windshake and seeing. Each telescope will feed a fused silica fiber with an 18-micron diameter core, corresponding to 1.4-arcsec on the sky, which will carry light to the spectrograph. Twenty units will be mounted in a steel frame on a common alt-az mount, providing 9 m² of collecting area. An array of 10 such systems will collect light equivalent to a traditional 10-m telescope; 132 systems will provide area slightly larger than the E-ELT.

Over the past two years we have designed and constructed a prototype unit telescope, and have been testing the system on-sky. Construction of a prototype 20-unit system is currently underway, and on-sky testing is planned for the second half of 2024. I will discuss the scientific opportunities offered by an inexpensive, scalable array telescope such as LFAST, provide a status update on our development progress, and describe our plans for the future development of large, multi-system arrays.

45. Precise inference of limb-darkening using a regularization technique: application for a sample of *Kepler* and TESS exoplanet transit light curves

K. Verma¹, P. F. L. Maxted², A. Singh¹ and Y. Sable¹, ¹Department of Physics, Indian Institute of Technology (BHU), Varanasi-221005, India (kuldeep.phy@itbhu.ac.in), ²Astrophysics group, Keele University, Staff, ST5 5BG, UK (p.maxted@keele.ac.uk).

Introduction: The contemporary high-precision measurements of the exoplanet transit light curves contain information about the planet properties, orbital parameters, and the stellar center-to-limb brightness variation (or the limb-darkening). Since the limb-darkening parameters typically have correlations with the other planet and orbital properties, it is important to measure them as precisely and accurately as possible. Furthermore, recent studies have shown that the limb-darkening profile depends on the mean magnetic field in the photosphere [1], and hence its precise determination can help us constrain the surface magnetic field. A number of limb-darkening laws with varying complexity have been proposed and used in the literature. The simplest of those may provide biased estimates of planetary and orbital properties [2], whereas the use of complex laws leads to substantial degeneracy among the limb-darkening parameters resulting in large uncertainty on them [3]. We have developed a new approach in which we use a reasonably complex limb-darkening model, the so-called Claret 4-parameter law, but with second derivative regularization during the fitting process [4]. Regularization helps in avoiding the over-fitting of data and leads to significantly reduced correlations among the limb-darkening parameters. We have used this new technique to re-analyze a sample of 43 exoplanet transit light curves observed by the NASA *Kepler* and TESS missions. In this presentation, I shall briefly discuss our fitting method, present a summary of the main results, and also point out the implications of our work in precisely measuring the exoplanet radii by the upcoming ESA PLATO mission.

References: [1] Ludwig et al. (2023) *Astronomy & Astrophysics* 679:A65. [2] Espinoza N. and Jordán A. (2016) *Monthly Notices of the Royal Astronomical Society* 457:3573–3581. [3] Maxted P. F. L. (2023) *Monthly Notices of the Royal Astronomical Society* 519:3723–3735. [4] Verma K. et al. (2024) *in prep.*

46. A search for auroral radio emission from β Pictoris b.

Yuta Shiohira¹, Yuka Fujii², Hajime Kita³, Tomoki Kimura⁴, Yuka Terada^{5,6}, and Keitaro Takahashi^{1,7} ¹Graduate School of Science and Technology, Kumamoto University, Kumamoto, Japan, ²National Astronomical Observatory of Japan, Tokyo, Japan, ³Tohoku Institute of Technology, Sendai, Japan, ⁴Tokyo University of Science, Tokyo, Japan, ⁵Institute of Astronomy and Astrophysics, Academia Sinica, Taipei, Taiwan, R.O.C., ⁶Department of Astrophysics, National Taiwan University, Taipei, Taiwan, R.O.C., ⁷International Research Organization for Advanced Science and Technology, Kumamoto University, Kumamoto, Japan

Abstract:

Measuring the magnetic fields of exoplanets can enhance our understanding of their intrinsic characteristics, including atmospheric escape and interior structure[1]. Because magnetized exoplanets would be the source of the auroral radio emission, observing this emission potentially enables us to constrain the strength of the planetary magnetic field[2]. So far, successful detections of auroral radio emissions from brown dwarfs, as well as from Jupiter[3], suggest that Jupiter-like planets in distant orbits may also generate radio emissions through a similar mechanism.

In this presentation, we present our search for 250-500 MHz emissions from β Pictoris b, one of the most extensively studied young Jupiter-like planets[4]. We conducted the search using the upgraded Giant Metrewave Radio Telescope (uGMRT). Despite a favorable orbital inclination, no signal was detected, putting 3σ upper limits on the radiation at 0.18 mJy. We translate this limit into constraints on the ionospheric and magnetospheric parameters, assuming that the emission is powered by the Hill current system. We will discuss the constraints on these parameters.

Reference:

- [1] Lazio J. et al., (2019) Bulletin of the American Astronomical Society, Vol. 51, Issue 3, id. 135
- [2] Zarka P. et al., (2001) Astrophysics and Space Science, v. 277, Issue 1/2, p. 293-300
- [3] Kao M. M. et al., (2016) The Astrophysical Journal, Volume 818, Issue 1, article id. 24, 17 pp.
- [4] Shiohira Y. et al., (2023) Monthly Notices of the Royal Astronomical Society, Advance Access

47. A NUMERICAL TRANSIT SIMULATOR FOR GENERATING LIGHTCURVES OF TRANSITING OBJECTS WITH WEIRD GEOMETRIES

Ushasi Bhowmick¹, ¹Affiliation (Space Application Centre, ISRO, Ahmedabad; ushasibhowmick@sac.isro.gov.in)

Introduction: The transit method is one of the most efficient means to identify exoplanets because of its simplicity. The increasing sensitivity and resolution of space-based telescopes like Kepler Space Telescope [1] and Transiting Exoplanet Survey Satellite (TESS) [2] have led to a shift from the identification of exoplanets to the in-depth study of its characteristics from transit photometry. A number of natural phenomena such as tidal distortions, apsidal precession, disintegrating systems have been identified from the deviations in the transit lightcurve from the standard exoplanet model (*Mandel and Agol (2002)* [3]).

In this work, we design a Monte-Carlo based transit simulator that numerically evaluates the transit lightcurve of a transiting object with any arbitrary input geometry. We demonstrate this as a suitable visualization for complex systems, by simulating the transit of tidally distorted exoplanets and eccentric eclipsing binaries. The simulator will enable a better analysis of the datasets of Kepler and TESS in its entirety. This also extends to further upcoming satellites. We show that we can simulate transits that arise due to hypothetical megastructures constructed by advanced extraterrestrial civilizations, using the case of a 2-D space mirror or solar-panel like structure. Therefore, this is a useful tool for finding technosignatures through transit photometry.

References:

- [1] Borucki, W. J., Koch et al. (2010). Kepler planet-detection mission: introduction and first results. *Science*, 327(5968), 977-980.
- [2] Ricker, G. R., Winn et al. (2015). Transiting exoplanet survey satellite. *Journal of Astronomical Telescopes, Instruments, and Systems*, 1(1), 014003-014003.
- [3] Mandel, K., & Agol, E. (2002). Analytic light curves for planetary transit searches. *The Astrophysical Journal*, 580(2), L171.

48. UNVEILING AND EXPLORING THE ATMOSPHERIC COMPOSITION OF SUPER-EARTH EXOPLANETS IN THE JWST ERA

Priyankush Ghosh¹ and Liton Majumdar²

Exoplanets and Planetary Formation Group, School of Earth and Planetary Sciences

National Institute of Science Education and Research, Jatni 752050, Odisha,

India 1 [2priyankush.ghosh@niser.ac.in](mailto:priyankush.ghosh@niser.ac.in), liton@niser.ac.in

Until recently, we have explored a vast array of planetary diversity through the detection of planets beyond our solar system. With the introduction of the James Webb Space Telescope (JWST), we have ushered in a new era, enabling us not only to detect exoplanets but also to characterize their atmospheres. This capability marks a crucial step in our understanding of the formation of the solar system itself. In this presentation, I will delve into two key aspects: (1) Nitrogen and Sulfur-based chemistry, and (2) Outgassing chemistry of the ultra-short-period rocky exoplanet 55 Cancri e. This planet has been observationally confirmed to host an atmosphere consisting of high mean molecular weight species and will be subject to observation using the JWST. I will introduce our cutting-edge, in-house forward exoplanet atmosphere model, which integrates radiative transfer under radiative-convective equilibrium with melt-vapor equilibrium and photo-chemical kinetics. This model explains the constraints on the physical structure of the atmosphere and its chemistry, considering variations in initial elemental abundances and eddy diffusivities. The presentation will be complemented by simulated transmission and emission spectra of the atmosphere of 55 Cancri e, highlighting the potential detectability of its modeled spectroscopic signatures using JWST. Gaining insights into the composition of such atmospheres will provide valuable information on the possible locations and environments in which these types of planets are likely to have formed in the protosolar nebula.

49. Exocomets, 35 years of discoveries

A. Lecavelier des Etangs¹,

¹Institut d'astrophysique de Paris, CNRS, 98bis boulevard Arago, 75014 PARIS, FRANCE

Transiting extrasolar comets have been observed for 35 years. The gas component of the evaporating comets has been first revealed using spectroscopy. Along the years, a very large number of observed lines provided information on the physical state of the gas. Statistical studies of hundreds of exocomets transiting the young star Beta Pictoris showed the presence of two different orbital families pointing toward two different origins of these small bodies [1].

Recently, the photometric accuracy of Kepler and TESS allowed to detect the dust tails of the transiting exocomets. The observed transit light curves look very similar to what was predicted 20 years ago [2]. Using TESS photometry, we discovered 30 exocomets transiting Beta Pictoris and derived the comets nuclei sizes [3]. The observed size distribution is strikingly similar to the one of the comets and asteroids in the Solar system. With a power law index of -3.5, this shows the importance of collisions and fragmentations in the late stages of the planetary formation.

To progress in this field, new observations of exocomets in a larger sample of planetary system is required. Observations with ground-based facilities to search for new exocometary systems must be undertaken ; Indian facilities, including PARAS and PARAS-2, can play a role in this domain.

References:

- [1] Kiefer F., Lecavelier des Etangs A., et al. (2014) *Nature* 514, 462
- [2] Lecavelier des Etangs A., et al. (1999) *Astronomy & Astrophysics* 343, 916
- [3] Lecavelier des Etangs A., et al. (2022) *Nature Scientific Report* 12, 5855

50. Exoplanet Demographics: Insights into Planet Formation Mechanisms and History

Manoj Puravankara¹, Mayank Narang², and Bihan Banerjee¹

¹ Tata Institute of Fundamental Research, Homi Bhabha Road, Mumbai – 400005

² Academia Sinica Institute of Astronomy & Astrophysics, 11F Astro-Math Bldg., No.1, Sec. 4, Roosevelt Rd., Taipei 10617, Taiwan Email: manoj.puravankara@gamil.com, mpuravankara@gmail.com

Abstract:

In the past three decades, astronomers have made remarkable strides in uncovering the vast population of exoplanets – planets orbiting stars other than our Sun. With the current count of confirmed exoplanets exceeding 5500, it is now possible to carry out detailed and statistically meaningful studies of planet properties (e.g. radius, mass) and planetary system architecture (e.g. orbital period, eccentricity) and how they are linked to the host star properties (spectral type, metallicity, and age). Results from such studies are beginning to challenge our traditional notions about planet formation that have been historically shaped by the observed properties of our solar system. In this talk, I will first present our recent results on the dependence of planet properties with host star metallicity: the host star metallicity dependence is different for Jupiters and super-Jupiters, indicating different formation mechanisms. I will then present our study on the dependence of planet properties with host star age. Our analysis shows that Jupiters are relatively young in our Galaxy, having formed in the last 6-7 Gyr after significant metal enrichment of the ISM. I will discuss our results and, in combination with the stellar metallicity-age relation, examine planet formation in the context of galactic evolution.

References:

[1] Narang, M., P. Manoj et al. 2018, AJ, 156, 221

[2] Narang, M., P. Manoj et al. 2024, MNRAS, under review

51. Age Distribution of Exoplanet Host Stars: Chemical and Kinematic Age Proxies from GAIA DR3

C. Swastik^{1,2}, Ravinder K. Banyal¹, Mayank Narang³, Athira Unni⁵, Bihan Banerjee⁴, P. Manoj, and T. Sivarani.

1. Indian Institute of Astrophysics, Koramangala 2nd Block, Bangalore 560034, India;
swastik.chowbay@iiap.res.in

2. Pondicherry University, R.V. Nagar, Kalapet, 605014, Puducherry, India

3. Academia Sinica Institute of Astronomy & Astrophysics, 11F of Astro-Math Building, No. 1, Section 4, Roosevelt Road, Taipei 10617, Taiwan, Republic of China

4. Department of Astronomy and Astrophysics, Tata Institute of Fundamental Research Homi Bhabha Road, Colaba, Mumbai 400005, India 5 Aryabhata Research Institute of Observational Sciences, Manora Peak, Nainital 263002, Uttarakhand, India

Abstract

The GAIA space mission is impacting astronomy in many significant ways by providing a uniform, homogeneous, and precise data set for over 1 billion stars and other celestial objects in the Milky Way and beyond. Exoplanet science has greatly benefited from the unprecedented accuracy of the stellar parameters obtained from GAIA. In this study, we combine photometric, astrometric, and spectroscopic data from the most recent Gaia DR3 to examine the kinematic and chemical age proxies for a large sample of 2611 exoplanets hosting stars whose parameters have been determined uniformly. Using spectroscopic data from the Radial Velocity Spectrometer on board GAIA, we show that stars hosting massive planets are metal-rich and α -poor in comparison to stars hosting small planets. The kinematic analysis of the sample reveals that stellar systems with small planets and those with giant planets differ in key aspects of galactic space velocity and orbital parameters, which are indicative of age. We find that the galactic orbital parameters have a statistically significant difference of 0.06 kpc for Z_{\max} and 0.03 for eccentricity, respectively. Furthermore, we estimated the stellar ages of the sample using the MIST-MESA isochrone models. The ages and their proxies for the planet-hosting stars indicate that the hosts of giant planetary systems are younger when compared to the population of stars harboring small planets. These age trends are also consistent with the chemical evolution of the galaxy and the formation of giant planets from the core-accretion process.

52. Investigating the influence of clouds on the reflectance spectra of exo-Earths using the HWO mission concept

Soumil Kelkar^{1,2}, Dr. Ravi Kopparapu², and Dr. Prabal Saxena²

¹Indian Institute of Science, Education and Research, Pune (email – soumil.kelkar@students.iiserpune.ac.in)

²NASA Goddard Space Flight Center, Maryland

Introduction: A primary goal of the upcoming Habitable Worlds Observatory (HWO) is to identify and characterize Earth-like exoplanets through reflected light spectroscopy. However, a planet's spectrum is dynamic and represents a time-dependent snapshot of its properties. Changing atmospheric conditions due to climate and weather patterns, particularly variation in cloud cover can significantly affect the spectrum in ways that complicate an understanding of a planet's baseline atmospheric properties. Variable cloud patchiness and cloud properties affect the detectability of atmospheric constituents [1,2], and also greatly influence the radiative transfer that determines a planet's spectrum. This has considerable implications for observations of potentially habitable exoplanets and thus it is critical to study and characterize the effects of clouds on their spectra. In this work, we construct accurate models of exo-Earths using NASA's MERRA-2 dataset [3] which assimilates data from a variety of satellites orbiting Earth. Utilizing the Planetary Spectrum Generator (PSG) [4], we simulate observations of these exo-Earths at different orbital and rotational phases and inclinations using the HWO mission concepts [5,6]. We identify periods of significantly high/low cloud coverage on Earth, construct exo-Earth atmospheres with a similar cloud distribution, and quantify the variations in the simulated spectra for these periods. Our findings also quantify the effects of clouds on the detectability of atmospheric constituents, specifically biomarkers like O₂, O₃, H₂O, etc. Through this work, we are developing a comprehensive suite of 'cloudy' spectra that will be vital in making accurate atmospheric retrievals and determining the optimal observation strategies for the HWO mission.

References:

- [1] Komacek T.D., Fauchez T.J., Wolf E.T and Abbot D.S (2020) *The Astrophysical Journal* 888 L20
- [2] Line M.R. and Parmentier V. (2016) *The Astrophysical Journal* 820 78
- [3] Gelaro R. et al (2017) *Journal of Climate* 30:5419—5454
- [4] Villanueva G.L., Smith M.D, Protopapa S., Faggi S., and Mandell A.M (2018) *Journal of Quantitative Spectroscopy and Radiative Transfer* 217:86—104
- [5] The LUVOIR Team (2019) *arXiv* 1912.06219
- [6] The HabEx Team (2020) *arXiv* 2001.06683

53. First measurement of seasonal variations of surface pressure over Hellas and Argyre basins from EMIRS on board EMM: Comparison with MCD model.

S. A. Haider¹, Siddhi Y. Shah¹, Hessa R. Al Matroushi² and H. Almazmi³

¹Planetary Science Division, Physical Research Laboratory, Ahmedabad

²Mohammed Bin Rashid Space Centre, Dubai, UAE

³United Arab Emirates Space Agency, Abu Dhabi, UAE

Abstract

Replace Emirates Mars Mission (EMM) inserted in the Martian orbit on February 2021 (MY36, Ls=0.6) providing 9 sol of Emirates Mars Infrared Spectrometer (EMIRS) observations. EMM orbital period is ~55 hour with a periapsis of 20000 km and an apoapsis of 43000 km. About 20 observations are taken in one orbit with one observation in 20 min at periapsis and 11 min at apoapsis. EMIRS measure the temperature, pressure and dust optical depth at all latitudes and longitudes. We have studied seasonal variability of surface pressures in northern and southern hemispheres. The diurnal variability of surface temperature is also studied in both hemispheres during the spring, summer, autumn and winter seasons. These observations are compared with Mars Climate Database (MCD) model. We report first measurement of atmospheric pressures ~13.0 mbar and 9.0 mbar over Hellas (42.4°S, 70.5°E) and Argyre (49.75°S, 316°E) basins respectively. This pressure is 50 % higher than the averaged pressure ~ 6.1 mbar. In southern hemisphere the average temperatures on the Mars' surface are observed to be ~300°K and ~160°K during the summer and winter seasons respectively. Thus, the temperature values plummet by ~ 140°K in the southern winter of Mars. In northern hemisphere the average temperatures on Mars' surface are observed to be ~ 270°K and ~150°K during the summer and winter seasons respectively. The temperature in southern hemisphere is higher than the northern hemisphere by ~20°K at all latitudes.

54. SUPRATHERMAL ELECTRON DEPLETIONS IN THE MARTIAN NIGHTSIDE UPPER ATMOSPHERE: ROLE OF MAGNETIC FIELD TOPOLOGY AND INDUCED MAGNETIC FIELDS

Pavan D. Gramapurohit¹, N.V. Rao¹

¹National Atmospheric Research Laboratory, Gadanki, India

pavandgp@gmail.com

Abstract

Understanding the interactions between the solar wind and planetary ionospheres is crucial for deciphering the complex dynamics of upper atmospheres. In the case of Mars, the absence of global magnetic fields allows direct interaction between the solar wind and the planetary atmosphere. The lack of photoionization on the Mars nightside ionosphere results in the depletion of suprathermal electrons. Previous studies have investigated the dependence of suprathermal electron depletions on the solar zenith angle, strength of the magnetic fields, and the solar wind dynamic pressure. In this study, we explore the role of induced magnetic fields and magnetic field topologies in the depletions. To investigate this, we used comprehensive sets of measurements from different scientific instruments on the Mars Atmosphere and Volatile EvolutionN (MAVEN) spacecraft during 2015 to 2019 within an altitude range of 200 km to 900 km.

We observed a pronounced dependence of suprathermal electron depletion occurrences on the strength of crustal magnetic fields, with strong field regions (>20 nT) exhibiting higher depletions than weak field regions (<10 nT). These results are concurrent with previous studies. The calculated magnetic field topologies along adjacent non-depleted regions provide critical insights, demonstrating that strong magnetic field regions favor closed fields at lower altitudes and draped fields at higher altitudes, while weak magnetic field regions showcase the dominance of open and draped fields. In strong magnetic regions, an increase in solar wind dynamic pressure leads to the compression of closed fields and a slight reduction in depletions. Weak crustal magnetic field regions lead to more opening of cusp regions, facilitating solar wind electron precipitation and resulting in a significant reduction in electron depletions. The induced magnetic field strength is enhanced in weak magnetic field regions compared to strong magnetic field regions and during strong solar wind dynamic pressures. This study highlights the importance of solar wind electron precipitation in the Martian nightside plasma environment and its role in suprathermal electron depletions.

55. Electromagnetic Ion Cyclotron wave with magnetic model in Jovian Magnetosphere.

Sankalp Jain¹ and R.S Pandey² , 1 Department of Physics, Amity Institute of Applied Science, Amity University, Sector – 125 Noida, Uttar Pradesh, India and sankalp.jain@s.amity.edu , 2Department of Physics, Amity Institute of Applied Science, Amity University, Sector – 125 Noida, Uttar Pradesh, India and rspandey@amity.edu.

Introduction: The analysis based on observations by Ulysess of Electromagnetic Ion Cyclotron (EMIC) wave in Jovian magnetosphere has been done in this paper. In Jovian's magnetosphere it has been observed that there are various types of large frequency radio emissions by the mechanism of resonant interaction. This paper we have considered the phenomenon of wave-particle interactions between EMIC wave along the magnetic field lines and fully ionized magnetospheric plasma particles with parallel propagation of wave which evaluates the elaborated dispersion relation for ring distribution finding also with and without magnetic field model. Using the method of characteristics solution and kinetic approach, expression of growth rate has been derived. Following a parametric examination of the plasma's temperature anisotropy, thermal velocity, and number density, the impact of these variables on growth rate was examined using graphs. **Keywords** Electromagnetic Ion cyclotron waves, Ring Distribution, Magnetic model, Jovian magnetosphere.

56. INTERPLANETARY DUST FLUX AT DIFFERENT PLANETS IN INNER SOLAR SYSTEM

J. P. Pabari*, S. N. Nambiar, Rashmi, S. Jitarwal and Aanchal Sahu, Physical Research Laboratory, Navrangpura, Ahmedabad – 380009, India. *E-mail: jayesh@prl.res.in

Introduction: The dust in solar system is found everywhere in the interplanetary space. The Interplanetary Dust Particles (IDPs) start their journey from a source like Asteroid belt or comets. The evolution of IDP could be over geological time scales to reach a planet [1], for example from Asteroid belt to Mars. Towards Venus, the scenario is complex due to occasional comets leaving particles because of sublimation of ice. Further, the nongravitational forces like P-R drag [2] are important in the dust particle evolution. Some direct or indirect observations of dust were taken by various instruments [3-8] onboard satellites. It can help understand the flux variation in the solar system. Recently, Solar Orbiter [9] has given dust impact observations using Radio and Plasma Wave (RPW) instrument during inward and outward movement towards Sun. The results of dust flux at various planets in inner solar system will be discussed.

References: [1] Pabari et al., (2021), 52nd LPSC, LPI Contrib. No. 2548, #1430. [2] Gor'kavyi, N. N. et al. (1997), ApJ, 474, 496. [3] Stenborg, G. et al. (2021), ApJ, 910:157, 13. [4] Andersson, L. et al. (2015), Science, 350, 6261, aad0398. [5] Hirai, T. et al. (2014), PSS, 100, 87-97. [6] Hirai, T. et al. (2017), ASR, 59, 1450-1459. [7] Dietzel, H. et al. (1973), J. Phy. E: Sci. Inst., 6, 209-217. [8] Krueger, H. et al. (2010), GO-D-GDDS-5-DUST-V4.1, NASA PDS. [9] Zaslavsky, A. et al. (2021), A & A, 656, A30.

57. ELECTROSTATIC CHARGING NEAR THE LUNAR POLAR REGION.

T. Sana^{1,2} and S. K. Mishra², ¹Indian Institute of Technology, Gandhinagar, 382055, India (sanatrinesh@gmail.com), ²

Physical Research Laboratory, Ahmedabad, 380009, India.

Exploration of the polar region of the Moon is a highly intriguing focal point in the current lunar research. After the recent success of Chandrayaan 3, the lunar community aspired to conduct long-term in situ measurements near the polar region of the Moon. Since the spin axis of the Moon is nearly perpendicular to the ecliptic plane and the existence of elevation variability, certain areas near the poles experience extreme variations in illumination. Many polar impact crater floors remain in permanent darkness, while elevated regions could potentially receive continuous sunlight [1-2]. These areas lacking direct sunlight experience extreme cold temperatures. These permanently shadowed cold traps reside just adjacent to sunlit regions, enabling the collection of migrating volatile substances as they transition into darkness. Since the lunar surface undergoes electrostatic charging due to UV-induced photoemission and solar wind /ambient plasma collection, these locations are electrically complex regions [3-4]. Due to dominant photoemission, the sunlit surface acquires positive potential; however, the darker region becomes negatively charged because of electron accretion from the solar wind/ambient plasma. So, the surface experiences a significant shift in potential, transitioning from the illuminated to the darker side of this location. This potential shift due to topographic shielding within a very small region creates a sufficiently large electric field (Figure 1), which may give rise to the electrostatic dust and volatile transport around this topographic region in the south pole region of the Moon. Since the permanently illuminated and shadowed region remains nearby, this large electric field sustained for a very long span of time, which may generate a local dust cloud around this region, associated with the large number of dust grains ejected from the surface and giving rise to migration of volatiles.

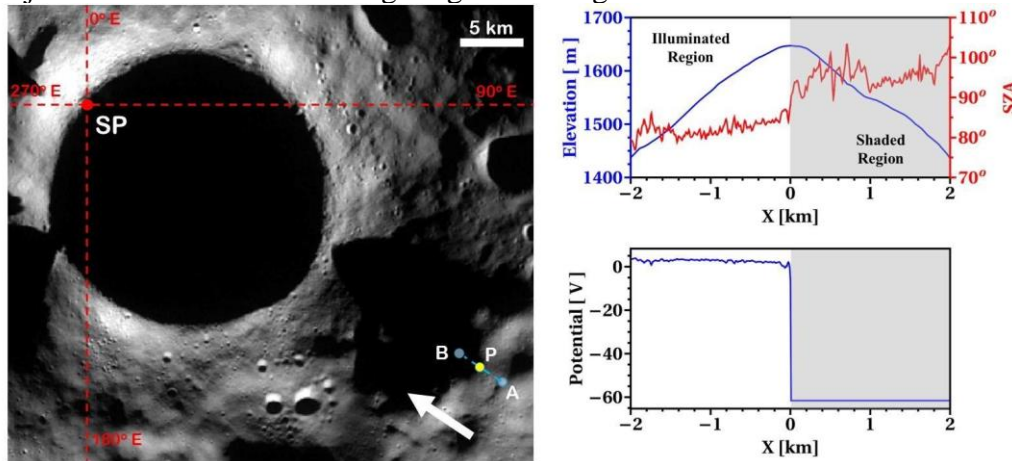


Figure 1. Left: The location of the Shackleton crater, in which the SP point indicates the location of the Lunar South Pole, and P is the location of 85.5% average solar illumination [2]. Line AB is the region of interest (spans 4 km) where the portion AP is illuminated, and PB is a shaded region. The arrow indicates the direction of solar illumination. Right: The top right figure indicates the elevation and variation of the solar zenith angle (SZA). Here, the horizontal distance is given with respect to point P. The bottom right figure indicates the surface potential at various locations of this topography. The surface acquires few positive potentials in the illuminated region, whereas in the darker side, the

surface acquires significantly high negative potential. The sharp potential shift in the sunlit shadowed boundary gives rise to an intense horizontal electric field, which is capable of electrostatic transport of dust and volatiles.

This presentation introduces underlying physics and the current understanding of the electrical environment of the lunar polar region. We also discuss ideas for test experiments for future lunar polar exploration missions based on our present knowledge.

References: [1] Bussey, D. B. J., Fristad, K. E., Schenk, P. M., Robinson, M. S., & Spudis, P. D. (2005). Constant illumination at the lunar north pole. *Nature*, 434(7035), 842-842. [2] Mazarico, E., Neumann, G. A., Smith, D. E., Zuber, M. T., & Torrence, M. H. (2011). Illumination conditions of the lunar polar regions using LOLA topography. *Icarus*, 211(2), 1066-1081. [3] Manka, R. H. (1973), Plasma and potential at the lunar surface, in *Photon and Particle Interactions With Surfaces in Space*, edited by R.J.L. Grard, p. 347, D. Reidel, Dordrecht, Netherlands. [4] Farrell, W. M., Stubbs, T. J., Delory, G. T., Vondrak, R. R., Collier, M. R., Halekas, J. S., & Lin, R. P. (2008). Concerning the dissipation of electrically charged objects in the shadowed lunar polar regions. *Geophysical research letters*, 35(19).

58. DEVELOPMENT OF PROCESSING PACKAGES FOR AKATSUKI RADIO SCIENCE EXPERIMENT OF VENUS ATMOSPHERE.

A. Shyam¹, A. Upadhyay² and P. K. Thapliyal¹, ¹Space Applications Centre (Bopal (Old) Campus, Bopal, Ahmedabad-58, abhineetshyam@sac.isro.gov.in), ²Vellore Institute of Technology (Vellore campus, Vellore, Tamil Nadu).

Introduction: The ISRO-JAXA joint science collaboration beginning with acquisitions of radio science data at Indian Deep Space Station (IDSN-32) at Byalalu in March 2017 has provided the first-ever opportunity to the authors to get engaged in observations of atmosphere of planet Venus by radio occultation technique. Retrieval algorithm and package has been independently developed for deriving atmospheric parameters from residual Doppler to bending angle, refractivity, geopotential, neutral number density and finally, atmospheric temperature and pressure profiles in the neutral atmosphere of Venus. The algorithm is validated through cross-comparison with products derived by our counterpart team at JAXA [1]. However, inversion of raw data (Level-1) [1] available in standard RDEF data format to observed Doppler has been performed currently for the IDSN collection of AKATSUKI Venus radio science (RS) experiment for 20th July 2017. The Observed Doppler is derived for the entire duration of the experiment spanning almost an hour, albeit, the meaningful portions of observed Doppler measured when AKATSUKI scans the Venusian atmosphere in the ingress (spacecraft moving behind Venus) and egress (spacecraft emerging from behind Venus) phases comprise of only a few minutes. These phases are marked by the time series of the signal power. Figure 1 (top) shows the derived observed Doppler from the raw signals recorded at IDSN-32 at Byalalu and broken plot shows the period of occultation behind the Venus when spacecraft signal is cut-off by the Venus planetary disk. For the duration of the experiment, figure 1 (bottom) delineates the distribution of power (in absolute units) with characteristic fall during the ingress (beginning at 18383 seconds) and rise during the egress (starting at 20100 seconds). The time duration spent behind the planetary disk is marked by the zero power at the IDSN-32 antenna. The observed Doppler estimation takes into account the effect of broadening and corrections have been done for precise frequency location in the spectral signature. The package for inversion of observed Doppler to residual Doppler for AKATSUKI IDSN-32 collections is in progress and involve the forward modeling of theoretical Doppler while also accounting for the relativistic terms and correcting for background contribution using the baseline fit.

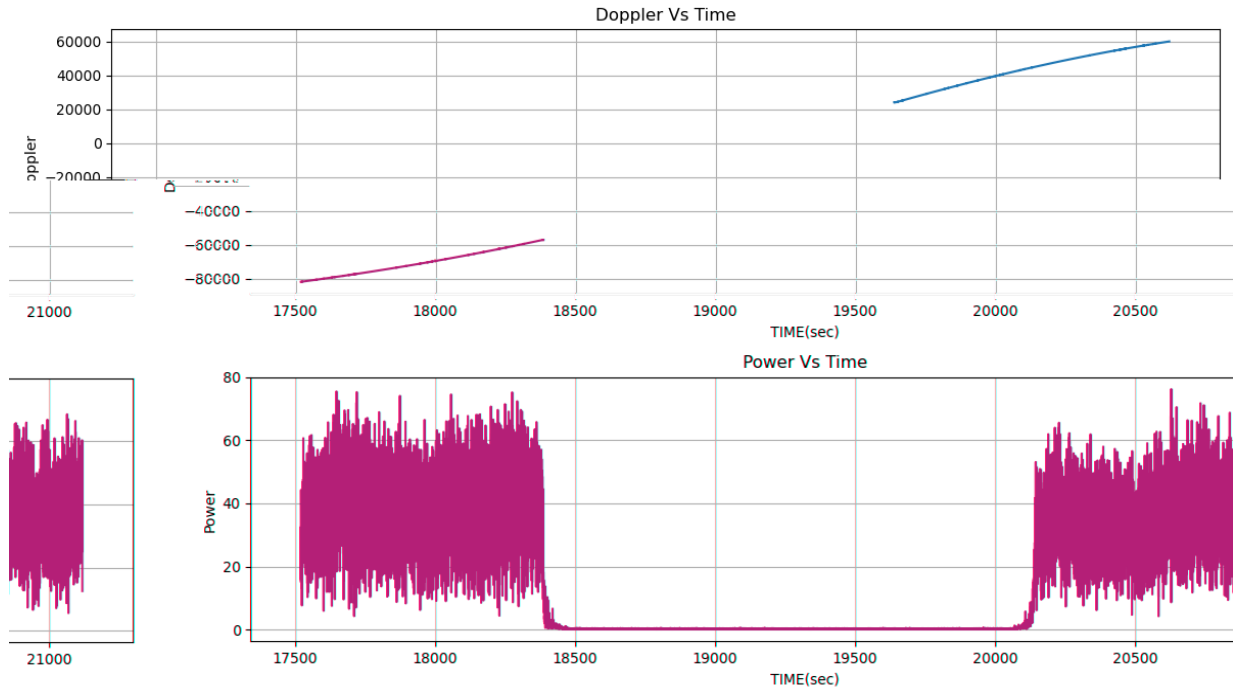


Figure 1. Observed Doppler (top) and power spectral density derived from raw prd data in RDEF format for AKATSUKI RS experiment on 20th July 2017 at IDSN-32 antenna at Byalalu.

References:

[1] Kleinbohl A. et al. (2023) vco_rs_sis_v10.pdf.

59. DEVELOPMENT OF A COAXIAL ROTOR SYSTEM FOR MARS EXPLORATION

Ajo Joseph Anto¹, Vellingiri Ramanujam R², Abraham George M³, Ranjith Mohan⁴ and Shamrao⁵

¹M.S Scholar, Dept. of Aerospace Engineering, IIT Madras, ²Research Associate, Dept. of Aerospace Engineering, IIT Madras, ³Project Associate, Dept. of Aerospace Engineering, IIT Madras, ⁴Associate Professor, Dept. of Aerospace Engineering, IIT Madras, ⁵Scientist/Engineer- 'SG', Space Mechanics Group, URSC - Bangalore

Introduction: The research focusses on the development of a helicopter rotor system for operation in the Martian atmosphere which is approximately 100 times less dense than Earth's atmosphere. On Mars, 98% of the atmosphere is composed of CO₂ and has an average surface temperature of 210K. In order for the helicopter to generate the necessary thrust at low density, a higher rotating speed of rotor is necessary which combined with low temperatures leads to a high Mach number flow. A coaxial helicopter rotor system is designed with aerodynamic profiles of the rotor blades being optimized for operation on Mars.

Experimental studies and Prototype development: A 2.4m vacuum chamber is set-up for simulating the atmospheric density on Mars. Experimental rotor is mounted on a test stand installed inside the chamber with an electric motor drive mechanism. Multi-axis loadcells are employed to measure the thrust and power. The test setup includes all essential components for the helicopter, although not optimized for weight. The experimental data consisting of thrust and power coefficients are compared with numerical results obtained from blade element momentum theory and RotCFD (a commercial tool that is specific for rotor applications and based on momentum source approach). Test data that brings out the effect of Reynolds number on propellers are also presented.

Keywords: Mars, Helicopter, Reynolds number, Mach number, BEMT, RotCFD

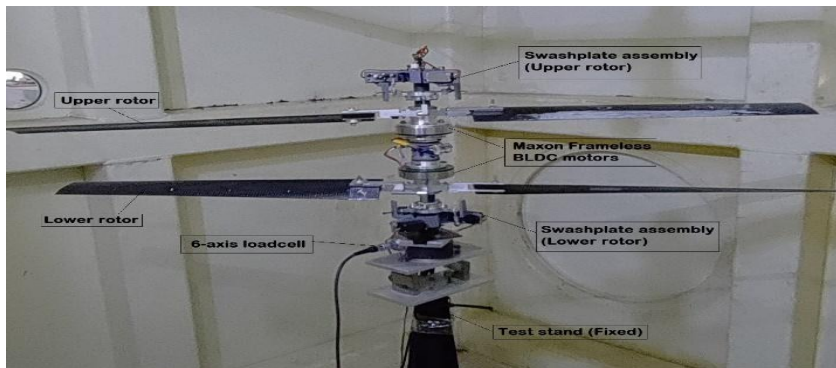


Figure 1: Coaxial rotor system prototype being tested inside a vacuum chamber.

References:

- [1] Young, L.A., et al. "Rotorcraft as mars scouts." Proceedings, IEEE Aerospace Conference. Vol. 1. IEEE, 2002.
- [2] J. Balam, et. Al. "Mars Helicopter Technology Demonstrator", 2018 AIAA Atmospheric Flight Mechanics Conference, AIAA 2018-0023.
- [3] Leishman, J. G., and Ananthan, S. "Aerodynamic Optimization of a Coaxial Proprotor," Proceedings of the 62nd Annual Forum of American Helicopter Society, Phoenix, AZ, May 2006.

60. THE SEARCH FOR LIFE ON EXOPLANETS: THE RELIABILITY OF O₂ AS A BIOSIGNATURE AND THE KEY ROLE OF UV SPACE TELESCOPES LIKE ASTROSAT AND INSIST

S. Ranjan¹

¹University of Arizona Lunar and Planetary Laboratory (Tucson, AZ 85719, USA; sukrit@arizona.edu)

Introduction: Exoplanet surveys have revealed temperate terrestrial planets to be common, and current (James Webb Space Telescope) and upcoming (Habitable Worlds Observatory) facilities will characterize their atmospheres in search of signs of life [1,2]. Oxygen (O₂) is the strongest biomarker of life in Earth's atmosphere, but scenarios have been put forward whereby abiotic mechanisms like photochemistry can abiotically generate high levels of O₂ (“false positive scenarios”) [3]. However, models are discrepant about these false positive scenarios: some models show O₂ false positives, while other models run under identical conditions find O₂ to be a robust biosignature gas [4,5].

Methods: We use model intercomparisons to determine the robustness of two of these O₂ false positive scenarios: the low-outgassing scenario and the M-dwarf scenario [5,6]. Our modeling illustrates the key role of molecular H₂O cross-sections and host star UV spectral energy distributions (SEDs) in controlling the buildup of biosignature gases: we use laboratory measurements to constrain the former, and explore the utility of ASTROSAT UVIT [7] to constrain the latter.

Results & Discussion: We show that discrepant assumptions regarding the near-UV absorption properties of temperate water vapor underly the low-outgassing false positive scenario, place the first-ever laboratory constraints on these cross-sections, and use these constraints to obviate this scenario [8]. We show that discrepant assumptions regarding planetary upper atmospheres and M-dwarf stellar emission underly the M-dwarf scenario, provisionally eliminating this scenario as well [9]. We confirm that the accumulation of biosignature gases is sensitive to the UV SED of the host star [10,11]. Prior to our work, the only operative facility capable of constraining such SEDs was the Hubble Space Telescope (HST). We conduct spectroscopy of the nearby M-dwarf star HIP 23309 with HST and UVIT to validate the ability of UVIT to characterize the SEDs of exoplanet host stars, and we show that while UVIT-derived spectra do not have the precision on their own to be useful for interpretation of exoplanet spectra, they can likely be used to calibrate stellar models to extract high-quality synthetic spectra useful for such purposes [11].

Conclusions: Our results strengthen the biosignature gas paradigm for exoplanet life detection in general, and for O₂ as a biosignature gas in particular. Our results highlight the utility of UVIT as a tool to complement HST in characterization of exoplanet host stars to aid interpretation of potential biosignatures. We advocate for the retention of UVIT-like UV spectral capability in ASTROSAT-2/INSIST [12].

References: [1] Kozakis T. et al. 2022. *Astronomy & Astrophysics* 665:A156. [2] Clery D. 2023. *Science* 379:123 [3] Meadows V. S. et al. 2018. *Astrobiology*, 18:630. [4] Harman C. E. et al. 2015. *The Astrophysical Journal* 812:137. [5] Hu R. et al. 2020. *The Astrophysical Journal* 888:122 [6] Hu R. et al. 2012. *The Astrophysical Journal* 761:166. [7] Tandon S. N. et al. 2020. *The Astronomical Journal* 159:158. [8] Ranjan S. et al. 2020. *The Astrophysical Journal* 896:148. [9] Ranjan S. et al. 2023b. *The Astrophysical Journal Letters* 958:L15. [10] Teal D.J. et al. 2022. *The Astrophysical Journal* 927:90. [11] Ranjan S. et al. 2023a. *The Astronomical Journal* 166:70 [12] Subramaniam A. 2022. *Journal of Astrophysics & Astronomy* 43:80.

61. INSIGHTS INTO THE GEOLOGICAL IMPORTANCE OF IMPACT CRATERING EVENTS

K. S. Sajinkumar^{1,2}, ¹Department of Geology, University of Kerala, Thiruvananthapuram 695 581, Kerala, India, ²Department of Geological & Mining Engineering & Sciences, Michigan Technological University, Houghton, MI 49931, USA

Introduction: Impact craters are the most prevalent examples of large-scale planetary events. The presence of hundreds of thousands of craters across planetary surfaces of Moon, Mars, Callisto, and several others, substantiate the fact that impact cratering is one of the most fundamental processes of the Solar System [1,2]. The tectonically dormant bodies such as Moon and Mars have been engraved with hundreds of thousands of impact craters yet, the terrestrial crater record stands at 210 owing to obliteration or shielding by the active tectonics and geomorphological processes on Earth. Irrespective of the planetary surface, the crater formation process occurs in 3 stages: (1) contact/compression stages - conversion of kinetic energy of incoming high-velocity projectile to shock waves on collision, (2) excavation stage - initiation and synchronous progression of extensive target modifications as shock waves propagate radially outward to form transient crater and (3) modification stage - refashioning of transient crater under combined influences of gravity, rock mechanics and geological processes [3,4]. The impact cratering processes produce a range of shock metamorphic effects on target such as shatter cones, breccia, impact melts, impact mineral polymorphs, planar deformation features (PDFs), planar fractures (PFs) in conjunction with the typical circular morphology of an impact crater [4]. Morphologically, impact craters are categorized into two types: (1) simple (diameter < 2km) and (2) complex craters (diameter > 4km). The transition from the simple to complex craters tend to occur within the diameter range of 2-3 km for sedimentary targets and 4-5 km in crystalline targets [4].

The consequences of impact events can vary from local to global based on the projectile size and velocity, with bigger impact craters being associated to the most catastrophic of effects. Earth has experienced planetary-scale collisions which eventually resulted in formation of the Earth's Moon (Giant Impact Hypothesis), evolution of primitive crust and the widely debated commencement of plate tectonics [5,6]. The relatively small number of terrestrial impact craters are the associated triggers for a variety of processes on our planet including: (1) formation of massive volumes of igneous rocks, (2) establishment of economic mineral deposits and hydrocarbons, (3) mass extinctions, (4) environmental and climatic changes and (5) introduction of chemical components and habitats to aid proliferation of life [6,7]. To elaborate, impact craters serve as windows into subsurface structure. The intense forces involved in their formation lead to distinct deformation of rocks, offering researchers a unique opportunity to study the underlying geological layers. The extreme conditions generated during impact events can concentrate valuable minerals, making these sites potential targets for resource exploration and thereby contributing to the knowledge of mineral formations and the potential for resource extraction. Sudbury, Ames and Vredefort are some examples of the associated as these are associated with Ni deposits, oil and natural gas deposits, and Au and U deposits respectively. The Chicxulub impact event is an example of manifestation of impact-induced global scale environmental and biotic changes, in the form of the Cretaceous-Paleogene Mass Extinction (most known for the mass extinction of non-avian dinosaurs) [8,9]. Lastly, the exploration of impact craters on other planets and moons offers a comparative perspective on geological processes. By studying these features in extraterrestrial environments, scientists can draw parallels and contrasts with Earth's geological history, contributing to a more comprehensive understanding of planetary evolution.

References: [1] Shoemaker, E. M. (1983). Asteroid and comet bombardment of the Earth. *Annual Review of Earth and Planetary Sciences*, 11(1), 461-494. [2] Kenkmann, T. (2021). The terrestrial impact crater record: A statistical analysis of morphologies, structures, ages, lithologies, and more. *Meteoritics & Planetary Science*, 56(5), 1024-1070. [3] Melosh, H. J. (1989). Impact cratering: A geologic process. *New York: Oxford University Press; Oxford: Clarendon Press*. [4] French, B. M. (1998). *Traces of catastrophe: A handbook of shock-metamorphic effects in terrestrial meteorite impact structures* (No. LPI-Contrib-954). [5] Canup, R. M., & Asphaug, E. (2001). Origin of the Moon in a giant impact near the end of the Earth's formation. *Nature*, 412(6848), 708-712. [6] Osinski, G. R., Grieve, R. A., Ferriere, L., Losiak, A., Pickersgill, A. E., Cavosie, A. J., ... & Simpson, S. L. (2022). Impact Earth: A review of the terrestrial impact record. *Earth-Science Reviews*, 232, 104112. [7] French, B. M., & Koeberl, C. (2010). The convincing identification of terrestrial meteorite impact structures: What works, what doesn't, and why. *Earth-Science Reviews*, 98(1-2), 123-170. [8] Alvarez, L. W., Alvarez, W., Asaro, F., & Michel, H. V. (1980). Extraterrestrial cause for the Cretaceous-Tertiary extinction. *Science*, 208(4448), 1095-1108. [9] Schulte, P., Alegret, L., Arenillas, I., Arz, J. A., Barton, P. J., Bown, P. R., ... & Willumsen, P. S. (2010). The Chicxulub asteroid impact and mass extinction at the Cretaceous-Paleogene boundary. *Science*, 327(5970), 1214-1218.

62. Asteroid impact craters on terrestrial planets and opportunity for planetary habitability

D. Ray, Physical Research Laboratory, Ahmedabad 380009, India

(dwijesh@prl.res.in)

Impact cratering is one of the fundamental processes of our solar system that shape the surface of planet/planetesimals [1]. An asteroid impact has been common since the earlier days of the solar system in fact at the time of accretion of planet/planetesimal. The best manifestation of impact cratering is well comprehended during late heavy bombardment (~3.8-3.9 Ga) when the frequency of impacts was several magnitudes higher as compared to the present-day record. The hypervelocity asteroid impact is known for its devastation, very unusual event (higher pressure, temperature in shorter time with higher strain rate), and at least in one case linked to the mass extinction during the Cretaceous-Paleogene boundary [2]. The shock diagnostic evidence in minerals remains helpful and is considered a potential proxy to infer the intensity of impact and to explore the planetary habitability scenario. Of course, the high-intensity impact sometimes delayed the habitability. The habitability may be punctuated due to the repetitive high-intensity impact events as inferred from the mineral shock excursion studies. However, a comparatively lower intensity shock, availability of water, and other environmental constraint can induce early life forms to thrive further. One of the important paradigms that is likely to be inherited in the impact structures is the occurrences of syn and post-impact induced hydrothermal alteration due to the warming up of groundwater and fluid-rock interaction facilitated scavenging of the elements. Thus, the new minerals formed due to the precipitation of hydrothermal solution are also sometimes capable of hosting some extremophiles and early signs of life. The importance of studying the terrestrial impact craters is further augmented due to its multifaceted potential for scientific research. The impact craters and its close vicinity remain the exploration scientist's first and foremost choice for the landing site selection for the ongoing planetary missions (Curiosity in Gale crater, Perseverance in Jezero crater, Zhurong in Utopia Planitia, close to Utopia basin on Mars) and even for future Mars (Oxia Planum, eastern margin of Chryse basin) and Moon (South Pole Aitken basin) mission.

References:

[1] French, 1998 A. B. and Author C. D. (1997) *Journal of Geophysical Research* 90:1151–1154. [2] Schulte, 2010 E. F. et al. 1997. *Meteoritics & Planetary Science* 32:A74.

63. End Member Models in Planet Formation: Constraints from different Achondrites

Rai, Nachiketa, Layak, Pipasa, Verma, Kalpana, Downes, Hilary, Mishra, Vijay, Vishwakarma, Rishi

¹Department of Earth Sciences, Indian Institute of Technology Roorkee, Roorkee-247667, India, ²Centre for Space Science and Technology, Indian Institute of Technology Roorkee, Roorkee-247667, India. ³ Dept. of Earth and Planetary Sciences, and Centre for Planetary Sciences, Birkbeck University of London, Malet London WC1E 7HX, United Kingdom.

The formation of terrestrial planets is thought to have occurred through accretion from an originally cold and chemically homogeneous cloud of gas and dust. The subsequent differentiation of a terrestrial planetary body, along with the associated chemical evolution, is typically the outcome of whole-scale or partial melting of the planetary body. Different achondrite meteorites are products of these early solar system processes and offer a window into investigating and understanding these early planetary processes. The HED parent body (asteroid 4 Vesta) is often thought to be the quintessential planetesimal left over from the formation of the Solar System and is commonly considered a reference model for planetesimal formation [1]. However, recent work and our new results provide a different view of the formation of asteroids and planetesimals [2].

Phase equilibrium results supplemented by additional criteria like trace element abundances, and O-isotopic signatures, were used to constrain the petrogenetic evolution of different achondrite meteorite groups from chondritic precursors. A combination of proxy material resembling Allende-type FeO-rich and MgO-rich chondrules can account for the ureilite oxygen isotope trend and a radial gradient in major elements and oxygen isotopes within its parent planetesimal that did not undergo a magma-ocean stage, can account for the entire range of observed ureilite compositions. Our new results demonstrate that a chondritic composition having undergone low degrees of partial melting could have generated the acapulcoite-lodranite clan of meteorites. Our results show that the angrites formed through a complex multi-stage crystallization mechanism in a molten chondritic body that had already undergone core-mantle differentiation.

References: [1] McSween H et al. (2014) *Elements* 10: 39-44. [2] Rai, N., et. al. (2020). *Geochemical Perspectives Letters*. 14, 20–25.

64. Search for the habitable worlds by their atmosphere characterization

Manika Singla

It is the most appropriate time to characterize the Earth-like exoplanets in order to detect biosignatures beyond the Earth because such exoplanets will be the prime targets of big-budget missions like JWST, Roman Space Telescope, HabEx, LUVOIR, TMT, ELT, HWO, etc.

We provide models for the transmission and reflection spectra for the present and prebiotic (3.9 Ga) Earth-like exoplanets orbiting within the habitable zone of stars of spectral types F, G, K and M. Molecules that are potential biosignatures and act as greenhouse agents are incorporated in our model atmosphere. Various combinations of solid and liquid materials such as ocean, coast, land consisting of trees, grass, sand or rocks determine the surface albedo of the planet. Geometric albedo and model reflected spectra for a set of nine potential habitable planets, including Proxima Centauri b, TRAPPIST-1d, Kepler-1649c and Teegarden's Star-b, are also presented. We employ the opacity data derived by using the open-source package Exo-Transmit and adopt different atmospheric Temperature-Pressure profiles depending on the properties of the terrestrial exoplanets.

We also calculated the phase curves of albedo and disk-integrated polarization by using appropriate scattering phase matrices and integrating the local Stokes vectors over the illuminated part of the disks along the line of sight. For this, we solve the 3D vector radiative transfer equations numerically. We present the effects of the globally averaged surface albedo on the reflection spectra and phase curves as the surface features of such planets are known to significantly dictate the nature of these observational quantities. Synergic observations of the spectra and phase curves will certainly prove to be useful in extracting more information and reducing the degeneracy among the estimated parameters of terrestrial exoplanets.

Thus, our models will play a pivotal role in driving future observations.

65. The Curious Case of Argon

M. Safonova¹ and A. Saini², ¹Indian Institute of Astrophysics (IIA), Bangalore, margarita.safonova@iiap.res.in, ²National Centre for Biological Sciences (NCBS), Bangalore.

Introduction: In the modern search for life elsewhere in the Universe, we are broadly looking for the following: the planets similar to Earth – physical indicators of habitability, and the manifestation of life – the biological signatures. A biosignature is a measured parameter that has a high probability of being caused by the living organisms, either atmospheric gas species or some surface features. Therefore, the focus of a search is on a product or phenomena produced by the living systems, mostly by microorganisms as these are the most abundant on our planet like, say, methane. However, we may need to distinguish the terms ‘biosignature’ and ‘bioindicator’.

A biosignature is what living organisms produce – a bioproduct, while a bioindicator may be anything necessary for life as we know it, such as water or a rocky planet. Oxygen in this case is a double biomarker: first, it is a byproduct of oxygenic photosynthesis and, second, it is a signature of a complex life, because complex highly organized life requires high levels of oxygen [1]. But it is possible that there are other such bioindicators.

For example, in the atmospheric compositions of terrestrial planets in our Solar System (including Titan), argon is one of the major constituents, moreover it was recently acknowledged to be a ‘biologically’ active gas [2], exhibiting organo-protective and neuroprotective properties, especially under hypoxic conditions, having essentially oxygen-like properties [3]. Here we propose [4] that argon in the atmosphere of a rocky planet is a bioindicator of a highly organized life, provided that the planet is already deemed potentially habitable: with water, atmosphere, and of a certain age allowing for the complex life to evolve. We also delineate its possible detection methods.

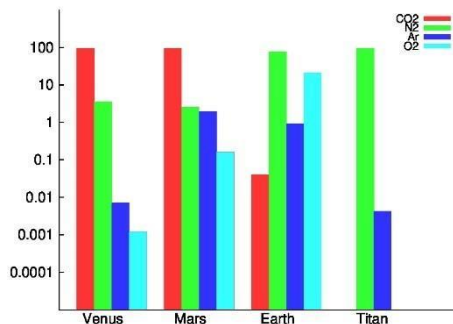


Fig. 1. Major Constituents in the Atmospheres of Terrestrial Planets (by volume).

References:

- [1] Catling, D. C. et al., 2005. *Astrobiology*, 5(3), 415-38. [2] Nespoli, F., Redaelli, S., Ruggeri, L., et al., 2019. *Ann. Card. Anaesth.*, 22, 122-35. [3] H'ollig, A. et al., 2014. *Int. J. Molecular Sciences*, 15(10), 18175–18196. [4] Safonova M. and Saini A., 2021. ArXiv preprint: arXiv:2103.15071v1

66. FROM PRESTELLAR CORE TO PLANETARY BODIES -ASTROCHEMICAL ORIGIN AND HABITABILITY

Dipen Sahu^{1,2}, Sheng-Yuan Liu², Naomi Hirano², Doug Johnstone³, Neal J Evans II⁴, Ken Tatematsu⁵, and the ALMASOP team ; ¹Physical Research Laboratory, India, dsahu@prl.res.in, & dipenthink@gmail.com ; ²Academia Sinica Institute of Astronomy and Astrophysics, Taiwan; ³NRC Herzberg Astronomy and Astrophysics, Canada; ⁴The University of Texas at Austin, USA; ⁵Nobeyama Radio Observatory, National Astronomical Observatory of Japan

Abstract: Low-mass prestellar cores are the birthplace of Solar-type systems. Unnumbered star formations are occurring in our galaxy and other galaxies. Therefore, our solar system is one of the many; similarly, Earth may be one of the many habitable and even inhabited planets. Now, organic elements and water are the basic ingredients of life. However, our knowledge is very limited regarding how temperate, rocky exoplanets have access to water and organic molecules. Additionally, how star and planet formation affect the chemical diversity of (exo)planets remains unclear. A holistic approach to answering these questions involves studying the astrophysical and chemical processes intricately, from core to protoplanetary disk and planets.

In this talk, I will summarize our efforts to understand the origin of complex organic molecules in solar-type protostars [3,4], prestellar cores [1,2], chemical signatures of planet formation via grain growth [ongoing], and the search for prebiotic molecules in space [3], among other aspects. As the habitability problem is complex, it should be addressed using facilities like ALMA, JWST, the Mount Abu telescope, uGMRT, and future facilities like TMT and SKA, in synergies. Additionally, support from laboratory astrochemistry is crucial as well.

References: [1] Sahu et al. (2023) *The Astrophysical Journal*, 156: 945. [2] Sahu et al. (2021) *The Astrophysical Journal Letters*, L15, 907 [3] Sahu et al. (2020) *The Astrophysical Journal*, 65: 899. [4] Sahu et al. (2019) *The Astrophysical Journal*, 196: 872. [5] ALMASOP project ([link](#))

67. Exploring the scaling relations of exoplanets and characterization of a potential habitable exoplanet system.

B. Prateek¹⁺, C. A. Sneha²⁺, M. Abirami^{3+#}, P. Mahesh⁴⁺, R.N. Aishwarya⁵⁺, ¹Ludwig Maximilian University, Germany, ^{2,4,5}Independent researcher, ³University of Aberdeen, Scotland. ⁺All authors have contributed equally to the presented work. #Corresponding author: a.muthusamy.23@abdn.ac.uk

Introduction: NASA Exoplanet Archive [1] is one of the most detailed catalogues for exoplanets' research. The presented work explores the 35000+ candidates catalogued in the above mentioned database which forms a statistically significant collection, ideal for correlation analysis and testing for scaling relations between different parameters viz. planet radius, planet mass, stellar radius, stellar mass, stellar luminosity, metallicity ([Fe/H]) and many more. The catalogue is then scrutinized for potential habitable candidates using systems with K-type stars for ideal irradiance, and filtering out the systems with planets out of the Goldilocks Zone [2]. Factoring in the availability of the data, a planet named 5 Vita b (named as per the nomenclature norms set by IAU) is hypothesized with radius that is an average of the filtered systems. The generated scaling relations of the exoplanet systems are used to predict the other parameters of the system. Potential surface composition, atmosphere composition [3, 4], and hence the spectra of such an exoplanetary atmosphere is also proposed and 3D modelled with Blender.

It is proposed that the life underneath would be formed from Abiogenesis. A Protobiont forms a basic microbe called "Kho", which eventually evolve to "Aang" and "Kora". A possibility of Panspermia after an asteroid impact on the exoplanet 5 Vita b which leads to the formation of the exomoon 'Diane' is also explored. The mass and radius of this exomoon is narrowed down upon using the ratios of Mass of habitable moons to that of their planet in our solar system. The considered moons were Dione, Callisto, Titan, Enceladus and Europa.

Potential future prospect of this work includes creating a framework and eventually cataloging of exoplanets that show similar conditions as the proposed 5 Vita b to study their planetary parameters and composition, and study their natural satellites as well, if any.

Acknowledgements: This work is a minor extension of the authors' work done during NASA SpaceApps Hackathon 2023. Authors acknowledge the inputs of Mr. Sundar M N (PhD.).

References:

- [1] NASA Exoplanet Archive, DOI:10.26133/NEA12
- [2] Whitmere D. and Reynolds R., 1996. *Circumstellar Habitable Zones*, 117-142.
- [3] Alessi M et al., 2017. *Monthly Notices of the Royal Astronomical Society*, Volume 464, Issue 1: 428–452.
- [4] Irwin P. G. J. et al. 2017. *European Planetary Science Congress Vol. 11, EPSC2017-192*.

68. ESTABLISHMENT OF LUNAR HABITAT: CONSIDERATIONS, REQUIREMENTS AND ESSENTIAL TECHNOLOGIES

Gnanasekar S¹, Bijoy Jacob K² and Vinod SS¹

¹Deputy Project Director, Small Satellite Launch Vehicle Project, Vikram Sarabhai Space Centre, Indian Space Research Organisation, Thiruvananthapuram, India, s_gnanasekar@vssc.gov.in,

²Head, Advanced Inertial Sensors Division, ISRO Inertial Systems Unit, Indian Space Research Organisation, Thiruvananthapuram, India, bijoy_jacob@vssc.gov.in

³Project Director, Small Satellite Launch Vehicle Project, Vikram Sarabhai Space Centre, Indian Space Research Organisation, Thiruvananthapuram, India, ss_vinod@vssc.gov.in

During last few decades the focus of the space fairing fraternity was on “habitat the space” like International Space Station, Tiangong Space Station and the focus have now shifted to “habitat the other planets”. Establishment of Lunar Habitat will act as base for further exploration and will be the first stepping stone in this aspect. Currently many space fairing nations are having or proposing programs to land man on the Moon. The objective of which includes 1) science exploration such as using Moon as base for observations, understanding of evolution of Earth, moon and solar system, 2) commercial exploration such as bringing lunar resources to Earth, 3) habitat the Moon using in-situ resources for long term sustainability and 4) using Moon as test-bed for future missions to go other planets. In order to establish Lunar Habitat, it is essential to study its Environment and identify technologies to address it. In addition, spinning off technologies developed for lunar exploration missions will find wide variety of application such as agriculture, medicine, environmental monitoring, robotic operations, mining, communications, health care, automobiles, waste management, renewable energies, automated vehicles, etc.,

This paper addresses aspects like the need to go to moon, Robotic versus manned mission, considerations and requirements with respect to lunar environment and lunar infra structure. This paper also includes different types of lunar habitat. Aim of this paper is to generate inputs and approaches for establishment of full-fledged lunar habitation with emphasis on the technologies to be developed.

69. NEXT GENERATION LUNAR SCIENCE THROUGH GEOPHYSICAL NETWORK ON THE MOON

K.Durga Prasad¹, Neeraj Srivastava¹, Pankaj Priyadarshi², J. John³, M. Shanmugam¹, S. Dattagupta⁴

¹Physical Research Laboratory, Ahmedabad (durgaprasad@prl.res.in); ²AERO Entity, Vikram Sarabhai Space Centre, Trivandrum; ³Laboratory for Electro-Optics Systems, ISRO, Bangalore; ⁴IIT (ISM) Dhanbad, Dhanbad

The understanding of the Moon is an important cornerstone in solar system exploration for not only deciphering the evolutionary history of our Earth but also the evolution of terrestrial planets as a whole. The interior of the Moon hides a treasure of information about its initial composition, differentiation, crustal formation, and subsequent magmatic evolution. Despite several exhaustive studies for nearly half a century (particularly through the manned Apollo missions), several aspects of the Moon specifically about its interior still remains to be unknown. In this scenario, it is imperative that any next generation science mission to the Moon should target in-depth geophysical investigations that will help is to understand its interior structure, bulk composition and thermal state. Results from recent missions have completely changed the existing geophysical perspective of the Moon. Significant to mention at this point are the reports about the globally distributed faults, young volcanism, dry granular flows and mass movements on the Moon. These observations therefore suggest that the Moon is more dynamic than thought before. However, the plausible sources behind these features are either tidal or impacts or internal heat remains puzzling which calls for detailed geophysical investigations. For the past two decades, extensive studies of the Moon through remote sensing, in-situ experiments and modelling have provided an enhanced understanding of its geology and geomorphology. Now the next logical step is to carryout geophysical measurements at diverse locations. Such geophysical measurements basically include heat-flow, seismic, magnetic field, selenodesy and other related studies that provide fundamental information on the formation of the Earth-Moon system, the evolution of the Moon (including its surface), and differentiation processes of terrestrial planets in general.

The next generation of geophysical measurements on the Moon are expected to be more advanced and improved upon the data obtained during the Apollo missions. As the deployment of several landers for geophysics at diverse locations of the Moon is not practical, an effective way of carrying out such investigations is to deploy penetrators at few pre-defined locations on the Moon to form a one-step geophysical network on the Moon. This geophysical network may be augmented with additional penetrators as necessary. Each penetrator proposed is deployed through an orbiter to the surface and carries geophysical instruments for heat flow, seismic and magnetic field measurements. Such investigations need to be included as a part of every future landing mission to the Moon. Rationale for such geophysical investigations and configuration of the proposed experiments will be discussed.

70. Development of Spectro-polarimeter for HAbitable Planet Earth (SHAPE) onboard Chandrayaan-3

Anand Jain¹, Swapnil Singh¹, Bhavesh Jaiswal¹, Smrati Verma¹, Reenu Palawat¹, Brajpal Singh¹, Ravishankar B T¹, Anuj Nandi¹,

¹Space Astronomy Group, ISITE Campus, U. R. Rao Satellite Centre, ISRO, Bangalore-560037, India
Email: anandj@ursc.gov.in

Earth is the only known habitable planet. Hence, disc-integrated signatures of Earth for a range of phase angles serves as a test bed to benchmark the observations of Earth-like exoplanets. SHAPE an experimental payload onboard ISRO's Chandrayaan-3 spacecraft, which is configured and designed to carry out a detailed discintegrated spectroscopic and polarimetric study of Earth from the Moon's orbit in the Near-Infrared (NIR; 1.0 – 1.7 μm) wavelength range. Placing an instrument around the Moon is ideal as Earth's angular size from Moon is $\sim 2^\circ$, which is small enough for it to be observed as an Exoplanet by the instrument. The instrument consists of two packages – EODS (Electro-Optical Detector System) and RFS (Radio Frequency Source) and is a compact lightweight spectro-polarimeter with an Acousto-Optic Tunable Filter (AOTF) at its heart. The AOTF is driven by a radio frequency signal generated with the in-house developed RFS system. On application of the RF signal, the AOTF filters incident light and produces two diffracted narrow-band beams, which are linearly polarized in mutually perpendicular directions. The instrument optics with an FOV of $\sim 2.6^\circ$ is configured to focus two output beams onto two Indium-Gallium-Arsenide (InGaAs) detectors. In-house front-end, processing and power electronics have been developed to read out the data. The instrument configuration along with the end-to-end development and calibration will be discussed. The usefulness of an AOTF-based spectro-polarimeter instrument has been established, and a similar technique is planned for the study of the atmospheric study of Venus for ISRO's upcoming Venus mission.

71. PROCESS VIABILITY STUDY IN THE LUNAR ISRU – PRODUCTION OF OXYGEN FROM LUNAR REGOLITH

Ganesh P¹, Vignesh G², and Raghu Meetei³

^{1,2}ISRO Propulsion Complex (IPRC), Mahendragiri – 627133, pganesh@iprc.gov.in ³ Directorate of Technology Development & Innovation (DTDI), ISRO-HQ, Bangalore Email: pganesh@iprc.gov.in

Introduction: In-Situ Resource Utilization (ISRU) covers all aspects of using or processing local resources for the benefit of robotic and human exploration of Moon, Mars and other planets. In-Situ Propellant Production (ISPP) is one of the important subset of ISRU that focuses on producing propellants from local resources. This propellant may be used e.g., in ascent vehicles, hoppers as well as in rovers and other surface mobility systems.

ISPP requires the least amount of infrastructure to support and provides immediate benefits to mission plans. Recent studies [1-2] show that ISRU can significantly reduce mass, cost, and risk of Mars exploration missions. Mass can be reduced mainly by In-Situ Propellant Production, since propellant is typically the largest mass fraction of the overall system. Development of ISPP technology plays a vital role to achieve human or robotic exploration to Moon.

There are potential lunar resources that can be utilized for propellant production namely (1) Metal oxides in lunar regolith containing typically >40 Wt.% Oxygen, (2) Water ice in regolith pores in permanently shadowed craters near the poles etc. Oxygen in the form of metal oxides proves to be the major and most obvious resource for production of Oxygen. Oxygen present in soil in the form of oxides in lunar regolith can be extracted through various physio-chemical processes. In the present paper, process engineering feasibility studies are carried out in detail for providing the valuable insights and information on process selection. Process viability matrix is discussed in detail for scrutinizing the potential processes. In addition, a new approach in lieu of conventional physio-chemical process technology is also studied in detail and included in the process viability matrix.

Process Technologies on Oxygen Extraction from Lunar Regolith: Based on analyses of various Luna and Apollo samples, it is known that oxygen is the most abundant element in lunar regolith, accounting for 40–45% by mass [3]. However, this Oxygen is chemically bound in the regolith material as oxides, in the form of minerals and amorphous glass, and is therefore unavailable for immediate use. The extraction and processing of Oxygen from the lunar regolith will be key technology for enabling future exploration. Numerous process technologies for extracting oxygen have been proposed and they are classified under the categories of (1) Chemical reduction, (2) Electrolytic and (3) Pyrolytic processes.

Results & Discussion: Process Viability Matrix for scrutinizing the potential process was made based on the factors of (1) Technology Readiness (2) Imported chemical reagents requirement (3) Process requisites (4) Feedstock processing requirement & (5) Yield. Assessment indicators e.g. high, moderate and low are used on the selected factors to rank the processes. Further, challenges and opportunities in each process technologies are presented with the current scenario on the technology readiness level. Based on the above studies it is found that pyrolysis technique has the potential on maturing the oxygen extraction process technology. However, electrolysis process is having the edge over the pyrolysis process if the complex technology on anode material is available under oxidation environment. In addition, conceptual process design on the new closed loop process using the ionic liquid is discussed in detail. Process viability matrix is applied for the new process and the assessment indicators are compared with the conventional process techniques.

Conclusion: Based on the process viability studies and characterization of lunar simulant soil characterization carried out to finalize the potential process routes for in-situ propellant production in

Moon, the more viable option is that oxygen can be produced using Lunar regolith through vacuum pyrolysis technique. In addition, conceptual process design on the new closed loop process using the ionic liquid is discussed in detail. Process viability matrix is used for the new process and the assessment indicators are compared with the conventional process techniques.

References:

- [1] Sanders, G., Duke, M. (2005), "NASA In-Situ Resource Utilization Capability Roadmap Final Report." Documents Archive, Lunar and Planetary Institute, Houston, TX, May 2005.
- [2] Rice, E., Gustafson, R. (2000), "Review of Current Indigenous Space Resource Utilization(ISRU) Research and Development", 38th Aerospace Sciences Meeting & Exhibit, AIAA2000-1057.
- [3] Schreiner, S.S., Dominguez, J.A., Sibille, L., Hoffman, J.A., (2016), Thermo physical property models for lunar regolith. Adv. Space Res.

72. SIMULATION OF BRIGHTNESS TEMPERATURE FROM LUNAR SUBSURFACE FOR RADIOMETRIC MODE OBSERVATIONS OF DFSAR/CHANDRAYAAN-2

Renju R¹, ¹Space Physics Laboratory, VSSC, ISRO, Trivandrum-695022, India, renju_r@vssc.gov.in

The microwave remote sensing techniques for planetary surface studies have several advantages due to its capability to sound surface and subsurface thermal structure and dielectric characteristics. The penetration property of microwaves is beneficial for analyzing dielectric properties of the medium and also to generate maps of lunar regolith. Dual Frequency Synthetic Aperture Radar (DFSAR) operating at L and S bands onboard Chandrayaan-2 (CH-2) has an experimental radiometric mode operation. A multi-layered microwave radiative transfer model coupled with thermal model has been used to account for the microwave thermal emission or the brightness temperature from the lunar subsurface at L and S band frequencies. Thermal emission from the lunar subsurface depend on the temperature and dielectric property and are deciding factor of depth of penetration of microwaves into lunar surface. The attenuation of the radiation through the medium is primarily due to absorption caused by imaginary part of the dielectric constant which is related to only the mineral content (FeO+TiO₂) in case of lunar regolith [1]. The net intensity of thermal radiation just beneath interface layer between the lunar surface and free space is thus the superposition of intensities emitted at various regolith layers. The thermal emission emerging out of the surface is decided by the emissive property or emissivity of the surface layer. Thus, the brightness temperature simulated using the incoherent RT approach can be formulated as a product of the planetary surface emissivity and the net radiation from the surface layers.

The temperature profiles are simulated using one-dimensional thermal model and validated using LRO/Diviner Radiometer observations. The brightness temperature simulated using different dielectric models are validated using radiometric observations. Microwave emissions at DFSAR/CH-2 operating frequencies such as 1.25 GHz and 2.5 GHz can be used for sounding dielectric discontinuity due to the presence of water ice, high minerals or densely packed rocky medium than thermal sounding as microwave thermal emissions at these channels are not sensitive to surface temperature [2]. Hence these frequencies are potential tool to study the sub-surface characteristics and for the discrimination of subsurface material type.

References: [1] Fa, W. and Jin, Y.Q. (2010) Analysis of microwave brightness temperature of lunar surface and inversion of regolith layer thickness: Primary results from Chang'E-1 multi-channel radiometer observation. *Icarus* 3:109–134. [2] Renju R and C. Suresh Raju (2023) Simulation analysis of microwave emission from lunar subsurface for SAR radiometric mode dual frequency (L/S Bands) observations onboard Chandrayaan-2, *Advances in Space Research* 72: 3499–3508.

73. Surface and Subsurface Regolith Characterization of Lunar South Pole using Chandrayaan-2 Dual-frequency Synthetic Aperture Radar (DFSAR)

Krishangi Kashyap¹ and Unmesh Govind Khati¹

¹Department of Astronomy Astrophysics and Space Engineering, Indian Institute of Technology Indore, Khandwa Road, Simrol, Indore 453552, Madhya Pradesh E-mail ID: msc2203121006@iiti.ac.in

Abstract: Despite its proximity to Earth, vast regions of the Moon remain unexplored quantitatively, particularly the Permanently Shadowed Regions (PSRs) which are located at the poles. Identified by LRO Diviner as the coldest lunar locations (temperature reaching > 100 K), these PSRs harbour potential volatiles such as water ice, ammonia, methane etc. implanted into the regolith by solar winds and meteorite impacts which are valuable for future robotic and manned missions, prompting a need for precise mapping of their distribution and abundance [1]. This research focuses on the south polar region 'Faustini Rim A' located at the latitude of 87.3° S, which was chosen as one of the potential landing sites for upcoming Artemis III mission. Moreover, ensuring a successful lander touchdown necessitates the selection of a terrain devoid of rocks. Therefore, this study utilizes Chandrayaan-2's Dual-frequency Synthetic Aperture Radar (DFSAR) fully polarimetric data acquired by simultaneous operation mode to perform a comparative analysis of the presence of different types of scatterers and volumetric rock abundance at surface and subsurface levels.

The DFSAR image covers portions of two south polar craters, Shoemaker and Faustini. The PSR within Shoemaker and the wall of Faustini crater are observed, leveraging the deeper penetration of L-band radar compared to S-band [2] to gain new insights into subsurface properties. Applying Pauli (coherent) decomposition [3] and model-based (incoherent) Freeman Durden decomposition [4] methods to the radiometrically calibrated data reveals a variety of scattering mechanisms across the study area. Seven distinct regions exhibiting mixture of these mechanisms were chosen for detailed analysis, aiming to characterize both surface and subsurface properties. In order to estimate the rock abundance, a recently developed CPR based linear model [5] was applied to both L-band and S-band data across the entire study area.

Analysis of single scatterers reveal distinct characteristics between Shoemaker and Faustini. Inside Shoemaker, the walls of small craters exhibit high double-bounce scattering in S-band, indicative of blocky ejecta or rocks on the surface. Conversely, the subsurface reveals a mixture of surface and double-bounce scattering implying mixed regolith with small blocks. On the other hand, Shoemaker crater floor reveals higher volume scattering at the subsurface level, suggesting loosely packed regolith particles. Faustini crater presents a different picture. Its wall and the small crater on its rim show prominent double-bounce scattering with surface scattering in L-band. This indicates compactly packed regolith particles at the subsurface, creating a smooth surface, while the walls themselves are rugged. Some volume scattering remains at the surface level due to multiple scattering from regolith particles. In terms of distributed scatterers, the crater on the Faustini rim displays volume scattering in both S-band and L-band, likely due to loosely held regolith and blocky ejecta on the surface and subsurface. This observation suggests increasing surface scattering with deeper penetration into the regolith, as L-band becomes less sensitive to smaller objects compared to S-band. Rock abundance analysis reveals maximum rock concentration on the surface of Shoemaker floor and on the wall of the small crater inside Shoemaker at its subsurface level.

References: [1] Sharma, A., Kumar, S., & Bhiravarasu, S. S. (2023). *Advances in Space Research*. [2] Kumar, S., Singh, A., Sharma, A., Chaudhary, V., Joshi, A., Agrawal, S., & Chauhan, P. (2022). *Advances in Space Research*, 70(12), 4000-4029. [3] López-Martínez, C., & Pottier, E. (2021). *Polarimetric Synthetic Aperture Radar: Principles and Application*, 1-58. [4] Freeman, A., & Durden, S. L. (1998). *IEEE transactions on geoscience and remote sensing*, 36(3), 963-973. [5] Gao, Y., Zhao, F., Hou, W., Han, Y., Liu, M., Dang, Y., Lu, P. & Wang, R. (2023). *IEEE Journal of Selected Topics in Applied Earth Observations and Remote Sensing*.

74. TERRESTRIAL IMPACT CRATERS AS AN IMPORTANT GEOMORPHIC FEATURE FOR THE FORMATION, PRESERVATION, AND IDENTIFICATION OF ENERGY RESOURCES

S. James¹, J. Aswathi¹ and K.S. Sajinkumar¹ ¹Department of Geology, University of Kerala, Thiruvananthapuram, Kerala, India(shaniajames@keralauniversity.ac.in), ²Department of Geological and Mining Engineering and Sciences, Michigan Technological University, Houghton 49931, MI, USA

Introduction: Impact craters on the Earth's surface are round morphological structures associated with mass extinctions, planetary-scale climatic and environmental changes, the formation of large igneous bodies, ore deposits, etc. As the world struggles with potential resource scarcity and an ever-growing population, it is essential to properly explore potential regions/structures. Impact craters are among the first, with 60 (29%) of the 208 surface impacts associated with natural resources. The resources of the 60 craters consist of hydrocarbons (19), base minerals (10), and materials such as agate and gypsum (Figure 1). Progenetic, syngenetic and epigenetic mineralization products can be observed in the crater [1,2,]

Materials and Methods: Systematic geological exploration is a long and complex process, so remote sensing is the most important tool for extensive exploration. The mineral resources associated with terrestrial impact craters was identified [1,2,3]. Prospective imaging to determine material properties at the Froid and Stobie (Sudbury) mines was carried out at four locations in each of the two mining units. PlanetLab (3 m resolution) and EO-1 Hyperion (242 bands) satellite images were acquired for false color compositing and hyperspectral analysis (USGS Earth Explorer). Google Earth imagery was used for Manicouagan Reservoir.

Result and Discussion: Crater morphology and resource mineralization are functionally equivalent. This can be attributed since (1) crater identification can be aided by mineral deposits, (2) mineral deposits occur within the crater and lastly, (3) mineral identification is catalyzed by remote sensing techniques. Each of the same are explained as follows:

(1) Crater identification aided by mineral deposits: The rounded, arched or basin/hemispherical shape of mineral deposits, or rather the mineralization itself, may indicate a crater. Mineralization can be expected along listtype or concentric fractures in the crater. In addition, regional variations in the distribution patterns of physical impact products (eg, molten rocks, breccias, cinder cones, ejecta) or metamorphic effects of the impact may also aid crater identification.

(2) Mineral deposition within the crater: Craters house minerals through various stages of mineralization that occur following crater formation. Descendant mineralization is seen in the early fossil stages of crater formation (eg, by opening of originally buried sediments), and synthetic mineralization is seen in the middle to late fossil stages (eg, melt-influenced hydrothermal mineralization). mineral-rich minerals). Pb, Zn, Fe, etc.) and epigenetic mineralization occurs during the deformation and post-deformation phases (e.g. preservation of hydrocarbons with the help of crater structural elements).

(3) Mineral identification aided by remote sensing techniques: Mineral detection can be performed using remote sensing methods. The metal deposits of the Froude and Stobie mines are distinct from the vegetation. In addition, the hyperspectral image curves peak in the absorption bands of several minerals: chalcopyrite (400 nm), bornite (600 nm), and pyrite (2100 nm) (Figure 1). 2). However, Daniel Johnson Dam, which blocked water from the Manicouagan Reservoir during the Manicouagan hydroelectric development process, stands out (Figure 1).

References: [1] Grieve, R., 2005. Economic natural resource deposits at terrestrial impact structures. *Geol.Soc., Lond. (Spl. Publ.)* 248 (1), 1-29. [2] Grieve, R., Masaitis, V., 1994. The economic potential of terrestrial Impact Craters. *Int. Geol. Rev.* 36 (2), 105-151. [3] Reimold, W.U., Koeberl, C., Gibson, R.L., Dressler, B.O., 2005. Economic mineral deposits in impact structures: a review. In: Koeberl, C., Henkel, H. (Eds.). *Impact Tectonics. Impact Studies.* Springer., Berlin, Heidelberg, pp. 479-552. [3] Osinski, G. R., Grieve, R. A., Ferriere, L., Losiak, A., Pickersgill, A. E., Cavosie, A. J., ... & Simpson, S. L. (2022). Impact Earth: A review of the terrestrial impact record. *Earth-Science Reviews*, 232, 104112.

75. Role of ice in the Martian erosional valley formation: A study from Thaumasia highland and adjacent region, Mars

Dibyendu Ghosh^{1*}, Alok Porwal¹, Guneshwar Thangjam²

¹Indian Institute of Technology Bombay, Mumbai- 400076, India

²School of Earth and Planetary Science, NISER, HBNI, Bhubaneswar-752050, India

*Corresponding Author E-mail: ghosh.dibyendu@iitb.ac.in

The presence of erosional and depositional surficial ice features is well-documented in the Thaumasia highland and surrounding region on Mars [1]. Therefore, there is a significant possibility that this surficial ice may contribute to the valley formational process or, at least, to the modification of valleys in this region. Based on the analysis of the morphometric parameters such as drainage pattern, junction angle, Hack's law, drainage density, and other details, early researchers attributed that the formation of the valley networks in parts of the Thaumasia region is associated with the surface runoff process [2-3]. This suggests a warm and humid ancient Mars. However, considering the climate model and morphometric parameters, some researchers also proposed that part of the valley networks in this region may result from a sub-glacial erosional process [4]. The climate model [5] also supports the cold and icy early Martian climate concept. Thus, the primary question arises: How can valley-networks-like features possibly be formed in a cold climate? Also, this raises the question of whether the surface runoff process was the sole factor in the valley network formational process or whether there was any role of surface and sub-surface ice in the valley formational process.

This research focuses on the second question, investigating whether surface and subsurface ice contributed to the valley formational process in this region. We selected 150 valley networks in the Thaumasia region using a high-resolution global scale imagery dataset (CTX). We categorised them based on their age as per the available geological map [6]. Further, we divided them categorically into different regions based on their spatial location, for example, valley networks in relatively lower latitudinal regions (15°S to 24°S), mid-latitudinal regions (24°S to 33°S), and higher latitudinal regions (33°S to 42°S). We examined the evidence of ice-erosion and deposition features within the valleys and their surroundings to understand the role of ice in the valley network formational process. Our study reveals that ice was an integral part of the many valley networks, as evidenced by moraine-like features, glacial flow features, and viscous flow features (VFF) indicating ice flow within the valley. On the contrary, pitted surfaces, lobate debris apron (LDA), concentric crater fill materials (CCF), and gullies near the valleys suggest ice accumulation. However, pitted surfaces, LDA, CCF, and gullies may or may not directly impact the valley formation process. Alcove features are another indicator of ice accumulation, especially from the mid- and high-latitude regions. However, alcove-like features may also form through seepage processes, which is not uncommon in this region. A close relationship between the presence of ice within the valleys and factors such as altitude, latitude, and age has also been observed. An increase in ice erosional and depositional features has been observed within the valley with increasing latitudes, and most of those valley networks date back to Noachian-Hesperian and Hesperian times. However, a further study of some other morphometric parameters from this region reveals that glacial/ice erosion was not the sole primary erosional mechanism, and, except in higher altitude regions, in the majority of the valley networks, ice acted as a secondary erosional agent responsible for valley modification.

References: [1] Rossi, A. P., et al. (2011). *Geol. Soc. Lond. spec.*, 356(1), 69-85. [2] Ansan, V., & Mangold, N. (2013) *J. Geophys. Res. Planets*, 118(9), 1873-1894. [3] Penido, J. C., et al. (2013). *Planet. Space Sci.*, 75, 105-116. [4] Buffo, J. J., et al. (2022). *Earth Planet. Sci. Lett.*, 594, 117699. [5] Wordsworth, R., et al. (2013). *Icarus*, 222(1), 1-19. [6] Dohm, J. M., et al. (2001). *ASSEMBLAGE*, 2(5), 16.

76. Morphological Scene Representations to Explore Small Solar System Bodies

Aditya Savio Paul¹

¹Tartu Observatory, University of Tartu

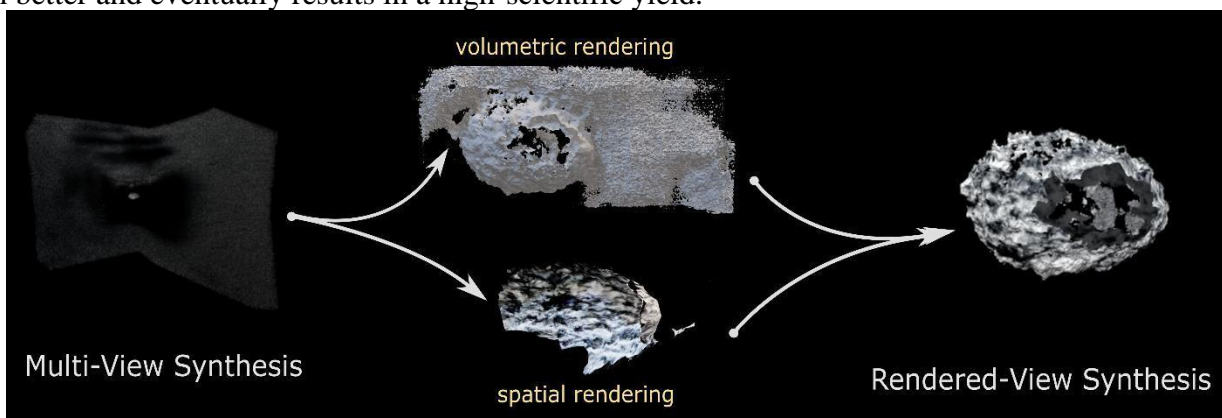
aditya.savio.paul@ut.ee

Small solar system bodies, in the likes of asteroids are expected to host environments which are quite dynamic in nature. They are known to exhibit characteristics that involve dynamic behavior including rotations on varied axis, rubble disintegrations and erratic surface activities. It is these activities and many others that have propelled solar system sciences to advance techniques and methods in order to explore, navigate and the study these bodies that continue to amaze us.

In order to study these bodies and concurrent activities in their vicinity, it is essential that preliminary scenarios are developed that provide early intuition about the possible states of the target body that could be encountered during various phases of a scientific mission.

This work leverages generative radiance field methodology to reconstruct morphological-scene representations. These are performed over spatial and volumetric rendering to synthesize minimum-loss environments. The images are obtained over a series of simultaneous fly-bys capturing the target body from spatially sampled positions. These scenes can produce educated representations of the environments that spacecrafts and satellites might encounter when they visit these pristine worlds. Not only do the scenes help us to understand specific morphology and physical entrails of the target bodies, but also to study the extent of the forces that affect the dynamics of these bodies. These scene representations help to model inherent forces like the gravitational influence and extent exerted by these bodies, or the motion effected by the solar radiation pressure or even rubble and dust modelling in the vicinity of these bodies.

These simulated environments and scene representations serve as initial understandings of the target body which further planning, control and analysis for potential space missions. This helps us to characterize them better and eventually results in a high-scientific yield.



77. Estimation of lunar soil parameters near southern polar regions of the moon from Chandrayaan-3 mission observations.

Devyani B. Visana¹, Megha Tomer², Rishitosh K. Sinha³, Sanjay K. Mishra⁴, Physical Research Laboratory, Ahmedabad 380009, (devyanibvisana@gmail.com)

Abstract: Chandrayaan-3 mission is a stepping stone for India's future space missions. India successfully demonstrated soft landing in the rough highland area of Moon near southern polar region. Pragyan rover traversed the lunar terrain for substantial distance of 103 meters. Movement of Pragyan rover sheared the lunar soil, resulting in static and dynamic sinkage of wheels. While travelling the rover also experienced considerable amount of slippage. This slippage and sinkage experienced by rover wheels are dependent on the soil bearing capacity of lunar regolith and pressure exerted by the rover wheels on the surface. Also, despite the complete lack of moisture in lunar regolith the images captured by Vikram lander clearly shows soil sticking on the wheels of rover which can be related to the triboelectric charging of rover wheels and electrostatic adhesion of soil. These phenomena were also observed in other major lunar missions like Apollo, Surveyor, ChangE and Luna. We analyzed data obtained from the Chandrayaan-3 mission to calculate these soil attributes at our landing site. Results obtained from this study will give a better understanding of soil properties and their interaction with alien objects, particularly to higher latitude where no other mission has gone before (i.e. near Southern pole) and many forthcoming campaigns are pipelined.

78. Noble gas isotope study in Chondrules of Ordinary Chondrite

D.K. Panda¹, R.R. Mahajan¹ and A. Kumar¹

¹Physical Research Laboratory Ahmedabad, e-mail: pdipak@prl.res.in

Introduction: Meteorites are the oldest material that can be used for analysis to understand origin and formation of solar system. Out of the fall meteorites more than 80 % are of ordinary chondrite. Chondrite, silicate spherule with igneous textures and accreted in the proto-planetary disk, an major component in chondritic meteorite. Primitive unequilibrated chondritic meteorite contain several primordial noble gas components that have been trapped during the formation of the meteorites in the early solar system. Depending on the Fe content ordinary chondrite are classified as L, H and LL type. In ordinary presence of different kinds, PO (Porphyritic olivine), POP (Porphyritic olivine-pyroxene), PP (Porphyritic olivine-pyroxene), radial pyroxene (RP), and cryptocrystalline (CC) textures, of chondrite are presents. These are chondrites are texturally and mineralogically different in nature which is due to the formation environment and condition. The noble gas isotopic study of these ordinary chondrites can provide us important information related to proto-planetary disk. Additionally, the bulk properties such as trapped noble gas isotopic ratios, cosmic-ray exposure ages, radiogenic ages of meteorites help us to constrain the compositional make up and understand the geological history of their parent objects [1,2]. In this study we aim to study mineralogical and noble gas and Nitrogen isotope analysis of the bulk meteorite to understand the origin and evolution of these ordinary chondrite.

Methodology: Separated chondrite from two ordinary chondrites has been chosen for this study. One is Bjubole type L4 and Dhajala a type H3.8 meteorites. The chondrites from each was broken into two halves, one half will be used to make thick section for mineralogical and other half will be used noble gas analysis. The mineralogical analysis (Na, Si, Mg, Al, P, K, Ca, Ti, Cr, Mn, Fe, Ni, Co) is being carried out using Cameca SX-100 EPMA whereas the noble gas measurement (He, Ne, Ar, Xe and N) has been carried out using Nu Noble gas Mass Spectrometer.

Result and Discussion: Early study in type H3.8 Dhajala chondrites shows variable amounts of radiogenic ^{129}Xe , incorporation of Q-type gas and variable amounts of N_2 . The chondrites have distinct trapped N isotopic composition ($\delta^{15}\text{N}$ varies from -24.1 ± 8.4 ‰ to 89.1 ± 12.7 ‰), which is inconsistent with Q-gas and solar wind [3]. These inconsistencies can be considered preliminary evidence in support of multiple trapped components in the chondrites. Similarly, the bulk analysis (metal separated) in few L-type chondrite shows ^{15}N ($\delta^{15}\text{N} \sim 168.7 \pm 23.9$ ‰ to 64.2 ± 3.4 ‰) compare to solar [4]. All these results were only from noble gas measurement. So to have a co-relation of these isotopic noble gas this study is focused on mineral along with noble gas and Nitrogen analysis. The new results from Dhajala and Bjubole chondrite (both mineral and noble gas data) will be presented.

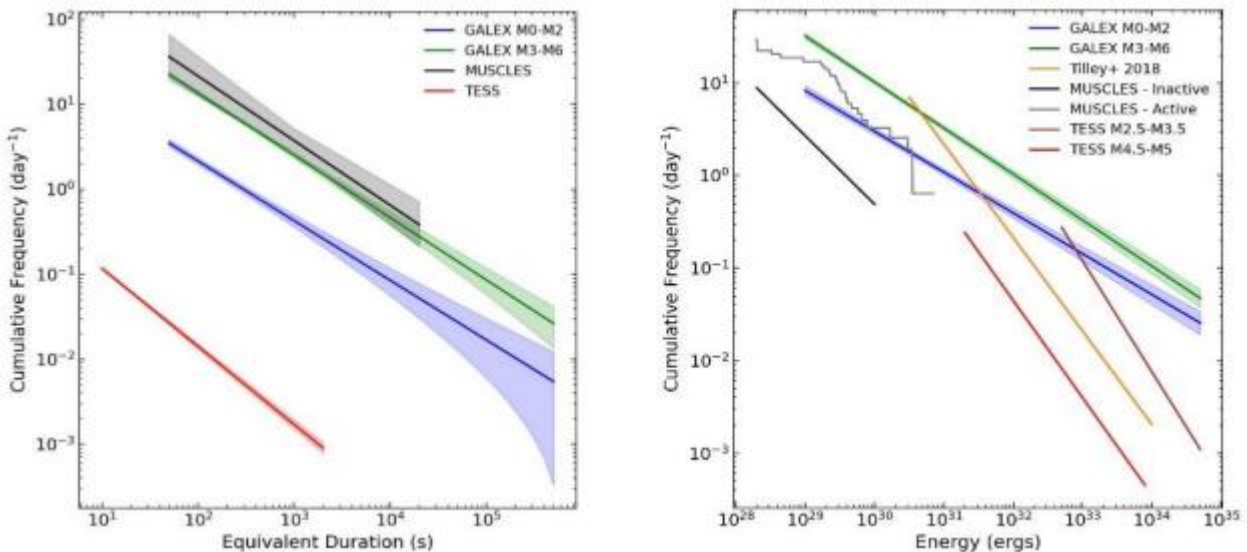
References

- [1] Mahajan R.R. [2022] *Advances in Space Research* 70:2112–2132
- [2] Huss G.R. et al. *Meteorites and the Early Solar System II*
- [3] Mahajan R.R., (2020), *MAPS*, 9:2141-2156.
- [4] Mahajan R.R., (2023), *Astrophysics and Space Science*, 368:101

79. EXPLORING NUV M-DWARF FLARES AND THEIR IMPACT ON HABITABILITY

Param Rekhi, Department of Particle Physics and Astrophysics, Weizmann Institute of Science, Israel
param.rekhi@weizmann.ac.il

Introduction: M-Dwarfs are of high interest as hosts of habitable exoplanets due both to their prevalence in the solar neighborhood and the relative ease of detecting rocky worlds orbiting them. Near-Ultraviolet (NUV) radiation from these stars can significantly influence the atmospheric and surface conditions of their planets and hence plays a key role in determining their habitability. In Rekhi et al. (2023) [1] we study the flaring activity of M-dwarfs in the NUV using archival data from GALEX processed with the new gPhoton2 pipeline. Our work presents the most extensive dataset of M-dwarfs in the NUV to date. Results: We identified and characterized 528 flares from a sample of more than 4000 M-Dwarfs and found ten flares with NUV energies greater than 1033 ergs, including one of the most energetic flares observed on M-dwarfs with NUV energy exceeding 4×10^{34} ergs. The dataset allowed us to constrain flare frequency distributions (FFDs) for stars from M0 to M6 in the NUV up to 105 s in equivalent duration and 1034 ergs in energy, orders of magnitude above any previous study in the UV. We find flare rates increase monotonically with spectral type, with a 2 OOM increase from M0 to M6. There is a commensurate increase in their contribution to total NUV stellar energy budgets, from ~5% at M0 to ~33% at M4. We also note that flare rates in the UV are several OOM above those in the visible/NIR bands, making the extrapolation of UV FFDs from optical data highly error prone.



Impact on Habitability: We obtained median quiescent NUV irradiances on planets in habitable zones (HZ) of M0-M6 stars and estimated the frequency of flares required to equal the NUV irradiance of a young Earth. The median quiescent irradiance is lower by ~2 OOM as compared to young Earth [2], possibly inhibiting abiogenesis on planets orbiting early and mid M-Dwarfs considering our assessment of flare rates. However, the large spread in NUV luminosities found across the sample, the presence of highly energetic flares, and the likely lower true limiting NUV irradiance required for abiogenesis [1,3] suggests it could occur on some fraction of these planets. On the other hand, we found the frequency of energetic UV flares and associated CMEs might inhibit the formation of an ozone layer, thereby exposing planetary surfaces to sterilizing levels of UV radiation. **Future Work:** In light of these results, it becomes imperative to accurately characterize the variation and interdependence of NUV flare rates and luminosities across spectral types and stellar ages, also considering the inward migration of HZs with age. We thus require an extensive campaign of long-term UV observations of M-dwarfs which will be provided by ULTRASAT, a wide FoV NUV telescope to be launched in 2026. We estimate

ULTRASAT will detect $\mathcal{O}(10^6)$ M-dwarf flares over 6 months of continuous exposure. When coupled with spectroscopic observations, this will enable the scientific community to form a better understanding of NUV flare activity on Mdwarfs, and its impact on atmospheric evolution and habitability.

References: [1] Param Rekhi et al. (2023) The Astrophysical Journal 955:24. [2] Sukrit Ranjan et al. (2017) The Astrophysical Journal 843:110. [3] Paul B. Rimmer et al. (2018) Science Advances 4:eaar3302.

80. UNDERSTANDING HABITABILITY AND LIMITS OF LIFE: OPPORTUNITIES THROUGH INDIAN SPACE PROGRAMME

C. P. Singh, Mehul R. Pandya and Rashmi Sharma

EPSA, Space Applications Centre, ISRO, Ahmedabad, Gujarat, India

cpsingh@sac.isro.gov.in, mrpandya@sac.isro.gov.in, rashmi@sac.isro.gov.in

Introduction: Habitability has been defined as the potential of an environment (past or present) to support life of any kind; it is a function of a multitude of environmental parameters whose study is biased by the effects that biology has on these parameters; and it may be a matter of degrees, depending on how much diversity, productivity, or spatial cover of life that an environment supports. Earth is the only inhabited world known to us. Astrobiologists are exploring to develop a catalogue of planets orbiting other stars to explore potential habitability with diverse and exotic chemistries and environmental settings. As we are limited with our experience with habitability, on Earth alone, it has limited understanding of the basic settings for a potential habitable world, however this experience may even serve as a helpful guide for the search for habitability beyond Earth. A direct understanding of habitability provides context for interpreting the apparent biosignatures, or their absence. Habitability indicators, including biosignatures (carbon and organic compounds), must be interpreted within a planetary and environmental context (water, temperature, pressure, radiation, atmosphere), while synthesising the information from a large range of spatial scales. Space telescopes and other national/ international future space and planetary missions are opening up new avenues to assist in the study of biosignatures on exoplanets, apart from zero gravity experimentation and radiation exposure experiments avenues on biological samples, on the anvil with upcoming Indian Gaganyaan and Bhartiya Antariksh Station.

Understanding the limits of life and mechanisms adopted by extremophiles on Earth is important step in developing our understanding towards habitability and terraforming on other planetary bodies. Ecosystem approach is important in this direction and drawing clue from Earth, lichens are the best biological material for such experiments as they are known to be extremophiles and first colonisers on any undisturbed surface. We propose to study the effect of microgravity on the return sample of lichens on morphological, anatomical, physicochemical properties and production of secondary metabolites in response to stimulus (microgravity and cosmic radiation). Secondary metabolites are created by lichens as a defence mechanism to protect themselves when they are exposed to various environmental stressors. Lichens are known for their adoptability towards extreme environmental conditions and therefore, they are of interest for astrobiological research [1]. Earlier only the *Rhizocarpon geographicum* and *Xanthoria elegans* lichens were used in space research. Both the species are high altitudinal distribution and having only green algal photobiont. It is well known that cyanolichens are more sensitive than the chlorolichens [2]. However, there is a need to find out the comparative effect of microgravity on lichens containing blue green algae as well as green algae. Apart from having universal space lichen, i.e. *R. geographicum*, containing green algal photobiont; *Leptogium deticulatum* containing blue green algae is also proposed to be exposed. Health of lichens photobiont (green algal/cyanobacterial component) may predict the future strategies of research in space for the purpose of terraforming experiments.

Discussion & way forward: Building a robust ground-based program on extremophiles as analogue study to planetary life systems (e.g. Antarctica, Arctic, Ladakh, Deep-Sea, Geysers, etc) is essential to predict habitability on other planetary bodies at different scales. Pre-investment studies can be taken up using data available in open domain like material property database of organic liquids, ices, and hazes on Titan (available at Astrobiology Habitable Environments Database - AHED, <https://ahed.nasa.gov>). These data can be used as inputs for various theoretical models to interpret current and future remote sensing and *in-situ* atmospheric and surface measurements. The material properties of the simple organics may also be applicable to giant planets and icy bodies in the outer solar system, exoplanets, interstellar medium, and protoplanetary disks. Bio-signatures (pigments, essential life forming elements) through remote sensing approaches essentially using data from JWST and such missions should be explored. Pursuing research in areas that are already having data in free domain from lander/rover missions related to finding biosignatures of life (phosphorous, amino-acids etc.). Lipid biomarkers from microbial mats on the McMurdo Ice Shelf, Antarctica, is signatures for life in the cryosphere apart from the hyperspectral signatures collected for lichens by Indian scientists in extreme environment of Antarctica [3]. ThermoBase is another global database that houses comprehensive descriptions for 1238 thermophilic or hyperthermophilic organisms, which can be utilized for the study.

References: [1] Sadowsky A., Hussner A. and Ott S. (2012) *Nova Hedwigia* 94(3–4):1–12. [2]. Gauslaa Y., Coxson D.S. and Solhaug K.A. (2012) *New Phytologist* 195(4): 812–822. [3]. Singh C.P., et al. (2023) *Polar Science*, doi: 10.1016/j.polar.2023.100976

81. Using mid-IR spectroscopy to study interstellar ice analogues

Sohan Jheeta

sohan@sohanjheeta.com

Introduction

It has not been reported to date that 90% of the organic molecules which were present on the surface of the early Earth were made in the vicinity of the interstellar medium from whence the Earth was accreted. The other candidate locations (such as at the boundaries of denser and less dense atmospheric layers as well as hydrothermal vents on the seabed) pale into insignificance. These organic compounds can be made via both gas phase and solid phase chemistry. In context of this abstract, only the latter will be considered when highlighting: “Using mid-IR spectroscopy to study interstellar ice analogues.”

82. Sustainable Lunar Habitat Design: Utilizing PEMFCs in Lava Tube for Creating an Artificial Atmosphere

Tuhina Bhuniya¹, Risabh Paul², Akshanth Sai K³,^{1,2}School of Electronics Engineering (SENSE),
Vellore Institute of Technology, Vellore, Tamil Nadu, India
632014,¹(tuhinabhuniya2688@gmail.com),

²(paulrisabh3@gmail.com),³School of Computer Science and Engineering (SCOPE), Vellore Institute
of Technology, Vellore, Tamil Nadu, India 632014(akshanthkakubal@gmail.com)

Introduction: Lava tubes have emerged as potential future lunar habitats since these naturally occurring structures, formed during volcanic activity, provide insulated environments beneath the moon's surface^[1]. Moreover, they offer protection against extreme temperature fluctuations, micrometeorite impacts, cosmic radiation, and lunar winds. The solidified remnants of lava within these tubes have resulted in stable and cavernous spaces that present unique opportunities for shelter and exploration^[2]. Literature emphasises the inefficacy of traditional electricity and atmospheric generation methods for sustainable dwelling. Establishing a reliable and perpetual energy source becomes imperative for long term lunar habitability. This paper explores the utilisation of Proton Exchange Membrane Fuel Cell (PEMFC) mechanisms within lava tubes for the generation of electricity and water.^[3] Thereafter, oxygen requirements can be met through extraction by carbothermal reduction of lunar regolith whereas hydrogen from the lunar atmosphere. These elements can also be obtained through electrolysis of water produced from the fuel cell reactions. Furthermore, the manuscript highlights the advantages of PEMFC over different sources of energy generation, additionally addressing issues regarding structural stability, atmosphere, ventilation, optimal pressure, and temperature inside an innovatively designed lava tube.

References:

[1] Theinat, A. K., Modiriasari, A., Bobet, A., Melosh, H. J., Dyke, S. J., Ramirez, J., ... & Gomez, D. (2020). Lunar lava tubes: Morphology to structural stability. *Icarus*, 338, 113442. [2] Martin, R. P., & Benaroya, H. (2023). Pressurized lunar lava tubes for habitation. *Acta Astronautica*, 204, 157-174. [3] Luo, Y., & Jiao, K. (2018). Cold start of proton exchange membrane fuel cell. *Progress in Energy and Combustion Science*, 64, 29-61.

83. DYNAMIC GEOPHYSICAL CONDITIONS AND PROBABILITY OF ADVANCED LIFE IN POTENTIALLY HABITABLE ROCKY EXOPLANETS.

Varnana M. Kumar¹, T. E. Girish², P. E. Eapen³, Thara N. Sathyan¹, Biju Longhinos⁴, K.S. Sony² and J. Binoy¹, ¹Department of Physics, Government College for Women, Trivandrum 695014, INDIA, e-mail: mvarnana@gmail.com, ²Department of Physics, University College, Trivandrum 695034, INDIA, ³Department of Physics, SG College, Kottarakkara 691531, Kerala, INDIA, ⁴Geology Section, Department of Civil Engineering, College of Engineering, Trivandrum 695016, INDIA.

Introduction: Earth remains still as the lone planet with confirmed advanced life in the Universe [1]. More than 5200 exoplanets have been identified till date and only 63 (1.2%) of them are considered to be potentially habitable. Different criteria [2] have been evolved for identifying potentially habitable extrasolar planets (PHESP hereafter). Probability of advanced life in potentially habitable exoplanets based on dynamic geophysical conditions is not attempted previously. This work is an update of our earlier paper [3].

Methods of Data Analysis: Based on our results on previous studies on the time evolution of volcanism in the inner solar system, we have tried to infer dynamical geophysical conditions in 53 potentially habitable extrasolar planets given in the Catalogue of University of Puerto Rico [4]. Using solar system rocky planet analogy we have inferred the phases of volcanism if any in these extrasolar planets at earth and host star ages. We have then calculated the magnitude of tidal heating [5] and magnetic moment of these PHESP using procedure available in published literature [6–7]. Based on these inferences and calculations we have inferred the probability of finding life favoring geophysical conditions such as water, oxygen, ozone and magnetic field shielding at earth and host star ages for these PHESP.

Results: 1. According to our calculations life favoring geophysical conditions can be found with high probability in extrasolar planets with an age greater than 3.75 Gyrs if their mass is comparable to Earth. The same is most probable in extrasolar planets at an age greater than 5 Gyrs if their mass is twice that of our Earth.

2. Only three planets out of 52 PHESP (listed by University of Puerto Rico in early 2023) are found to have high habitability probability from our studies based on the inference of dynamic geophysical conditions.

3. Two conditions possess challenges to the development of advanced life in extrasolar planets near M stars. They are (i) hazardous space weather conditions due to super flares near M stars. (ii) Long night periods of M star extrasolar planets due to their inferred slow rotation periods.

4. The probability of finding advanced life in extra solar planets in our galaxy is inferred to be very low from our investigations.

References:

[1] Spiegel D. and Turner E. L. (2011) *Proceedings of the National Academy of Sciences*, 109:395–400, <https://doi.org/10.1073/pnas.1111694108>. [2] Kopparapu R. K. et al. (2019) *Characterizing Exoplanet Habitability*, arXiv:1911.04441[astro-ph.EP] [3] Varnana M. Kumar et al. (2023) Inference of Dynamic Geophysical Conditions and Probability of Advanced Life in Potentially Habitable Rocky Exo Planets. *Preprints 2023*, 2023030327, <https://doi.org/10.20944/preprints202303.0327.v1> [4] University of Puerto Rico (2023) The Habitable Exoplanets Catalog,

available at <https://phl.upr.edu/projects/habitable-exoplanets-catalog>, accessed on January 10, 2023. [5] Hector Javier Durand-Manterola (2009) *Planetary and Space Science*, 57:1405–1411, <https://doi.org/10.1016/j.pss.2009.06.024>. [6] Driscoll P. E. and Barnes R. (2015) *Astrobiology*, 15:739–760, <https://doi.org/10.1089/ast.2015.1325> [7] Varnana M. Kumar et al. (2023) In: Bisikalo D. et al. eds. The Predictive Power of Computational Astrophysics as a Discovery Tool, *Proceedings IAU Symposium No. 362*: 175–176, <https://doi.org/10.1017/S174392132200148X>.

84. LONGEVITY OF HYDROLOGICAL REGIME AND WATER ACTIVITY AS IMPORTANT PARAMETERS IN SEARCH FOR ASTROBIOLOGICAL TARGET SITES

D. Singh^{1*}, K. Acharyya¹ and R.K. Sinha¹ ¹Planetary Science Division, Physical Research Laboratory, Ahmedabad, Gujarat, India- 380009 (deeps301090@gmail.com)

Introduction: For a long time, there has been a search for evidence of water in the Martian past since it is the main solvent of all life on Earth. In this context, certain chlorides have shown the potential to provide a harbour for microbes to survive and propagate in extreme conditions [1,2]. This work, therefore, explores a chloride-rich sedimentary basin within the Terra Sirenum region of Mars [3-6] and reconstructed its hydrological regime to understand its potential as an astrobiological target site.

Methods: The habitability potential of an area is a function of a conducive environment and the longevity of those sustainable conditions [4]. To ascertain the duration of hydrological activity we carried out fluid and sediment discharge analysis[7,8] using ConTeXt (CTX) Camera its Digital Elevation Model [9,10]and subsequently modelled the availability of water, or water activity, within the basin by considering it as a multicomponent system [11] and deriving the ionic forms from its mineralogical profile.

Results and discussion: Sediment transport modelling of the surrounding network of valleys suggests that the basin was hydrologically active for at least a thousand years with periods of drying and wetting. We categorized the possibility for habitability into three fields using two isolines at 0.75 [12,13] and 0.55 based on the saturation points of the dominant chloride species and lowest known limit of life i.e., 0.565 [14,15]. Water activity modelling of the system and its comparison with Earth-based playas suggests this mineralogical combination does not adversely decrease the availability of water (i.e., beyond 0.75) for living systems since microorganisms have been found in even poorer environments on Earth. **Conclusion:** We propose that duration of hydrological regime within an area and ions conducive to high water activity must be included as important factors for site selection for future astrobiologically oriented missions.

References: [1] Davila et al. (2008). *JGR: Biogeosci.* 113 (1), 1–9. [2] Wierzchos et al. (2011). *Geobiology*, 9(1), 44–60. [3] Osterloo et al. (2008). *Sci.*, 319(5870), 1651-1654. [4] Osterloo et al. (2010). *JGR: Planets*, 115(E10). [5] Singh et al. (2023). *LPS.*, Abstract #2806. [6] Singh et al. (2024). Manuscript submitted. [7] Kleinhans (2005). *JGR: Planets*, 11(E12). [8] Wilson et al. (2004). *JGR: Planets*, 109(E9). [9] Malin et al. (2007). *JGR: Planets*, 112 (E5). [10] Quantin-Nataf et al. (2018). *Planet. and Sp. Sci.*, 150, 157-170. [11] Pitzer (1991). CRC Press, 75-153. [12] Grant (2004). *Phil. Trans. of the Royal Soc. Lon. B: Bio. Sci.*, 359(1448), 1249–1267. [13] Lee et al. (2018). *FEMS Micro. Rev.*, 42(5), 672–693. [14] Stevenson et al. (2015). *ISME Jour.*, 9, 1-19. [15] Stevenson et al. (2017). *Env. Micro.*, 19(2), 687-97.

85. Automatic Crater Detection on Lunar Surface.

A. Das¹, M. G. N. Lala², A.P. Krishna³ and S. Garg⁴
¹²³⁴Birla Institute of Technology, Mesra

Abstract: Craters are the main morphological feature with the help of which we can get almost 70% information about the Geology and Stratigraphic time scale of a rocky planet or satellite like our Moon. The moon has been studied since the advent of space exploration still the polar region in particular the South Pole region of the moon is still a mystery to us. With the help of India's first orbiter ever Chandrayaan-1 Terrain Mapping Camera DEM image we tried to automate the location of craters on the lunar surface with the help of Deep Learning and Transfer Learning.

The Automation of Crater with our model gave us a good accuracy of 80.26% where we were able to detect both shallow as well as deep craters on the lunar surface

Keywords: Automatic Crater Detection, Lunar Surface, Transfer Learning, TMC-1 DEM

References:

[1] Bandeira L., Ding W., Stepinski T.F., (2012). Detection of subkilometer craters in high resolution planetary images using shape and texture features. *Advances in Space Research* 49, 64-74. [2] Crater Analysis Techniques Working Group, (1979). Standard Techniques for Presentation and Analysis of Crater Size-Frequency Data. *ICARUS* 37, 467-474. [3] DeLatte D.M., Crites S.T., Guttenberg N., Yairi T., (2019). Automated crater detection algorithms from a machine learning perspective in the convolutional neural network era. *Advances in Space Research*. 64, 1615-1628. [4] Silburt A., Ali-Dib M., Zhu C., Jackson A., Valencia D., Kissin Y., Tamayo T., Menou K., (2018). Lunar Crater Identification via Deep Learning. *ICARUS*. [5] Wang Y. and Wu B., (2019). Active Machine Learning Approach for Crater Detection from Planetary Imagery and Digital Elevation Models. *IEEE Transactions on Geoscience and Remote Sensing*. [6] Zhou Y., Zhao H., Chen M., Tu J., Yan L., (2018). Automatic detection of lunar craters based on DEM data with the terrain analysis method. *Planetary and Space Science*.

86. Lunar Launchpad to Cosmic Frontiers: Navigating Interplanetary Exploration from the Moon

Gourav Mohanan, Dayananda Sagar University (DSU), gouravmohanan12@gmail.com

Sindhu MG, Dayananda Sagar University (DSU), sindhumg25@gmail.com

As the frontier of interplanetary travel unfolds, innovative solutions become paramount. This research sets a course toward new horizons by exploring the integration of advanced technologies into the operational framework of lunar missions. The objective is to empower spacecraft originating from the Moon with autonomous navigation capabilities, thereby reducing dependence on Earth-based commands and propelling us into deeper realms of exploration beyond our lunar neighbour.

Interplanetary travel presents inherent challenges, such as communication delays and the need for real-time decision-making. This research advocates for spacecraft equipped with the ability to analyse data onboard and autonomously make informed decisions. The goal is to redefine the efficiency and adaptability of interplanetary exploration, beginning with missions launched from the Moon.

The primary aim is to maximize the scientific potential of interplanetary missions by leveraging autonomous systems onboard spacecraft. These systems are designed to adapt trajectories dynamically, responding to unexpected phenomena and optimizing resource utilization to enhance the overall scientific yield.

The research methodology involves the development and rigorous testing of navigation algorithms tailored specifically for interplanetary missions originating from the Moon. These algorithms undergo training using simulated mission scenarios and historical data, ensuring robust performance in navigating the vastness of space. The study addresses challenges associated with autonomous navigation in deep space, including trajectory planning, course corrections, and optimized resource allocation.

Anticipated outcomes include a demonstration of the feasibility and effectiveness of autonomous navigation for interplanetary exploration. The research aims to provide insights into the transformative potential of this technology for the future of interplanetary travel, showcasing how autonomous systems proactively contribute to mission objectives. The findings emphasize the role of autonomous navigation in shaping the future of interplanetary exploration, unlocking the full scientific potential as humanity ventures beyond the Moon into the cosmic unknown.

This research signifies a critical contribution to the evolution of interplanetary travel methodologies, highlighting the pivotal role of autonomous navigation in unlocking the full scientific potential of exploration as we extend our reach into deep space from the Moon.

References:

Filip, J., Azkarate, M., and Visentin, G. (2017). "Trajectory control for autonomous planetary rovers," in 14th Symposium on Advanced Space Technologies in Robotics and Automation (ASTRA).

Fraunhofer-Institut für Kommunikation, Informationsverarbeitung und Ergonomie FKIE (2017). *Fkie multimaster for ros*. Available at: https://github.com/fkie/multimaster_fkie. Accessed on 2022-10-20

Gerdes, L., Azkarate, M., Sánchez-Ibáñez, J. R., Joudrier, L., and Perez-del Pulgar, C. J. (2020). Efficient autonomous navigation for planetary rovers with limited resources. *J. Field Robotics* 37, rob21981. doi:10.1002/rob.21981

German Research Center for Artificial Intelligence GmbH (2022). *Rimres - reconfigurable integrated multi robot exploration system*. Available at: <https://robotik.dfki-bremen.de/en/research/projects/rimres.html>. Accessed on 2022-02-22

Gläser, P., Oberst, J., Neumann, G. A., Mazarico, E., Speyerer, E. J., and Robinson, M. S. (2018). Illumination conditions at the lunar poles: Implications for future exploration. *Planet. Space Sci.* 162, 170–178. doi:10.1016/j.pss.2017.07.006

87. Surface and Subsurface Regolith Characterization of Lunar South Pole using Chandrayaan-2 Dual-frequency Synthetic Aperture Radar (DFSAR)

Krishangi Kashyap¹ and Unmesh Govind Khati¹

¹Department of Astronomy Astrophysics and Space Engineering, Indian Institute of Technology Indore, Khandwa Road, Simrol, Indore 453552, Madhya Pradesh E-mail ID: msc2203121006@iiti.ac.in

Abstract: Despite its proximity to Earth, vast regions of the Moon remain unexplored quantitatively, particularly the Permanently Shadowed Regions (PSRs) which are located at the poles. Identified by LRO Diviner as the coldest lunar locations (temperature reaching > 100 K), these PSRs harbour potential volatiles such as water ice, ammonia, methane etc. implanted into the regolith by solar winds and meteorite impacts which are valuable for future robotic and manned missions, prompting a need for precise mapping of their distribution and abundance [1]. This research focuses on the south polar region 'Faustini Rim A' located at the latitude of 87.3°S , which was chosen as one of the potential landing sites for upcoming Artemis III mission. Moreover, ensuring a successful lander touchdown necessitates the selection of a terrain devoid of rocks. Therefore, this study utilizes Chandrayaan-2's Dual-frequency Synthetic Aperture Radar (DFSAR) fully polarimetric data acquired by simultaneous operation mode to perform a comparative analysis of the presence of different types of scatterers and volumetric rock abundance at surface and subsurface levels.

The DFSAR image covers portions of two south polar craters, Shoemaker and Faustini. The PSR within Shoemaker and the wall of Faustini crater are observed, leveraging the deeper penetration of L-band radar compared to S-band [2] to gain new insights into subsurface properties. Applying Pauli (coherent) decomposition [3] and model-based (incoherent) Freeman Durden decomposition [4] methods to the radiometrically calibrated data reveals a variety of scattering mechanisms across the study area. Seven distinct regions exhibiting mixture of these mechanisms were chosen for detailed analysis, aiming to characterize both surface and subsurface properties. In order to estimate the rock abundance, a recently developed CPR based linear model [5] was applied to both L-band and S-band data across the entire study area.

Analysis of single scatterers reveal distinct characteristics between Shoemaker and Faustini. Inside Shoemaker, the walls of small craters exhibit high double-bounce scattering in S-band, indicative of blocky ejecta or rocks on the surface. Conversely, the subsurface reveals a mixture of surface and double-bounce scattering implying mixed regolith with small blocks. On the other hand, Shoemaker crater floor reveals higher volume scattering at the subsurface level, suggesting loosely packed regolith particles. Faustini crater presents a different picture. Its wall and the small crater on its rim show prominent double-bounce scattering with surface scattering in L-band. This indicates compactly packed regolith particles at the subsurface, creating a smooth surface, while the walls themselves are rugged. Some volume scattering remains at the surface level due to multiple scattering from regolith particles. In terms of distributed scatterers, the crater on the Faustini rim displays volume scattering in both S-band and L-band, likely due to loosely held regolith and blocky ejecta on the surface and subsurface. This observation suggests increasing surface scattering with deeper penetration into the regolith, as L-band becomes less sensitive to smaller objects compared to S-band. Rock abundance analysis reveals maximum rock concentration on the surface of Shoemaker floor and on the wall of the small crater inside Shoemaker at its subsurface level.

References: [1] Sharma, A., Kumar, S., & Bhiravarasu, S. S. (2023). *Advances in Space Research*. [2] Kumar, S., Singh, A., Sharma, A., Chaudhary, V., Joshi, A., Agrawal, S., & Chauhan, P. (2022). *Advances in Space Research*, 70(12), 4000-4029. [3] López-Martínez, C., & Pottier, E. (2021). *Polarimetric Synthetic Aperture Radar: Principles and Application*, 1-58. [4] Freeman, A., & Durden, S. L. (1998). *IEEE transactions on geoscience and remote sensing*, 36(3), 963-973. [5] Gao, Y., Zhao, F., Hou, W., Han, Y., Liu, M., Dang, Y., Lu, P. & Wang, R. (2023). *IEEE Journal of Selected T*

88. Morphological, Mineralogical, and Chronological Mapping of Nernst Crater Using Lunar Remote Sensing Datasets

Keerthana R ^{1*}, Annadurai R ¹ and Kusuma K.N ²

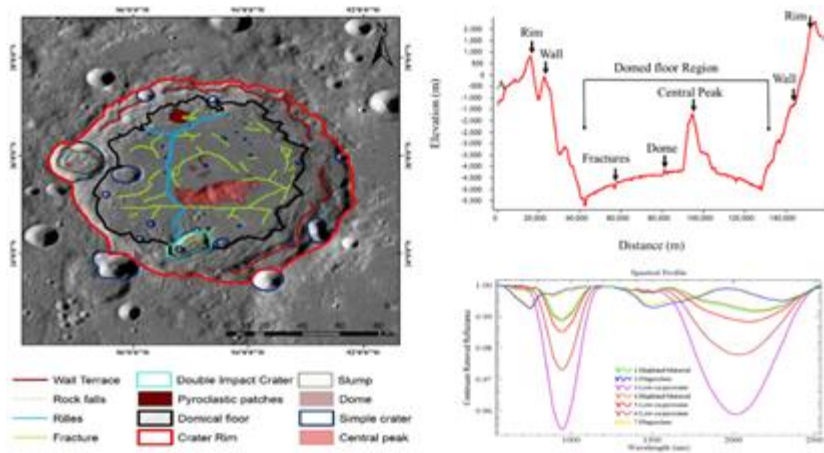
¹ Department of Civil Engineering, SRM Institute of Science and Technology, Kattankulathur - 603 203

² Department of Earth Sciences, Pondicherry University, Puducherry – 605 014

*Corresponding author email –keerthcivil10@gmail.com

Abstract

Nernst impact crater is located in the highland region and has a diameter of 116 km. It is situated on the northwestern limb of the Oceanus Procellarum [1]. It has a Floor Fractured Crater (FFC) associated with a series of concentric fractures and a domical floor profile. This study investigates the morphology and mineralogy of the crater. From the mineralogy, analysis was carried out in the present study area to identify various minerals such as LCP, Highland Material, and Plagioclase. Using M3 datasets, an Integrated Band Depth-based Color Composite Image was generated to differentiate among similar spectral profiles [2] [3]. The Nernst crater lies on the feldspathic Highland Terrane, which exhibits an anorthosite signature on the crater rim, floor, and central peak. The morphological analysis was carried out using the Lunar Reconnaissance Orbiter and Kaguya DEM images identified features such as uplifted central peak, dome, fractures, rilles, rim, rolling stone, Double Impact crater, convex floor, and wall terrace are marked on the morphological map. There is an additional impact crater, Nernst T, just on the western rim edge of the Nernst crater. Nernst T crater contains rolling stone, rock boulders, domes, lunar slump, and minerals such as low calcium pyroxene (LCP) and pure crystalline plaque. Combining CSFD-based chronology with morphology and mineralogy revealed that the Nernst crater ejecta and its floor fell from pre-Nectarian to early Imbrian periods (4 Ga and 3.8 Ga, respectively). The concentric and polygonal fractures show an age of 3 Ga, indicating that they might have originated during the formation of the FFC due to the tensional forces and associated rebound. The radial fractures and dome show a much younger age of 1.2 Ga, hinting towards a much later volcanic intrusion, which is also responsible for the convex floor profile of Nernst's crater and pyroclastic deposit. The presence of much younger basalts in the Procellarum terrain about 600 km East of Nernst crater hints that the origin and evolution of the Nernst crater is closely related to the late-stage magmatic activity in the Oceanus Procellarum Terrane. The integrated analysis reveals that anorthosite was present in and around the Nernst crater and that the study area is classified as a class 2 floor fractured crater.



References:

[1] Donaldson et al. (2014) *Journal of Geophysical Research Planets*, 119 1516–1545, [2] Mustard. (2011) *Journal of Geophysical Research*, 116. [3] Besse et al. (2011) *Journal of Geophysical Resource*, 116, 1-15

89. COMPOSITIONAL DIVERSITY OF MANILIUS CRATER AND SURROUNDING REGION USING CHANDRAYAN HYPERSPECTRAL DATASETS.

Suyash Sharma¹ (*ssharmaco07@gmail.com*), Nabamita Chaudhuri², K.N.Kusuma³ and Subhadip Bhadra⁴

^{1,2,3,4}Department of Earth Sciences, Pondicherry University

Introduction: The Manilius crater (14.452 ° N 9.0737° E), is a complex crater near the side of the Moon with a diameter of 38.29 km on the eastern edge of Mare Vaporum exhibits various morphological features such as a central peak, a raised rim, and asymmetrical ejecta deposits. Notably, the Manilius crater and its surrounding area are known to exhibit diverse lithologies. To gain a deeper understanding of this compositional diversity, we have conducted a detailed study using Chandrayaan datasets.

Datasets and Methodology We have analysed one data from the Chandrayaan-2 Imaging Infrared Spectrometer (IIRS) and three reflectance data from the Chandrayaan-1 Moon Mineralogy Mapper (M³) acquired in the OP2C optical period.

IIRS data provides radiance information in the 700-5000 nm spectral range. IIRS radiance data were converted to reflectance values using the method of [1], which also does photometric and thermal correction of the data. The derived reflectance image was georeferenced with respect to the Lunar Reconnaissance Orbiter Camera (LROC) Wide Angle Camera (WAC) global mosaic image. In the spectral subset (700 to 2500 nm), bad bands removed data were used for further analysis. M³ data were georeferenced and mosaicked. Integrated band depth (IBD) parameters around 1000nm and 2000nm were found to be useful in differentiating compositional variation using M³ [2] [3]. We applied IBD analysis on both IIRS and M³ data. Since IIRS has a different spectral range from the M³, the shoulder positions and number of bands for IBD parameters were modified accordingly. The IBD colour composites were generated for IIRS and M³ data by assigning IBD1000, IBD2000 and 1500nm reflection bands to red, green and blue channels, respectively.

Results: The Manilius crater on the M³-derived IBD colour composite showcases blue rim and ejecta rays, indicating a plagioclase composition. Additionally, blue colour patches are visible on the crater floor, while the crater wall and floor exhibit green and yellow hues. The southwest side of the blue-coloured ejecta gets abruptly truncated by a yellow-coloured patch, which indicates a basalt composition younger than the Manilius Crater. The green-coloured area with patches of orange and yellow hues denotes variation in basalt composition and the presence of spinel.

IIRS data covers the eastern part of the Manilius crater and, compared to M³, exhibits a lot of vertical stripes, making it appear noisy. Despite this, the IIRS-derived IBD image highlights variations in lithology indicated by different colours, which match fairly with the M³-derived IBD. The southern part of the study area comprises part of Rima Hyginus and patches of lunar pyroclastic deposits (LPDs).

Representative spectra were extracted from M³ and IIRS reflectance data corresponding to different IBD colours revealing a mixture of plagioclase, pyroxene, chrome spinel and olivine from M³ spectra.

However, IIRS spectral analysis poses a challenge due to a spectral shift of the 1 μm feature and the presence of bad bands. The 2 μm features are broader and deeper than the M^3 spectra.

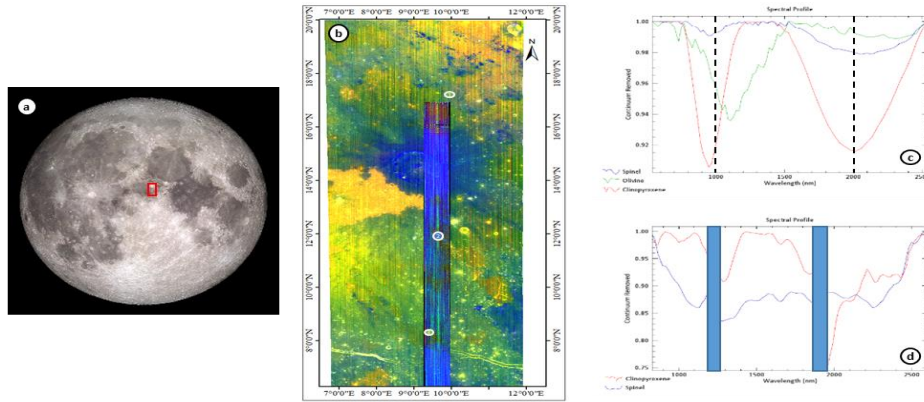


Figure a. Study area (in red box) on near side of moon. b. IBD color composite image (R: IBD1000G:IBD2000B:1500nm) derived from IIRS image of the Manilius crater and surrounding region overlaid on IBD color composite image derived from M^3 image. c. Spectral profiles from M^3 . d. Spectral profiles from IIRS

References: [1] Verma et al, (2022), Icarus 383(115075); [2] Mustard, J. F. et al (2011). JGR: Planets, 116(E6); [3] Besse, S. et al (2011). JGR: Planets, 116(E6)

90. IMBRIAN TO ERATOSTHENIAN VOLCANISM AND THE COMPOSITIONAL DELINEATION OF MARE UNITS OF MARE INGENII USING M3 , IIRS, TMC-2, AND KAGUYA DATA.

C.R Neeraja and S.Arivazhagan*, Centre for Applied Geology, The Gandhigram Rural Institute-Deemed to be University, Dindigul, Tamilnadu-624 302, India (*arivusv@gmail.com, neerajarajan577@gmail.com)

Introduction: Mare Ingenii is a significant volcanic basin in the northwest corner of South Pole Aitken Basin (SPA) situated at 33.7°S 163.5°E. Mare Ingenii witnessed geological activities from basin forming impact event at Preneectarian to volcanic activities spanning to Eratosthenian[1]. The Present study focused on the basaltic flows of Mare Ingenii covering the inner ring of the basin along with the lithological discrimination. Orbital remote sensing data collected from different lunar missions are used classify the basaltic units of the Mare Ingenii along with chronology of each mare units of the basin.

Data and Methodology: Ch-1 M3 ,Ch-2 IIRS, TMC-2, Kaguya TC, Kaguya Lunar Multiband Imager (MI) derived FeO weight percent map[2] and LROC WAC titanium distribution map[3] were used in the present study. Lithological discrimination is done by Standard Band Ratio mapping by using M3 data with the RGB band combination of R-750/540 nm, G-750/950 nm, and B-540/750 nm[4,5]. 1um and 2um IBD have been done using M3 and IIRS data to discriminate mafic lithology. Kaguya MI derived FeO weight percent map, the LROC WAC titanium distribution map and IBD color composite map is used for the compositional analysis. Comparing the color differences of FeO, TiO₂ map, and IBD color composite image (generated by IBD1000, IBD2000, and R1578 to red, green, and blue channels respectively using M3 data) the mare can be delineated into different units[6]. Crater Size Frequency Distribution (CSFD) has been used to determine the absolute model ages of Mare basalt of the Ingenii basin. Kaguya TC is used for crater counting studies and 200m to 10km diameter craters are used for the study.

Result and Discussion: FeO value ranges up to 22 wt.% and TiO up to 7.2 wt.% for Mare Ingenii. Based on the color variations in FeO, TiO₂ map and IBD color composite images, the basaltic units of the study area have been divided into 19 units. The highest iron and titanium values are observed in unit T3 of Thomson crater (>21 wt.% FeO, up to 7.2 wt.% TiO₂), indicating the presence of intermediate Ti basalts in the region and the age corresponds to 2.8 Ga. Lowest age 2.3Ga is shown by a melt pond associated with a relatively fresh sinuous rille in the northern portion of inner ring Ri, has a FeO wt% of 8–13 % and ≤2 wt% TiO₂. All the 19 units and their FeO, TiO₂ wt% and corresponding age have been calculated. The age of the unit ranges from 3.8 to 2.3 Ga. Western units of the basin are the oldest, then multiple volcanic episodes to the eastern part covered Thomson M and Thomson crater. The initial volcanic event took place at the boundary between early and late Imbrain at 3.8Ga emplacing low Ti– basalt in the unit Ig5. Later volcanic events supplied intermediate titanium basalt in the region during the Eratosthenian period around 2.8Ga. It infers the possibility of heterogeneous melt sources supplied for different episodes of mare volcanism.

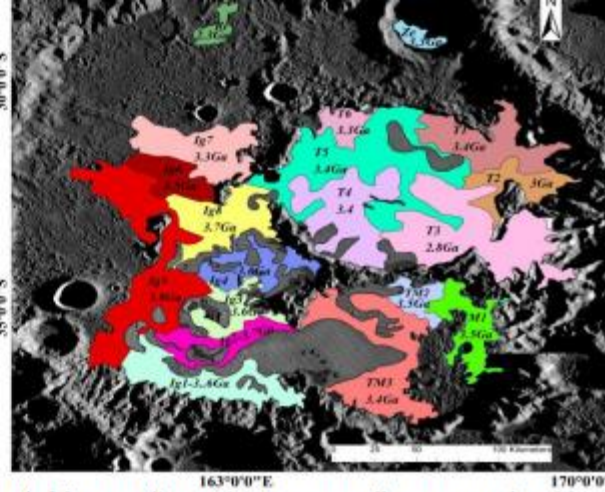
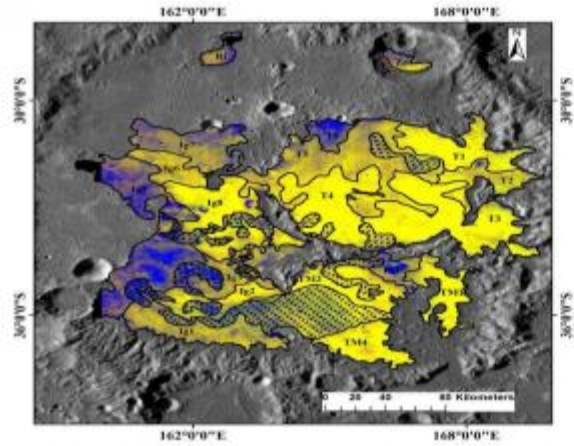


Figure 1. IBD color composite image (generated by IBD1000, IBD2000, and R1578 to red, green, and blue channels respectively using M^3 data

Each Mare units and corresponding age using Kaguya TC Merge

Reference: [1] Pasckert et al., 2017 *icarus*.2017.07.023., [2] Lemelin et al 2016, 47Th LPSC Abstract #2994. [3]Sato et al 2017, *Icarus* 296, Pp 216-238 [4] Arivazhagan and Anbazhagan 2012, 43rd LPSC [5] Arivazhagan and Karthi 2018, *Planet. Space Sci*161, Pp. 41–56., [6] Thesniya et al., 2020, *Meteorit Planet Sci* 1-29.

91. AUTOMATIC CRATER DETECTION AND CLASSIFICATION ON LUNAR SURFACE USING NEURAL NETWORKS

Vaishnavi Sharma¹, Suchit Purohit¹, Jyoti Pareek¹

¹Department of Computer Science, Gujarat University- 380009.

E-mail: vrsharma2003@gmail.com

Introduction: Secondary craters contaminate the process of crater counting through CSFD method leading to spuriously high age estimation. Therefore, it is necessary to eliminate them beforehand. So far, secondary crater detection has been done through manual or rule-based automatic methods. This study proposes an approach to automatically discriminate a secondary crater from the primary ones using neural network framework. The investigation area surrounds the Orientale impact basin, i.e., region covering an area of about six radii from the rim of Orientale, with the help of DEMs obtained from TMC-2 instrument onboard Chandrayaan-2. The proposed methodology consists of selecting the region of interest, the one which overlap with secondary crater database (surrounding Orientale impact basin) provided by [1], preparing the dataset and exporting it into YOLO format and then finally training a neural network architecture, using an Ultralytics implementation of YouOnlyLookOnce (YOLO) version 8 [2]. To test the approach, the detected craters are checked with the already reported secondaries by [1]. The new detections are verified by rule-based approach, by extracting the morphological parameters and observing the spatial distribution encompassing chain or cluster arrangements. The objective of this study is to prepare global map of secondaries on lunar surface utilizing TMC-2 data set.

References: [1] D. Guo, J. Liu, J. W. Head, and M. A. Kreslavsky, "Lunar Orientale Impact Basin Secondary Craters: Spatial Distribution, Size-Frequency Distribution, and Estimation of Fragment Size," *J Geophys Res Planets*, vol. 123, no. 6, pp. 1344–1367, Jun. 2018, doi: 10.1029/2017JE005446.[2] G. Jocher, A. Chaurasia, and J. Qiu, "Ultralytics YOLOv8." 2023. [Online]. Available: <https://github.com/ultralytics/ultralytics>

92. DUST DETACHMENT FROM THE LUNAR SURFACE

S. K. Mishra*¹, and T. Sana^{1,2}

¹Physical Research Laboratory, Ahmedabad, 380009, India.

²Indian Institute of Technology, Gandhinagar, 382055, India (*Corresponding Author: sanjaym@prl.res.in)

The phenomenon of the dust detachment from the lunar surface has been of immense interest since long [1-2]. In literature, the electrostatic processes are fundamentally important in understanding particle dynamics and the complex dusty plasma environment over the Moon [3-5]. Based on the charge fluctuation approach in connection with photoemission current, this presentation addresses the fundamental problem of dust detachment from the lunar surface. By applying the charge fluctuation at the microscopic scale [6], we have quantified the magnitude of fluctuating charge density over the sunlit lunar surface and illustrate that it could induce sufficient electric field to overcome the dust–surface adhesive Van der Waals bonding through the electrostatic Coulomb repulsion.

Herein this presentation, we examine the fact and quantify the magnitude of the charge fluctuation and subsequent electric field due to the dominant photoemission charging at the microscopic scale in the context of the sunlit lunar surface. Accounting for the dynamic equations for the statistical variables [7-9], corresponding to the charge distribution over the microscopic spots exposed to solar radiation, the fluctuating charge and field strength have been derived. The calculations suggest that the electrostatic fluctuation may trigger significantly large charge density over the microscopic spots compared to the mean value of the charge [10]. As an illustrative example, it is shown that one square micrometer spot may acquire ~15 electronic charges and might induce the local electric field equivalent to ~ 10kV/m, which can support the detachment of the submicron dust particles from the lunar surface.

The presentation gives a conceptual and quantitative basis for understanding the significance of the statistical charge fluctuation in the dust particle detachment from the lunar surface. It suggests that the microscopic charge fluctuations due to photoelectric charging may induce the detachment of the submicron particles from the lunar surface.

References: [1] J. J. Rennilson and D.R. Criswell, *Moon* 10, 121 (1974). [2] J. E. McCoy and D. R. Criswell, *Proc. Lunar Sci. Conf. 5th*, 2991 (1974). [3] H. Zook and J. Mc. Coy, *Geophys. Res. Lett.* 18, 2117 (1991). [4] X. Wang, M. Horanyi and S. Robertson, *Jour. Geophys. Res.* 114, A05103 (2009). [5] X. Wang, J. Schwan, H. W. Hsu, E. Grun and M. Horanyi, *Geophys. Res. Lett.* 43, 6103 (2016). [6] E. V. Rosenfeld and A. V. Zakharov, *Icarus* 338, 113538 (2020). [7] T. E. Sheridan and A Hayes, *Phys. Plasmas* 98, 091501 (2011). [8] T. E. Sheridan, *Phys. Plasmas* 113, 143304 (2013). [9] B. Shotorban, *Phys. Rev. E* 83, 066403 (2011). [10] S. K. Mishra, *Phys. Plasmas* 27, 052901 (2020).

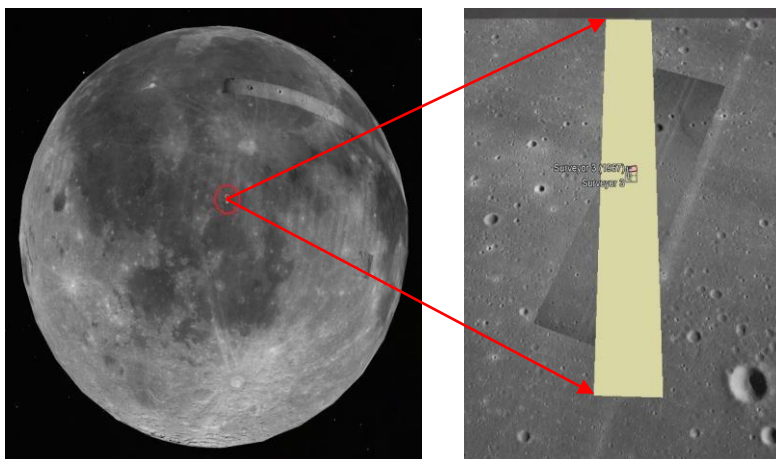
93. Advance Lunar Surface Exploration: A Comparative Analysis of Deep Learning Models for Crater Detection Using Chandrayaan-2 OHRC Data

Harshaditya Gaur¹, Shaifali Garg² and Vinay Kumar³, ¹PRSD Dept. Indian Institute of Remote Sensing, Dehradun, Uttarakhand, ²GID Dept. Indian Institute of Remote Sensing, Dehradun, Uttarakhand.


Abstract: The study of planetary science has reached new heights with recent technological advancements in remote sensing that have transformed our understanding of distant celestial bodies, enabling us to analyze surface composition, atmospheric dynamics, geographical features etc [1]. Planetary geographics, such as lunar terrain, are vastly covered with craters. The collision of extraterrestrial objects such as asteroids, comets, and meteorites on the lunar surface forms these circular surface depressions. These impact zones pose challenges for planetary missions in various domains, such as landing site selection of landers, navigation of extra-vehicular activities, rover path planning etc [2]. Crater detection is a formidable challenge due to their diverse and complex characteristics. The study focuses on the automated identification of lunar craters using the panchromatic dataset of the Chandrayaan-2 Orbiter High-Resolution Camera (OHRC), which provides a high spatial resolution of 0.25m with a swath of 3km (nadir view) for comprehensive insights into the lunar topography and morphology [3]. The area selected for this study covers the landing sites of Apollo 12 (April 1967) and Surveyor 3 (November 1969) missions, respectively. A comparative analysis of deep learning models such as YOLOv8 (You Only Look Once), which provides real-time object detection capabilities, and Mask R-CNN (Mask Region-based Convolutional Neural Network), which uses pixel-level segmentation for object detection, was used for crater detection and segmentation [4], [5], [6]. The output generated by the deep learning models was visualized using Streamlit, a Python framework for web application development for interactive visualization of the detected craters [7]. Also, by comparing the above results with UNET, an established semantic segmentation model provides a benchmark for understanding the drawbacks and advantages of each approach in the context of lunar surface feature extraction [8] [9]. The approach used in this research eliminates the need for manual intervention and streamlines the analysis of large lunar datasets. This study contributes valuable insights to the planetary science community by shedding light on the robustness of different deep-learning models for automated crater segmentation and detection using Chandrayaan 2 datasets.

Dataset and Study Area:

Dataset Details	
Acquisition Data	05-04-2021
Spectral Range	500-800nm
GSD	0.25m
Orbit Altitude	100km
Swath	3km (Nadir)
Platform	Chandrayaan 2 (Orbiter)



Type of Data	Panchromatic (Calibrated)
Sensor	OHRC
Study area visualization using Google Earth Pro (Moon)	



References: [1] Tewari, A., Prateek, K., Singh, A., & Khanna, N. (2023). Deep learning based systems for crater detection: A review (arXiv:2310.07727). [2] Hashimoto, S., & Mori, K. (2019). Lunar crater detection based on grid partition using deep learning. 2019 IEEE 13th International Symposium on Applied Computational Intelligence and Informatics (SACI), 75–80. [3] Tripathi, P., & Garg, R. D. (2021). Initial results from the Optical HighResolution camera (Ohrc) onboard Chandrayaan-2 (EPSC2021-83). [4] Terven, J., & Cordova-Esparza, D. (2023). A comprehensive review of yolo architectures in computer vision: From yolov1 to yolov8 and yolo-nas. Machine Learning and Knowledge Extraction, 5(4), 1680–1716. [5] He, K., Gkioxari, G., Dollár, P., & Girshick, R. (2018). Mask r-cnn (arXiv:1703.06870). [6] Ankeeta, M & K N, Pushpalatha. (2022). SMALL SCALE CRATER DETECTION USING DEEP LEARNING. [7] Khorasani, M., Abdou, M., & Hernández Fernández, J. (2022). Web application development with streamlit: Develop and deploy secure and scalable web applications to the cloud using a pure python framework. [8] Ronneberger, O., Fischer, P., & Brox, T. (2015). U-net: Convolutional networks for biomedical image segmentation (arXiv:1505.04597). [9] Jia, Y., Wan, G., Liu, L., Wu, Y., & Zhang, C. (2020). Automated detection of lunar craters using deep learning. 2020 IEEE 9th Joint International Information Technology and Artificial Intelligence Conference (ITAIC), 1419–1423.

94. Mapping the Moon: A Deep Learning Strategy for Lunar Crater Detection from Chandrayaan-2 Satellite Captures

Kunal Thapar^{1*} and Unmesh Govind Khati¹

¹Department of Astronomy, Astrophysics and Space Engineering, Indian Institute of Technology, Indore.

*Corresponding author's email – msc2203121009@gmail.com

Abstract: The moon has its geological information sustained for billions of years now. With the absence of an atmosphere and no tectonic activities, surface features like craters, rilles, pits, etc. are well preserved [1]. Craters are one of the most predominant features of the lunar surface. Crater counting serves as a crucial methodology, providing key insights into lunar surface evolution, impact history, and other geological processes. With the development of computer vision and image processing [2], crater counting has switched from the traditional manual counting, which is time-consuming and prone to error, to using deep learning methods with the help of object detection models which has become much faster and precise in just a few years. This project harnesses the power of Convolutional Neural Networks (CNNs) to detect lunar surface craters using satellite images from the Orbiter High-Resolution Camera (OHRC) aboard Chandrayaan 2 [3]. The methodology involves image labelling, model training, weight function identification during validation, and subsequent testing of the model on unlabeled images. The project leverages YOLOv8's adept architecture, which is designed to be fast and accurate, making it an excellent choice for a wide range of object detection, instance segmentation, image classification and pose estimation tasks.

For the project, more than 500 images taken from the OHRC were manually labelled as crater. Precision and recall were the two metrics used to measure the model's efficiency. It was observed that as the number of epochs, which refers to the number of times the model iterated through the labelled data, increased, the model could detect more and more craters with increase in the confidence score, indicating improvement in the model's knowledge on the targeted object. Subsequently, the precision value increase from 42% for 10 epochs to roughly 58% percent for 100 epochs. The recall also jumped from 21% to roughly 30% for 10 and 100 epochs respectively.

References: [1] Heiken, Grant, David Vaniman, and Bevan M. French, eds. Lunar sourcebook: A user's guide to the Moon. No. 1259. Cup Archive, 1991. [2] Krizhevsky, Alex, Ilya Sutskever, and Geoffrey E. Hinton. "Imagenet classification with deep convolutional neural networks." Advances in neural information processing systems 25 (2012). [3] Chowdhury, Arup Roy, et al. "Orbiter high resolution camera onboard Chandrayaan-2 orbiter." Current Science 118.4 (2020): 560-565.

95. Towards Understanding Role of Transient Lunar Volcanism in Enriching Lunar Polar Volatile Deposits

E. Kabra^{1,2}, M. Bhatt², S. Biswas^{2,3}, and A. Bhardwaj²

¹Interdisciplinary School of Science, Savitribai Phule Pune University, Ganeshkhind, Pune-41100, India, ²Physical Research Laboratory, Ahmedabad, 380009, India, ³Atmospheric Science Department, Marine and Atmospheric Sciences Group, Indian Institute of Remote Sensing, Indian Space Research Organization, Dehradun-248001, India. Email: sci.eeshakabra@gmail.com

It is well known that the Moon is deficient in volatile elements relative to the Earth. It has been established by missions like Clementine [1], Lunar Prospector [2], Chandrayaan-1 [3], LCROSS and LRO [4] that the lunar poles have comparatively enriched deposits of volatiles in contrast to equatorial regions. Permanently shadowed regions (PSRs) on lunar poles are the most attractive targets, likely to have reserves of such volatiles [5]. The volatile which is currently a focus of several lunar polar missions, is water. Significant amounts of water/ice buried or mixed with the surface soil is expected in the lunar polar regions based on remote sensing measurements using neutron [6] and near-infrared spectrometers and radars operating in the microwave wavelengths [7] and these findings are supported by extensive modeling works [8]. But another moderately volatile element or ‘MVE’ that has been discovered in noteworthy amounts in the PSRs by LCROSS during the LCROSS impact event, is sodium [9]. Multiple theories have been put forward to explain enhanced volatile deposits towards the lunar poles. The most plausible theory to explain the amount of sodium present in the PSRs is volcanism (majorly till two billion years of the Moon formation) [10]. There have been various indications that the ancient Moon had active volcanism on very large scales [11]. The degassing followed by such an eruption should be rich in volatiles, a part of which could have escaped and reached the cold traps of the poles to be preserved there due to the frigid environment.

The objective of this work is to quantify Na presence and find out its sources in paleo-lunar conditions. Using paleo-lunar volcanism as the source, a General Circulation Model (GCM) - ROCKE-3D (Resolving Orbital and Climate Keys of Earth and Extraterrestrial Environments with Dynamics) [12] – has been employed to understand the dynamics of this objective. Our approach is to first understand the GCM, modify it as per paleo lunar conditions and derive the Na variation trends from equatorial to polar regions. In this work, we will report on the present status of the work as this work is in progress.

Acknowledgement: E. Kabra and S. Biswas carried out research work on this topic as summer research fellows under the INSA-IASc-NASI Summer Research Fellowship for two months each. This work was conducted with immense support and guidance from M. Bhatt, A. Bhardwaj and the scientists at PRL.

References: [1] Sorensen, T.C. and Spudis, P.D. (2005) *J Earth Syst Sci* 114, 645–668 [2] W. C. Feldman et al., (1998) *Science* 281,1496-1500 [3] C. M. Pieters et al. (2009), *Science* 326,568-572 [4] Anthony Colaprete et al. (2010), *Science* 330,463-468 [5] Fisher E.A. et al. (2017), *Icarus*. 2017 Apr 2; Volume 292:74-85. [6] R. Richard Hodges, Jr., 2002, *Journal of Geophysical Research*, 107, 5125 [7] Vilas, F., Jensen, E.A., Domingue, D.L. et al. (2008), *Earth Planet Sp* 60, 67–74 [8] Aleinov, I., Way, M., Harman, C. E., Tsigaridis, K., Wolf, E. T., & Gronoff, G. (2019). *Geophysical Research Letters*, 46, 5107–5116; Bénédicte D. Stewart, Elisabetta Pierazzo, David B. Goldstein, Philip L. Varghese, Laurence M. Trafton (2011), *Icarus*, Volume 215, Issue 1, 2011, Pages 1-16, ISSN 0019-1035 [9] Killen, R. M., A. E. Potter, D. M. Hurley, C. Plymate, and S. Naidu (2010), *Geophys. Res. Lett.*, 37, L23201 [10] Liu, Y. and Ma, C. (2022), *Icarus* 382, August 2022, 115044, ISSN 0019-1035 [11] Debra H. Needham, David A. Kring, (2017), *Earth and Planetary Science Letters*, Volume 478, Pages 175-178, ISSN 0012-821X [12] M. J. Way et al. 2017 *ApJS* 231 12

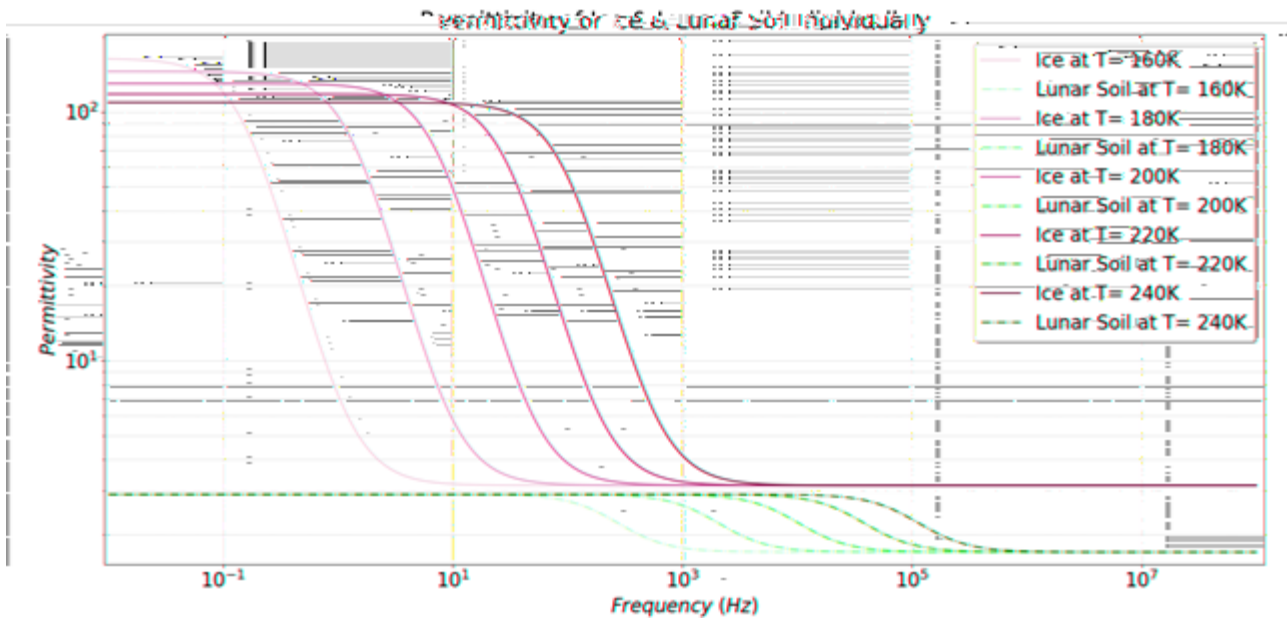
96. ELECTROSTATIC CHARACTERISTICS OF ROCK-ICE MIXTURES AND DETECTION OF ICE ON LUNAR SURFACE.

Antariksha Mitra¹ and Debabrata Banerjee², ^{1,2}Physical Research Laboratory, Ahmedabad (mailing address: PRL, Thaltej, Ahmedabad 380058, e-mail address: antarikshamitra@prl.res.in)

Introduction: Potential resources for future lunar exploration can be identified and further quantified by studying the subsurface structure of the Moon, up to depths of hundreds of meters. The lunar volatiles are expected to be preserved in cold traps or buried beneath the surface layer near the poles. This study aims to construct a fundamental model for detecting ice or water on rocky planets, moons, asteroids, and comets. It has been achieved by utilising the dielectric properties of ice-rock mixtures. The dielectric constants of dry materials are typically between 1 and 5. Since the permittivity of water is both a function of frequency and temperature (Banerjee, 2022), mutual impedance probe and ground-penetrating radar measurements can differentiate the electric permittivity of water from other materials for static fields. The permittivity value is almost two orders of magnitude compared to the value for extremely high frequencies. At very high frequencies, the molecules have no time to change their orientation in response to the applied electric field, resulting in low dipolar polarizability (and dielectric constant). Whereas in a static field, the polar molecules will prefer a slight orientation parallel to the applied field.

Here, we extend Banerjee's (2022) earlier study^[1] and determine the electric permittivity of two or more component ice-rock mixtures for various ice-rock concentrations using various mixing models, viz., Landau-Lifshitz, Maxwell-Garnet, Multiphase Mixture, Polder-van Santen / Bruggeman, Coherent Potential, Birchak modelling, Linear Mixture, Random Mixture, Cubic Model, Lichtenecker, modified Bruggeman and the Monte Carlo – Finite Element Method. The limitations and usefulness of these methods have also been scrutinized. The effects of different soil components have been investigated, and the impact of porosity has been considered. The present modelling has been realized using new Python codes. Results show that for around 1% ice concentration in the lunar regolith, the change in the permittivity of the mixture at 220 K is around ~2-20% for various mixing models in the range 0.1 Hz – 10 kHz. Mars, having 10% water concentration and considering a surface temperature of 300 K, exhibits a permittivity change of ~25-60% for various models in the frequency range of 10 Hz – 1 MHz. Similarly, Mercury with 10% ice concentration at 160 K indicates ~30-110% change for different mixing models outlined above in permittivity in the frequency range 0.1 mHz-10 Hz.

Digital Formats: The following plot shows the temperature and frequency dependence of permittivity for Lunar soil and ice individually, which motivates us to investigate the mixing models for the detection



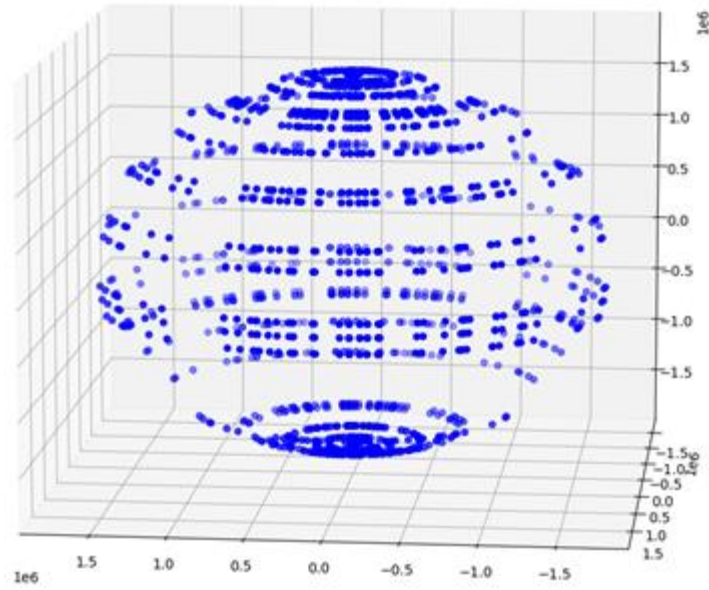
References:

[1]Banerjee, D., Modelling electric permittivity of ice-rock mixtures and implications regarding permittivity-based ice detection techniques in the 1-1000 Hz range, Current Science, 123, 841-843, 2022

97. VOLATILE MIGRATION ON THE LUNAR SURFACE.

Antariksha Mitra¹ and Debabrata Banerjee^{2, 1,2}Physical Research Laboratory, Ahmedabad (mailing address: PRL, Thaltej, Ahmedabad 380058, e-mail address: antarikshamitra@prl.res.in)

Introduction: Samples returned from the moon have established that widespread lunar volcanism ceased around 3.2 Ga, and only impact craters reshaped the lunar surface over the last billion years. ^{222}Rn (half-life ~ 3.8 days) produced in a decay chain of ^{238}U , can be expected to be released from the upper layers of the hot sunlit side of the lunar surface by thermal diffusion and be trapped in the permanently shadowed regions of the moon and other cold traps in the polar regions. The mean free path of a radon atom's random walk is not determined by collisions with other gas molecules in the extreme lunar vacuum but rather by collisions with soil grain surfaces. ^{222}Rn decays to ^{210}Pb , and hence, a thin layer of ^{210}Pb and ^{210}Po is expected in the permanently shadowed regions of the lunar surface. Several models have been proposed for the transport of radon from the lunar interior to the lunar surface and then across the terminator to the colder regions. Permanently shadowed regions near lunar poles should have high concentrations of ^{222}Rn , ^{210}Po and an alpha particle spectrometer and a gamma ray spectrometer on a future lunar lander/rover mission should be able to determine their concentrations and help us understand the transport and deposition of volatiles on the lunar surface. This study presents a Monte Carlo simulation (using new Python codes) for the migration of molecules on the surface of the Moon and Mercury. The molecules are placed on a planetary surface and then permitted to migrate until they are lost to the system. Whereas migration occurs by ballistic hops, loss of water and CO_2 occurs due to photodissociation, photoionization, or due to capture by a (near-polar) cold trap. Our results show that about $\sim 60\text{-}75\%$ of water placed randomly either escapes or photo-destroys in 100 migrations, and of the remaining $\sim 16\%$ migrate to the stable polar regions ($70^\circ\text{-}90^\circ$) for Mercury. In comparison, for the Moon, about $\sim 35\%$ gets deposited in the polar regions. Similarly, carbon dioxide migration deposit appears to be $\sim 3\%$ on Mercury and $\sim 10\%$ on the Moon. These results are consistent with existing calculations and support the notion of ice at the poles. We have simulated the migration of volatile radon gas for the first time, and note that $\sim 90\%$ of radon molecules placed randomly decay before reaching the poles. Of the remaining, about $\sim 30\%$ moves to the polar region on Mercury, while around $\sim 33\%$ reaches the polar region on the Moon.



References:

[1]Butler, B. J. (1997), The migration of volatiles on the surfaces of Mercury and the Moon, *J. Geophys. Res.*, 102(E8), 19283–19291, doi:10.1029/97JE01347.

98. Evaluating Latitudinal Dependency in Depth-to-Diameter Ratios of Lunar Polar Craters: Do They Truly Indicate the Presence of Water Ice?

Sachana Sathyan^{1, 2}, K. S. Sajin Kumar², Megha Bhatt¹

¹Physical Research Laboratory, Ahmedabad, Gujarat, India. 380059 (sachana@prl.res.in) ²University of Kerala, Thiruvananthapuram, Kerala, India. 695581

Introduction: The lunar poles are of great scientific interest due to permanently shaded regions (PSRs) and the likelihood of water ice accumulation [1, 2, 3, 4]. The depth/diameter ratio (d/D) from impact craters, gradually decreasing over time due to infilling, has been used to detect ice in a recent work [5]. [5] observed a poleward decrease in d/D for both Mercury and the Moon, particularly pronounced at the lunar south pole in case of Moon, suggesting potential water ice infilling. However the lunar north pole differs, showing no clear d/D decrease, contrary to other observations pointing to the presence of ice. This study integrates d/D with various parameters to explore trends at both lunar poles.

The objective was to discern whether the observed lower depth-to-diameter ratio indeed corresponds to the presence of water ice or if other factors play a significant role in this relationship. Our approach involved utilizing the crater catalogue provided in [6], encompassing over 9000 craters spanning both lunar poles within a latitudinal range of 65° N/S to 90° N/S, with crater diameters falling between 5-20 km. Similar to [5], our analysis focused on simple craters. To correlate the depth to diameter ratio results with the existing evidence for water ice, we have included additional parameters such as illumination, temperature, radar based circular polarization ratio (CPR) and spectral detections from M3 corresponding to water ice. In this study, the OMAT parameter was introduced to impose constraints based on the relative age of the craters, considering that numerous studies have highlighted ancient craters as primary locations for hosting water ice [7]. We systematically examined and plotted the values of all these factors for each crater in relation to the depth-to-diameter ratio and latitude for both lunar poles.

Discrepancies in the trends of the depth-to-diameter ratio (d/D) were identified between the North and South lunar poles. The theoretical anticipation of a declining trend, mirroring observations in the south pole [5], did not align with the data for the north pole, where mean d/D values exhibited an increase toward higher latitudes. Noteworthy, a gradual decrease in d/D for the south pole was observed, specifically between 80° S to 90° S. Contrary to the hypothesis that d/D ratios directly correspond to ice filling in craters [5], our analysis did not reveal lower values of depth to diameter ratio for craters identified as water ice rich using radar and Near-Infrared (NIR) techniques. However, a notable correlation was identified between M³ and DFSAR detections. These findings highlight that the lower depth-to-diameter ratio of craters towards the poles might be influenced by additional factors and should not be singularly relied upon for estimating water ice filling. Further insights were gained by examining Optical Maturity (OMAT) based trends for the selected craters where a clear association emerged between higher OMAT values (indicative of fresh craters with deeper depths) and higher latitudes in the

case of the north pole. Conversely, for the south pole, higher OMAT values were concentrated in the -70° to -80° latitudinal range. Craters with lower OMAT values (indicative of older craters) were predominantly found at lower latitudes (< 70° N/S) for both poles. This observation could provide a plausible explanation for the observed parabolic trend in mean d/D for the north pole and high depth to diameter ratio at 70-80° latitudes for south pole. Consequently, we draw the conclusion that the observed lower depth-to-diameter ratio trend toward the poles cannot be solely ascribed to the presence of water ice.

References: [1] Lawrence D. J. (2006) *JGR Planets*, 111(E8). [2] Putrevu D. et al., (2023) *JGR Planets*, 128(12), e2023JE007745. [3] Li S. (2018) *PNAS* 115(36), 8907-8912. [4] Williams J. P. et al., (2019) *JGR: Planets*, 24, 2505– 2521. [5] Rubanenko L. et al., (2019) *Nat. Geosci.*, 12(8), 597-601. [6] Wu B. et al., (2022) *GRL* 49(20), e2022GL100886. [7] Deutsch A.N. (2020) *Icarus*, 336, 113455.

99. EXPLORING THE POTENTIAL OF USING CHANDRAYAAN-2 IMAGING INFRA RED SPECTROMETER (IIRS) AND LRO-DIVINER DATA TO ESTIMATE SURFACE TEMPERATURES OVER PARTS OF THE ARISTARCHUS PLATEAU PYROCLASTIC DEPOSITS ON THE MOON

Subhadyouti Bose¹ (subhabose@prl.res.in), Annu Kumari², and Neeraj Srivastava¹ (sneeraj@prl.res.in)

¹Physical Research Laboratory, Ahmedabad - 380009, Gujarat, India; ²Department of Remote Sensing, Birla Institute of Technology, Mesra, Ranchi – 835215, India

Widespread pyroclastic deposits (also known as Dark-Mantle Deposits, DMDs) have been detected and mapped on the lunar surface using remotely-sensed data as well as from the samples of lunar regolith brought back to Earth. Such deposits can be identified by their low albedo with respect to other features, their apparent smooth surfaces, their emplacement in areas adjacent to maria and in and around elevated regions, and how they are mantled with respect to the surrounding terrain [1, 2]. Pyroclastic deposits have been classified as regional and local, based on their areal extents as well as by their formation mechanisms [2, 3]. Imaging Infra-Red Spectrometer (IIRS), launched on-board Chandrayaan-2, is a 250-band spectrometer. IIRS is the first spectrometer sent to the Moon that can capture lunar surface radiance between ~700 and ~5000 nm. In this study, we have performed thermal correction on lunar spectroscopic data from IIRS to remove the effects of thermal emission from the lunar surface, following the approach of [4]. Additionally, data from the Lunar Reconnaissance Orbiter's (LRO) Diviner Lunar Radio Experiment (DLRE) instrument has also been used. Data from both IIRS and Diviner have been used to generate surface temperatures, which were then used to study possible temperature variations over parts of the Aristarchus Plateau. The study of temperatures can help reveal information about the regolith and near-subsurface material (within a few centimeters) and help establish possible relationships between different materials and their contribution to the observed temperatures.

Calibrated radiance data from IIRS have been used to estimate surface temperatures (T_S). T_S have also been derived from the Diviner sensor, while contextual information about the Aristarchus Plateau was obtained from LRO's Wide Angle Camera (WAC). An IIRS radiance image (CH2_IIR_NRI_20210129T1432285315_d_img_d32) was downloaded from the *Pradan* online archive. The image was then thermally corrected in QuantumGIS (version 3.23.3) to remove the thermal emission component from the IIRS reflectance data. Following this, temperatures were estimated by inverting the Planck function. In order to compare and validate the temperatures obtained from the IIRS images, derived T_S have been used from Chandrayaan-1 Moon Mineralogy Mapper (M^3) images [5] as well as from the Diviner data [6], where brightness temperature (T_B) data from channels 6 to 9 were converted to (T_S) using an emissivity value of 0.95.

Surface temperatures indicate significantly higher temperatures (~318-380K) on the equator-facing wall of the Vallis Schröteri rille. On the other hand, the pole-facing slope of the rille show temperatures of ~280-330K, thus presenting an overall difference of ~38-50K. The reason for this is that the equator-facing slope receives relatively greater solar insolation than the pole-facing slope, which leads to the large temperature difference, as observed here. In addition to the rille, T_S have also been mapped over a part of the extensive pyroclastic deposits that blanket the Aristarchus Plateau. Observed temperatures over the pyroclastic deposits range between ~303-316K. The measured values suggest they are comparable to the surface temperatures estimated using M^3 data [5], where the overall temperature range

was estimated to be ~267-364K, over a part of the rille as well as over some of the pyroclastic deposits studied here. With respect to the overall temperature range (~263-332K) observed in the image, the pyroclastic deposits exhibit relatively higher temperatures as compared to the other features. On the other hand, T_s values obtained from Diviner indicate an offset of ~10-20K from the IIRS-derived values, similar to what was found for M^3 data for the Aristarchus Plateau region [5]. The underestimation of T_s values from IIRS could possibly result from a variety of factors, some of which are surface topography, viewing geometry orientations, different acquisition time of Diviner data with respect to other dataset like IIRS or M^3 , etc. In this regard, photometric and topographic corrections will be performed on the IIRS images to remove the effects of errors induced due to varying viewing geometry conditions as well as surface topography, which could reduce the observed temperature offset.

References: [1] Gustafson et al. (2012) *JGR*, 117, 1151–1154. [2] Head (1974) *LPS V*, 32, A74. [3] Gaddis et al. (1985) *Icarus*, 61(3), 461-489. [4] Prabhakar et al. (2022) *Icarus*, 383, 115075 [5] Li and Milliken (2016) *JGR*, 121, 2081-2107. [6] Hayne et al. (2017) *JGR*, 122, 2371–2400.

100. Differentiating wrinkle ridges for the analysis of displacement-length ratios in Mare Tranquillitatis.

Shubham Magar*, Nabamita Chaudhuri, Suyash Sharma, Subhadip Bhadra, Kusuma K.N
Dept. Earth Sciences, Pondicherry University, Kalapet, Puducherry – 605014
*magarshub01@gmail.com

Introduction: Wrinkle ridges are one of the prominent, yet complex, geomorphic features on the near side of Lunar mare basins. Wrinkle ridges originate as thrust-related folds above a subjacent blind thrust. Similar to other planetary bodies, the displacement (D) to length (L) ratio ($\square = D/L$) [1, 2, 3, 4] of wrinkle ridges bears significant clues to contractional tectonics, either local or global, during the lunar evolution. However, some cross-sectional profile across a wrinkle ridge shows a complex morphology that is probably affected by craters, its ejecta, and the overlapping of wrinkle ridges [6]. In this study, two wrinkle ridges are selected from the Lamont region of Mare Tranquillitatis, a low-mascon mare basin, to calculate the throw distribution along the ridge. Forty-eight acrossridge profiles (Fig. 1) are extracted and throw is measured for each profile from Lunar LRO- LOLA – Kaguya DEM (SLDEM with 60 m resolution), Chandrayan 2 Terrain Mapping Camera (TMC -2) DEM, with 5m resolution, data that has partial coverage. Throw is the elevation difference between the highest and lowest point on the wrinkle ridge profile [6]. Using the measured throw, along-ridge profiles have been obtained for the two selected ridges (Fig. 2). In Fig. 2a, fault throw alternately increases and decreases along LM, MN and NO. Either it could be three single faults overlapping each other or connected by relay ramps. In Fig. 2b, fault throw increases along AB and BC. This procedure was used to differentiate segments of the wrinkle ridges to calculate the Displacement-Length ratios. A part (blue portion) of the wrinkle ridge in Fig. 1 has been used for further analysis. The displacement– length ratio, calculated using the retrieved fault dip data, suggest a value of 1.67×10^{-2} for the Lamont region (Fig. 3). The value is significantly affected if precise profiles and segments along wrinkle ridges are not observed.

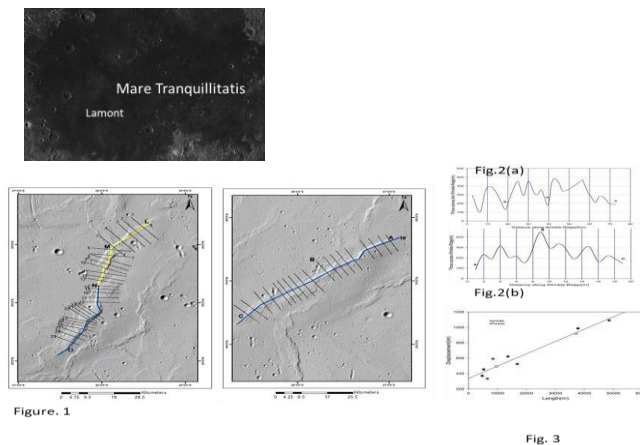


Figure. 1

Fig. 3

References: [1] Cowie, P. A., & Scholz, C. H. (1992) *Journal of Structural Geology*, 14(10), 1133-1148.; [2] Walsh, J. J., & Watterson, J. (1988) *Journal of Structural geology*, 10(3), 239-247.; [3] Watters T.R et al (2000) *Geophysical research letters*, 27(22), 3659-3662. [4] Schultz R.A. (2010) *Journal of Structural Geology* 32, no. 6 (2010): 855-875. [5] Watters T.R et al (2022) *Journal of Geophysical Research: Planets* 127, no. 3 (2022): e2021JE007058; [6] Li, BLing, Z., Zhang, J., Chen, J., Ni, Y. and Liu, C., 2018. Displacement-length ratios and contractional strains of lunar wrinkle ridges in Mare Serenitatis and Mare Tranquillitatis. *Journal of Structural Geology*, 109, pp.27-37.

101. INVESTIGATION OF TEMPERATURE DEPENDENT THERMAL CONDUCTIVITY OF LUNAR ANALOGUES UNDER SIMULATED LUNAR ENVIRONMENT.

G. Ambily^{1,2}, P Kalyan Reddy¹, K Durga Prasad¹, ¹Physical Research Laboratory, Ahmedabad, India, ²Andhra University College of Engineering, Visakhapatnam, India (ambilyg@prl.res.in).

Introduction: The Moon's surface is covered by a layer of dust and rocks known as regolith, which undergoes continuous modification from impacting meteorites, resulting in dynamic and ever-changing surface properties [1,2]. The thermal behavior of the lunar surface is heavily influenced by various factors, including solar insolation, internal heat flux, and thermophysical properties such as thermal conductivity, bulk density (or porosity), rock composition, and specific heat [3,4]. Therefore, understanding these properties and their variations becomes crucial for both scientific exploration and practical applications. Recent discoveries, including the presence of water on the Moon, have led to the exploration of numerous theoretical models and high-resolution remote sensing datasets with this focus [2,3,5,6,7]. However, current efforts rely on rough estimates of basic parameters that could ideally be measured under carefully controlled laboratory conditions. Despite some in-situ studies providing ground truth, the interpretation of results and extraction of valuable information significantly benefit from data obtained through laboratory experiments. Here we try to understand the effect of temperature on thermal conductivity of various analog materials by means of laboratory experiments.

Methodology & Results: The analogue materials utilized in the current investigation include both lunar highland and mare representatives. To ensure a comprehensive analysis, the powdered samples are categorized into three grain sizes: <100 μm , 100-160 μm , and >250 μm . The thermal conductivity of each sample is measured using the line-heat source technique under vacuum conditions. The experiment involves varying the temperature of the sample and observing the corresponding fluctuations in thermal conductivity. The dependence of thermal conductivity on temperature and ambient pressure is investigated and compared with earlier literature. This experiment holds significance in enhancing our understanding of how regolith parameters vary under different conditions. The insights gained from this study will be presented and discussed.

References: [1] Heiken, Grant, David Vaniman, and Bevan M. French, eds. *Lunar sourcebook: A user's guide to the Moon*. No. 1259. Cup Archive, 1991. [2] Vasavada, A. R., Paige, D. A., & Wood, S. E. (1999). *Icarus*, 141(2), 179-193. [3] Hayne, Paul O., et al., *Journal of Geophysical Research: Planets* 122.12 (2017): 2371-2400. [4] Prasad, K. D., & Murty, S. V. S. (2013), *Acta Astronautica*, 89, 149-153. [5] Paige, D. A., et al., *Space Science Reviews* 150 (2010): 125-160. [6] Durga Prasad, K., Rai, V. K., & Murty, S. V. S. (2022). *Earth and Space Science*, 9(12), e2021EA001968. [7] King, Oliver, et al., *Planetary and Space Science* 182 (2020): 104790.

102. MOON AS A GATEWAY FOR FUTURE SOLAR SYSTEM EXPLORATION

Harpreet Kapoor¹ and Rishab Kumar Agrawal², ¹Propulsion Engineer at Om Space Rocket & Exploration Pvt. Ltd, harpreetkapoor2000@gmail.com, ²Aerospace Engineer at Brahmastra Aerospace Systems, Rishabagrawal.100@gmail.com

This paper explores the strategic utilization of the Moon as a pivotal gateway for advancing human and robotic exploration throughout the solar system. Examining the Moon as a staging point for future space endeavors, we discuss the potential benefits and applications that arise from establishing a sustainable human presence on its surface. Key aspects include the Moon's role as a launch and testing platform,

resource repository, communication relay, and training ground for astronauts. The paper emphasizes the significance of international collaboration and technology development in realizing the full potential of the Moon as a springboard for deep space exploration, ultimately paving the way for human missions to Mars and beyond. Through a comprehensive analysis of ongoing initiatives like NASA's Artemis program, this paper aims to underscore the importance of the Moon as a strategic gateway for unlocking the mysteries of the solar system and expanding our human presence in space.

103. LABORATORY REFLECTANCE SPECTROSCOPY OF SITTAMPUNDI ANORTHOSITE, A LUNAR ANALOGUE

Denesh K.1,2 (deneshkarunakaran@gmail.com), Dhwanil Patel1,3 , Foziya Modan1,4 , Tejash D. Dave 1,4 , Neha Panwar1,5 , Subhadyouti Bose1 , Abhishek J. Verma1 , Neeraj Srivastava 1 (sneeraj@prl.res.in) 1Physical Research Laboratory, Ahmedabad; 2National Institute of Technology, Hamirpur; 3M.G. Science Institute, Ahmedabad; 4Gujarat University, Ahmedabad; 5 Indian Institute of Technology, Gandhinagar

The Lunar Highland Terrain is composed almost entirely of anorthosite, formed as a result of crystallization and flotation of plagioclase feldspar at the top when the Lunar Magma Ocean was solidifying. Therefore, the task of quantifying and modelling the anorthosite compositions is essential for understanding lunar surface compositions and gaining insights into crustal evolution processes. The study presented below focuses on the use of the terrestrial anorthosites to understand the spectroscopic behaviour of the lunar anorthosites. The anorthosites from the Neoproterozoic Sittampundi Anorthosite Complex (SAC), which are composed of relatively pure Anorthite (An₈₀₋₁₀₀), have been established as an analogue to the lunar highland anorthosites [1, 2]. Anorthosites display diagnostic absorption features at 380–387, 700–740, 930–1100, 1160–1200, 1415, 1920, 2200 and 2330 nm wavelengths within the electromagnetic spectrum. The primary objective of this study is to characterize the scattering properties of the anorthosites as a function of the viewing geometry and further the case for the SAC as an important lunar analogue.

The bidirectional reflectance spectra were measured for powdered anorthosite samples belonging to three different grain size classes (<45 μm , 45-100 μm and 100-200 μm) using an ASD Fieldspec4 Hi-Res spectroradiometer mounted on a custom-made goniometer in use at the PRSL (Planetary Remote Sensing Laboratory) facility at PRL, Ahmedabad. The spectra were acquired with 1 nm spectral sampling between 0.35 and 2.5 μm with 5° FOV incident at -45° and emergence angles varying from -30° to 60° in the principal plane at room temperature. The acquired spectra were plotted and analyzed in MATLAB. The Hapke model [3] has been used to derive the VNIR optical constants of the SAC sample for different grain sizes [4]. Using the Hapke equation of bidirectional reflectance [3], we retrieved the single scattering albedo (w) for each wavelength [5]. With this ' w ' values, the phase function coefficients were derived. Then, the ' w ' values and derived phase function coefficients have been used to model the spectra of the SAC sample. Following this, we fixed the grain-size distribution and the real part of the refractive index ($n + ik$), and inverted the formulation of w to compute the imaginary part (k , the extinction coefficient) for the entire wavelength range [6]. The computation of the wavelength-dependent phase function coefficient offered nuanced perspectives on the scattering behavior of the anorthosites samples. The optical constants derived in this work will assist in quantifying mineral abundances from mineral

mixtures. The study presents an efficient way to understand the spectral properties of anorthosite having important implications in the interpretation of spectra from the planetary remote sensing missions.

References: [1] Arivazhagan, S. & Anbazhagan, S. (2010) *Planetary and Space Science*, Volume 58, Issue 5, 752-760. [2] Arivazhagan, S. & Anbazhagan, S. (2012) *Second Conference on Lunar Highland Crust*. [3] Hapke, B.W. (1981) *Journal of Geophysical Research* 86: 3039-3054. [4] Sudhakar, A., Sklute, E.C., Carey, C., Glotch, T.D., Dyar, M. (2021) *52nd Lunar and Planetary Science Conference*. [5] Carli, C., Ciarniello, M., Capaccioni, F., Serventi, G., Sgavetti, M. (2011) *EPSC-DPS Joint Meeting 2011* 2011, 847. [6] Ye, C., Sklute, E.C., Glotch, T.D. (2021). *Earth and Space Science*, 8, e2021EA001834.

104. REFLECTANCE SPECTROSCOPY OF CLAY MINERALS FROM THE MATANUMADH LOCALITY, A MARTIAN ANALOGUE.

Dhwanil B. Patel^{1,2}(dhwanilpatel747@gmail.com), Denesh K.^{1,3}, Foziya Modan^{1,4}, Tejash D. Dave^{1,4}, Neha

Panwar^{1,5}, Subhadyouti Bose¹, Abhishek J. Verma¹, Neeraj Srivastava¹(sneeraj@prl.res.in),

¹Physical Research Laboratory, Ahmedabad; ²M. G. Science Institute, Ahmedabad; ³National Institute of Technology, Hamirpur; ⁴Gujarat University, Ahmedabad; ⁵Indian Institute of Technology, Gandhinagar.

The Matanumadh locality has been identified as a potential Martian analogue, holding a significant value for studying minerals. The overall geological setting of the Matanumadh area, with an unusual mineral assemblage developed within altered basalts and in the overlying sedimentary sequence, mimics the geological environment of many of the identified jarosite localities on Mars and can be considered as a Martian analogue from this perspective [1]. The primary objective of this study is to characterize the scattering properties of the minerals of the Matanumadh locality based on viewing geometry. A comparative analysis with the Naredi formation, a nearby locality underlying the Matanumadh formation, is also included in the study.

The bidirectional reflectance spectra were measured for powdered samples belonging to different grain size classes using an ASD Fieldspec4 Hi-Res spectroradiometer mounted on a custom-made goniometer in use at the PRSL (Planetary Remote Sensing Laboratory) facility at PRL, Ahmedabad. The spectra were acquired with 1 nm spectral sampling between 0.4 and 2.4 μm with 5° FOV incident at -45° and emergence angles varying from -30° to 60° in the principal plane at room temperature. The acquired spectra were plotted and analysed in MATLAB. The Hapke model [2] has been used to derive the optical constants of the samples for different grain sizes and phase angles [3]. Using the Hapke equation of bidirectional reflectance [2], we retrieved the single scattering albedo (w) for each wavelength [4]. Following this, we fixed the grain-size distribution and the real part of the refractive index ($n + ik$), inverted the formulation of w to compute the imaginary part (the extinction coefficient, k) for the entire wavelength range [5]. The derived k values have then been used to model the spectra of the samples. The computation of the wavelength-dependent phase function coefficient offered nuanced perspectives on the scattering behaviour of the samples.

References: [1] Bhattacharya S., Mitra S., Gupta S., Jain N., Chauhan P., Parthasarathy G., Prof. A., (2016) *Journal of Geophysical Research: Planets*. 121.10.1002/2015JE004949. [2] Hapke, B.W. (1981) *Journal of Geophysical Research* 86: 3039-3054. [3] Sudhakar, A., Sklute, E.C., Carey, C., Glotch, T.D., Dyar, M. (2021) *52nd Lunar and Planetary Science Conference*. [4] Carli, C., Ciarniello, M., Capaccioni, F., Serventi, G., Sgavetti, M. (2011) *EPSC-DPS Joint Meeting 2011*, 847. [5] Ye, C., Sklute, E.C., Glotch, T.D. (2021). *Earth and Space Science*, 8, e2021EA001834.

105. Transition of a pristine crater to sepulchered: A tale of Morella crater, Mars

Hiral P.B.¹, Sajinkumar K.S.¹

¹Department of Geology, University of Kerala, Kariavattom P.O., Thiruvananthapuram-695581, Kerala

pbhiral@gmail.com

Morella Crater on Mars unveils a multitude of tales narrating its transition from a fresh crater to a degraded crater. The crater with a diameter of 76.97 km is breached on its eastern side by the Elaver Vallis outflow channel and houses an extremely deep collapse structure, called Ganges Cavus. This crater has undergone diverse geologic and geomorphic processes like cavus formation, water pooling, breaching and outflow channel. An understanding of all these processes can shed light on several geological conundrums that modified the Martian surface environment as this late Noachian crater has such a large diameter that it can encompass several planetary-scale processes. In this study, we utilized Mars Orbiter Laser Altimeter (MOLA) Digital Elevation Models (DEMs) and MRO Context Camera (CTX) data as preliminary data for dating the different surface on Morella and its hinterlands. The chronological sequence, identification of minerals, and hydrologic modelling were done to decipher the temporal changes that have modified this crater. Furthermore, a schematic model depicting the entire sequels of the evolution of this crater was done using Interactive Erosion simulation in Web Browser (Webgl-Erosion).

The evolution of Morella crater history is unfolded through a five-stage process. Stage 1 reveals the formation of the Morella Crater with an age of $3.7_{-0.05}^{+0.04}$ Ga depicting a late Noachian period. The crater was subjected to sepulchering probably due to impact-induced volcanism (Stage 2) between $3.7_{-0.05}^{+0.04}$ Ga and $3.5_{-0.1}^{+0.07}$ Ga. This material has preponderance of olivine and pyroxene, indicating volcanic activity. Later, in the third stage, Ganges Cavus, a deep collapsed part was formed by the faulting mechanism due to Ophir Catenae Structural Complex, near the southern region of Morella crater [1]. Subsequently, through the heat from this Ophir Catenae, the confined groundwater was melted in the Cavus, which produced a lake in Morella [2]. This is the fourth stage in the odyssey of a fresh crater to a highly modified one. Eventually, the lake level rose until the wall of the crater was overtopped and breached, leading to catastrophic release of water and the carving out of the Elaver Vallis channels at $3.0_{-0.8}^{+0.3}$ Ga, indicating an early Amazonian period. The hydrologic modelling of Morella reveals a volume of 2.7×10^{12} m³, and an estimated peak velocity of 8.98×10^7 m³/s. Morella also witnessed a second fluvial activity, which resulted in the carving of dark-tone channels. The age of dark-toned channels was estimated as $1.8_{-0.3}^{+0.3}$ Ga and it indicates an age of the early Amazonian period. By these inferences, important evidence for the sediment deposits in the crater, subsidence of Ganges Cavus, source of water that filled the crater and the catastrophic release of ponded water were revealed. Thus, this study shed more, but convincing evidences, on the odyssey of one of the oldest craters on Martian terrain.

References:

[1] Coleman, N.M., Dinwiddie, C.L. and Casteel, K., 2007. High outflow channels on Mars indicate Hesperian recharge at low latitudes and the presence of Canyon Lakes. *Icarus*, 189(2), pp.344-361. [2] Komatsu, G., Di Achille, G., Popa, C., Di Lorenzo, S., Rossi, A.P. and Rodriguez, J.A.P., 2009. Paleolakes, paleo foods, and depressions in Aurorae and Ophir Plana, Mars: Connectivity of surface and subsurface hydrological systems. *Icarus*, 201(2), pp.474-491.

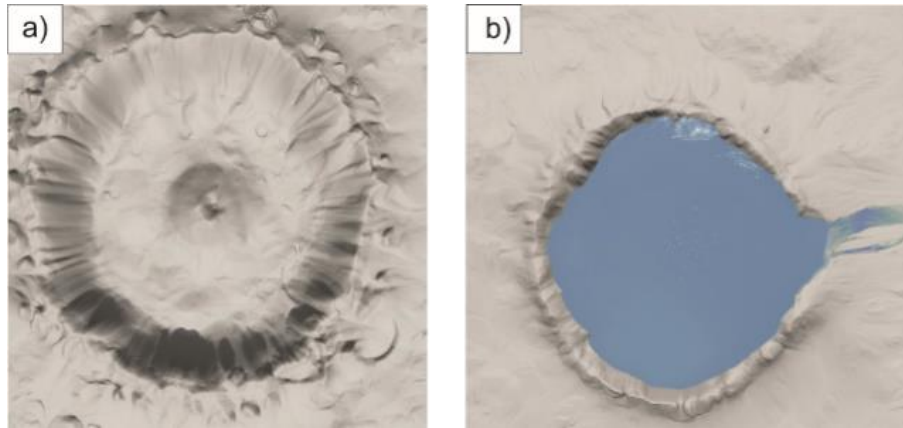


Figure 1: Schematic sketches showing the evolutionary history of Morella Crater (a) Morella in its transient form (b) breaching in the eastern crater rim, leading to the creation of outflow channels.

106. Designing a toolkit to delineate the ejecta rays of fresh craters on lunar surface

Arya Nandakumar, Subhami Mohan, Sajinkumar K.S.

Department of Geology, University of Kerala, Thiruvananthapuram-695581, Kerala, India
aryaharitham@gmail.com

The geology of the moon is primarily shaped by meteorite impacts and volcanism with associated tectonics. In the past, the moon was thought to lack an atmosphere. However, scientific studies signify the presence of a tenuous atmosphere. Thus, the absence of free oxygen and water on moon prevents erosion caused by weathering. This delicate layer of atmosphere provides minimal protection against asteroid impacts on the lunar surface [1]. Due to the pristine nature of the impact craters on the Moon, it provides a unique gateway to understand the geological records of space explosions and several other geological processes. Craters are widespread across the moon irrespective of its most distinctive geological units like the dark maria and the light anorthositic highlands. Substantial amount of information about the craters is revealed through its ejecta [2]. The distinct rays of material ejected from recently formed impact craters remain well-preserved with minimal changes, attributed to the Moon's thin atmosphere and the absence of significant weather phenomena. The younger and older ejecta materials are distinguished through the albedo effect, determined by the optical maturity (OMAT), a unitless quantity that acts as a relative measure of the extent to which lunar soil has been physically modified by exposure to space [3]. Smaller OMAT values indicate greater optical maturity and vice versa. Based on OMAT, we developed a toolkit to delineate the ejecta rays. As a preliminary work, we studied the Copernicus crater of Copernican age by using the Moon Kaguya Terrain Camera (TC) Global Mosaic, Kaguya lunar multiband imager derived OMAT and Clementine OMAT data. The process of delineating the fresh ejecta from younger craters was done utilizing OMAT imagery and the Terrain Camera global Mosaic. This was achieved with the assistance of modern high-level programming languages like Python. The following concept was developed as a toolkit to simply track the impact crater spallation on the moon. The toolkit operates by combining various image enhancement techniques, such as contrast stretching, which highlights image details; density slicing, which splits a single band image into distinct brightness intervals; contouring, which locates contours in an image and inverting which extracts ejecta around a younger, fresh crater. As a result, this toolbox integrates several remote sensing techniques to extract the ejecta spallation expanse. Thus, this study paves the way for a comprehensive exploration of impact craters of moon and the ejecta rays delving into their formation, implication for our understanding of lunar and other planetary bodies.

References:

[1] Taylor, S.R., Pieters, C.M. and MacPherson, G.J., 2006. Earth-Moon system, planetary science, and lessons learned. *Reviews in Mineralogy and Geochemistry*, 60(1), pp.657-704. [2] Schmitt, H.H., Heiken, G., Vaniman, D. and French, B.M., 2005. *Lunar sourcebook: A user's guide to the Moon*. Lunar and Planetary Institute. [3] Grier, J.A., McEwen, A.S., Lucey, P.G., Milazzo, M. and Strom, R.G., 2001. Optical maturity of ejecta from large rayed lunar craters. *Journal of Geophysical Research: Planets*, 106(E12), pp.32847-32862.

107. STUDY OF TRACES OF BIO-SIGNATURES ON MARS AND INDIAN ANALOG SITES

A. Gaur¹, M. Chauhan¹, R.S. Chatterjee¹ and R.P. Singh¹ ¹Indian Institute of Remote Sensing (IIRS),
I.S.R.O.,

Dehradun, Uttarakhand-INDIA (gaurankita951@gmail.com)

Introduction: The term ‘Bio-signature’ can be defined as an object, substance, and/or pattern whose origin specifically requires a biological agent [1]. Macro structures and mineral composition are two major geological evidences used to assess past environmental condition over terrestrial surface [2], [3]. The geologic deposits with or without biotic traces are significant because they might document prebiotic conditions. The relationship between the physical and chemical condition for preservation of bio-signatures and various processes that are able to alter the signature can be crucially understand using Earth Analog sites. The present study is focused on the study of two major geological features as potential biosignatures; *mud volcanoes* and *biostromal structures*. With characteristic pattern and distribution conducive to the biotic habitability [4], [5], these features have been selected to be analyzed and characterize for lithology, morphology and structural patterns using high-resolution remote sensing data from Martian surface. The selected Indian analog sites datasets will be analyzed in a similar trend along with field study to have comparative analysis for the analogical interpretation.

Datasets and Method: The present study attempts to characterize the major geomorphic features of different craters using high-resolution optical images attain from NASA PDS archives such as CTX(6m), HiRISE(0.3m/pixel) under Mars Reconnaissance Orbiter Mission (MRO), Mars Express’s HRSC (12.5m/pixel for nadir; 25m/pixel for off nadir). The terrain topography has been analyzed and interpreted using DEM and its derivative along with morphometric parameters to have a quantitative aspect using Mars Global Surveyor (MGS) MOLA DEM (~463m) and high resolution DTM. The hyperspectral data analysis for mineral characterization of selected Martian terrain includes the pre-processing of the dataset followed by identification of characteristic absorption of minerals and classification and abundance map generation by collecting endmember of pure pixels using MRO CRISM (362-3920nm with spectral sampling of 6.55nm/channel) dataset. For Indian analog site dataset like Sentinel-1(10m spatial resolution), ResourceSat LISS-IV, ALOS PALSAR RTC DEM (12.5m), NASA JPL AVIRIS-NG (5 nm \pm 0.5 nm; 20m) followed by samples procured from field observation.

Initial Findings: For mud volcanism volcanic terrain of Elysium Planitia (at 3°0’N, 154° 42’E) have been studied that reveals the presence of features like fissure volcanism, subdued flow-like structure, pitted cones/mounds with sediment flow, volcanic vein-like linear features. The overall slope of the terrain is influenced by three major volcanic vents present at the north of Elysium Planitia. Similar conditions have been observed at Barren Island active volcano and associated mud volcanoes of Baratang island (BI), Middle Andaman that lies in proximity to Barren Island. These mud volcanoes at BI have been studied critically using remote sensing and field observations.

Similarly, for biostromal structures, study have been carried over degraded impact craters of Mars such as Gale (5°24’S, 137° 48’E) and Gusev (14°30’S,175°24’E) that are reported to have preserved fluvial and eolian deposited sediments. The age of the Gusev crater determined using Crater Size Frequency Distribution (CSFD) technique reveals its age ~3.6 Ga (Early to Mid-Noachian) suggesting sedimentary deposition found in the crater probably host the signature of earliest microorganisms. Several preserved depositional features observed includes, Central highland showing layering, multiple drainage flow networks, black crescent shape dunes, preserved ripples, river inflow across the rim, smooth crater floor with features such as, flow lobes, clustered mounds, possible hydrothermal spring, canyons, yardang type structures, shallow water depositional features, river flow traces, alluvial fan etc. The dolomite hosted phosphate deposition of Jhamarkotra, Udaipur contains preserved stromatolitic structures is an indicative of shallow water deposition condition. This region has been analyzed for understanding the distribution pattern and formation condition for biostromal structures using remote sensing and field based approach.

Acknowledgement: We would like to thank PDS geoscience node, USGS-Earth Explorer, NASA-JPL, Alaska Satellite Facility and ISRO-Bhoonidhi for providing data in public domain.

References:

[1] Hays, L. E et al. (2017) *Astrobiology*, 17(4), 363-400 [2] Petruny, L. M. (2010) *41st Lunar and Planetary Science Conference* #1533, 1410 [3] Tanaka, K. L. et al. (2014) [4] Joseph, R. G., et al. (2020) *Advances in Astronomy*, 1-15 [5] Ivanov, M. A et al. (2014) *Icarus*, 228, 121-140.

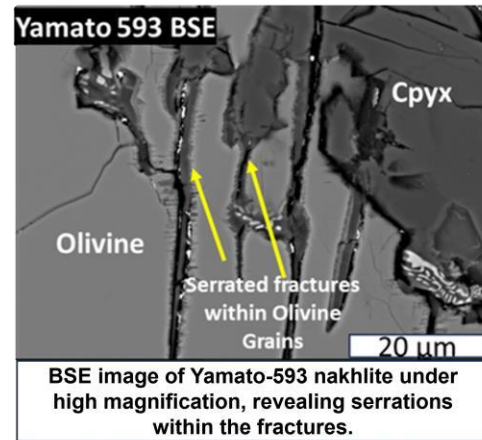
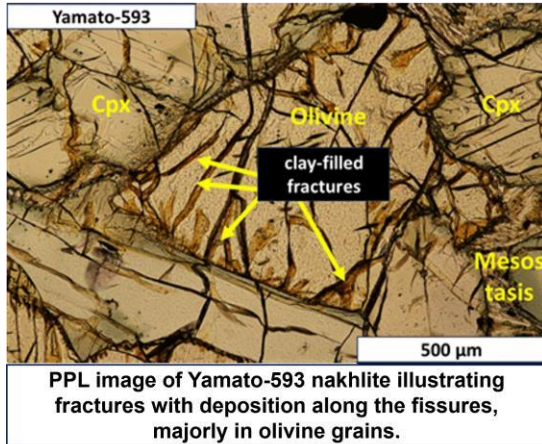
108. Unraveling Martian Mysteries: Nakhrites as Key Proxies for Water Activity in the Younger Amazonian Epoch

A. Das^{1,2} and D. Ray², ¹Indian Institute of Technology Gandhinagar, Gujarat 382355 (adityadas23081996@gmail.com), ²Physical Research Laboratory, Ahmedabad, Gujarat- 380009.

Introduction: Nakhrites among the Martian meteorites are the best proxy for signs of water activity during the younger Amazonian era, which is evidenced by the deposition of altered minerals along the fractures of primary minerals [1]. The Nakhrites are a type of cumulate igneous rock found on Mars, characterized by a substantial abundance of clinopyroxene minerals where alteration occurred at around 630 Ma [2]. The pre-terrestrial origin of these clay minerals is determined through petrography [3], age [4], and isotopic fingerprinting [5]. Multiple Nakhrites have been placed in a depth profile based on their cooling rates [6]. The focus of this study involves an in-depth examination of the alteration products, intending to provide a comprehensive understanding of the underlying factors that led to the observed transformations.

Petrography: The Nakhrite cumulate is characterized by a prevalence of augite grains, with minor occurrences of olivine grains. Furthermore, the Nakhrites display fractures, within which altered clay minerals, particularly in the olivine grains, are deposited. Upon closer examination through petrographic analysis at higher magnification, it was revealed that these fractures possess serrated features, high relief, and, most significantly, the resultant altered products exhibit a poorly crystalline nature.

Discussion: The high relief of the serrated fractures implies low-temperature alteration. Additionally, the geochemistry of this altered product indicates that the clays are affiliated with the smectite group of minerals, representing a low-temperature alteration consistent with the petrographic observations. The amorphous quality of the altered product indicates that the cooling process occurred very rapidly. These modifications took place during the Amazonian epoch, marked by minimal water-rock ratios, substantiated by the prevailing alteration predominantly affecting olivine grains. This implies that the alterations within these conditions were influenced by the compositions inherent to the host rock.



References: [1] Bridges J. C., & Grady, M. M. (2000) Earth and Planetary Science Letters, 176(3-4), 267-279. [2] Borg L., & Drake, M. J. (2005) Journal of Geophysical Research: Planets, 110(E12). [3] Treiman A.H. (1993) Meteoritics & Planetary Science 28: 86-97. [4] Swindle T.D. et al. 2000. Meteoritics & Planetary Science 35: 107-115. [5] Leshin L.A. et al. 1996. Geochimica et Cosmochimica Acta 60: 26352650. [6] Mikouchi T. et al. (2006) LPS XXXVII, Abstract #1865.

109. COMPARATIVE STUDY OF LADAKH PERIGLACIAL FEATURES FROM MARTIAN ANALOGUE PERSPECTIVE

A. S. Borkar¹, M. Chauhan¹, P. Pandey¹, R. S. Chatterjee¹ and R. P. Singh^{1,1}, Indian Institute of Remote Sensing (IIRS-ISRO), Dehradun, Uttarakhand, India 248001 (akankshabrkr@gmail.com).

Introduction: Many of the surficial features observed on the Mars show morphological similarity to that of periglacial features on the Earth. The present study has analyzed various periglacial features of Ladakh, NW Hima laya and compared them one to one with similar features present on the mid-latitude regions of Mars. The Ladakh region in northwestern Himalaya, receives very low annual rainfall, has a very high UV radiation, average annual mean temperature below freezing point, extreme climatic conditions with very low oxygen levels and till now has low anthropogenic activities [1], that makes the terrain more like a cold desert. Mars has no atmosphere with significant temperature drops at night and higher insolation receiving conditions during days. The harsh cold and semi-arid environment of Ladakh enables it as a potential region for Martian analogue studies. Periglacial features formed by cyclic freezing and thawing action are abundantly present in Ladakh terrain. Mars, due to the axial tilt, shows variations in the seasons owing to the amount of insulation received [2], thereby increased obliquity tends to warm the ice-rich polar regions and redistribute water-ice equatorward, suggested by general circulation models [3]. The general circulation theory, supports the formation and evolution of glacial landscapes at mid-latitudes in Mars, hence the presence of periglacial features [4].

Data and Methods: In this study, we have acquired the photographic field data and high-resolution satellite data of Resourcesat-2A LISS IV (5.8 m) data of Ladakh. For Mars

surface, MRO-HiRISE (25 cm) and CTX (~6 m) data was utilized. ALOS PALSAR RTC DEM (12.5 m) for Ladakh and MGS-MOLA DEM (463 m) data for the Mars features was used to generate the 3-D models of features for further morphological analysis using ArcGIS and ENVI soft wares.

Result and Conclusion: Cyclic frost and heave actions leave behind traces of their activities in the form of periglacial features viz., solifluction lobes, gullies and alcoves, polygonal features etc. To get proper insights, morphological parameters (e.g. Slope angle, aspect, etc.) were calculated along with profiling wherever required. Comparison of the features have been done on the basis of morphology and topography; several 3-D models of features were generated using the DEM datasets in ENVI software at various locations from Ladakh and selected study area (mid-latitude) from Mars. The extent of the gully system in Ladakh and Mars shows striking similarity.

Results showed resemblance between some features, for instance, alcove depression of the gully system at hill crest and down the slope debris cone deposition, both connected by the channel or gully. Periglacial solifluction lobes were observed near Tso-Morari, Ladakh and polygonal cracks were observed near Lamayuru region. Similar features were captured from Mars near Mojave crater. Such features indicate diurnal cycle of creeping of the active layer present on permafrost. Polygonal patterned ground suggests the continuous presence of permafrost beneath active layer during the entire period of gully emplacement and these crack polygons may also constrain the gully formation sequence [5,6].

The present morphological analysis provides the indication that the compared features show morphological similarity and existence of above features on Mars suggests presence of glacial environments. Thus, this study holds an importance to understand well-preserved periglacial features and thereby their significance to comprehend glacial climatic conditions on Mars during millions of years of its climatic history.

Acknowledgements: This study uses data from NASA's MRO and MGS mission, ISRO-ResourceSat, NASA-JAXA ALOS provided in public domain.

References: [1] Pandey, P., et al. (2021), *Current Science*, 120(2), 429 [2] Zent, A. P. (2013), *Comparative Climatology of Terrestrial Planets*, 505-538 [3] Head, J. W., et al. (2005), *Nature*, 434(7031), 346-35 [4] Madeleine, J. B., et al. (2009), *Icarus*, 203(2), 390-405 [5] Levy, J. S., et al. (2008), *Antarctic Science*, 20(6), 565-579 [6] Levy, J. S., et al. (2010), *Icarus*, 206(1), 229-252.

110. INSIGHTS ON MARTIAN ALTERATION PROCESS FROM TERRESTRIAL ANALOG STUDY ON OLIVINE-TO-CLAY REPLACEMENT.

A. Bose¹, A. Das², A. S. Majumdar¹ and D. Ray² (¹ Department of Applied Geology, IIT (ISM) Dhanbad, Jharkhand 826004, India ² Planetary Sciences division, Physical Research Laboratory, Ahmedabad, Gujarat 380009, India E-mail: 21dr0035@agl.iitism.ac.in(A. Bose), asmajumdar@iitism.ac.in(A. S. Majumdar))

Introduction: Ongoing (and future) Mars missions are (and would be) aiming to search for life on Mars, which relies on identifying suitable energy sources and electron donors like H₂ and CH₄ in Martian conditions. Despite substantial evidence of olivine hydration in generating H₂ and CH₄ and thus supporting primordial metabolism in terrestrial systems, information on olivine hydration process in the Noachian Mars is scarce. However, Martian crust is substantially comprised of olivine that can readily react with aqueous solution to produce phyllosilicates and H₂. In fact, most of the hydrous phases found to date on Mars are phyllosilicates, predominantly clay minerals, chlorite, serpentine and iddingsite and they have major influence in shaping the Martian crust during the Noachian (4.5 – 3.7 Ga). The controlling physical and chemical parameters that led to the origin of these phases are still poorly understood although they are important to validate orbiter data from Mars and the ocean world Europa and understand the Martian alteration process in depth. Accordingly, this study presents a detailed textural-compositional investigation on olivine-to-clay replacement process in olivine-gabbro system, which has analogous primary mineralogy to that of SNC meteorites.

Sample and Analytical Techniques: The textural and compositional features are investigated in polished thin sections using Electron Probe Micro Analyzer (EPMA), whereas mineral phases are identified by Raman spectroscopy technique.

Results: In studied samples, the primary olivine (Ol) has an X_{Mg} [= Mg²⁺ / (Mg²⁺ + Fe²⁺), where Mg²⁺ and Fe²⁺ is in atoms per formula unit i.e. apfu] value of 0.88 ± 0.01 and primary plagioclase (Pl) exhibits bytownitic composition with X_{Ca} [= Ca²⁺ / (Ca²⁺ + Na⁺), where Ca²⁺ and Na⁺ is in apfu] = 0.80 ± 0.02. Clinopyroxene has an augitic composition with an X_{Mg} value of 0.90 ± 0.01. Degree of alteration is highest in olivine followed by plagioclase and clinopyroxene is less altered compared to other components. Serpentine, chlorite, clay mineral and magnetite are common secondary phases, which compositionally varies based on micro-mineralogical composition at the interface scale. Serpentine is present throughout whereas chlorites are present mainly at plagioclase interfaces. Serpentine has variable FeO (t) (2.9 - 6.5 wt%) and Al₂O₃ (0.1 - 1.4 wt%) content and X_{Mg} values (0.92 - 0.95) at different olivine interfaces. Chlorites are of clinoclinal composition with an X_{Mg} value of 0.80 ± 0.04. They further exhibit variation in both FeO (t) (9.5 - 13.5 wt%) and Al₂O₃ (9.5 - 15.5 wt%). Clay minerals are also widespread throughout the sample and mostly sazonitic in composition with variable Al₂O₃ content (0 - 7 wt%) and X_{Mg} values (0.81 - 0.82) based on their textural positions. Alteration of plagioclase by prehnite has also been observed in places.

Discussion: Based on the textural-compositional observations, it is evident that the secondary mineral compositions are highly variable across different interfaces and are mainly controlled by the primary mineralogical assemblage at replacement interface. Furthermore, aluminum concentration in the reacting fluid also appeared to play a significant role in defining the replacement interface. This study thus provides important insights on the control of protolith and reacting fluid composition in defining the secondary phyllosilicate composition in Marslike alteration environment.

References: [1] Majumdar, A.S., Ray, D. and Shukla, A.D., 2020. Serpentinization of olivine–gabbro in Central Indian ridge: Insights into H₂ production during alteration in lower oceanic crust and sustenance of life at slow– spreading ridges. *Lithos*, 374, p.105730. [2] Nozaka, T., Fryer, P. and Andreani, M., 2008. Formation of clay minerals and exhumation of lower-crustal rocks at Atlantis Massif, Mid-Atlantic Ridge. *Geochemistry, Geophysics, Geosystems*, 9(11). [3] Pens, M., Andreani, M., Daniel, I., Perrillat, J.P. and Cardon, H., 2016. Contrasted effect of aluminum on the serpentinization rate of olivine and orthopyroxene under hydrothermal conditions. *Chemical Geology*, 441, pp.256-264. [4] Ehlmann, B.L. and Edwards, C.S., 2014. Mineralogy of the Martian surface. *Annual Review of Earth and Planetary Sciences*, 42, pp.291-315.

111. On the Relationship of Dichotomy of Mars and Occurrence of Dust Devils

Shivam Saxena^{1*} and Jayesh P. Pabari², ¹J S University, Shikohabad – 205135 (Last Attended) (dieshivamsaxena@gmail.com), ^{2*}Physical Research Laboratory, Ahmedabad - 380009, (jayesh@prl.res.in).

The Dust Devils referred to as DD's are very common on Earth and Mars as well. These atmospheric convective vortices, induced by daytime surface heating and planetary boundary layer turbulence, as the air heated up and starts to rise in the upward direction and the vorticity becomes more vertical and starts to intensify, whirling around a low-pressure region that develops in the vortex core uplift surface dust particles, significantly contributing to Mars' atmospheric dynamics [1][2]. Studying Martian dust devils offers valuable insights into the planet's atmospheric processes, including convective activity and surface-atmosphere interactions [3].

And another feature of Mars is “The Dichotomy”. The Martian dichotomy, a geological partition cleaving Mars into its Southern and Northern hemispheres, is a prominent feature with distinct characteristics. This division creates a stark contrast between the heavily cratered terrain of the Southern Hemisphere and the relatively smoother plains of the Northern Hemisphere [4], a phenomenon known as North-South Asymmetry [5]. Our study investigates the dynamic correlation between Mars' geological dichotomy, crustal magnetic field zones, and the presence of Dust Devils on Mars. Our research focuses on the observation and mapping of Dust Devil locations during multiple Martian years. We have studied and categorized our observations into two different groups: Direct Observations, where Dust Devils were captured in real time during their active phase or activity, and Indirect Observations, which involve tracking of Dust Devil's Tracks left in their wake after passage.

Our analysis of these observations unveils a relationship between Dust Devil occurrences and Mars' dichotomy. Specifically, we have identified a pronounced correlation between the Martian dichotomy's intricate, serpentine trajectory and the prevalence of Dust Devils. Most of the dust devils have occurred on the Dichotomy and the nearby regions of it and these Dust Devils locations follow the serpent-like trajectory of the dichotomy of Mars. Furthermore, our analysis of dust devil characteristics, including size, duration, and frequency, illuminates the diverse nature of these atmospheric phenomena. It is noteworthy that dust devils predominantly occur in the -4 to +4 kilometer range of relative elevation and depth zones, with a significant concentration around the 0-kilometer range. This information underscores the elevational preferences of these Martian whirlwinds. Our conclusions lie in the Martian Dichotomy, which is an inspiring geological feature that bisects the planet into Northern and Southern hemispheres,

each marked by strikingly divergent topographies. The Southern Hemisphere has countless craters, forming a heavily cratered terrain. and relatively, the Northern Hemisphere is a vast expanse of smooth. Our findings underscore the pivotal role played by the Martian Dichotomy in influencing the prevalence of dust devils. It appears that this geological boundary acts as a catalyst for dust devil formation.

This synergy between Dust Devils, the Martian Dichotomy, and Crustal Magnetic Fields offers fresh insights into the genesis and distribution of dust devils across the Martian landscape, marking a significant contribution to our understanding of the Red Planet.

References:

[1] Balme, M., & Greeley, R. (2006), Dust devils on Earth and Mars, *Reviews of Geophysics*, 44, RG3003. [2] Spiga, A., Barth, E., et al. (2016), Large-Eddy Simulations of Dust Devils and Convective Vortices, *Space Science Reviews*, 203 (1-4), 245–275. [3] Newman, C. E., et al. (2019), Mars WRF Convective Vortex and Dust Devil Predictions for Gale Crater Over 3 Mars Years and Comparison With MSL-REMS Observations, *Journal of Geophysical Research: Planets*, 124 (12), 3442–3468. [4] Watters, T. R., McGovern, P. J., & Irwin III, R. P. (2007), Hemispheres Apart: The Crustal Dichotomy on Mars, *Annual Review of Earth and Planetary Sciences*, 35 (1), 621–652. [5] Carr, M. H. (1981), *The Surface of Mars*, New Haven, CT: Yale Univ. Press. 232 pp.

112. MAGNETIC TOPOLOGY DEPENDENCE OF ELECTRON IMPACT IONIZATION FREQUENCY IN THE MARTIAN NIGHTSIDE IONOSPHERE

Arnob Sarkar¹ and N. V. Rao^{1*}

¹National Atmospheric Research Laboratory, Gadanki, Tirupati, India

Presenting author: Arnob Sarkar (arnobsarkar@narl.gov.in)

*Corresponding author: nvr Rao@narl.gov.in

Abstract

Photoionization and electron impact ionization are the two main sources of ionization contributing to the formation of the Martian ionosphere. While photoionization predominates over the dayside, on the nightside and beyond the terminator where photoionization is absent, impact ionization becomes the primary ionization source. The Electron Impact Ionization Frequency (EIIF), a key parameter, is commonly employed to quantify the efficiency of impact ionization on the nightside ionosphere ([1] Lillis et al. (2018)). [1] Lillis et al. (2018) have demonstrated that EIIF depends on the solar zenith angle, the strength of the crustal magnetic field, and the upstream solar wind dynamic pressure (Lillis et al., 2020).

Given the highly dynamic nature of the magnetic field configuration in the Mars space environment, which undergoes transitions between closed, open, and draped fields, it is crucial to characterize the EIIF in these three field topologies. In this study, we address this aspect by utilizing suprathermal electrons, the strength of the measured magnetic fields, and the solar wind dynamic pressure obtained by a suite of instruments on the Mars Atmosphere and Volatile Evolution (MAVEN). The EIIF at each altitude is derived from the differential electron energy spectra measured by the solar wind electron analyzer instrument aboard the MAVEN spacecraft. Altitude variations of EIIF in open and closed field configurations exhibit similarities in weak and strong magnetic field regions. However, significant variations are observed in closed field topologies, indicating that regions with strong magnetic fields and closed configurations hinder the precipitation of suprathermal electrons, consequently reducing EIIF. Furthermore, the altitude variation of EIIF in response to changes in solar wind dynamic pressure is more pronounced in closed field regions compared to open and draped field regions. The results of the present study are discussed in the light of the current understanding of the solar wind interaction with the Mars space environment.

Reference:

[1] Lillis, R. J., Mitchell, D. L., Steckiewicz, M., Brain, D., Xu, S., Weber, T., Halekas, J., Connerney, J., Espley, J., Benna, M., Elrod, M., Thiemann, E., & Eparvier, F. (2018). Ionizing Electrons on the Martian Nightside: Structure and Variability. *Journal of Geophysical Research: Space Physics*, 123(5), 4349–4363. <https://doi.org/10.1029/2017JA025151>.

113. Characteristics of Gravity Waves in Lighter and Heavier Species

114. in the Martian Thermosphere

V. Leelavathi and N. V. Rao

National Atmospheric Research Laboratory, Gadanki, Tirupati, India, (leela@narl.gov.in;
nvrao@narl.gov.in)

Gravity waves (GWs) are omnipresent in all stably stratified planetary atmospheres such as Earth, Venus, Mars, and Titan. The primary sources of their generation are orography, convection, thermal variations, wind shear instabilities, weather fronts, and thunderstorms. These waves can propagate both horizontally and vertically from their sources of generation and can reach thermospheric altitudes. In this study we investigate the characteristics of GWs in the thermosphere using densities measured by the Neutral Gas and Ion Mass Spectrometer aboard the Mars Atmosphere and Volatile Evolution spacecraft. We specifically examine the characteristics of GWs in lighter (He) and heavier (Ar) species. The analysis shows that GWs are a persistent phenomenon in Martian thermospheric He densities, similar to their presence in heavier species like Ar and CO₂. The amplitudes of GWs in both species typically fall below 30% of their respective background densities, with the most probable amplitudes being 7.6% for He and 3.5% for Ar. Horizontal wavelengths of the GWs in both species span from 30 km to 330 km, with the frequently occurring wavelengths being 55 km for He and 140 km for Ar. Larger GW amplitudes are observed in He during the afternoon hours, whereas the amplitudes in Ar peak in the early morning hours. This local time variation in GW amplitudes demonstrates an almost opposite pattern between He and Ar.

A significant finding is the identification of a temperature-dependent transition wavelength that distinctly separates short and long wavelengths. This transition wavelength increases with an increase in background temperatures and significantly influences the dominance of He and Ar. In the short-wavelength limit, GW amplitudes in He prevail, while GW amplitudes in Ar take precedence in the long-wavelength limit. Furthermore, the study emphasizes that the transition wavelength exhibits local time dependence due to temperature variations. During periods of lower temperatures, transition wavelengths fall within the observed horizontal wavelength range, enabling the study of He and Ar dominance. Conversely, higher temperatures (>180 K) during daytime and the dusk terminator eliminate transition wavelengths within the observational range. As a result, the amplitudes of GWs in He dominate over those in Ar. This different responses of GWs in He and Ar is explained by considering the roles of vertical advection of air parcels and flow divergence. Additionally, during the 2018 global dust storm (GDS), GW amplitudes in Ar show significant enhancement, while GW amplitudes in He do not exhibit any notable variations during this time. This analysis underscores that during the 2018 GDS, Martian thermospheric GWs in heavier species are more influenced and there is almost no considerable effect on the GWs in lighter species.

115. CHASING MARTIAN GLACIAL LANDFORMS: ANALYSIS OF ACHERON FOSSAE GLACIAL FORMATION USING HIGH RESOLUTION SATELLITE IMAGERY.

T. Ghosh¹, R.K. Tiwari² and R.K. Sinha³

^{1,2}Geomatics lab, Department of Civil Engineering, IIT Ropar, Punjab – 140001 and email-tanisha.20cez0009@iitrpr.ac.in, ³ Planetary Remote Sensing Section, Planetary Sciences Division, PHYSICAL RESEARCH LABORATORY, ISRO (A unit of Department of Space, Government of India), Navrangpura, Ahmedabad

Introduction: In this study, we focus to address the critical gaps in our understanding of Martian glaciation, concentrating on the unexplored Acheron Fossae region which is just above Olympus Mons in the Mid latitudes of Mars. Acheron Fossae which is located at 37.67° north latitude and 135.87° west longitude, provides a unique opportunity to expand our knowledge of Martian landscapes and the specific factors influencing glacial formation. In this research, we have used high-resolution remote sensing images acquired by Mars Reconnaissance Orbiter (MRO) ConText Camera (CTX) to create detailed maps that served as the foundation for our investigation. We manually digitized regional glacial landforms, ejecta superposed on glacial landforms and glacial landforms formed inside larger craters. The topographic parameters of the region were extracted from Mars Orbiter Laser Altimeter (MOLA) data sets to acquire the downslope flow characteristics such as slope, aspect, Length, width for insights into the flow patterns of Martian glaciers. And with the help of mapped landforms, we determined best fit ages by the integration of ages derived from three sources—regional glacial landforms, glacial landforms within craters, and ages derived from crater counts over ejecta, to analyze the comprehensive chronological framework for Acheron Fossae. This, in turn, will enable us to construct a detailed

chronological history of glaciation and glacial modification during the Late Amazonian period. We are committed to interpreting the climatic regime within which glaciers would have formed on Mars. Finally, we integrated our findings with the global glacial history of Mars, allowing for meaningful comparisons with other regions of the planet. The flow features were also compared with their terrestrial analogues to analyze the process of formation. This study will lead us to imply areas for future exploration and enhance our understanding of the geological intricacies of other celestial bodies.

Keywords: Martian glaciation, Acheron Fossae, chronological framework, crater counting method, conceptual model, planetary science, Mars exploration, geological processes, extraterrestrial dynamics.

116. GEOLOGICAL EVOLUTION OF A COMPLEX TOPOGRAPHIC DEPRESSION WITHIN TERRA SIRENUM, MARS

D. Singh^{1*}, R.K. Sinha¹ and K. Acharyya¹

¹Planetary Science Division, Physical Research Laboratory, Ahmedabad, Gujarat, India- 380009
(deeps301090@gmail.com)

Introduction: Amongst the evaporites, chlorides are most interesting species to study geological evolution of an area. They are the last to precipitate following the geochemical divide [1,2] in a solution consisting of other ions associated with evaporites such as carbonate and sulfate. Thus, the presence of chlorides in an area also depicts last hydrological activity of an area thereby helping in deriving environmental conditions during that period. They have often been observed as bright-toned regions overlying desiccated polygons [3-6] and as small patches within inter-crater plains with fluvial morphologies in close distance [3,4,7]. Chlorides have been found along with Fe/Mg smectites but not in association with other hydrated minerals such as Al-phyllsilicates, hydrated silica or evaporites such as sulfates and carbonates which has restricted our understanding of chlorides with several formation hypotheses in play [4,7,8,9,10]. Thus, the present work examined chloride-rich topographic depression within the Terra Sirenum with the aim to determine its potential as a lacustrine basin and decipher its geological evolution over time.

Methods: We began the study with detailed morphological analysis of the study area and its surrounding using high resolution ConTeXt (CTX) Camera and High-Resolution Imaging Science Experiment (HiRISE) datasets and their Digital Elevation Models [11-13] to find features that are associated with the presence of water. This was followed by Crater Size-Frequency Distribution (CSFD) analysis of the entire region [14] was carried out to find the time of last geological activity and find the relative age of different units. We further conducted mineralogical profiling of the study area to detect the presence of secondary minerals whose presence corresponds to different hydrological regimes. For this, we used long wavelength regions of CRISM datasets [15,16] for spectro-morphological analysis and created a geological map of the area.

Results and Discussion: The basin is a topographic depression which varies in depth from ~50-120m and is covered with bright toned polygonal cracks. On the southern side of the basin, we observed a large network of valleys on the termini of which are several layered fan-like structures. The variation in shape of the valleys, presence of concentric ringed crater suggests towards cycles of wetting and drying. We also observed bright-toned polygonal cracks in the surrounding terrain, suggesting that the basin

extended beyond its present boundary. Mineralogical investigation of the basin showed the presence of Fe/Mg-rich smectite, serpentine, kaolinite and its mixture with hydrated silica along the eroded edges near the basin boundary. The basin also featured other hydrated phases, possibly sulfates, which have previously not been associated with chloride-rich terrains. Age dating of the different unit and the surrounding area indicates that the basin witnessed its first hydrological cycle ~3.7Ga ago whereas, chlorides formation occurred ~3.4Ga ago. The mineralogical diversity within the area indicates that the region witnessed complex geochemical environments.

Conclusion: We deciphered that it is a part of a large sedimentary basin that extended beyond its present boundaries. It has undergone several wetting and drying cycles and contains signatures indicative of different environments. We propose that the topographic depressions can serve as sites for water to the pond, and localized in-depth investigations are necessary in such areas to model their astrobiological potential and contribute towards paleolake records on Mars.

References: [1] Eugster, H. P., & Hardie, L. A. (1978). *Springer*, 237–293. [2] Tosca, N. J., and S. M. McLennan (2006), *Earth Planet. Sci. Lett.*, 241(1–2), 21–31. [3] Osterloo et al. (2008). *Sci.*, 319(5870), 1651-1654. [4] Osterloo et al. (2010). *JGR: Planets*, 115(E10). [4] El-Maarry et al. (2013). *JGR: Planets*. E118 (11), 2263-78. [6] Ye et al. (2019). *Jour. of Earth Sci.*, 30, 1–10. [7] Leask, E. K., & Ehlmann, B. L. (2022). *AGU Advances*, 3(1). [8] Hynek et al. (2015). *Geology*, 43(9), 787-790. [9] Glotch et al. (2016). *JGR: Planets* 121(3), 454-471. [10] Daswani, M. M., & Kite, E. S. (2017). *JGR: Planets*, 122(9), 1802-1823. [11] Malin et al. (2007). *JGR: Planets*, 112 (E5). [12] McEwen et al. (2007). *JGR: Planets*, 112 (E5). [13] Quantin-Nataf et al. (2018). *Planet. and Sp. Sci.*, 150, 157-170. [14] Michael, G.G. & Neukum, G. (2010). *Earth Planet. Sci. Lett.*, 294 (3-4), 223–229. [15] Murchie et al. (2007). *JGR: Planets*. 112(E5), 1–57. [16] Viviano-Beck et al. (2014). *JGR: Planets*, 119, 1403–1431.

117. Archean stromatolites: a possible terrestrial analog to Mars.

S. Sarkar¹, A. Das¹, and D. Ray¹. ¹Physical Research Laboratory, Ahmedabad, India
(subham@prl.res.in)

Introduction: Stromatolites are the product of complex organo-sedimentary processes, including trapping, binding, and precipitation of sediments by Prokaryotic microorganisms [1]. Owing to their occurrence in numerous Archean formations worldwide, they are often regarded as the earliest known evidences of life [2]. Prokaryotic life, about half of the current biomass, may flourish in harsh environments, including deep crustal settings, salt pans, peritidal marine environments, and geothermal spring systems [3]. Thus, constraining the formation condition and biosignature preservation potential of different stromatolites will help search for extraterrestrial life. Various rover and orbiter-based studies have revealed that Mars once had more or less similar climatic conditions and environment, like our Earth, that have been habitable to life [4]. The search for biosignature on Mars is also the top science priority for Mars 2020 Perseverance Rover [4].

Mesoarchean Stromatolite: Stromatolite deposits are easily recognized by visual investigation due to their distinct morphologies. In this study, we have tried to constrain geological setting and formation scenario based on the mineralogy and geochemistry of Mesoarchean (2.97 Ga) stromatolite from the White Mfolosi, Nsuzi Group, South Africa [5]. The stromatolite unit comprises meta-limestone of greenschist facies layered above lapillistone and gradually grades into quartzite. The quartzite most likely represents a metamorphosed quartz arenite formation deposited in a coastal environment with shallow intertidal zones. Stromatolite drapes are frequently seen over quartzite with wave ripples. Shallow water is suggested by the relationship with wave ripples, and wave activity is indicated by the thin beds (>30 cm) of stromatolite-chip pebble conglomerates. The White Mfolosi stromatolites are interpreted as

peritidal marine in nature [6]. The presence of wave deposits and lack of diagnostic tidal structures suggest a microtidal [7] or even a non-tidal regime. The base (which rests on lapillistone) may have served as a shore platform.

Probable terrestrial analog to Mars: Hesperian siliceous structures exposed on flat surfaces near low cliffs at the edge of the Gusev Crater have been interpreted as possible biosignatures and likened to the contemporary siliceous hot spring microbialites of El Tatio, Chile [8]. We propose that contemporary microbialite occurrences are consistent with the existence of putative "shore platforms" and low cliffs [9]. The recent discovery of a shore platform from Utopia Planum, Mars, further comprehends that the ocean probably existed on Mars. Furthermore, the siliceous structures of Gusev Crater are found to be associated with the volcanic rocks at the edge of the crater on which they rest. The White Mfolosi stromatolites are also associated with volcanic deposits, including the lapillistones [7]. The difference in mineralogical composition of both the settings, i.e., opaline silica for Gusev Crater and carbonate in the case of Mfolosi, can be answered by their variation in the redox regime.

References:

[1] Allwood, A. C. et al. (2006) *Nature* 441(7094): 714-718. [2] Nutman et al. (2016) *Nature* 537(7621): 535-538. [3] Rodell et al. (2005) *Earth Interactions* 9(2), [4] Farley et al. (2020) *Space Science Reviews* 216: 1-41. [5] Smith et al. (2018) *Biogeosciences* 15(7): 2189-2203. [6] Siah et al. (2016) [7] Smith et al. (2020) *Precambrian Research* 278: 244-264. [8] Ruff and Farmer (2016) *Nature Communications* 7(1): 13554. [9] Cooper et al. (2022) *Journal of Sedimentary Research* 92(7): 619-634.

118. UNVEILING MARTIAN MAGMATIC PROCESSES: GEOCHEMICAL PERSPECTIVES ON POIKILITIC SHERGOTTITES

V. M. Nair^{1,2}, A. Basu Sarbadhikari¹, Y. Srivastava¹, N. Sorcar³, S Mukherjee³ (varsha@prl.res.in)
¹Physical

Research Laboratory, Ahmedabad, 380009, India; ²Indian Institute of Technology Gandhinagar, Gujarat, 382355, India; ³National Centre for Earth Science Studies, Akkulam, Thiruvananthapuram 695011, India

Introduction: In recent decades, Mars exploration missions, including Landers, Rovers, and Orbiters, have provided valuable insights into the chemical and mineralogical properties of the Martian surface. However, the instruments used on Mars lack the precision of Earth's laboratories and cannot analyze multiple sample parameters crucial for understanding the planet's evolution. Martian meteorites are the primary source for in-depth laboratory studies without sample return missions, offering valuable information on diverse geological processes and Mars' evolutionary history.

Shergottites, the most common type of Martian meteorites, comprise approximately 90% of the collection. Based on texture and mineralogy, they are classified into different categories, including basaltic, olivine-phyric, poikilitic, and gabbroic [1]. Among them, poikilitic shergottites are the most abundant, accounting for over 20% of the collection. Poikilitic shergottites are distinguished by their unique bimodal texture [2], [3]. This texture provides insights into their evolution, with an early slow-cooling poikilitic stage and a later, rapidly cooled interstitial stage [2]. They may constitute a significant portion of the Martian crust, making them crucial for studying Martian magmatism. These meteorites are geochemically categorized based on the variations in

Incompatible Trace Elements [4], [5] and radiogenic isotopic compositions [6] into enriched, intermediate, and depleted varieties, revealing insights into their mantle sources and the planet's geological history. In this study, we will be discussing the mineralogy, trace element mineral chemistry, and petrology of two suits of poikilitic shergottites, NWA 7397 (enriched) and NWA 1950 (intermediate), to constrain the mantle source characteristics for poikilitic shergottites, advancing our understanding of Martian igneous processes.

Methods: The polished sections of NWA 1950 and NWA 7397 were analyzed for major-element compositions of mineral phases using Electron microprobe (EMP) analyzer. Elemental X-ray maps of the samples were also obtained. Subsequently, modal abundances (expressed in volume percentages) of different mineral phases were calculated. The calculations were performed using ImageJ software, utilizing pixel count analyses of elemental X-ray maps for Mg, Fe, Ca, and Si. This comprehensive approach provides valuable insights into the composition and distribution of mineral phases in NWA 1950 and NWA 7397.

Results: The meteorite samples NWA 1950 and NWA 7397 display distinctive textural regions, namely poikilitic and non-poikilitic. Both the samples exhibit poikilitic textures characterized by pyroxene oikocrysts enclosing multiple olivine and spinel chadacrysts. The non-poikilitic regions are found interstitial to the pyroxene oikocrysts. In NWA 1950, poikilitic areas feature large low-Ca pyroxene crystals enclosing substantial euhedral olivines and chromites. Conversely, non-poikilitic regions contain augitic pyroxenes, pigeonite, maskelynite, and various accessory minerals, with olivine abundance surpassing that of pyroxenes and plagioclase glass. In NWA 7397, the poikilitic region showcases anhedral pyroxene oikocrysts with low-Ca cores and high-Ca rims, enclosing olivine chadacrysts of varying sizes and subhedral morphology, along with euhedral, smaller chromite grains. The non-poikilitic region in NWA 7397 is primarily composed of olivine, low-Ca pyroxene, high-Ca pyroxene, and maskelynite, accompanied by minor phases such as phosphates, spinel, pyrrhotite, and ilmenite. These findings contribute to the understanding of the complex mineralogical compositions in these Martian meteorites.

REFERENCES: [1] Udry, A. et al. (2020) e2020JE006523. [2] Howarth, G. H. et al. (2014) *Meteorit. Planet. Sci.*, 49(10), 1812–1830. [3] Combs, L. M. et al. (2019) *GCA* 266, 435–462, [4] Basu Sarbadhikari, A. et al. (2009) *GCA* 73(7), 2190-2214 [5] Basu Sarbadhikari, A. et al. (2011) *GCA* 75(22), 6803-6820. [6] Day, J.M.D. et al. (2018) *Nat. Commun.*, 9(1), 1-8.

119. Volcano-tectonic and fluvial interplay on Mars: insights from geomorphic landforms in Syria Planum

Anil Chavan^{1*}, K.B. Kimi¹, S Vijayan¹ and Subhash Bhandari²

¹*Planetary Sciences Division, Physical Research Laboratory, Ahmedabad, India*

²*Department of Earth and Env. Science, K.S.K.V. Kachchh University, Bhuj, India*

Email: asac.anil@gmail.com

The timing and formation of the Syria Planum volcano-tectonic province are critical in understanding the progression of the mantle, environment, and climate of eastern Tharsis province [1]. The tectonic feature linked with the upwelling of the mantle from Noachian to the early Amazonian epoch has to carry the specific characteristic of local and regional tectonism. Analyzing the ages of the tectonic and volcanic features may provide fresh insight into the history of volcanic domes and related fractures [2]. In the Syria Planum region, the number, the total length, and the linear density of faults and deformation rates are analyzed for each of the following 5 stages i.e., early to late Noachian (stage I); late Noachian to early Hesperian (stage II); early to late Hesperian (stage III); late Hesperian (stage IV), and early Amazonian (stage V). A total of 1076 Syria Planum related tectonic features, which are radial, tangential, and concentric to the center of the Syria Planum were assigned to their particular stages based on their stratigraphic and cross-cutting relationships based recent geological map. The attributes of each stage indicate that the deformation rate in the early/middle Noachian, late Hesperian, and early Amazonian was lower. At the same time, it has acquired a peak in late Noachian to early Hesperian. The volcanic activity in the area separates each episode of tectonism. The age relationship of the smaller shield volcanoes in the area indicates shifting of the root from south to northwest direction with respect to time. The area witnesses fluvial activity in the northern parts of Syria planum viz. Noctis fossae and Noctis Labyrinthus with a probable water source from the glacial melt in the southern highland caused by heating due to Tharsis volcanism. The Noctis Fossae with extensive fluvial erosional channels situated on the transition zone between Valles Marineris and Tharsis has preserved evidence of flowing water. The area has recorded NNE-SSW trending channels maintaining U-shaped glacial valleys at higher altitudes and V shape fluvial valleys at lower altitudes forming parallel to subparallel drainage system, fluvial terraces, surfaces, and deep gorges on the Hesperian volcanic rocks [3]. Faulting centered at Pavonis-I induced the collapse of Noctis Labyrinthus in the south, concentrating water to the troughs, implying the decline in the fluvial processes in the early stages of Amazonian time.

References: [1] Bouley et al. (2018) EPSL, 488, 26-133. [2] Hauber et al. (2009) J. Volc. & Geo Res. 185, 69-95. [3] Chavan et al. (2022) ASR. 70(10), 3205-3219.

120. Modeling of Schumann Resonance of Mars by using FDTD Method

Manauti Chaudhari¹, Foram M Joshi², Jayesh Pabari³

¹CVM University, Vallabh Vidyanagar, Anand, Gujarat, manoutichaudhari22@gmail.com, ²Madhuben and Bhanubhai Patel Institute of Technology, CVM University, Vallabh Vidyanagar, Gujarat, India, foram.joshi@cvmu.edu.in, ³Physical Research Laboratory, Ahmedabad

Abstract

Natural electromagnetic waves generated near the surface by electrostatic discharges in dust devils could be trapped in the resonant cavity formed by the surface and lower ionosphere of mars. In this paper we have calculated Schumann resonance value in extremely low frequency on martian surface by finite difference time-domain (FDTD) method lightning discharge on mars. The FDTD techniques are used to analyze ELF propagation on planetary atmosphere used to determine Schumann resonance. After solving 1D Maxwell equation by using FDTD algorithm, the frequency as a function of time for electromagnetic wave. The comparisons will be discussed during the conference.

References

- 1) J.P.Pabari Dust In Solar System, Volume-5, Issue – 3, July 2015.
- 2) S.tolendo- Redondo at.el., Schumann resonance at mars: Effect of the day-night asymmetry and the dust-loaded ionosphere, Geophysical Research Letters, RESEARCH LETTER,10.1002/2016GL071635
- 3) Heng Yang and Pasko, Three-Dimensional Finite Difference Time Domain modeling of the Earth-ionosphere cavity resonance, Geophysical Research Letters, VOL.32, L03114
- 4) J.P.Pabari, Trinesh Sana, Dependence of Martian Schumann Resonance on Dust Devil's Shape and Its Implications.
[Current Science](#), Vol 121, No 6 (2021), 769-774
- 5) A. Soriano et. al, A numerical study of the Schumann Resonance in mars with the FDTD method, Journal Of Geophysical Research, 112(A6), 2007.

121. Geological evaluation of the Martian analogue site in Kachchh basin of western India and its Geoheritage value

A. N. Dharaiya¹, R. Singh², M. G. Thakkar³ and S. K. Gaikwad⁴

¹M.Sc. Geology (II), Department of Geology, Savitribai Phule Pune University, Pune, India, adiradhu@gmail.com,

²Scientist E, Space Application Center (SAC), ISRO, Ahmedabad, India, ram@sac.isro.gov.in,

³Director, Birbal Sahni Institute of Paleosciences (BSIP), Lucknow, India, mgthakkar@rediffmail.com,

⁴Associate Professor, Department of Geology, Savitribai Phule Pune University, Pune, India, satyajit.gaikwad@gmail.com

Introduction: The exploration and understanding of Mars have captivated the scientific community and the public alike. Terrestrial analogues are places on Earth that have one or more geological or paleo-environmental characteristics that are similar to those found on extra-terrestrial planets, therefore identifying and studying such sites resembling Martian geology or paleo-environment, valuable inferences of the geological processes and potential habitability on the Mars could be gained [1]. The Kachchh basin has conserved several traditional terrestrial analogue locations, that could be explored as Martian counterpart regions such as Mawrth Valles, Meridianum Planum, Valles Marineris, etc. provide opportunities to study planetary science [2]. Matanomadh Formation exhibits geological characteristics that bear striking similarities to the Martian landscape. Its sedimentary rock formations, surface morphology, and mineral composition resemble those found on Mars, making it an ideal site for conducting detailed investigations [3]. The formation, dating to the late Paleocene, exhibits sedimentary layers, clay pockets, cross-stratified sandstone, and weathered laterite, reflecting complex depositional and weathering histories. The geological setting, marked by jarosite and hydrous sulphates, mirrors Martian environments [3]. The present study aims to identify and investigate the span of Matanomadh Formation in western Kachchh and establish it as a terrestrial Martian analogue. A comprehensive study and analysis of the Matanomadh Formation was conducted through detailed field observations, geological mapping, geochemical analysis (XRD, XRF, SEM & EDS), and petrography of the field samples in order to establish its status as a terrestrial Martian analogue. Geological fieldwork unveils distinct lithological sequences, providing insights into the region's complex sedimentary transportation

processes. Furthermore, remote sensing analysis aids in identifying clay and carbonate minerals, while XRD analysis confirms the presence of Alunite and Jarosite in field samples. Through implying these merits, the rock formations, mineralogy, stratigraphy, and sedimentary processes within the study are characterized. This investigation has enabled, studying the Martian analogue to identify specific geological features and processes that closely resemble those found on Mars, thereby contributing to understanding of the Martian geological history. The detection of Paleocene-age Jarosite in Matanomadh holds terrestrial relevance, offering insights into Earth's geological and environmental history during the Paleocene Eocene Thermal Maxima (PETM). The study concludes by proposing Matanomadh as a Geoheritage site, emphasizing its scientific, educational, and conservation significance as the site serves as a significant link to perform a comparative paleoenvironmental analysis of the Earth with that of the Mars [4]. Due to its several geomorphic and mineralogical analogues, the Kachchh basin serves as a stand-in for the Martian conditions that were prevalent throughout the Noachian to Hesperian transition. The Cenozoic environment of Kachchh has similarities to the conditions that prevailed during the Noachian to Hesperian transition on Mars. The occurrence of jarosite not only suggests the existence of oxidizing and acidic water on the surface, but also that the water is transient/ephemeral. Therefore, jarosite may indicate the end of water-rock interaction on the Martian surface and constrain the termination of water activity on Mars. It is necessary to develop the peculiarity of this Martian analogue geosite located in the Kachchh basin. Both the promotion and development of sustainable geotourism as well as conservation need sanctioning of the management.

References:

- [1] Osinski, G. R., L veill , R., Berinstain, A., Lebeuf, M., & Bamsey, M. (2006). Terrestrial analogues to Mars and the Moon: Canada's role. *Geoscience Canada*, 33(4), 175-188.
- [2] Chavan, A., Sarkar, S., Thakkar, A., Solanki, J., Jani, C., Bhandari, S., Bhattacharya, S., Desai, B.G., Ray, D., Shukla, A.D., Sajinkumar, K.S., Mitra, S., Gupta, S., Chauhan, G., & Thakkar, M. G. (2022). Terrestrial Martian Analog Heritage of Kachchh Basin, Western India. *Geoheritage*, 14(1), 33.
- [3] Bhattacharya, S., Mitra, S., Gupta, S., Jain, N., Chauhan, P., Parthasarathy, G., & Ajai. (2016). Jarosite occurrence in the Deccan Volcanic Province of Kachchh, western India: Spectroscopic studies on a Martian analog locality. *Journal of Geophysical Research: Planets*, 121(3), 402-431.
- [4] Chauhan, G., Biswas, S. K., Thakkar, M. G., & Page, K. N. (2021). The unique geoh heritage of the Kachchh (Kutch) Basin, Western India, and its conservation. *Geoheritage*, 13, 1-34.

122. MORPHOLOGICAL CHARACTERIZATION OF LIU HSIN CRATER, MARS

S. Ebrahim¹, A. Porwal², and M.Nithya^{3, 1,3}(Department of PG Studies & Research in Geology, MES Ponnani College (University of Calicut), Malappuram District, Kerala, 679577, e-mail: shabnaebrahim@gmail.com), ²(Centre of Studies in Resources Engineering, Indian Institute of Technology Bombay, Powai, Mumbai, 400076, e-mail: aporwal@iitb.ac.in).

Liu Hsin Crater is a crater in the Phaethontis quadrangle of Mars, located at 53.6°S latitude and 171.6°W longitude. The Noachian aged crater is an example of a peak-ring basin containing a central peak and a low peak ring with 137 km in diameter [1]. The key objective of the study is to analyze the morphological features found within the crater including gullies, fan deposits of granular sediments that accumulate on downhill formations, and dark dunes. A preliminary morphological mapping method is approached. Our work combines a study with processed CTX (5-6 m/pixel, 30 km swath) and HRSC (~12.5-50 m/pixel, 52 km swath) images, complemented by higher resolution HiRISE (25-30 cm/pixel, ~6 km swath) [2] [3] . The location of the crater towards the south pole region makes the landform formation in association with the glacial and periglacial activities. The plausible reason for the origin of the valley channels can be subsurface seepage, and/or precipitation which supports the climatic conditions. One particularly striking feature is the presence of dark dunes encircling the crater's inner rim, which might be the result of dust devils currently active on the Martian surface, whereas fluvial and glacial-periglacial are crucial in comprehending the history of water activity on Mars [4].

References: [1] Carlton, C.A (2015) LPSC XLVI, Abstract #32729. [2] Malin, M. C. et al. 2007. *Journal of Geophysical Research: Planets*, 112:E5. [3] McEwen, A.S. et al. 2007. *Journal of Geophysical Research: Planets*, 112:E5. [4] Mangold, N (2012) *Planetary and Space Science*, 62(1), 69-85.

123. Electromagnetic Ion Cyclotron wave with magnetic model in Jovian Magnetosphere

Sankalp Jain and R.S. Pandey

Department of Physics, Amity Institute of Applied Science, Amity University, Sector – 125, Noida, Uttar Pradesh, India

sankalp.jain@s.amity.edu; Corresponding author - rspandey@amity.edu

Abstract:-The analysis based on observations by Ulysess of Electromagnetic Ion Cyclotron (EMIC) wave in Jovian magnetosphere has been done in this paper. In Jovian's magnetosphere it has been observed that there are various types of large frequency radio emissions by the mechanism of resonant interaction. This paper we have considered the phenomenon of wave-particle interactions between EMIC wave along the magnetic field lines and fully ionized magnetospheric plasma particles with

parallel propagation of wave which evaluates the elaborated dispersion relation for ring distribution finding also with and without magnetic field model. Using the method of characteristics solution and kinetic approach, expression of growth rate has been derived. Following a parametric examination of the plasma's temperature anisotropy, thermal velocity, and number density, the impact of these variables on growth rate was examined using graphs.

Keywords

Electromagnetic Ion cyclotron waves, Ring Distribution, Magnetic model, Jovian magnetosphere

124. Understanding the effect of Fe in the interstellar nanosilicates : A first principles study

Debdatta Banerjee^{1*}, Swastika Chatterjee¹

¹Department of Earth Sciences and National Centre for High Pressure Studies, Indian Institute of Science Education and Research Kolkata, Mohanpur, Nadia – 741246, West Bengal, India

*db20ip003@iiserkol.ac.in

The planetary interiors are abundant in silicate minerals. In our own planet, silicates like olivine and pyroxene dominate the upper mantle. Apart from the deep Earth they are also prevalent in the astronomical environment. Their occurrence may not be in bulk form but as proposed by astrochemists, they take the form of “nanoclusters” in the interstellar medium. These cosmic dust grains are thought to be the origin of the planetary silicates [1]. Infrared spectroscopy-based studies indicate that the nanosilicates bear the stoichiometries corresponding to olivine (M_2SiO_4) and pyroxene ($MSiO_3$), where M is predominantly Mg [2]. Since the concentration of Fe in these nanoclusters is small, it is usually neglected while determining the properties (namely, formation energy, structural variations, dipole moments, heat capacities, infrared spectra) of the nanoclusters. Fe, being a transition metal ion, can significantly influence the physical properties of these nanoclusters. Moreover, the contribution of silicate dust in the reduction of Fe is still unclear [3]. The goal of this study is to understand the influence of Fe concentrations on the fundamental changes in characteristics of the olivine and pyroxene nanoclusters and their relationship to astronomical observations, from a quantum-chemical view point. As a result, we have simulated the infrared spectra of the olivine and pyroxene nanoclusters of varying size and Fe-concentration. As expected Fe modulates the properties of the nanoclusters. Our observations may have important implications in the interpretation of the JWST data for planet forming silicates present in the interstellar medium.

References:

- [1] Plane et al. (2012) *Chem. Soc. Rev.* 41 (19), 6507.
- [2] Jager et al. (2003) *Astron. Astrophys.* 408 (1), 193–204.
- [3] Roy et al. (2022) *Monthly Notices of the Royal Astronomical Society* 517.4: 4845-4855.
- [4] Serra-Peralta et al. (2022) *Physical Chemistry Chemical Physics* 24.46 : 28381-28393.
- [5] Escatllar et al. (2019) *ACS Earth and Space Chemistry* 3.11: 2390-2403.

125. Unraveling Phaethon's Comet-Like Activity: Expected Spectral Variations in the December 2024 Encounter

N. Keshav^{1*}, P. Shalima¹ & S. Narendranath²

¹Manipal Centre for Natural Sciences, Centre of Excellence, Manipal Academy of Higher Education, Manipal - 576104, India

²Space Astronomy Group, U R Rao Satellite Centre, ISRO, Bengaluru - 560017, India

*Corresponding Author E-mail: kshhhv.nikhil@gmail.com

Meteor showers, visible phenomena in the night sky, result from Earth's passage through dust particle trails, which are often the remnants of disintegrated comets. Notably, the Geminids shower exhibits a distinctive link to the Apollo asteroid Phaethon, which evident in its spectral properties and orbital trajectory [1],[2]. This asteroid blurs the line between asteroids and comets due to its highly eccentric orbit around the Sun, with a perihelion distance of only 0.14 AU. The extreme heat prompts Phaethon to exhibit comet-like activity and causes it to develop a tail [3].

Due to these enigmatic characteristics, JAXA has planned DESTINY+, a fly-by mission to Phaethon [4]. Observations from Phaethon's recent pass-by revealed spectral variations across latitudes in the lower visible range. The cause of these discrepancies remains poorly understood and can be attributed to factors such as compositional differences, physical properties like grain size, or space weathering effects [5]. A better understanding of the underlying causes can shed light on the impact of a highly eccentric orbit and extreme temperatures on planetary processes.

We have computed the asteroid's visibility using ephemeris data and the asteroid's shape model. An upcoming pass-by in December 2024 provides an excellent opportunity to observe this asteroid and understand its nature. Extending the reflectance spectra into the near-UV range, along with near-simultaneous ground-based observations at NIR-VIS wavelengths, could provide new insights to explain the observed spatial variations in visible reflectance. We will show how these observations in multiple wavelengths at different aspect and phase angles will provide a more comprehensive explanation for the active processes. This study will thus improve our insight into Phaethon's composition, activity, and origin.

References: [1] Williams, I. P. and Wu, Z. D., 1993, *Monthly Notices of the Royal Astronomical Society* 262: 231–248. [2] Gustafson, B. A. S., 1989, *Astronomy and Astrophysics*, 225: 533–540. [3] David Jewitt et al., 2013, *The Astrophysical Journal* 771 L36. [4] Ozaki, N., 2022, *Acta Astronautica* 196: 42–56. [5] Lazzarin, M., 2019, *Planetary and Space Science* 165:115–123.

126. Future Mining Candidate Among the Quali-hilda Group of Asteroid & Comet Dhanraj S Warjurkar¹ and Prasad V. Arlulkar²

¹Zade Plot, Bhadrawati, Inida (author was affiliated to SNU, South Korea, during the Observation) ²Kalyani Strategic Systems Ltd. Inida (Corresponding Author e-mail: warjurkar@hotmail.com)

Abstract: This work refines a previously proposed classification of quali-hilda group of asteroids & comets for mining purposes and will be based on updated information about their physical, and taxonomical classification. The process leading to the successful mining of quali-hilda asteroid and comets, may consist of 1) viable targets must be identified and confirmed 2) the targets must be either retrieved or a mining team be deployed to it 3) the target must be mined 4) the material must be returned to the Earth or wherever they are destined to go. Due to less know physical and chemical properties and taxonomical classification of quali-hilda asteroid and comets, further observation and investigation are necessary in order to enlighten the nature and potential target candidate of quali-hilda asteroid and comets mining. Asteroid sample return research missions, such as Hayabusa, Hayabusa2, and OSIRIS-REx illustrate the challenges of collecting ore from space using current technology. As of 2023, less than 7 grams of asteroid material has been successfully returned to Earth from space. In progress missions promise to increase this amount to approximately 60 grams (two ounces). Asteroid research missions are complex endeavors and return a tiny amount of material (less than 1 milligram *Hayabusa*, 100 milligrams *Hayabusa2*, 60 grams planned *OSIRIS-REx*) relative to the size and expense of these projects (\$300 million *Hayabusa*, \$800 million *Hayabusa2*, \$1.16 billion *OSIRIS-REx*).

References:

- [1] Dhanraj Warjurkar , P V Arlulkar (2020)-arXiv:2004.08928 [astro-ph.EP- Quasi-Hilda Comet 231P/LINEAR-NEAT: Observation at aphelion using Himalayan Chandra Telescope [2] Myung-Jin Kim; Hong-Kyu Moon; Masateru Ishiguro; ...Dhanraj S Warjurkar;... et. al.(2013)-A&A-550 Pages-L-11-Lightcurves of Near-Earth Asteroid 162173 (1999 JU3).
- [3] Masateru Ishiguro; Daisuke Kuroda; Sunao Hasegawa; Myung-Jin Kim; ...Dhanraj S Warjurkar;... et. al.-(2014)- AJ-Optical Properties Of (162173) 1999 JU3:In Preparation For The JAXA Hayabusa 2Sample Return Mission
- [4][The tale of 2 asteroid sample-return missions". *cen.acs.org*. Archived from the original on 2021-06-02. Retrieved 2021-05-30.](https://arxiv.org/abs/2021.06.02)
- [5] *The Planetary Society*-The OSIRIS-REx mission is expected to cost \$1.16 billion. [6] J. Correa-Otto, E. García-Migani, R. Gil-Hutton- (2023) -MNRAS- 1-7The population of Comet candidates among quasi-Hilda objects revisited and updated.
- [7] Matt Anderson-(2015)-Planetary Sciences- Mining Near Earth Asteroids-

127. Understanding the Mode of Occurrence of Granite and Other Felsic Rocks in Mars and Moon and their Role in Planetary Crustal Evolution: An Earth Analogous Study

R. Dutta¹(email: riyadutta@prl.res.in) and D.K. Panda¹(email: pdipak@prl.res.in)

¹Physical Research Laboratory, Ahmedabad, Gujarat

Introduction:

Earth is the only planetary body with reported continental crust. Understanding the evolution of continental crust of planet Earth requires a much more comprehensive picture of granite as it is the key component of earth's continental crust. Granite is formed by various magmatic processes regardless of plate tectonics. Yet such felsic rocks have not been widely exposed on other planetary bodies, but the recent discovery of silicic domes on the lunar surface and granitic fragments returned by the Apollo missions have provided evidence for the presence of SiO₂-rich lithology on the Moon. Crustal melting is considered as a possible model for explaining the formation of silicic lithology on lunar surface. Besides that, the presence of granitic compositions with quartz, feldspar, some combination of sheet silicates and high silica glass in the Martian surface collectively reveal a more complex picture of Mars crustal diversity. The felsic compositions plausible suggest their formation through prolonged magmatic activities, mainly through fractional crystallization of Martian magma. A comparative study of petro-geochemical signature and isotopic character of Martian and lunar granite and other felsic rocks with that of earth granitic analogue is considered to understand the mode of granitisation and its role in crustal evolution of inner solar planets. For this study Precambrian Mount Abu granitic batholith and surrounding granitic rocks are chosen as earth analogue.

Objective and Methodology:

The work will be focused on the detailed petrographic study, mineral phase analysis, bulk rock major trace element and isotope analysis of selected granitic samples from the study area using Electron Probe Micro-Analyzer (EPMA), X-Ray diffraction (XRD), X-ray fluorescence (XRF) Spectrometry, Inductively Coupled Plasma Mass Spectrometry (ICPMS). The magmatic differentiation modelling through various thermodynamic parameters using MELTS- software may be used to understand on formation of granitic and other felsic magma from protoliths. A complete database of Martian and Lunar igneous compositions will be used to statistically and analytically compare felsic composition of Mars, Moon with that of terrestrial compositions from Earth continental crust and intraplate volcanism.

Discussion:

The keen interest of the present study is to elucidate petrogenetic processes of granite and other felsic rock formation in planetary bodies and try to understand their role in planetary crustal evolution. This study will also offer a new insight to the possible existence of evolved granitic crust in planetary history.

Keywords: Granite, Earth Continental crust, Silicic lithology on lunar surface, Mars crustal diversity, Prolonged magmatic activity.

References:

[1] Udry A. et al. 2018. *Journal of Geophysical Research: Planets* 123: 1525-1540 [2] Steven A. et al 2002. *Journal of Geophysical Research* 107: 1-19 [3] Hagerty and Reid M. R. (2014) *LPSC XXXV*, Abstract # 2277 [4] McLeod L. et al. 2016. *Journal of The Geochemical Society and The Meteoritical Society* 187: 350- 374 [5] Ostwald A. et al. 2022. *Earth and Planetary Science Letters* 585: 1-13 [6]: CAO H. et al. 2021. *Meteoritics & Planetary Science*: 1-33 [7] Xue Z. et al. 2019. *Journal of The Geochemical Society and The Meteoritical Society* 266: 74- 108. [8] Wray J.J. et al. 2013. *Nature Geoscience* 6: 1013- 1017.

128. Effect of Different Forces on IDP in Inner and Outer Solar System

Aanchal Sahu* and J. P. Pabari

Physical Research Laboratory, Navrangpura, Ahmedabad - 380009, India

* E-mail: aanchalsahu@prl.res.in

Dust is ubiquitous in our Solar System. These dust particles are originated by various sources like Asteroid Belt, Kuiper Belt, Oort cloud etc. [1]. Measurements of the Venera 9 and 10 spacecraft served as first evidence for a co-orbital dust ring around Venus. These measurements were tested later by the Helios mission [2] and were confirmed with observations from STEREO [3]. The acquisition of data was undertaken by space probes, namely Pioneers 10 and 11, Galileo, and Ulysses, spanning distances from 0.7 to 18 Astronomical Units (AU) from the sun. Within the inner solar system, extending to approximately 3 AU, identification of zodiacal dust particles is facilitated through methods involving scattered light, thermal emission, and in-situ detection by space probes. These particles orbit the sun on low inclination ($i \leq 30^\circ$) and moderate eccentricity ($e \leq 0.6$) orbits, while beyond 3 AU, the dust population is predominantly comprised of particles on high inclination or even retrograde trajectories. [4]. We studied and compared the dynamics of orbital dust in the inner Solar system that is the role of Solar Radiation pressure, the Poynting Robertson effect and the Solar Wind force [5] on the location of micron-sized dust grains by variation in heliocentric distance and size of dust grain. We have analyzed the forces by taking Interplanetary Dust mass range from 10^2 kg to 10^{-21} kg [6]. We have considered mainly protons and alpha particles as Solar wind species [7]. Since Gravitational force always dominates and therefore, we have considered only the effects of Non-Gravitational forces on dust for the better understanding of dynamics in Inner and Outer Solar System. The study can be useful to understand the effects of various forces on dust at outer planets.

References: [1] Krasnopolsky & Krysko (1979), Planetary and Space Science, Volume 27, Issue 7, Pages 951-957; [2] Leinert & Moster (2007), Astronomy and Astrophysics, Volume 472, Number 1; [3] Jones et al. (2013, 2017), Astronomy and Astrophysics, Volume 602; [4] Eberhard Grun (1993), IAUS Volume 160; [5] T. Minato and Yamamoto (2004), Astronomy and Astrophysics, Volume 424, Number 2; [6] Grün, E. et al. (1985), Icarus, 62, 244; [7] Neugebauer et al., (2001), Neugebauer (2001), Geophysical Research Letters, Volume 28, Issue 7

129. HIGH-PRESSURE PHASES AND IMPACT-INDUCED TEXTURES IN SHOCKED INDIAN METEORITES.

Kishan Tiwari^{1,*}, Sujoy Ghosh², Masaaki Miyahara³, Dwijesh Ray¹, ¹Planetary Sciences Division, Physical Research Laboratory, Ahmedabad – 380059, India (kishan@prl.res.in), ²Department of Geology and Geophysics, Indian Institute of Technology, Kharagpur - 721302, India, ³Graduate School of Advanced Science and Engineering, Hiroshima University, Higashi-Hiroshima, Hiroshima 739-8526, Japan

Introduction: Impact events have been one of the most crucial and fundamental cosmic processes that have played an important role in the shaping and evolution of the planetary surfaces and interiors. Such

impact events on planets and asteroids are also responsible for the delivery of meteorites on the Earth's surface. Meteorites are broken pieces of the asteroids or some planet that got dislodged from the asteroid's surface when two celestial bodies collide with each other. These broken pieces are later get sucked in by the Earth's gravity and fall on the Earth's surface as meteorites. These collisions result in the formation of shock waves. The main property of these waves is that they deform the rocks and immensely increase the pressure. Furthermore, such collisions give rise to the formation of numerous fractures in the parent body. During the collision, the friction produced as the surface of these fractures moves past each other, causes temperature spike and subsequent melting. Therefore, these fractures become localized zones of high-pressure and high-temperature and are called shockmelt veins (SMVs). These high-pressure and high-temperature conditions are similar to the condition prevailing at depths of ~400-700 km on Earth resulting in formation of high-pressure phases in and around these SMVs.

Kamargaon: Asteroids are mostly made up of a mineral called olivine which is also a major constituent of the Earth. Consequently, understanding the behavior of olivine at high pressure and temperature becomes important to unravel the secrets of Earth's deep interior. Olivine becomes unstable at around pressure of ~23-25 GPa, which is equivalent to the depth of ~660 km on Earth, and breaks down into bridgmanite + magnesiowüstite. Bridgmanite is the most abundant mineral on Earth, which makes this one of the most important reactions that control the physical and chemical properties of the Earth's interior. This breakdown may occur where the olivine remains in the solid state or may also form by melting of the olivine. The breakdown assemblage of bridgmanite and magnesiowüstite formed by both of these mechanisms has been reported in few Martian meteorites. However, no such assemblage formed by melting has been found in meteorites originated from the asteroid belt. We studied a meteorite named 'Kamargaon' that fell on November 13, 2015, near the town of Kamargaon, Assam, India [1]. We, for the first time, reported the possible occurrence of bridgmanite and magnesiowüstite formed by the melting of olivine in Kamargaon meteorite, a meteorite that came from the asteroid belt [2]. This assemblage may have formed at pressure and temperature of ~25 GPa (equivalent to the depth of ~660 km on Earth) and ~2500 °C [2]. These observations suggest that the breakdown of olivine in the natural systems can also take place by the melting of olivine.

Katol: Additionally, we studied another meteorite that originated in the asteroid belt named 'Katol' that fell near the town of Katol in the Nagpur district of India after a large meteor shower occurred on May 22, 2012 [3]. We tried to understand and decipher the composition and formation mechanisms of various minerals that are present in the shock-melt veins of Katol meteorite. We found that the bridgmanite is present as a very finegrained (100-1000 nanometer in size) assemblage in the shock-melt veins [4]. Natural bridgmanite has been reported in only a few meteorites; however, the composition of these specimens differs from the plausible composition of bridgmanite that is expected to be present in the Earth's interior. This study reports the first natural occurrence of bridgmanite, observed in Katol meteorite, with a composition closest to the bridgmanite present in the Earth's mantle. The bridgmanite in the Katol chondrite has high Fe³⁺ and other compositional traits that agree with experimental predictions. Additionally, the pressure we have estimated (~25 GPa) based on the occurrence of bridgmanite and the duration for which such conditions persisted can be used to calculate the impact velocity and parent body size of these meteorites. According to our calculations, Katol meteorite was produced during an impact where impact velocity was ~2.54 km/s and the parent body from which it broke off was at least ~3 km in diameter [4]. For Kamargaon meteorite, our calculations suggest that it is a result of impact velocity of ~2.3 km/s and the parent body size was ~6.4 km in diameter [2].

References: [1] Goswami T.K. et al. (2016) *Current Science* 110(10), 1894. [2] Tiwari K. et al. (2021) *Geophysical Research Letters* 48:e2021GL093592. [3] Suresh G. et al. (2013) *Journal of Geological Society of India*, 81(2), 151-157. [4] Ghosh S. et al. (2021) *Proceedings of the National Academy of Sciences*, v. 118, p. e2108736118.

130. Insights on the Ion Composition of Comet 67P/C-G during the Rosetta Mission: A Multi-instrument Analysis

Sana Ahmed¹, Kinsuk Acharyya¹ and Vikas Soni¹

¹Planetary Sciences Division, Physical Research Laboratory, Ahmedabad, India
(ahmed.sana92@gmail.com)

Comet 67P/Churyumov-Gerasimenko (67P/C-G) is a Jupiter family comet that was the target of ESA's Rosetta mission [1] that orbited in its vicinity for nearly 26 months. Rosetta typically remained at cometocentric distances ranging from tens to hundreds of kilometers during the mission period. The sublimation of volatile ices from the comet nucleus forms the coma. The neutral species in the coma are partially ionized due to photoionization, electron impact ionization and charge exchange with the solar wind [2], thereby forming the cometary ionosphere. Changes in the comet's heliocentric distance lead to alterations in the outgassing rate and activity patterns. The continuous monitoring of 67P/C-G by the suite of instruments carried by Rosetta has enabled us to study the evolution of the coma for varying heliocentric distances and spatial locations. The instruments carried by Rosetta included the Rosetta Orbiter Spectrometer for Ion and Neutral Analysis (ROSINA; [3]) and the Rosetta Plasma Consortium (RPC; [4]). ROSINA included the Double Focusing Mass Spectrometer (DFMS) that operated in low and high resolution modes, giving mass spectra of cometary ions and neutral species lying in the range 13-140 u/q. ROSINA's COMet Pressure Sensor (COPS) provided us with time-series measurements of the total neutral density. Among the instruments of the RPC, the Mutual Impedance Probe (MIP) and the Langmuir Probe (LAP) measured the in situ plasma density, while the Ion Composition Analyzer (ICA) had limited mass resolving capabilities and provided density measurements of some ions.

DFMS had a small field of view and the counts obtained from the mass spectra cannot be directly converted into number densities of ions. However, the total ion density can be known by combining the measurements from MIP and LAP. Additionally, the density of some ions such as H⁺ and H₂O⁺ can be known from the ICA measurements. We used multi-instrument dataset in order to estimate the ion abundances and their formation/loss mechanisms in the coma of 67P/C-G. We modeled the coma using a combined chemical-hydrodynamical multi-fluid model. This model uses the fluid approximation for a spherically symmetric coma in the steady state, and is based on the fluid conservation equations of number density, momentum and energy [5]. Lauter et al. (2020) [6] used the COPS and DFMS data to obtain the densities of neutral volatiles in the coma for a number of intervals on the orbit of 67P/C-G at the time of the Rosetta mission. We selected 38 of these intervals and used the neutral densities reported by [6] as inputs in our model runs. The total ion densities at different cometocentric distances obtained from our model outputs match well with the in situ density measured by MIP and LAP, while the modeled H₂O⁺ density matches well with the ICA observations. We also made a comparison of the ion ratios of NH₄⁺/H₂O⁺ and H₃O⁺/H₂O⁺ obtained from our model and from the observed DFMS mass spectra. We find that these ion ratios can be used to comment on the extent of ion-neutral chemistry occurring in the coma at different heliocentric and cometocentric distances. Finally, since our modeled values match well with the total ion density measurements, we can make density profiles of all the ions whose presence in 67P/C-G has been confirmed by high resolution DFMS spectra.

References:

[1]Schulz R. (2009) *Solar System Research* 43: 343. [2] Cravens T. E. et al. (1987) *Journal of Geophysical Research* 92: 7341. [3] Balsiger H. et al. (2007) *Space Science Reviews* 128: 745. [4] Carr C. et al. (2007) *Space Science Reviews* 128: 629. [5] Ahmed S. and Acharyya K. (2021) *The Astrophysical Journal* 923: 91. [6] Lauter M. et al. (2020) *Monthly Notices of the Royal Astronomical Society* 498: 3995.

131. Venus Exploration Challenges and Future Research Opportunities

G. ARORA and D. RAY*

Physical Research Laboratory, Ahmedabad, India

**Corresponding author E-mail: garima@prl.res.in*

Venus being the closest neighboring planet (0.7 AU) among the terrestrial planets closely resembles Earth and is rightly considered as its ‘Twin sister’. It has about the same mean radius, mass, and mean density. For many decades, these fundamental similarities suggested that Venus and Earth might have similar climatic environments, water abundances, tectonic styles, and geological histories. Early space exploration missions like Mariner, Venera, Vega, & Pioneer, and the more recent Magellan, Venus Express, and Akatsuki missions have given us significant details about Venus’s history, evolution, and current geological and atmospheric conditions. The surface morphology of Venus is dominated by the signatures of basaltic volcanism resulting in the formation of vast regional plains and tectonic deformation. Earth-based observations have revealed Venus’s opaque ‘runaway greenhouse’ atmosphere (dense 93 bar surface pressure), dominantly CO₂ composition with H₂SO₄ clouds and high surface temperatures reaching 475°C.

Yet, many fundamental questions remain unanswered like the nature of interior-surface-atmosphere interactions over time (including whether liquid water was ever present), evolution of the surface and interior of Venus, etc. Comparable levels of Venus exploration were significantly inhibited by the global dense, acidic, and optically opaque atmosphere, penetrable only by descent probes to the surface, and imaging and altimetry at radar wavelengths.

Improvements in imaging and topography from the upcoming missions will enable seeing key geologic contacts, individual volcanic flows, fault blocks, and other details of surface geology. Considerable advancements in our knowledge of compositional information will come from both infrared and SAR imaging. The surface and subsurface observations in the upcoming missions like Radar-equipped ESA-led EnVision M5 orbiter mission, NASA-JPL’s VERITAS (Venus Emissivity, Radio Science, InSAR, Topography, and Spectroscopy) orbiter mission, NASA-GSFC’s DAVINCI (Deep Atmosphere Venus Investigation of Noble Gases, Chemistry, and Imaging) entry probe/flyby mission and Indian radar-equipped orbiter, Shukrayaan-1 will help in understanding geologic and resurfacing history, aeolian features on the surface, impact processes including detection of buried impact craters, vertical structure and stratigraphy of geological units including active volcanic hotspots and lava flows.

References:

[1] Thomas Widemann et al. (2023) *Space Science Reviews* 219:56 [2] James W. Head et al. (2023). *Geological Society, London, Special Publications*, 541, [3] Allan H. Treiman (2006) *A chapter in the AGU Chapman Conference Book* [4] Ivanov M.A., Head J.W. (2013) *Planet. Space Sci.* 2013 V. 84. P. 66-92.

132. Observations of V0 layer from Venera 15 and 16

Satyandra M. Sharma^{1,2}, Varun Sheel¹ and Tirtha J. Kalita¹ ¹Physical Research Laboratory, Ahmedabad-380009 (smsharma@prl.res.in), India, ² Indian Institute of Technology Gandhinagar, Gandhinagar-382055, India.

The dayside ionosphere of Venus is characterized by V2 and V1 layers, produced by Solar EUV and Soft X-ray radiation. The solar and non-solar driven space weather elements affect the Venusian ionosphere significantly causing disturbance in its plasma distribution. The full structure of the planetary ionosphere is obtained using the remote sensing Radio Occultation (RO) technique. The retrieval parameter of the RO technique is electron density as a function of distance with respect to the center of planet. We have analyzed the archival data of electron density profiles obtained from Radio Occultation Experiment (ROE) of Venera 15 and 16 [1]. Apart from the main characteristic ionospheric layers V2 (at ~140km) and V1 (at ~130km) a sporadic layer V0 below 120km is observed with peak electron density of $\sim 1.2 \times 10^4 \text{ electrons/cm}^3$ [Fig.]. The source of V0 layer is still debatable. The possible candidates may be the dust ablation, solar energetic particles and solar X-ray radiations which needs further investigation.

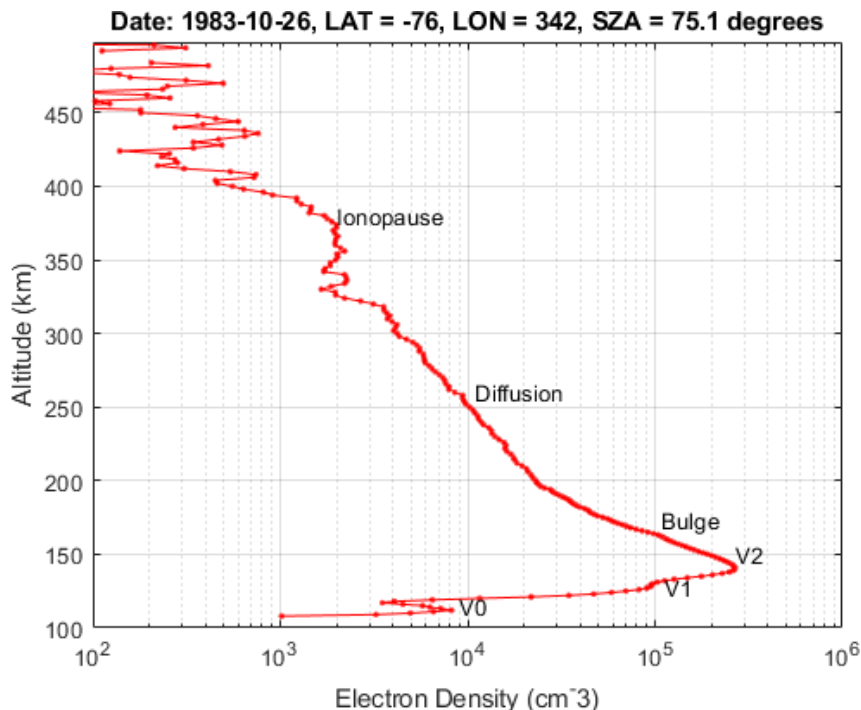


Figure. An example of electron density profile showing an additional layer below V1 layer with peak electron density of $\sim 8.2 \times 10^3 \text{ electrons/cm}^3$ at an altitude near 112 km.

References: [1] A. L. Gavrik, Yu. A. Gavrik, P. Withers, S. Joy, Venera 15 and 16 Radio Occultation Ionospheric Electron Density Profiles, Version 1.0, V15/V16-V-ROE-5-OCC-ELECTRON-DENS-V1.0, NASA Planetary Data System, 2010.

133. Ejection age and Noble Gas Study of Rantila Meteorite

Avadh Kumar¹ and R. R. Mahajan²,

^{1,2}Physical Research Laboratory, Ahmedabad-380009

e-mail: avadh@prl.res.in

Introduction: Meteorites are the segment of rocks or stones which come from different asteroid or planets to Earth. With the availability of existing catalogue of meteorites gave us a boost for their study for unravel the secrets of our Solar system in many ways. Although plenty of work has been done on meteorites to understand how our Solar system has been formed and modified since ages but many points are need to be clarified yet. In this work we analysed the Rantila meteorite. This meteorite fall was observed in two nearby villages, Rantila and Ravel, 10.5 km apart. Several fragments of the meteorite were found scattered around a field. This meteorite is an aubrite (enstatite achondrite). This is the second reported aubrite fall in India, the last aubrite before this was in Basti, Uttar Pradesh. So in this work we measured the abundance of all stable isotopes of noble gases and their ratios as well. So the new results from Rantila meteorites will be presented.

Methodology: Here, we extract the gases from sample using the technique of single grain analysis. We used ND-YAG laser of wavelength 1.06 μm . The Laser is operated in CW mode.

Significance of Ejection age: The scientific significance of CRE ages of meteorite is advancing our understanding of the solar system. Its contributions to unravelling the chronology and dynamic processes in the solar system. Cosmic rays, predominantly high-energy particles from outer space, constantly bombard the surfaces of celestial bodies, including meteoroids and asteroids.

Results and Conclusion: By determining the cosmic ray exposure ages of meteorites, we can establish a chronology of events in parent asteroid body. The CRE ages of different meteorites provide insights into the timing and duration of various processes, such as asteroid fragmentation, collisional evolution, and transport in the solar system. Study of the CRE age of meteorites can help in understanding the regolith evolution of asteroids.

Acknowledgements: We are very thankful to Department of Space. Government of India for the financial support.

References: [1] Grady M. et al. (2014) *Atlas of Meteorites* [2] Eugster O. et al. (1988) *GCA Acta Vol. 52*, 1649-1662 [3] Dalcher N. et al. (2013) *Meteoritic and Planet. Sci.* 48, Nr 10, 1841-1862 [4] Mahajan R. R. et al. (2018) *Planet. And Space Sci.* 152, 136-141 [5] Mahajan R. R. (2020) *Earth, Moon and Planets* 124, 3-13.

134. Active radio sounding of Solar Corona - Results From MOM and Akatsuki Missions.

Richa Naja Jain¹, R.K. Choudhary¹, Anil Bharadwaj², Umang Parikh³ and T. Imamura⁴

¹Space Physics Laboratory, VSSC, ISRO, India, 695022 (richanajajain@gmail.com), ²Physical Research Laboratory, Ahmedabad, India, ³ISRO Telemetry and Tracking Centre, Bangalore, India, ⁴University of Tokyo, Japan

Abstract: The study of dynamics at Solar Corona and acceleration of solar wind holds a significant importance in refining our understanding of Space-weather events. To unveil the origin and expansion of the solar wind, it is crucial to map its speeds closer to the Sun. However, the inner-middle coronal region's complex dynamics, involving high temperatures, plasma, and magnetic flux, pose challenges for in-situ measurements. Active remote sensing through radio signals emerges as a reliable tool to investigate the solar corona's structure and dynamics. Several missions have effectively employed downlink radio signals from spacecraft to study the solar corona during solar conjunction trajectories [1,2,3].

Solar conjunction occurs when the Sun, Earth, and spacecraft align, allowing radio signals transmitted from the spacecraft to traverse the solar corona before reaching ground stations. The ionized corona induces frequency-dependent Doppler signatures in these signals due to fluctuating electron density, enabling spectral inversion for studying various coronal properties like plasma turbulence, velocity, density, magnetic field fluctuations, and solar wind acceleration. This is an ingenious method to employ the radio telemetry technology already onboard a planetary mission spacecraft to study solar coronal dynamics.

In our work, we developed an algorithm to extract the “differential Doppler-frequency residual” values, from the signal recorded in the RDEF file, and the range rate doppler estimated from the SPICE kernels provided by UDSC/IDSN teams. By analyzing Doppler frequency residuals, we derived valuable insights into plasma turbulence characteristics, estimated electron density fluctuations and flow speeds based on isotropic quasistatic turbulence methods [4]. We used the coronal radio sounding experiments performed by Indian Mars Orbiter Mission (MOM) spacecraft during the Mars-Solar Conjunction period in May/June 2015 and by Akatsuki (JAXA Mission around planet Venus) during Venus-Solar Conjunctions in 2019, 2021, 2022 to study the frequency fluctuation spectrum, which is indicative of plasma density fluctuations and magnetohydrodynamic waves and turbulence in the inner-middle corona. We are able to probe the region as close as 3-20 Rs, spanning equatorial to polar heliolatitudes. We have interesting results from the comparative study of the turbulence spectrum and solar wind velocity estimates from various experiments across the maxima of solar cycle 24 and minima of solar cycle 25. The MOM results highlighted the transition in the turbulence regime indicated by the change in the slope of turbulence spectrum from 0.3 to 0.7 between the heliocentric distances 5 to 15 Rs. This helped us to substantiate the process of turbulent energy transport and dissipation of magnetohydrodynamic wave, that lead to Coronal heating and solar wind acceleration in the coronal region [2]. The Akatsuki experiments gave us the unique opportunity to track the evolution of fast solar wind streams emanating from a polar as well as from a rare occurrence of trans-equatorial coronal hole, as they propagated to increasing heliocentric distances. Our study provides unique insights into the least-explored inner coronal region by corroborating radio sounding results with EUV observations of the corona [3]. In my presentation, I will be exploring the enigmatic mechanisms of the solar corona. I will explain the methodology used in active radio sounding of the solar corona, which is a reliable and unique technique. Additionally, I will provide insights into the findings of previous sounding experiments. We will also discuss the potential of using spacecraft signals as radio beacons for improved prediction of space weather events that may be triggered by high-speed solar wind streams directed towards Earth.

References:

- [1] Pätzold, M., B. T. Tsurutani, and M. K. Bird (1997), *J. Geophys. Res.*, 102(A11), 24151–24160 [2] Jain, R.N., et.al, (2022), *MNRAS*, 511, 2, 1750-1756 [3] Jain, R.N., et.al, (2023), *MNRAS*, 525, 3, 3730–3739 [4] Armand N. A. et. al., 1987, *Astronomy and Astrophysics*, 183, 135

135. ELECTROSTATIC SOLITARY WAVES IN THE VENUSIAN PLASMA ENVIRONMENT

R. Rubia^{1*}, S. V. Singh², G. S. Lakhina³, S. Devanandhan², M. B. Dhanya¹ and T. Kamalam⁴

¹*Space Physics Laboratory, Vikram Sarabhai Space Centre, Thiruvananthapuram – 695022*

²*Indian Institute of Geomagnetism, Navi Mumbai – 410218*

³*Retired, Vashi, Navi Mumbai – 410218*

⁴*School of Physics and Astronomy, University of Southampton, Southampton, SO17 1BJ, UK*

* rubi.r92@gmail.com

ABSTRACT

The solar wind interaction with the Venusian atmosphere generates an “induced magnetosphere” which is analogous to Earth’s magnetosphere with respect to plasma regions but varies in the spatial extent [1]. The solar wind - Venus interaction results in particle acceleration, energy and momentum transfer to the Venusian plasma particles as well as generation of varied plasma waves [2]. Electrostatic solitary waves (ESWs) are ubiquitous in the space plasma environment and often manifests as broadband electrostatic noise (BEN) in the frequency domain. The ESWs are often associated with ion and/or electron beams [3]. The ESWs account for the electrostatic turbulence and acceleration of particles in space.

The occurrence of the ESWs in the Venusian plasma environment by virtue of its interaction with the solar wind are studied using a homogeneous, collisionless, and magnetized multicomponent plasma comprising of Venusian H⁺ and O⁺ ions, background electrons following Maxwellian distribution and streaming solar wind protons, and suprathermal electrons following κ - distribution. The model supports the existence of positive potential O⁺ and H⁺ ion-acoustic solitons. The characteristics and evolution of the solitons existing in two sectors, viz., dawn-dusk (DD) and noon-midnight (NM) sector of the Venus ionosphere at an altitude of (200–2000) km, are studied. The theoretical model supports the existence of solitons with amplitude \sim (0.067–56) mV, width \sim (1.7–53.21) m, velocity \sim (1.48–8.33) km s⁻¹, bipolar electric field amplitude \sim (0.03–27.67) mV m⁻¹ with time duration \sim (0.34–22) ms. The Fourier transform of these bipolar electric field pulse results in a BEN, with frequency varying in the range of \sim 9.78 Hz – 8.77 kHz. The model is relevant in explaining the electrostatic waves (frequency \sim 100 Hz–5.4 kHz) observed in the Venus ionosphere by the Pioneer Venus Orbiter (PVO) mission [4, 5] and in the Venus magnetosheath by the Solar Orbiter during its first gravity assist manoeuvre of Venus [6].

References:

[1] Futaana Y, Wieser G. S., Barabash S., and Luhmann J. G, (2017) *Space science Review*, 212, 1453-1509.

[2] Afify M., Elkamash I., Shihab M., & Moslem W., (2021) *Advances in Space Research*, 67, 4110.

[3] Lakhina G. S., Singh S. V., Rubia R., & Sreeraj T., (2018) *Physics of Plasmas*, 25, 080501.

[4] Scarf F. L., Taylor W. L., & Green I. M., (1979) *Science*, 203, 748.

[5] Strangeway R. J. 1991, (1991), *Space Science Review*, 55, 275.

[6] Hadid L. Z., Edberg N. J. T, Chust T., (2021) *Astronomy and Astrophysics*, 656, A18.

136. UTILIZING PSINSAR FOR MONITORING SUBSIDENCE IN RAMGARH CRATER, INDIA: AN INNOVATIVE APPROACH

J. Aswathi¹, S. James¹ and K. S. Sajinkumar^{1,2}, ¹Department of Geology, University of Kerala, Thiruvananthapuram 695 581, Kerala, India, ²Department of Geological & Mining Engineering & Sciences, Michigan Technological University, Houghton, MI 49931, USA

Introduction: Ramgarh crater, situated in Baran district of Rajasthan, India, stands as a distinctive topographic feature, characterized by its nearly circular shape. This structure has been a longstanding intrigue among Indian geologists since the 19th century [1], [2], with the latest study proving it as an impact crater [3], [2]. Being in a flat sedimentary terrain of the Neoproterozoic Vindhyan Supergroup [1], this crater is an ideal candidate for quantifying erosion through the state-of-the-art microwave remote sensing technique called Persistent Scatterer Interferometric Synthetic Aperture Radar (PSInSAR) by detecting and monitoring ground displacements and subsidence in and around Ramgarh crater. Recent study suggests a 10 km diameter complex crater with denuded rims, postulating the current structure as a remnant of the central elevated area (CEA) [1].

Data and Method: Using 65 Sentinel-1A Single Look Complex (SLC) images spanning from April 2016 to October 2022 and leveraging advanced PSInSAR techniques, we conducted a comprehensive analysis covering a 12 km diameter region of the crater. ENVI SARscape analytics of ENVI software has been used for the analysis. Employing PSInSAR represents a robust remote sensing method utilizing satellite radar signals to precisely observe and measure Earth's surface displacement at a mm scale [4].

Results and Discussion: PSInSAR results yielded 36,581 Persistent Scatterer (PS) points, exhibiting velocities ranging from -26.51 to +27.18 mm/yr. Negative values signify subsidence/erosion, while positive values indicate uplift. Based on both crater morphology and with the field knowledge, as well as based on visual interpretation of PS points, we classified the entire area into five distinct zones (Zone A, B, C, D, and E). Zones A, B, and C were chosen within the suspected 10 km diameter of the crater, while Zone D represents the presumed Central Elevated Area (CEA), and Zone E is situated within the topographic high structure. The findings reveal no deformations in the 10 km diameter and the elevated area, but moderate subsidence is observed within the crater, characterized by colluvial material, which are liable to deformation.

But, there are areas showing positive and negative values but those coincide with badland topography, loose sediment deposits, flood plains, and to some extent, agricultural fields. Conversely, regions with thick vegetation, water bodies, and streams exhibit no subsidence zones. In contrast to the recent studies, this study does not find supporting evidence for the collapse of the CEA or notable erosion in the suspected 10 km rim area. Furthermore, fieldwork in this area aligns with a simple crater morphology. In conclusion, this research provides valuable perspectives on the morphological and deformation features of the Ramgarh crater, contributing to a deeper understanding of its geological history.

References: [1] Kenkmann, T., Wulf, G., & Agarwal, A. (2019). Indiás Third Impact Crater: Ramgarh, Rajasthan. *Large Meteorite Impacts and Planetary Evolution VI*, 2136, 5007. [2] Aneeshkumar, V., Chandran, S. R., James, S., Santosh, M., Padmakumar, D., Aswathi, J., ... & Sajinkumar, K. S. (2022). Meteorite impact at Ramgarh, India: Petrographic and geochemical evidence, and new geochronological insights. *Lithos*, 426, 106779. [3] Kenkmann, T., Wulf, G., & Agarwal, A. (2020). Ramgarh, Rajasthan, India: A 10 km diameter complex impact structure. *Meteoritics & Planetary Science*, 55(4), 936-961. [4] Ferretti, A., Prati, C., & Rocca, F. (2000). Non-linear subsidence rate estimation using permanent scatterers in differential SAR interferometry. *IEEE Trans-actions on geoscience and remote sensing*, 38(5), 2202-2212.

137. Magnetosphere Formation of a Tidally Locked Planet or Satellite.

Deepanshu Chouhan¹, Department of Physics, University of Hyderabad, Telangana, India

Introduction: The magnetosphere, a crucial defense mechanism against harmful solar winds, has long been thought to be absent in tidally locked planets due to the absence of convection currents in their cores. However, recent studies on exoplanets suggest that tidal heating can lead to core melting, potentially resulting in the formation of a magnetosphere. This paper explores the conditions necessary for the formation of a magnetosphere in a tidally locked planet or satellite. The study proposes that a highly eccentric orbit and close perihelion are essential for achieving the required high velocity, leading to a changing electric field.

The research examines four points on the orbital path, considering aphelion, perihelion, and two diametrically opposite points. Tidal forces cause the planet to expand and contract, generating heat within the core. The ionization of iron in the core, driven by the high temperature, produces a partially charged core. As the planet moves, charge separation occurs, generating a changing electric field. According to Ampere-Maxwell law [1][2], this varying electric field results in the formation of a magnetic field around the planet.

The intensity and direction of the magnetic field are influenced by the planet's rotational velocity and eccentricity. The study provides equations predicting the magnetic field strength, highlighting its proportionality to the square of the core radius. Contrary to common belief, tidally locked planets may possess a magnetic field, challenging previous assumptions about their habitability. The study opens avenues for understanding how planets generate magnetic fields, despite their proximity to host stars.

Digital Formats:

Figure 1. Here blue arrows denote the direction of motion of the planet.

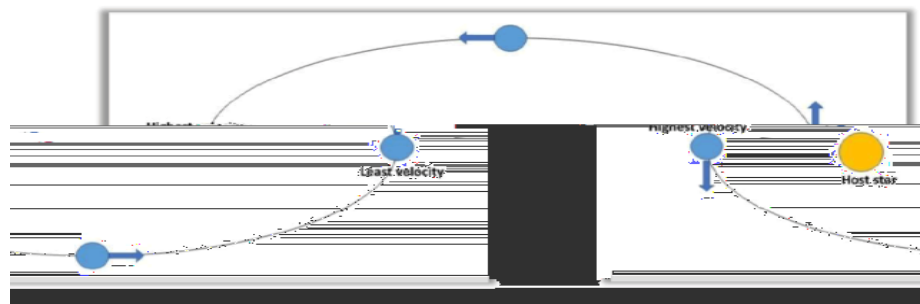
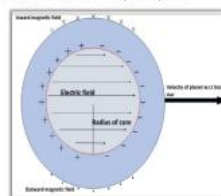


Figure 2. Due to motion core separation of charges takes place.



Figure 3. Direction of magnetic field, electric field and velocity of the planet.



References:

- [1] James Clerk Maxwell et al. 1865
- [2] Andre-Marie Ampere et al. 1820.
- [3] Ludwig Boltzmann et al. 1870.
- [4] Bruce HM. College of Chemistry, University of California Berkeley; 1962.

138. Autonomous Systems for Data Analysis on Space Probes

Gourav Mohanan, Dayananda Sagar University (DSU), gouravmohanan12@gmail.com

Kinit Sai Devatha, Vellore Institute of Technology (VIT), kinit said@gmail.com

Jatin Dhall, Vellore Institute of Technology (VIT), jatindhalla@gmail.com

Introduction:

As space exploration advances, the demand for enhanced scientific output from space missions becomes increasingly vital. This research explores a pioneering approach to meet this demand by integrating advanced artificial intelligence (AI) and machine learning (ML) algorithms into the operational framework of space probes. The goal is to empower these probes with autonomous data analysis and decision-making capabilities, thereby reducing reliance on Earth-based commands and opening new frontiers for scientific discovery.

In traditional space missions, the time delay in transmitting commands to and receiving data from probes poses a significant bottleneck in scientific exploration. The proposed paradigm shift towards autonomous systems aims to address this challenge by enabling space probes to analyze data onboard and make informed decisions in real time. By doing so, this research seeks to revolutionize the efficiency of scientific data analysis during space missions.

The primary objective is to maximize the scientific output of space missions by leveraging the computational power of onboard AI and ML systems. These autonomous systems are designed to swiftly identify and prioritize significant findings, allowing space probes to adapt their mission parameters dynamically. This adaptability is crucial in responding to unexpected discoveries and optimizing the allocation of resources, ultimately enhancing the overall scientific yield.

The research methodology involves the development and rigorous testing of AI and ML algorithms tailored specifically for spaceborne applications. These algorithms undergo training using simulated mission scenarios and historical data, ensuring their robust performance in recognizing scientifically relevant patterns and anomalies. Additionally, the study addresses the challenges associated with autonomous decision-making in the unforgiving space environment, including limited computational resources and the implementation of robust error-handling mechanisms.

Anticipated outcomes include not only a demonstration of the feasibility and effectiveness of autonomous systems for data analysis on space probes but also insights into the transformative potential of this technology for the future of space exploration. The findings are expected to showcase how the integration of intelligent systems can proactively contribute to mission objectives, enabling space probes to play a more active and responsive role in the quest for scientific knowledge beyond Earth.

This research contributes to the ongoing evolution of space exploration methodologies, emphasizing the critical role of onboard intelligence in shaping the future of autonomous interplanetary missions. As the frontier of space exploration expands, autonomous systems represent a promising avenue for unlocking the full scientific potential of space missions.

References:

- [1] Lucian Murdock, Ferdinando Figueroa, and Lauren Underwood, "Autonomy Voice Assistant for NPAS (NASA Platform for Autonomous Systems)," NASA Stennis Space Center, AIAA Paper, 2020.

- [2] Ellande Tang, Patrick Spieler, Matthew Anderson, and Soon-Jo Chung, "Design of the Next-Generation Autonomous Flying Ambulance," Caltech (2021), AIAA SciTech, January 2021.
- [3] Stewart Aslan, Kyle Krol, and Mason Peck, "Pathfinder for Autonomous Navigation: Low-Cost Architecture for Autonomous CubeSat Rendezvous and Docking" Cornell Engineering AIAA SciTech Forum Paper 2021, January 2021.
- [4] Doga Yucalan and Mason Peck "Autonomous Navigation of Relativistic Spacecraft in Interstellar Space." Cornell Engineering AIAA SciTech Forum Paper 2021, January 2021.

139. SPACE SURVEILLANCE NETWORK AS A MEANS OF MAXIMIZING SCIENTIFIC OUTPUT FROM SPACE MISSIONS

S V SHRIGANDHA, 2nd YEAR UG STUDENT, DR. AMBEDKAR INSTITUTE OF TECHNOLOGY, BENGALURU

svshrigandha@gmail.com

Introduction: Space Surveillance Network (SSN) is a system that detects, tracks, catalogs and identifies man-made objects in space. Today's issue of Space debris demands continuous observation and SSN tracks them to secure the Earth's orbits. This report explores how innovation in the field of SSN is highly potential of maximizing the scientific output from space missions. Space surveillance helps prevent collisions between satellites and space debris, therefore, minimizing the risk of damage and ensuring the longevity of the spacecraft. By optimizing the routes and timing of spacecraft, missions can be designed to maximize the scientific data collected. Surveillance data aids in planning communication with spacecraft and by knowing the precise location of a satellite, mission controllers can optimize communication windows, ensuring efficient data transfer and reception.

To observe and track the debris for operating missions in orbit safely, several ground-based observations (optical telescopes, radar sensors, etc.) have been implemented as a part of Space Surveillance Network. But these ground-based observations having a size threshold ranging from 10cm in LEO to 1m in GEO, are further limited by brightness/ magnitude. To overcome these limitations specifically by: obtaining information on debris smaller than 10cm, orbit determination of space debris objects and enhancing space-based observations play a vital role in securing future space activities and ensuring maximum scientific output from operating missions as well.

Space Surveillance Payload Camera: A low-cost payload camera similar to star trackers (STRs) using COTS (commercially off-the-shelf) devices is developed which performs under-cataloged space debris detection. The camera is capable of detecting, tracking and calculating the orbit position to automatically control the rendezvous for space debris by predicting the limiting magnitude of the system and correlating the observable debris sizes that the sensor can detect if it is on the ground or in space. Since the COTS devices have been proved to be capable of detecting objects of different sizes in several conditions of distance and phase-angle, the camera is approved in the vibration, thermal and thermal-vacuum tests and proved to be in-orbit tolerant.

Combined use of Radar, Laser and Optical Measurements for the Orbit Determination of Space Debris: Orbital determination makes it possible to define the state vector of an object in orbit at different instants of time. It is therefore possible to calculate the trajectory of an orbiting object in a given reference system by solving this problem. It is of a great importance specifically in the LEO which has the highest concentration of objects, GEO ring and at heights close to the constellations of navigation satellites. The combined use of these different observation techniques provides certain advantages in the orbit determination process by increasing the number of available observations, improving the observability of the orbit by merging observed angles and distances and determining the orbit of more objects in different orbital regimes due to the higher density of sensors. Once the orbit of an object has been defined, it is possible to predict future positions by means of different propagation techniques.

Expanding the SSN with Space-Based Sensors: The Space-Based Sensors provide many advantages over the Earth-Based optical telescopes and radar sensors by providing dynamic fields of view relative to the Earth's surface and views of Resident Space Objects (RSOs) unobstructed by atmospheric effects. They also circumvent the technological limitations or political pitfalls that ground-based sensors face in areas in deep oceans, harsh climates or unstable geopolitics. Two options for the sensors proposed for the present application includes an inexpensive sensor to explore the viability of microsatellites for Space Domain Awareness (SDA) and the expensive sensor to resolve distant GEO objects, but, in general, both options are electro-optical, consistent with the current SDA practices. Orbits are selected so the space-based sensors will be positioned to collect on targets in a way that prioritizes network performance. Also, certain types of sensors provide the additional possibility of making quasi-real time corrections to the orbit.

If a mission can only promote technology development, not science, it shall not be a part of the space science program. Therefore, in conclusion, outputs from space missions provide us the data helpful to create a better life on Earth and provide the perspective about the universe around us. Hence, it is crucial to adopt new technologies that maximize these scientific outputs and promote scientific culture.

References:

[1] J.Filho, P.M.R. Duarte and N.Peixinho, Rui Melicio and Ricardo Gaferia *Applied Sciences* 13 (6), 3682, 2023
[2] Sanchez Piedra, Manel and Sanjurjo Rivo, Catalan Morollon (2023) *2nd NEO and Debris Detection Conference*
[3]Cameron Harris, Dylan Thomas, Jonathan Kadan and Dr. Kevin Schroeder, Dr. Jonathan Black (2021) *Advanced Maui Optical and space surveillance Technologies Conference*
[4]Ji Wu and Alvaro Gimenez (2020) *Springer Nature*

140. Advancements in volatiles and In-Situ Resource Utilization: Efficient Extraction Methods for Sustainable Space Exploration.

Riya Dewangan¹ and Arka Roy Chowdhury², ¹B. Tech Aerospace engineering, Lovely Professional University(riyadewangan0211@gmail.com) for first author, ²B. Tech Computer Science Engineering, Lovely Professional University(roychowdhury.arka02@gmail.com).

Abstract: The discovery and settlement of extraterrestrial environments pose distinct difficulties that demand creative approaches to resource management. We explore the developing area of In-Situ Resource utilization (ISRU) in this abstract, with an emphasis on the creation and use of effective extraction techniques for space exploration that is sustainable. The extraction of volatiles—substances with low boiling points that are frequently present on celestial bodies as ice or gases—is a critical component of ISRU. Water has received a lot of attention because it is an essential resource for both life support and propulsion. Since electrolysis makes it possible to extract oxygen from the water ice found in lunar regolith, it appears to be a promising technique for lunar missions. This method not only helps humans survive, but it also creates the foundation for possible fuel production on the moon.

One common thread in ISRU initiatives is the use of regolith, the loose material layer covering planetary surfaces. Different approaches are being considered to extract valuable resources such as oxygen from regolith. These include using chemical methods to extract substances containing oxygen or heating regolith to liberate oxygen. By utilizing the local environment, these methods seek to lessen the dependency on materials from Earth, increasing the sustainability and economy of space operations.

For this reason, we have thought of a robotic initiative to pop out the in-situ resources present in the surrounding , which is named as roboX. RoboX, with its unique design and function will be solely responsible for extracting out the materials for various applications.

A new facet of ISRU is asteroid mining, which concentrates on obtaining volatile minerals like water ice. Drilling into asteroids, heating surfaces to release volatiles, or using solar concentrators to collect and store these precious materials are some of the methods that have been proposed. The success of asteroid mining could open up new routes for collecting crucial components for space missions without the need for resource-intensive launches from Earth.

In the quest for space self-sufficiency, in-situ propellant manufacturing systems are becoming more and more popular. The ideas are to take carbon dioxide out of the atmospheres of planets like Mars and mix it with hydrogen that is brought in from Earth or created locally by processes like water electrolysis. By reducing reliance on Earth for propellant, this strategy hopes to allow more extended and sustainable space missions

A new facet of ISRU is asteroid mining, which concentrates on obtaining volatile minerals like water ice. Drilling into asteroids, heating surfaces to release volatiles, or using solar concentrators to collect and store these precious materials are some of the methods that have been proposed. The success of asteroid mining could open up new routes for collecting crucial components for space missions without the need for resource-intensive launches from Earth.

In the quest for space self-sufficiency, in-situ propellant manufacturing systems are becoming more and more popular. The ideas are to take carbon dioxide out of the atmospheres of planets like Mars and mix it with hydrogen that is brought in from Earth or created locally by processes like water electrolysis. By

reducing reliance on Earth for propellant, this strategy hopes to allow more extended and sustainable space missions

References: [1]K.L. Ferrone, A.B. Taylor, and H. Helvajian, In situ resource utilization of structural material from planetary regolith, *Advances in Space Research*, Volume 69, Issue 5, 2022, Pages 2268-2282, ISSN 0273-1177.

141. Design and development of Neutral and Ion Mass Spectrometer (NIMS) for future planetary space missions

(P. Sharma^{1*}, A. Verma¹, S.K. Goyal¹, R.R. Mahajan¹, N. Upadhyay¹ and V. Sheel¹)

¹Physical Research Laboratory, Ahmedabad

* E-mail: piyush@prl.res.in

Over the past half-century of space exploration, Mass Spectrometry has played a crucial role in providing unique chemical and physical insights into the characteristics of celestial bodies within our Solar System. Various types of Mass Spectrometers, such as Quadrupole, Time-of-flight, and Ion trap, have significantly contributed and will continue to enhance our comprehension of the formation and evolution of exploration targets, including the surfaces and atmospheres of planets and their moons. The exploration of the Moon, Mars, and Venus is driven by the essential goal of evaluating the habitability of these celestial bodies and, ultimately, the quest for extraterrestrial life—a monumental undertaking that can be advanced through the application of mass spectrometry. Modern, flight-capable mass spectrometers, when coupled with sophisticated ionization techniques, facilitate the sensitive detection of exospheric ions and atmospheric gases, thereby strengthening our ability to identify traces of potential bio-signatures.

The Neutral and Ion Mass Spectrometer (NIMS), based on the Quadrupole Field technique, is under development at PRL. NIMS comprises four cylindrical rods with applied direct-current (DC) and radio-frequency (RF) electric fields used for ion separation. It includes the detector probe and its processing electronics, with the Ionizer, Quadrupole Mass Filter, and Detector sub-assemblies forming the Detector head. NIMS operates within a mass range of 2-200 amu and a peak width (m) of 0.5 amu. The detector head is enclosed within a shield tube that also serves as a common ground for the instrument. NIMS will function in two modes: a) The Neutral Mode and b) The Ion Mode. The ongoing development aspects of NIMS are briefly discussed below: The successful design of NIMS ensures the following:

The instrument will employ a Faraday cup and a CEM as detectors, with the CEM needing to be biased at -2.5 kV (ranging from 0 to -3 kV) to achieve the appropriate gain for detecting targeted species. The electronics' breadboard development has been carried out, including Electronics for Ionizer Control, RF scanning, HV circuit for CEM biasing, FPGA-based processing electronics, and LabVIEW-based data acquisition. The current status of the development and its results will be discussed along with the next course of action.

The Electron Impact ionization mechanism demands intricate circuitry, particularly tailored for managing the ionization process. This involves applying a focused voltage ranging from -90V to -120V to facilitate electron impact ionization. The system accommodates electron emission currents of up to 3.5 mA, ensuring efficient ion conversion within the ionizer. As ongoing advancements are pursued, the focus remains on refining these electronic components to achieve optimized sensitivity and reliable operation in diverse mass spectrometry applications.

142. Characterization of Silicon Photomultipliers and Scintillators based detector modules for hard X-ray measurements

Shiv Kumar Goyal*^{1,2}, Amisha P. Naik², Piyush Sharma¹, Abhishek J. Verma¹

¹Physical Research Laboratory, Ahmedabad

²Institute of Technology, Nirma University, Ahmedabad

*Email: goyal@prl.res.in

Silicon Photomultiplier (SiPM) is a semiconductor device, which has very high internal gain (~1e6) [1], Photo Detection Efficiency (PDE) very similar to the Photo Multiplier Tube (PMT) [2] and can be used to detect single photons. Here, we are exploring the usage of CeBr₃ and NaI (Tl) Scintillation detectors coupled with an array of Silicon Photomultipliers (SiPMs) [3] for potential applications in the field of planetary exploration [4] and high – energy astrophysics as position sensitive hard X-ray spectroscopic detectors [5] and charge particle detectors [3]. These detectors are being developed and characterized for the future space exploration programs. The interaction of the X-rays onto the scintillation detectors produces optical photons where number of the photons is proportional to the deposited energy [6] [7]. The distribution of these photons is detected by the SiPM array, which provides the spectral and spatial information of the position of the incident X-ray photon. Development of two types of detector modules i.e. CeBr₃ and NaI (Tl), coupled with an array of SiPM is being carried out. The development of the front end electronics (FEE) for the charge collection from SiPM is carried out for the X-ray spectrometer application. Characterization of each of the detector modules is carried out with SiPM's over-voltages and shaping amplifier's time constant. The detector modules are subjected to a wide temperature range to establish a relationship of the SiPM's gain, energy resolution, and yield of output photons of both CeBr₃ and NaI (Tl) with operating temperature. The test results show that energy resolution improves with higher overvoltage of SiPM and also with lower operating temperature. The SiPM's gain is a function of the temperature which can be made constant by keeping the overvoltage fixed under varying temperature conditions.

In this paper, the type of detector modules, comparison with existing semiconductor detectors, test results with electronics parameters, SiPM's operating parameters and variations of the performance with the operating temperature will be presented.

References

- [1] F. Acerbi and S. Gundacker, "Understanding and simulating SiPMs," *Nuclear Instruments and Methods in Physics Research Section A: Accelerators, Spectrometers, Detectors and Associated Equipment*, vol. 926, pp. 16-35, May 2019.
- [2] K. Hamamatsu Photonics, "PHOTOMULTIPLIER TUBES - Basics and Applications," 2017.
- [3] S. K. Goyal, A. P. Naik, N. S. Mithun and S. V. Vadawale, "Development of position sensitive detector module using scintillator and Si photomultiplier for hard x-ray imaging and spectroscopy," *Journal of Astronomical Telescopes, Instruments, and System*, vol. 5, no. 1, December 2018.
- [4] S. Goyal, P. Kumar, P. Janardhan, S. Vadawale, A. Sarkar, M. Shanmugam, K. Subramanian, B. Bapat, D. Chakrabarty, P. Adhyaru, A. Patel, S. Banerjee, M. S. Shah, N. K. Tiwari, H. Adalja and T. Ladiya, "Aditya Solarwind Particle Experiment (ASPEX) onboard the Aditya-L1 mission," *Planetary and Space Science*, vol. 163, pp. 42-55, November 2018.

- [5] T. Chattopadhyay, S. V. Vadawale, S. K. Goyal, M. N. P. S, A. R. Patel, R. Shukla, T. Ladiya, M. Shanmugam, V. R. Patel and G. P. Ubale, "Development of a hard x-ray focal plane compton polarimeter: a compact polarimetric configuration with scintillators and Si photomultipliers," *Experimental Astronomy*, vol. 41, p. 197–214, October 2015.
- [6] Z. Cho, Tomography, 3rd edition, 3rd ed., Encyclopedia of Physical Science and Technology, 2003.
- [7] U. Kramar, X-ray Fluorescence Spectrometers, Encyclopedia of Spectroscopy and Spectrometry, 1999.

143. Development and Characterization of a Multi-Detector Large Area X-Ray Spectrometer using Silicon Drift Detectors with ASIC Based Readout

Nishant Singh^{1*}, M. Shanmugam¹, Arpit Patel¹, Sushil Kumar¹, Deepak Kumar Painkra¹, Tinkal Ladiya¹, and S. Vadawale¹

¹Physical Research Laboratory, Ahmedabad

*nishant@prl.res.in

Abstract

The use of silicon-based X-ray spectroscopy has been increasingly widespread in various fields such as planetary elemental studies, solar studies, X-ray imaging, and astronomical observations. We have already developed a single-channel X-ray spectrometer with discrete components- Solar X-ray Monitor, flown on Chandrayaan-2 orbiter. In this work, we have developed a large area Silicon Drift Detector (SDD) based X-ray spectrometer using multiple SDDs and which are readout by a multi-channel Application Specific Integrated Circuit (ASIC). This will be compact instrument with very low power consumption. The developed system employs the VERDI ASIC, which is capable of readout from eight detectors simultaneously. The ASIC comprises of a preamplifier, a shaper with adjustable shaping times, and a peak stretcher with a baseline holder in each channel. The system enables to stack multiple SDD modules in a compact assembly with excellent energy resolution in the range of 0.5 keV to 15 keV with fast readout.

The performance of the large area X-ray spectrometer was characterized for various electrical parameters such as shaping time, channel gain, detector temperature and dynamic range of the ASIC. The spectrometer provides an energy resolution of ~145 eV at 5.9 keV with 5 detector channels for the optimum shaping time of ~2 μ s, at a detector temperature of approximately -30°C. The instrument is an excellent candidate for future planetary exploration missions and X-ray astronomy missions. The performance and results from the instrument will be presented at the conference.

144. In-Situ Measurement of Water-ice on Moon for Future Missions: Challenges, Techniques and Current Understanding

Sanjeev Kumar Mishra^{1*}, Chandan Kumar¹, Kalyan Reddy¹, Janmejay Kumar¹, K. Durga Prasad¹

Introduction: With the confirmation of presence of water on Moon by Chandrayaan-1 [1], the interest in studying, mapping, quantifying and modelling water and water-ice on Moon has gained immense interest in the scientific community. Recent observations from remote sensing instruments indicate considerable presence of water-ice in the polar regions [2], particularly in the Permanently Shadowed Regions called PSRs [3], [4]. While remote sensing observations provide an idea of presence of water-ice, validation of the same using in-situ experiments is not yet done. In-situ measurement of water-ice in the subsurface is immensely challenging and requires a novel approach to instrument development.

At PRL, we have been working on development of an instrument for measurement of water-ice on Moon. The instrument is based on the principle of Wenner Array type- α [5] and derives the science data using the principle of dielectric spectroscopy [6], with the phenomenon of dielectric relaxation being at its heart. We have conceptualized the instrument, have carried out numerous experiments to establish the proof of concept and have been carrying out modelling studies to see the effect of water-ice in the presence of other components such as the lunar regolith. Additionally, in the laboratory, we have carried out experiments with various Lunar analog samples mixed with different proportions of ices of different kinds such as water-ice and CO₂ ice to see the effect of the presence of other components on the dielectric signature of water-ice. We have established that a presence of water-ice as low as 2% (by volume) can be detected using the custom-made sensors. Our modelling results show that the quantification of water-ice can be done using linear mixing models and multi-component mixtures can be modelled to arrive at the volume fraction of the water-ice present in the investigation volume.

In this conference, I will be discussing the challenges of water-ice measurement, the instrument conceptualization, the techniques of measurement and their viabilities. I will also discuss some of the results from our experiments and modelling studies.

References: [1] R. Sridharan, S.M. Ahmed et al. (2010), Planetary and Space Science, vol. 58, pp. 947-950 [2] Paul O. hayne, Amanda Hendrix et al (2015), Icarus, vol. 255, pp. 58-69 [3] Colaprete, Schultz et al (2010), Science, vol. 330, pp. 463-468. [4] Kristen M. Luchsinger, Nancy J. Chanover, Paul D. Strycker (2021), Icarus, vol. 354, 114089 [5] Wenner, F. (1915), Bulletin of National Bureau of Standards, 12, 469-478. [6] Mark A. Nurge (2012), Planetary and Space Science, vol. 65, pp. 76-82

145. Digital Pulse Processing based readout electronics for Alpha Particle Spectrometer (APS)

Sushil Kumar¹, Arpit Patel¹, M. Shanmugam¹, Nishant Singh¹, Deepak K. Painkra¹, Tinkal Ladiya¹,

and D. Banerjee¹ ¹Physical Research Laboratory sushil@prl.res.in

ABSTRACT: Alpha particle spectrometer (APS) is one of the proposed instruments of future lunar mission of India. The primary objective of APS is to understand the radon transport on lunar surface by the detection of 5.490 MeV and 5.304 MeV alpha particles from ²²²Rn and ²¹⁰Po near the south pole region. It is proposed to use 4 Si PIN detectors of 100 μm thickness and active area of 9 cm², providing a total active area of 36cm². These detectors can provide precise measurement of alpha particles in the energy range of 1 MeV to 10 MeV. For the signal readout electronics from Si PIN detectors, analog and digital pulse processing techniques are considered. The design and development of analog pulse processing technique has been carried out with similar Si PIN detector and extensively evaluated the system performance demonstrating an energy resolution of 100 keV at 5.486 MeV.

To optimize the overall instrument in terms of mass, size, and power, the performance assessment using digital pulse processing signal readout technique has been initiated. At first, a MATLAB-based simulation has been carried out with a recursive algorithm that converts exponential pulses into symmetrical trapezoidal pulses. The algorithm employs delay parameters to achieve the desired digital shaping time, ensuring optimal pulse characteristics for improved signal/noise ratio. The same algorithm is being implemented on FPGA using Verilog programming language that enables digital pulse processing of the output pulse acquired from fast ADC (40MSPS) preceded by CSPA, and CR stage output. The results of these two approaches will be presented and discussed at the conference.

References:

- [1] Jordanov, Valentin T., et al. "Digital techniques for real-time pulse shaping in radiation measurements." *Nuclear Instruments and Methods in Physics Research Section A: Accelerators, Spectrometers, Detectors and Associated Equipment* 353.1-3 (1994): 261-264.
- [2] Jordanov, Valentin T., and Glenn F. Knoll. "Digital synthesis of pulse shapes in real time for high resolution radiation spectroscopy." *Nuclear Instruments and Methods in Physics Research Section A: Accelerators, Spectrometers, Detectors and Associated Equipment* 345.2 (1994): 337-345.
- [3] Vaghela, Mohindar, Rachna Jani, and Keyur Mahant. "FPGA Implementation of Digital pulse processing techniques for Radiation Measurement." *2016 International Conference on Microelectronics, Computing and Communications (MicroCom)*. IEEE, 2016.

146. Development of Cadmium Telluride (CdTe) based high-energy X-ray spectrometer for Venus Solar Soft X-ray Spectrometer (VS³) on-board Venus Orbiter

Deepak Kumar Painkra^{1,*}, Tinkal Ladiya¹, Nishnat Singh¹, Arpit Patel¹, M. Shanmugam¹, Santosh Vadawale¹, Varun Sheel¹

¹Physical Research Laboratory, Ahmedabad

deepakp@prl.res.in

ABSTRACT

Planetary atmospheres are exposed to a variety of ionizing radiation, including solar wind, solar extreme ultra violet (EUV) and X-ray photons, solar energetic particles (SEP) and cosmic ray particles. Among these, solar soft X-rays play a significant role in energizing the upper atmosphere of Venus producing an ionization peak around 130km. The Venus Solar Soft X-ray Spectrometer (VS³) is a shortlisted payload designed to measure the solar irradiance in the energy range of 1-100keV. The measurements will enhance our understanding of the interaction of solar irradiance with the Venusian atmosphere.

The proposed detector configuration comprises a suit of two different detectors to cover the wide energy range of 1-100keV. The low-energy photons in the energy range of 1-20keV will be measured using a Silicon Drift Detector (SDD) and a Cadmium Telluride (CdTe) detector will be used to measure the high energy photons from 20keV to 100keV. The performance of SDD detector has already been demonstrated in the XSM and APXS payloads in Chandrayaan-2 and Chandrayaan-3 missions. Currently, we are developing a readout methodology to optimally detect the photons with the CdTe detector. The front end readout electronics (FEE) of the detector includes a charge-sensitive preamplifier (CSPA) and a Gaussian shaper circuit to enhance the charge collection from the detector and to improve the signal-to-noise ratio (SNR). We have tested the detector & FEE using a ²⁴¹Am-59.54 keV radioactive source with varying bias voltage, shaping times and operating temperatures. The optimal energy resolution (ER) of 2.0keV FWHM at 59.54keV was achieved with a shaping time of 3μsec with a detector bias voltage of 500V for the detector operating temperature of ~ -30°C. Furthermore, various other performance assessment including linearity, flux measurements and temperature effects is in progress and the results will be presented in the symposium.

147. Developmental aspects of Impact Ionization Dust Detector

S. Jitarwal^{1*}, J. P. Pabari¹, S. Nambiar¹, Rashmi¹, K. Acharyya¹, A. Patel¹, H. Adalja¹, V. Sheel¹, A. Bhardwaj¹, R.K. Singh², S.M.K. Praneeth³, B. Shah³, V. K. Singh³, P. Suthar³, D. Kumar³, J. B. Rami³, S. Pandya³, V. Purohit³, S. Somani³, R. Khadekar³ & Team

¹Physical Research Laboratory, Navrangpura, Ahmedabad

²Institute of Plasma Research, Gandhinagar, Gujarat

³Space Application Centre, Ahmedabad

[Email: sonam@prl.res.in*](mailto:sonam@prl.res.in)

Abstract: The Interplanetary Dust Particles (IDPs), also known as micrometeoroids and cosmic dust particles, are found everywhere in our solar system [1]. During their evolution, they may undergo collision and evaporation or get ejected from the solar system depending on their size and properties. These IDPs are nanometer to micrometer-sized dust particles travelling at hypervelocity, i.e. greater than one km/s [2,3,4]. We have developed an Impact Ionization dust detector to study the interplanetary dust particles at and around Earth's orbits.

The signal generated by the dust particle's impact on the detector's target plate is measured, and using its rise time and peak voltage, the particle's physical properties, i.e., mass, velocity and flux, will be derived. In this work, the design, development and testing results of Dust Experiment (DEX) electronics using simulated input pulse from function generator will be presented. Further, detector is being characterized using nano second pulse laser impact at IPR, Bhat, Gandhinagar which will also be discussed.

References: [1] Grun E. et al. (1985), Icarus, 62, 244-272. [2] Pabari J. P. et al. (2021), COSPAR, C3.2-0030-21 [3] Pabari J. P. et al. (2018), PSS, 161, 68-75 [4] Pabari J. P. et al. (2022), PSS, 215, 105452.

148. NEW WAY OF OPTIMIZING SURFACE MISSIONS TO INCREASE SCIENTIFIC OUTPUT

S. S. Deshpande¹ (Student, Podar International School, Nerul, Navi Mumbai, sumedhsdeshpande@gmail.com)

Introduction: Since the first surface mission Luna-2, surface missions have improved significantly with time, with improvements in technology and capabilities. There have been many surface missions to Moon and Mars with developments to gather more data and to study those celestial bodies further. There has been a steady developments in technological trends from one mission to other. In recent missions included a lander, a single rover, which explores its surroundings, collects samples, etc. and a satellite or satellite network, which helps it navigate, communicate with Earth, etc. The challenge here is that the satellite can map the area to a certain extent of precision, as it is viewing from afar, and a single rover can study a single place or direction at once and there are many more limitations.

Concept: To address this limitation, we propose a concept to use a swarm of rovers, which will scatter around in different directions to gather more data at once and increase the efficiency (as per data collected per unit time) and cover a greater area. The rovers can also map the surface more precisely as compared to the satellite as they are closer to the ground and the swarm will compensate for the less area coverage.

In this work, illustrate possibilities of deploying swarm, additional efforts required, and challenges we might face.

Challenges and solutions: Additionally, there might be few difficulties in sending a swarm of such small rovers, such as adding systems of thermal control, and to store the samples to collect even more samples. This can be solved by following ways:

- A home module lander or a parent rover, which will store the swarm if the temperatures cannot be sustained by the rovers.
- if there is not enough sunlight for the solar panels use a RTG (Radioisotope Thermoelectric Generator) to charge the rovers while they are in the home module.
- The small size of the rovers mean that they can explore small caves as well.
- If there is a dense rock that weighs more than a rover's capacity, each rover in the swarm can be modular to collectively lift the sample. This can also be used if there is a gap that is comparatively large to the rover.

Present paper highlights methodologies to implement the rover swarms and provides a basic outline of the concept of operations of the proposed design.

149. BUOYANT ASCENSION: AN INGENIOUS PROBE DESIGN USING CONTROLLED VOLUME EXPANSION

Harshit Sharma¹, Anagha Ramesh², Divyanshi³ and Harman Singh Modi⁴

¹School of Computer Science and Engineering(SCOPE), Vellore Institute of Technology, Vellore, Tamil Nadu, India 632014 (harshitsharma182021@gmail.com), ²School of Electronics Engineering(SENSE), Vellore Institute of Technology, Vellore, Tamil Nadu, India 632014 (rameshanagha30@gmail.com), ³School of Mechanical Engineering(SMEC), Vellore Institute of Technology, Vellore, Tamil Nadu, India 632014 (divt2410@gmail.com), ⁴School of Computer Science Engineering and Information Systems(SCORE), Vellore Institute of Technology, Vellore, Tamil Nadu, India 632014 (harman.07.modi@gmail.com)

Penetrating dense realms like oceans and planetary atmospheres demands reconciling efficient data collection with rapid retrieval which is a struggle exacerbated by crippling drag forces that severely restrict exploration depth and range. This challenge demands ingeniously designed Controlled Volume Expansion (CVE) probes to bypass the necessity for high-thrust propulsion or constraints related to terminal velocity. These morphing explorers seamlessly transition between streamlined descent and buoyant ascent configurations, employing CVE through pressurization, microfluidic valves [1] and chemical reactions [2] significantly broadening the scope of exploration possibilities in these challenging environments. Furthermore, CVE probes employ sophisticated graph-based representations [3] to optimize their maneuverability and fluid interaction. These dynamic models are based on pressure waves,

expansion paths, and real-time data acquisition, allowing accurate drag force prediction, precise buoyancy control and dynamic path planning that leads to the fastest and safest retrieval trajectories. Beyond exploration, emergency escape systems utilizing CVE can broaden mission horizons. Additionally, the behavior of the probe in dense fluids will explain the dust particle dynamics in protoplanetary disks, volcanic plume eruptions, and biosignatures using the same mechanism of volume expansion, suggesting the presence of life forms.

References

- [1] Demello, A. J. (2006). Control and detection of chemical reactions in microfluidic systems. *Nature*, 442(7101), 394-402.
- [2] Fan, Y., Lim, Y., Wyss, L. S., Park, S., Xu, C., Fu, H., ... & Wang, B. (2021). Mechanical expansion microscopy. In *Methods in cell biology* (Vol. 161, pp. 125-146). Academic Press.
- [3] Li, Z., & Farimani, A. B. (2022). Graph neural network-accelerated Lagrangian fluid simulation. *Computers & Graphics*, 103, 201-211.

150. Optical Observation of Midnight Temperature Maximum using a Doppler Fabry-Perot Interferometer: First results from an equatorial Indian station.

Md. Mosarraf Hossain¹ and Tarun Kumar Pant¹, ¹Space Physics Laboratory, Vikram Sarabhai Space Centre, Trivandrum, Kerala, 695022, mosarraf_hossain@vssc.gov.in, mosarraf_sw@yahoo.co.in

We present first results on optical observations of thermospheric midnight temperature maximum (MTM) phenomenon using a Doppler Fabry-Perot Interferometer (DFPI) from Trivandrum (8.5°N, 77°E, 0.5° dip latitude), an Indian station close to the geomagnetic equator. The state-of-the-art solid etalon DFPI system provides thermospheric neutral wind and temperature based on measurements of Doppler parameters of OI630 nm nightglow emissions. Description of the DFPI system and method of extraction of geophysical parameters are available in [1]. MTM is significant enhancement in thermospheric neutral temperature observed in the equatorial and low-latitude thermosphere around midnight. However, recently, MTM has been reported even in the mid-latitude (up to ~ 42° N) region, and well before midnight as well as in the pre-dawn period [2]. In presence of MTM, observed neutral temperature variability may well be considered as the superposition of a background thermal variation and a temperature disturbance attributed to the MTM. We have used a harmonic model to eliminate thermal background from the temperature data to estimate MTM amplitudes (temperature residuals). We treat significant increase (>50K) in temperature with respect to the thermal background as MTM, where a simultaneous brightness increase in 630 nm airglow must be evident. Figure 1 (a) and 1(b) show respectively the DFPI temperature with thermal background and the derived MTM amplitude variability on 17.01.2018.

We find clear signature of MTM in all seasons with maximum of 8 MTM nights each in December 2017 and February 2018. Maximum MTM peak amplitude observed throughout all seasons is 213 K. We observe temperature variability alongside the meridional wind, zonal wind and airglow brightness, and the F layer height h'F and frequency foF2 on both the MTM and non-MTM nights. We notice near-

simultaneous occurrences of MTM and ‘Brightness wave’ with temporal shifts between 0 - 1.25 hr throughout the seasons. We observe that MTM causes a decrease in both the southward and eastward propagating wind speeds. In some nights, southward winds start reversing just after occurrence of MTM peak and complete the reversal into northward within 1-1.5 h, when temperature reaches its minimum. In other occasions, winds start reversing about 1 h before the MTM peak and completes the reversal within ~1h, when temperature also reaches the peak. Zonal winds are seen to decrease about 1 - 3 h before the MTM peak throughout the seasons. During the MTM nights, h'F is seen to decrease to about 200-220 km, whereas the foF2 increases to the maximum.

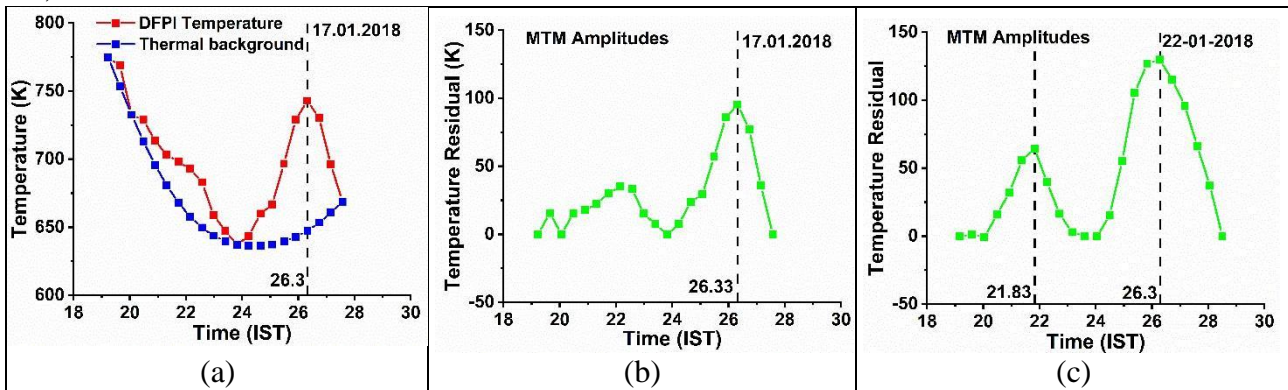


Figure 1: (a) DFPI temperature variability with thermal background on 17.01.2018, (b) MTM amplitude variability on 17.01.2018 and (c) MTM amplitude variability on 22.01.2018

A major finding on temperature variability specifically in autumnal equinox and winter solstice is doublepeaked MTM structure between 21:00-22:00 hrs. and 25:30-27:00 hrs. (figure 1(c)), which has been reported so far mainly from mid-latitudes, and confirmed by Whole Atmosphere Model as mid-latitude thermospheric feature. We find that double MTM peaks typically occurs when equatorward to poleward wind reversal happens in multiple sub-phases spanning longer duration (~ 3 - 4 h) unlike shorter duration single-phase reversal for normal MTM peak. However, zonal winds do not show any specific behavior during the double peak events. We also observe transition of the double-peaked structure into a well-defined temperature minimum of that night at or near midnight specifically during winter solstice (figure 1(c)). This temperature minimum may be termed as Midnight temperature minimum (MTMI) in analogy with MTM. The details will be provided during the presentation.

References:

- [1] Md. Mosarraf Hossain, Tarun Kumar Pant, C. Vineeth (2023) *Advances in Space Research* 72, 598–613. [2] Rafael L. A. Mesquita et al. (2018) *Annales Geophysicae* 36, 541–553.

151. Design and development of speckle imager for PRL 2.5m telescope

Nikitha Jithendran* ¹, Rishikesh Sharma ¹, Kevikumar Lad ¹, Neelam JSSV Prasad ¹, Nafees Ahmed ¹, Akanksha Khandelwal ¹, Kapil Bharadwaj ¹, Vivek Mishra ¹, Ashirbad Nayak ¹, Abhijit Chakraborty ¹ Physical Research Laboratory, Ahmedabad, Gujarat, India-380009 *nikitha@prl.res.in

Speckle Imaging / Lucky Imaging is one of the ways to image and resolve very close to the diffraction limit or the EE80 (80% of the encircled energy) of the telescope. Due to the presence of the earth's atmosphere and air turbulence, stars twinkle; as a result, their images are blurred, with an angular diameter of 1-3", which is known as the seeing parameter of a particular astronomical site. However, if one takes very short exposures with timescales of 2-10 ms, during which the atmosphere is partially frozen, and hence the atmospheric turbulence effect is reduced. So, in principle, this technique of acquiring cumulative short exposures and co-adding them can produce near diffraction limited images of stars, with FWHM of 0.1-0.3". The integration of speckle imaging with radial velocity (RV) measurements is a powerful approach to characterizing exoplanet candidates and understanding the dynamics of star systems. It helps in disentangling signals from different sources, such as planets and stellar companions, contributing to more accurate and comprehensive assessments of exoplanetary systems. We have designed and developed a speckle imager for the PRL 2.5m telescope at PRL Mount Abu Observatory, Gurushikhar, Rajasthan. This instrument has been used to find the diffraction limit of the PRL 2.5m telescope and resolve the close binary systems. The speckle imager has been installed on side port-1 of the telescope. It has a FOV of 1.5' X 2.0' and has the capability to give exposure times of 2-50 ms in the fixed V-band. The speckle imager can resolve stars as close as 0.3 - 0.4". In this presentation, I will give an overall overview of the design, development, and commissioning of the speckle imager and discuss the results.

152. DEVELOPMENT OF STABLE PRESSURE ENVIRONMENT FOR PARAS-2

Kevikumar Lad * ¹, Kapil Kumar Bharadwaj ¹, JSSV Neelam Prasad¹, Rishikesh Sharma ¹ and Abhijit Chakraborty ¹

¹ Physical Research Laboratory, Ahmedabad, Gujarat, India-380009

*kevikumar@prl.res.in

PRL Advanced Radial-velocity Abu-sky Search -2 (PARAS-2) is a fiber-fed high resolution spectrograph with resolution $R \sim 110,000$. It operates in a 380-690 nm wave-band. Development of such high precision and high resolution spectrograph requires a highly stable environment for its optical components. 1 mbar change in the pressure or 1 °C change in temperature of optics environment can introduce Radial Velocity (RV) variations of the order of 100 m s⁻¹ [1]. As we aimed to achieve sub m/s (≤ 50 cm s⁻¹) RV precision with PARAS-2 spectrograph, a dedicated vacuum chamber has been designed to ensure the stringent environmental stability criteria [2]. Further, Housing optics inside the chamber protects the optics from dust and humidity, and also prevents the spectrograph from stray light. We

designed the vacuum chamber and its necessary subsystems i.e. optical bench and mounts for optics, 6 degree of freedom platform for 6K X 6K detector, feedthrough for optical fiber etc. for the PARAS-2 spectrograph. Since the PARAS-2 optics are large size with long lead time and high cost, extreme care has been taken during the entire development process. The vacuum chamber has been fabricated and assembled by Ahmedabad based Aditya High Vacuum Private Limited. Opto-mechanical assembly and alignment of the spectrograph was done by PRL. Vacuum chamber was installed successfully at PRL Mount Abu Observatory located at Gurushikhar, Mount Abu, India during 2021-2022.

In this poster, we are presenting a detailed design of the vacuum chamber, testing, installation and final performance at PRL Mount Abu Observatory.

[1] Pepe, F., Mayor, M., et al. 2002. *The Messenger* , 110:9-14.

[2] Chakraborty, A., et al. 2018. *Ground-based and Airborne Instrumentation for Astronomy VII*, volume 10702 of SPIE, page 107026G

153. Searching for Organic beyond the Visible: Unveiling Biosignature Potential in Super-Earths through Combined Near-Infrared Spectroscopy and Polarimetry

Harshank Matkar, Government College of Engineering
Aurangabad

Introduction: The exploration of exoplanets has entered a new era with the advent of advanced space telescopes and observational techniques. Understanding the atmospheric composition, dust dynamics and potential habitability of exoplanets has become a primary focus of contemporary astronomical research. This research seeks to contribute to this burgeoning field through a combined approach of high-resolution spectroscopy and polarimetry, The super-Earth Ross 508b^[1] (*Mass* $0.1774 \pm 0.0045 M_{\odot}$, *Radius* $0.2113 \pm 0.0063 R_{\odot}$, *Surface Gravity* ($\log g$) 5.039 ± 0.027 cgs, *Temperature* $3071 + 34$ K *Luminosity* (bolometric) $0.003589 + 0.000067 L_{\odot}$) nestled within the habitable zone of its M-dwarf star, ignites excitement in the quest for life beyond Earth. This study proposes a novel approach utilizing combined high-resolution spectroscopy and polarimetry from JWST (NIRISS and COS), and Spitzer (IRAC)^[2], in deciphering dust mysteries of magnetic fields around exoplanets of its atmosphere and assess its biosignature potential. Our primary aim is to hunt for the elusive oxygen signature, a vital biosignature, while simultaneously elucidating its atmospheric dynamics and dust distribution, crucial for understanding habitability. The detection of oxygen in exoplanetary atmospheres holds paramount importance as it is a key biosignature and a critical component for the sustenance of life as we know it. Previous studies have underscored the challenges associated with accurately discerning oxygen signals amidst the complex spectra of exoplanetary atmospheres^[3]. Therefore, a multi-instrument approach, integrating the capabilities of the Near-

Infrared Imager and Slit less Spectrograph (NIRISS), Cosmic Origins Spectrograph (COS), and Infrared Array Camera (IRAC), is employed to enhance the precision and reliability of our findings. Super-Earths occupy a tantalizing niche in the planetary spectrum, potentially blurring the lines between Earth-like worlds and gas giants. Ross 508 b, with its estimated mass 4-5 times Earth's and comfortable orbital position, emerges as a prime candidate for harboring biosignatures. Potential biosignatures for extraterrestrial life include atmospheric spectral features (like O₂, O₃, CH₄, N₂O, CH₃Cl) and the reflectance spectra of biological surfaces (like pigments and vegetation's red edge)^[4]. The temporal variation of these signatures is also considered. However, traditional exoplanet characterization methods often fall short, particularly when probing for faint molecules like oxygen and Sodium whispers through the orange hues, revealing scorching clouds high above. Water vapor hums in the infrared's lower registers, hinting at the potential for liquid oceans below. Methane's signature methane lingers in the mid-infrared 1.3 μm to 3μm, possibly signaling biological activity. And the coveted oxygen, a potential biosignature, subtly alters the blue wavelengths, sending chills down the spines of astrobiologists. Water vapor hums in the, hinting at the potential for hidden oceans below. Methane's signature vibrates in the, a tantalizing clue for biological activity. In high-resolution spectra, spectral methods can be used to separate the planetary component from the combined star and planet spectra. The Doppler-shifted planetary atmospheric lines, which appear different from the telluric and stellar lines, can be used to identify the planetary component, along with the planetary line-of-sight velocity. Even though the stellar flux is much brighter and obscures the planetary signal^[5], cross-correlating the observed spectra with the modeled ones using multiple lines can improve the signal-to-noise ratio. This technique has been successfully used to extract planetary components from high- resolution spectra. The coveted oxygen, a potential biosignature, subtly alters the near-infrared's upper octave Doppler spectroscopy incorporating high-resolution COS spectra for shifts in spectral lines revealing wind speeds and directions, providing insights into atmospheric circulation patterns helps us chart the winds whipping across their surfaces, their velocities betraying the forces sculpting their atmospheric landscapes. We track escaping gases' whispers by analyzing hydrogen and helium signatures. This has greatly advanced astronomical instrumentation, particularly in the development of innovative spectrographs^[6] to understand the rate of atmospheric erosion and its impact on a planet's potential habitability. We will explore methods for characterizing the astronomical properties (mass, radius, orbit) and chemical/climatological properties (atmosphere, surface, etc.) of Ross 508, which may involve a comprehensive strategy for probing its atmospheric composition.

References:

- [1] Berta-Thompson.et al. (2014). *Astrophysical Journal Letters*. 790(1), 14. [2] Szentgyorgyi.et al.2022. *Publications of the Astronomical Society of the Pacific*, 134(1037), 092001. [3] Kreidberg.et al.2018. *The Astronomical Journal*, 156(1), 17. [4] Fujii.et al. (2018). *Astrobiology*, 18(7-8), 739-778. [5] Snellen.et al.2010.. *Nature*, 465(7299), 1049-1051. [6] Szentgyorgyi.et al.2015.*The Astronomical Journal*, 149(3), 111.

154. Further Probing the Plausible Causes of TTV in the TrES-2 system with TESS data

Shraddha Biswas¹, Parijat Thakur¹, Ing-Guey Jiang², Devash Path Sariya², John Southworth³. ¹Guru Ghasidas Vishwavidyalaya (A Central University), Bilaspur(C.G.)-495009,India;hiyabiswas12@gmail.com, ²Department of Physics and Institute of Astronomy, National Tsing-Hua University, Hsinchu, Taiwan ³Astrophysics Group, Keele University, Staffordshire, ST5 5BG, UK

Abstract

The multi-epoch, high-precision transit photometry provides an opportunity to examine the transit timing variations (TTVs) of known planets and TTVs are proving to be a very valuable tool in the field of exoplanetary detection. TrES-2b, discovered in 2006, is a gas giant exoplanet that orbits a G-type star, with an orbital period of 2.47 days and it is detected in tight orbit ($a = 0.03563$ AU) to its host star. For our work, we have analyzed total 214 transit light curves of TrES-2b, which include 47 recently observed transits by the Transiting Exoplanet Survey Satellite (TESS) in multiple sectors, 59 light curves with data quality < 3 from the Exoplanet Transit Database (ETD) and 108 from the literature to investigate the possibility of transit timing variation (TTV). We found that the sequence of transits occurred 31.48s later than had been predicted, based on transit-timing measurements spanning 15 yr. To explore the possible origins of TTV, the orbital decay and apsidal precession ephemeris models are fitted to the transit time data and to identify the theoretically correct model, we calculated the Bayesian information criterion (BIC). The Δ BIC metric favors the orbital decay model over a constant period, but it does not favor the apsidal precession model over a constant period and the decay timescale for the orbit is $P/\dot{P} = 24$ Myr. Our timing analysis shows that the orbital period of the hot Jupiter TrES2b appears to be decreasing at a rate of -8.64 ± 2.1 ms yr⁻¹. To investigate further, we probed whether the observed period change originated from Rømer effect or Applegate mechanism, but it does not seem to be originated either due to Rømer effect or Applegate mechanism. In order to confirm these findings, further high-precision transit, occultation and radial velocity observations of the system for a few more years will be required.

References:-

- [1] O'Donovan, F. T., Charbonneau, D., Mandushev, G., et al. 2006, ApJL, 651, L61
- [2] Rabus, M., Deeg, H. J., Alonso, R., Belmonte, J. A., & Almenara, J. M. 2009, A&A, 508, 1011
- [3] Mislis, D., & Schmitt, J. H. M. M. 2009, A&A, 500, L45
- [4] Kipping, D., & Bakos, G. 2011, ApJ, 733, 36
- [5] Schröter, S., Schmitt, J. H. M. M., & Müller, H. M. 2012, A&A, 539, A97
- [6] Raetz, S., Maciejewski, G., Ginski, C., et al. 2014, MNRAS, 444, 1351
- [7] Gazak, J. Z., Johnson, J. A., Tonry, J., et al. 2012, AdAst, 2012, 697967
- [8] Jiang, I.-G., Yeh, L.-C., Thakur, P., et al. 2013, AJ, 145, 68
- [9] Claret, A. 2017, A&A, 600, A30
- [10] Fulton, B. J., Petigura, E. A., Blunt, S., & Sinukoff, E. 2018, PASP, 130, 044504
- [11] Watson, C. A., & Marsh, T. R. 2010, MNRAS, 405, 2037

155. Pushing Efficiency of Planet Formation: Detection and Characterization of a Saturn around an M dwarf star.

1

1

2

Varghese Reji , Joe Philip Ninan , Shubham Kanodia

1. Department of Astronomy and Astrophysics, Tata Institute of Fundamental Research, Mumbai, India-400005
2. Department of Astronomy & Astrophysics, 525 Davey Laboratory, The Pennsylvania State University, University Park, PA, 16802, USA

According to our current understanding of planet formation, since the protoplanetary disc mass around proto-M-dwarf stars is small, it is difficult to form giant planets around M-dwarf stars. The discovery and detection of these extreme planets provide the tightest constraints to the efficiency of planet formation models. Under the umbrella of GEMS (Giant Exoplanets around M dwarf stars) collaboration, we identify potential giant planet candidates from the TESS (Transiting Exoplanet Survey Satellite) dataset and conduct ground-based photometry follow-ups with RBO, APO, etc. and extreme precision radial velocity measurements using the Habitable Zone Planet Finder (HPF), NEID and Planet Finding Spectrograph(PFS)s. This program has already significantly increased the number of GEMS available in the literature, providing insights into the mass budget of protoplanetary discs to form giant planets around M dwarf stars and formation pathways of GEMS in protostellar phase[1]. In this poster, we will specifically focus on one of our latest GEMS discoveries of a Saturn around an M-dwarf star. I will present our simultaneous Bayesian modelling of large photometry data (both TESS and ground-based follow-ups) along with HPF radial velocity measurements.

[1] Kanodia, S., Libby-Roberts, J., Cañas, C. I., Ninan, J. P., Mahadevan, S., Stefansson, G.,

Lin, A. S. J., Jones, S., Monson, A., Parker, B. A., Kobilnicky, H. A., Swaby, T. N.,

Powers, L., Beard, C., Bender, C. F., Blake, C. H., Cochran, W. D., Dong, J., Diddams,

S. A., ... Wright, J. T. (2022). TOI-3757 b: A Low-density Gas Giant Orbiting a

Solar-metallicity M Dwarf. *The Astronomical Journal*, 164(3), 81.

<https://doi.org/10.3847/1538-3881/ac7c20>

156. Comparative analysis of atmospheric characteristics of M-Dwarf Systems.

Mayuri Patwardhan^{1a}, Madhu Salavurao^{1b}, Pavithra Sekhar^{1c} (¹Amity Centre of Excellence in Astrobiology, Amity Institute of Biotechnology, Amity University Mumbai, MH 410206; (^{1a}mayuri.patwardhan@s.amity.edu), (^{1b}madhu.salavurao@s.amity.edu), (^{1c}psekhar@mum.amity.edu)

Our solar system, home to our Earth, is a benchmark for habitability. Our Sun is a main sequence G-type star which hosts our Earth, and its characteristics provides an important point of reference to understand habitability in other systems. In contrast, M-dwarfs stars are smaller, cooler, and have a lower mass than G-type stars and their habitable zone is much closer to the parent star. M-dwarfs have long lifetimes and have higher incidences of detecting potential habitable planets around these stars. Both ground and space observations have shown the presence of planetary systems with habitable planets around these stars [1]. M-dwarf systems like TRAPPIST 1, Wolf 1061, and Proxima Centauri have been explored so far and they present opportunities for future habitability studies [2]. Some of the previous works on the above-mentioned M-dwarf systems focused on observation of planetary systems and their terrestrial planets along with atmospheric composition, as well as mass radius relationship with respective stellar rotation and mass.

A notable area of investigation involves analysing the habitability potential of planets orbiting M-dwarf stars, such as those found in systems like TRAPPIST1, Proxima Centauri, and Wolf 1061. Identifying atmospheric patterns, such as the composition of gases and its characteristics [3], will shed light on the specifics of this comparative exploration. Prior research done has laid the essential groundwork for deeper exploration and understanding of these unique cosmic environments, providing a robust foundation for the current study's comparative analysis.

In this work, based on data available in archives from NASA and ESA; a comparative analysis of these three M-dwarf systems is being carried out. The work encompasses details on stellar characteristics, habitable zone parameters, and atmospheric conditions. This comprehensive approach aims to unravel the nuances that shape habitability beyond our celestial neighbourhood. Our study anticipates unveiling distinctions and shared elements between the three different M-dwarf systems. The study compares the stellar properties (For ex: radii, mass) between three stars systems and the correlation of spectroscopic analysis of the star systems and their respective planets. Beyond the intrinsic value of understanding diverse atmospheres, these findings will carry implications for refining the habitable zone model.

References:[1] Aomawa L. Shields, Sarah Ballard, John Asher Johnson,2016, *Physics Reports*, Vol. 663, p. 1â38 [2] Andrew Peter Lincowski; 2020; *The Nature and Characterization of M Dwarf Terrestrial Planetary Atmospheres: A Theoretical Case Study of the TRAPPIST-1 Planetary System*. [3] Thaddeus D. Komacek and Dorian S. Abbot. 2019. *The Astrophysical Journal*, Volume 871, Number 2.

157. SEARCHING FOR VARIABLE STARS AND MICROLENSING EVENTS IN THE GLOBULAR CLUSTERS PALOMAR 1 AND PALOMAR 2

A. D. Parikh and B.P Sridevi, Christ University (Hosur Main Road, Bhavani Nagar, S.G. Palya, Bengaluru, Karnataka 560029), Christ University (Hosur Main Road, Bhavani Nagar, S.G. Palya, Bengaluru, Karnataka 560029)

Introduction: The objects of our research are globular clusters (GCs) Palomar 1 (Pal 1) and Palomar 2 (Pal 2) discovered in the 1950s by the Palomar Observatory Sky Survey[1]. Located at a distance of 11.176 Kpc[2] Pal 1 has extended tidal tails stretching about one degree from either side of the cluster[3]. Due to the low surface brightness, sparse red giant branch, young age and its chemistry, Pal 1 has been considered unusual. Since it is an ultra-faint cluster[4], it is not that extensively studied and we do not have a knowledge of any variables in this cluster.

Similarly, Pal 2 is an outer halo GC with intermediate metallicity, at a distance of around 30 Kpc and in a direction towards the galactic anticenter. Therefore, it is heavily obscured by gas and dust and also appears faint while showing evidence of differential reddening[5]. Although some study has been conducted previously, only 18 variable stars are known in Pal 2[6].

Our objective is to study the Pal 1 and Pal 2 globular clusters using the five years (2010 to 2015) of observations taken using the Himalayan Chandra Telescope. In order to find variables in the images, we employ a differential image analysis technique using the DIAPL package and then form the light curves of the candidate sources. An extension to our study will be to detect microlensing events which is a time-varying phenomenon that can also be caused by exoplanets. Detecting a microlensing event towards any globular cluster would be a unique event and would open a new window to study the dark halo and other objects in the line of sight using globular clusters as background.

References: [1] Abell, G. O. (1955) *Publications of the Astronomical Society of the Pacific* 67(397):258–261. [2] Baumgardt, H. and Vasiliev, E. (2021) *Monthly Notices of the Royal Astronomical Society* 505(4):5957–5977. [3] Niederste-Ostholt, M. et al. 2010. *Monthly Notices of the Royal Astronomical Society: Letters* 408(1):L66–L70. [4] Sakari, C. M. et al. 2011. *The Astrophysical Journal* 740(2):106. [5] Bonatto, C. and Chies-Santos, A. L. (2020) *Monthly Notices of the Royal Astronomical Society* 493(2):2688–2693. [6] Ferro, A. A. et al. 2023. *Revista Mexicana de Astronomía y Astrofísica* 59(1):3–10.

158. Photometric and Spectroscopic observations of the transiting exoplanets from Devasthal Observatory

Y. C. Joshi (yogesh@aries.joshi.res.in)

Aryabhata Research Institute of Observational Sciences (ARIES), Manora Peak, Nainital-263001, India

Abstract: Over 5000 transiting exoplanets have been discovered so far, ranging in size from Earth to larger than Jupiter. We can probe the atmospheres of these planets through photometric and spectroscopic observations in the optical to infrared bands, particularly during transit. Since transit depth is a wavelength-dependent phenomenon, and spectroscopic features reveal the atmospheric constituents and structure, multi-wavelength observations of transiting planets can together investigate the physical properties of the planetary system. In this talk, I will provide the details of the photometric and spectroscopic facilities available at ARIES to conduct such a study. I will particularly emphasize how our observational facilities can complement other groups to enhance the scientific outcome of such planetary study.

159. Estimating the fundamental limit to RV precision taking into account the stellar activity

Joe. P. Ninan¹ ¹Tata Institute of Fundamental Research, Mumbai, India;
joe.ninan@tifr.res.in

Poster Abstract: Can we ever detect Earth like planets around sun like stars using extreme precision radial velocity (EPRV) in light of stellar activity induced jitter? This is a fundamental question that the EPRV community has been asking. The Carmer-Rao bound on the precision by which one can estimate a parameter from an observation is independent of the method used for estimation. It is completely determined by the sensitivity of the observed quantity to the parameters. If one has a forward model of stellar activity, that is sufficient to calculate the Fisher Information in the data to obtain the fundamental limit of precision by which we can measure the radial velocity shift hidden in the data. Here, we present a simple framework and tool to calculate this limit for any given spectroscopic observation and a forward model of stellar variability.

160. Probing the Biosignatures on Rocky Exoplanets: Methods, Current hurdles and Future Horizons

A. R. Rajkumar¹ , ¹Affiliation (Instituto de Investigación en Astronomía y Ciencias Planetarias, Universidad de Atacama, Chile; anitha.raj.21@alumnos.uda.cl)

Exoplanetary research has witnessed a transformation era since the ground breaking discovery of Pegasi 51 b in 1995, marking the inception of a monumental shift in our understanding of extraterrestrial planets. With the advanced telescopes and the observational methods, NASA Exoplanet archive has documented over 5500 confirmed exoplanets of different categories [1]. Yet, among this extensive collection, only a small fraction of 500 exoplanets are classified as terrestrial, creating an intriguing prospect of supporting life potentially [2]. Their relatively diminutive size gives complexities to characterize terrestrial exoplanets . Despite the fact that only 5% of these exoplanets are well-characterized, the search for Biosignature spectral features in the potential rocky

planets [3] are currently being implemented with the application of powerful telescopes like JWST, ALMA, and the upcoming Extremely Large Telescope (ELT).

This review work addresses:

- (i) Methods involved in characterizing the atmosphere of rocky exoplanets for the quest of Microbial Biosignatures
- (ii) The most promising biosignature gasses that can be remotely detected in the atmosphere of exoplanets and how can their unique spectral features be identified?
- (iii) A brief comparison of potential Earth microorganism in the surface of rocky exoplanets.
- (iii) How can the potential biosignatures can be distinguished from the abiotic process?
- (iv) Limitations and challenges associated with the remote detection of biosignatures in exoplanetary atmospheres and how can these challenges be addressed to enhance the reliability of biosignature detection?

References:

[1] Seager S. (2014) *PNAS* 111(35):12634-12640. [2] Seager S. (2013) Exoplanet habitability *Science* 340, 577-581. [3] Stam D M. (2008) *A&A* 482, 989-1007.

161. EXOPLANET DETECTION USING NEURAL NETWORK FOR TIME SERIES DATA

A. Choudhary¹, S. Bandari², and B.S. Khushvah³

^{1,3} Department of Mathematics and Computing, IIT(ISM), Dhanbad

² Department of Electronics Engineering, IIT(ISM), Dhanbad

(¹ 22dr0020@iitism.ac.in)

Abstract: The planets outside of our solar system are known as exoplanets. Finding exoplanets is a major area of research in the hopes of discovering a habitable, earth-like planet. There are various analytical methods related to the detection process, Like the radial velocity method, the transit method, etc. Initially, people use these methods to classify exoplanets, but it is a time-consuming process. As things are done manually, there is an issue related to accuracy. The merging of machine learning (ML) and neural network techniques has significantly advanced the area of exoplanet discovery in recent years. Researchers and space agencies are working with TESS, K2, and Kepler data and applying that to convolution neural network models. The accuracy of the suggested model is being enhanced through multiple adjustments and tuning of hyperparameters. In this area, several AI models have already been generated. So, we have used the powerful Transformer model to handle time series data due to its ability to capture long-term dependencies, combining that with the recurrence plot technique. The model was applied to massive data, resulting in an impressive accuracy rate of 99.87% and a precision rate of 68.7%. This impressive accuracy indicates the model's reliability in classifying cases and distinguishing between exoplanets and non-exoplanet objects. It also has a precision rate of 68.7%, indicating its ability to accurately predict exoplanet presence.

Keywords: Exoplanets. Transit method. Vision Transformer. Convolution Neural Network. Light curve.

References:

- [1] Salinas H.et al. (2023). Monthly Notices of the Royal Astronomical Society, 522(3): 3201-3216.
- [2] Mandel K. and Agol E. (2002). The Astrophysical Journal, 580(2): p.L171.
- [3] Agol E., Luger R., and Foreman-Mackey D. (2020). The Astronomical Journal, 159(3): 123.
- [4] Shallue C. J., and Vanderburg A. (2018). The Astronomical Journal, 155(2): 94.

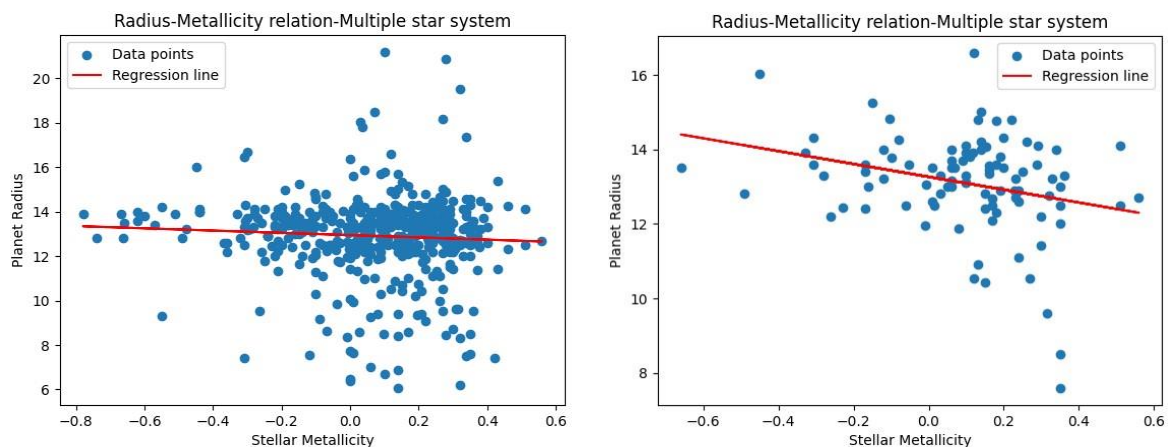
162. Do low metallicity stars contain giant planets? Large exoplanet relation with stellar Metallicity around G class star.

S. R. Pronoy¹ and J. Ahmed², ¹ Shahjalal University of Science & Technology (sumitroypronoy@gmail.com),

² Shahjalal University of Science & Technology

Introduction: As more accurate Telescopes and missions are developed, the number of exoplanet detections keep increasing. The characterization of these planets and their statistical investigations are important steps to understand the formation of the planet and planetary system. Additionally metallicity plays a critical role in planet formation mechanisms. An updated version of the parameters for stars and planets from the NASA Exoplanet Archive is used to investigate the relationship between the planet radius and stellar metallicity of massive exoplanets orbiting around G-class stars. Here, we concentrate on planets with radii greater than $6 R_{\oplus}$ (earth radius), that appear to suggest a probable inverse relationship between radius and Stellar metallicity. With declining metallicity and rising planet size, this correlation steepens. Moreover in the case of multiple star system the slope steepens more. Though it has relatively small data points, It contains both low R-squared value (0.07) and low P-value(0.006). Till now the calculation of uncertainty values and the effect of other parameters are being analyzed. The observed inverse exponential relation may not be fully explained by observational biases alone. More accurate data will be needed for further confirmation.

Digital Formats:



163. A Quench Level Approximation Approach for Rapid Retrieval of Chemical Abundances in Spectral Observations

Vikas Soni¹ (soniv100@gmail.com) and

Kinsuk Acharyya¹ Physical Research

Laboratory, Ahmedabad.

Exoplanet atmospheres' observed spectra are intricately linked to the atmospheric composition and thermal structure and influenced by chemical and physical processes. Retrieval models employ these spectra to constrain parameters by navigating an N-dimensional parametric space through numerous forward models. A forward model with detailed physics takes considerable computation time, making it unrealistic to use in retrieval models [1]. However, in the forward model, some approximations, such as the chemical relaxation method and quenching approximation, decrease the computational time by orders of magnitude [2,3]. This approximation requires considerable knowledge of the chemical timescales of several chemical species in a large parameter space [3,4].

We have created a Python-based model function that employs the quenching level approximation to determine atmospheric abundance in the presence of vertical mixing. This model function calculates the chemical abundances of the atmosphere using previously computed quenched curve data of CH₄, CO, CO₂, H₂O, NH₃, N₂, and HCN species [3,4]. The quenched curve identifies the initial quench pressure on a given thermal profile for each specific species. Subsequently, these initial quench levels undergo further refinement using the Smith method [2] to determine the quenched abundance of the respective species. CH₄, CO, CO₂, H₂O, NH₃, and N₂ abundances are taken as the thermochemical equilibrium abundance below their quench level, while HCN abundance is calculated from the NH₃ and CO quenched values. The frozen mixing ratio is taken above the quench level of the species.

The computation time of the model function is orders of magnitude faster than the 1D chemical-transport model and computes the model abundance in the order of milliseconds. We tested the model in petitRADTRANS retrieval [5]. The synthetic JWST spectrum is generated from PandExo [6] for an output of the photochemical transport. Our retrieved values for atmospheric metallicity, eddy diffusion coefficient, surface gravity, equilibrium temperature, and internal temperature are within 10% of the actual values.

[1] Madhusudhan, N. 2019, *Annual Review of Astronomy and Astrophysics*, 57, 617

[2] Smith, M. D. 1998, *Icarus*, 132, 176

[3] Soni, V., & Acharyya, K. 2023a, *The Astrophysical Journal*, 946, 29

[4] Soni, V., & Acharyya, K. 2023b, *The Astrophysical Journal*, 958, 143

[5] Mollière, P., Wardenier, J. P., van Boekel, R., et al. 2019, *Astronomy & Astrophysics*, 627, A67

[6] Batalha, N. E., Mandell, A., Pontoppidan, K., et al. 2017, *Publications of the Astronomical Society of the Pacific*, 129, 06450

164. EXOPLANET TRANSMISSION SPECTROSCOPY WITH 2m HIMALAYAN CHANDRA TELESCOPE

Bestha Manjunath¹, T Sivarani¹, Athira Unni², Arun Surya¹, Akhil

Jaini³, Parvathy M^{1,2,3}

Indian Institute of Astrophysics, University of California, Swinburne University of Technology.

Abstract: Transmission spectroscopy has been successfully used to study exoplanet atmospheres. Most of these observations are made using space-based instruments such as HST, Spitzer, and JWST. Low-resolution transmission spectroscopy, even with large 8m ground-based telescopes, often does not yield conclusive results due to systematic errors. Recently, Athira et al. demonstrated that a 2m HCT could be used for transmission spectroscopy of hot Jupiters using low-resolution spectroscopy. In this study, we attempt to use the slitless mode of HCT-HFOOSC to understand various systematic errors that would limit us from reaching the photon noise limit. We also present high-resolution transmission spectroscopy with the Hanle Echelle spectrograph, which allows individual spectral lines to be studied. Sodium D-lines are detected in many hot Jupiters and cover a very large scale height of the planet's atmosphere, helping to constrain the atmospheric structure.

165. Unraveling the atmospheres of faraway worlds with adaptable planetary atmosphere model.

Avinash Verma¹, Jayesh Goyal¹

¹National Institute of Science Education and Research, Bhubaneswar - 752050, India

Are we alone? This is the age-old question that human civilization has been asking since time immemorial. In today's era, this question has evolved and now we ask if there are other planets with life-supporting conditions, and one of the most crucial part of this is the planet's atmosphere. To date, more than 5500 exoplanets have been discovered and this number is increasing each day. Detection of an exoplanet is just the beginning of profiling and characterization of its atmosphere. Planets having an atmosphere impart this information as a unique fingerprint on the starlight, that pass through it during transit. Different techniques are applied to extract this information from the observed spectra of an exoplanet. Interpretation of these observed spectra requires planetary atmosphere models that can realistically simulate the atmospheric conditions and therefore provide constraints on the chemical compositions, pressure-temperature (P-T) profiles, energy transport, habitability, etc. in exoplanetary atmospheres. We present the development of an adaptable planetary atmosphere model that could be used to simulate Earth-like, super-Earth terrestrial exoplanets, as well as warm Neptunes, hot Jupiters, and similar gas giants. We also show an extensive opacity database covering a wide range of temperatures (70 - 3000 K) and pressures (7E-10 to 1000 bar) developed for this model. Here, we present the first results from the transmission spectroscopy module of our model coupled to a Bayesian sampler, interpreting Earth's satellite observations, thus showing important chemical species that could be detectable in the spectra and constraints on their abundances, if we look at Earth as an exoplanet. We also present an interpretation of recent James Webb Space Telescope (JWST) observations of K2-18b using our model. Finally, we present limitations of our current adaptable planetary atmosphere model and future planned developments to interpret solar system planetary atmosphere observations.